AD-A098 433 FOREIGN TECHNOLOGY DIV WRIGHT-PATTERSON AFB OH F/G 17/9
REDUCTION OF STATIONARY CLUTTER IN RADAR,(U)
OCT 80 J KROSZCZYNSKI
UNCLASSIFIED FTD-ID(RS)T-0132-80 NL

1 OF 1
AD
A098433

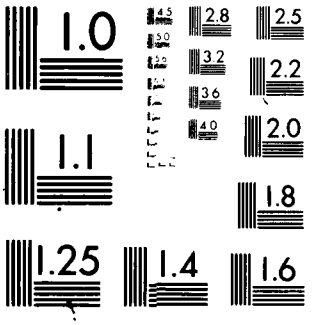

MICROCOPY RESOLUTION TEST CHART
NATIONAL BUREAU OF STANDARDS 1963 A

Corrected Copy DTIC

FTD-ID(RS)T-0132-80

(2)

AD A098433

FOREIGN TECHNOLOGY DIVISION

REDUCTION OF STATIONARY CLUTTER IN RADAR

by

Jan Kroszczynski

DTIC
ELECTE
MAY 0 4 1981
S D
E

DTIC FILE COPY

Approved for public release;
distribution unlimited.

81 5 01 029

FTD-ID(RS)T-0132-80

(12.) 295

EDITED TRANSLATION

(14) FTD-ID(RS)T-0132-80 (11) 30 October 1980

MICROFICHE NR: FTD-81-C-000086

(6) REDUCTION OF STATIONARY CLUTTER IN RADAR,

By: (10) Jan Kroszczynski

English pages: 290

(21) Edited trans. of [redacted] Tlumienie ech Stalych w Radiolokacji
Warsaw, 19[redacted]. [redacted]223, [redacted]

Country of origin: (Poland) v 4 p 1-[illegible] 1965.
Translated by: SCITRAN
F33657-78-D-0619
Requester: FTD/TQFE
Approved for public release; distribution unlimited.

THIS TRANSLATION IS A RENDITION OF THE ORIGINAL FOREIGN TEXT WITHOUT ANY ANALYTICAL OR EDITORIAL COMMENT. STATEMENTS OR THEORIES ADVOCATED OR IMPLIED ARE THOSE OF THE SOURCE AND DO NOT NECESSARILY REFLECT THE POSITION OR OPINION OF THE FOREIGN TECHNOLOGY DIVISION.	PREPARED BY: TRANSLATION DIVISION FOREIGN TECHNOLOGY DIVISION WP-AFB, OHIO.

INDEX

Introduction 1
I. Basic applications and methods in the technology of reduction of stationary clutter 2
1. The need for reduction of stationary clutter . . 2
2. Review of the basic methods for reduction of stationary clutter 6
2.1 Selection by distance 7
2.2 Selection by direction 9
2.3 Selection by polarization 13
2.4 Selection by signal envelope 16
2.5 Selection by Doppler frequency 22
3. Examples of design of radiolocation devices which use stationary clutter reduction. 48
II. Outline of the theory of signal detection systems operating against a background of correlated interference 54
4. Methods of radiolocation systems optimization . . 54
4.1 General discussion of the signal selection problem 55
4.2 Optimization of signal detection 66
5. Basic properties of signals and interference . . 92
5.1 Phenomena occuring in space scanning 92
5.2 Reflection properties of detected objects . 96
5.3 Properties of passive interference 104
6. The optimal reception algorithm 127
6.1 Solution of the basic integral equation. . . 127
6.2 Optimal algorithm of signal reception for correlated interference. 137
7. Characteristics of optimal filters 152
7.1 Signal and interference spectra..... 152
7.2 Optimal filter for stochastic signals . . . 157
7.3 Optimal filter for signals with a distinct Doppler component 167

8. Outline of the theory of intermittent (periodic) filters 174
8.1 Transfer functions of some intermittent (periodic) filters 174
8.2 The transformant and its application in the analysis of periodic filters 181
8.3 Synthesis of periodic filters 187
9. Evaluation of the detectability of signals against an interference background 202
9.1 Calculation of the quality of optimal decisions in the binomial case 202
9.2 Evaluation of the detectability in a multichannel system 207
9.3 Passage of signals and interference through optimal and non-optimal filters . . 215
9.4 Evaluation of the detectability of noncoherent signals 227
10. Some methods for improving the detectability of signals 240
10.1 Decrease of the influence of "blind velocities" 240
10.2 Decrease of the influence of the modulation arising in the course of space scanning 248
10.3 Some prospects of development 254

APPENDICES

1. The form of signals refected in the course of space scanning 261
2. Some properties of narrow-band stochastic processes 268
3. Solution of the Fredholm equations of the first kind by the method of orthogonal expansions 270
4. The displacement theorem for integral equations 277
5. On the Modulation of stationary stochastic processes 280
6. Some interrelations for the signal and interference spectra 286
7. Some aspects of the radar reception with noncoherent integration 289

Accession For
NTIS GRA&I ☒
DTIC TAB ☐
Unannounced ☐
Justification
By
Distribution/
Availability Codes
Dist | Avail and/or Special
A

INTRODUCTION

The technique of stationary clutter reduction is one of the most important and most interesting areas of modern radar. Thanks to the development of this technique it is possible to detect desired objects even in the presence of very strong passive interference, which greatly increases the range of radar application. Reduction of stationary clutter thus plays an ever more important role in civil as well as in military radar.

The present volume has as its goal to present an outline of the theory and the technique of stationary clutter reduction in radar. The first volume discusses the basic applications and the methods of stationary clutter reduction, and the necessary theoretical foundations; the second volume addresses the problems of the realization of appropriate devices and the measuring methods.

A presentation of the overall problems of stationary clutter reduction - even in the form of an outline - requires, on one hand, using rather advanced mathematical methods, and on the other, a detailed discussion of technical problems. Because of such a broad range of problems considered in this book, it seems appropriate to include in the introduction some methodological remarks. The material has been purposely arranged in such a form as to permit the use of this book by readers of verious interests and theoretical background. Generally, we assume familiarity with the basics of radar coverd by the monograph "Principles of Radar", PWN, 1956, I-X. A reader interested mainly in the technical problems may, after reading Chapters 1-3, look briefly at Chapter 4, cover more carefully Chapter 5,

look over and read the conclusions of Chapter 6, read Chapter 7 and 8.1, depending on the needs more or less thoroughly cover the rest of Chapter 8, read Chapters 9 and 10, and read completely the Chapters in the second volume. A reader more interested in the theoretical aspects of the problems discussed may cover Chapters 1-3, read Chapter 4, look through Chapter 5, read carefully Chapters 6-10; the second volume, which covers mainly technical problems, may be - depending on his interest profile - looked over or omitted. Additional literature in the area of the theory of signal detection includes a monograph by J. Seidler, "Statistical theory of signal reception", PWN, 1963. Readers with less of a theoretical background and interested more in the practical problems, will find an easier discussion of the basic problems of signal detection in a collective work edited by J. Seidler, "Modern methods of optimization of telecommunication systems", Communication Publ., 1965. **The author wishes to thank Prof. S. Slawinski, who suggested writing this book and Prof. Dr. J. Seidler for discussions on problems of statistical theory of signal reception. I also wish to thank Dr. J. Kulikowski for his valuable suggestions.**

I. Basic Applications and Methods in the Technology of Reduction of Stationary Clutter.

1. The need for reduction of stationary clutter.

In radar scanning of space there are often - aside from images produced by objects whose detection is the goal of a given radar system - numerous images of other objects. Images derived from objects whose detection is not required in a given application interfere with the process of obtaining and processing of information, and in many cases may completely prevent the detection of desired object. In radar, such interference is called <u>passive interference</u>. Since this interference is derived from stationary objects or from objects which move relatively slowly, and because their variability in time is

much slower than, e.g.that of images derived from airplanes, a term often used is stationary clutter.

Passive interference occurs most often as a result of reflection by field objects, clouds, atmospheric precipitation, or artificially introduced interfering objects.

Detection of desired objects against a background of passive interference is extremely important for radar methodology, in civilian and in military applications. Thus, radar stations serving to control air traffic encounter very strong images of filed objects which often surpass the level of the detector heat noise by tens of decibels. Fig. 1.1 shows as an example the graph of the intensity of stationary clutter surrounding a typical intermediate range radar station and Fig. 1.2 is a photograph taken from the screen of this station with the systems for reducing stationary clutter turned off. As can be seen, without applying special methods for interference reduction, stationary clutter completely prevent observation of airplanes within a radius of tens of kilometers around the airport, a range of particular interest and importance. [1.1][1] By application of appropriate methods it is possible to reduce the interference from field objects to an extent sufficient for detection of airplanes.

In addition, clutter originating from the reflections of clouds and from atmospheric precipitation may, in some cases, make it impossible to detect objects over relatively large areas, which could significantly decrease the operational value of radar. Thus, it is necessary to reduce clutter of meteorological origin.[2]

---

[1] In mountaineous areas, of course, one can observe permanent echos at even larger distances. For instance, a graph of permanent echos occurring in the Alps may be found in the work /1.2/.

[2] Examples of such interference and the effectiveness of its reduction by appropriate systems are discussed in Chapter 2.3.

The importance of the problem is even clearer for military applications since in this case it is necessary to reduce not only the stationary clutter of natural origin, but also to counteract the passive interference generated by the opponent.

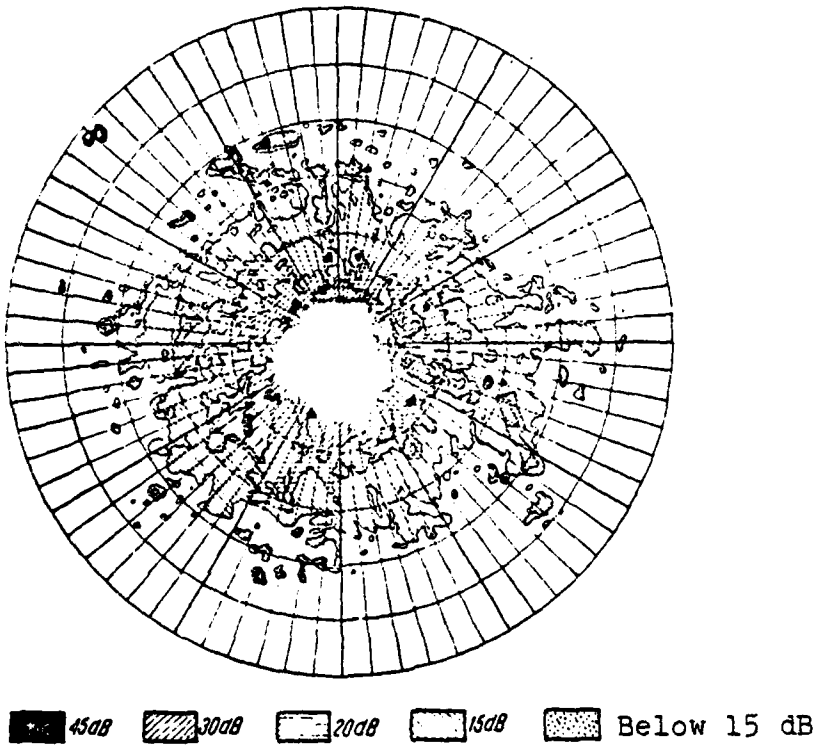

Fig. 1.1 Results of intensity measurements for stationary clutter around a radar station of range control. One mark every 10km.

Fig. 1.2 Photograph of the display screen of a radar station for area control (conditions as in Fig. 1.1)

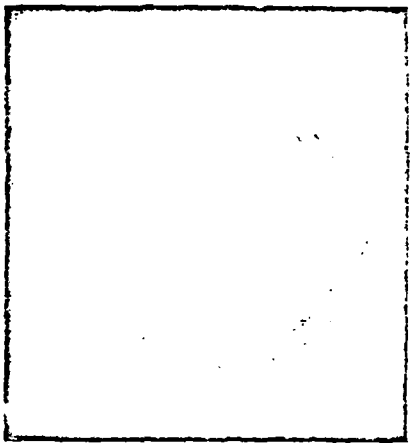

Fig. 1.3. Passive interference - imaging obtained on an indicator of type I [1.3]

For instance, during II World War use of passive interference (in the form of metallized paper strips scattered in the air) practically eliminated the effectiveness of German radar equipment. Investment costs in such equipment was estimated to have been several hundred million dollars, and the crippling of air defenses resulted in even greater losses. Fig. 1.3 shows a photograph of a indicator of J type of a German

radar station in the presence of passive interference; it may be seen that detection of airplanes was made impossible under these conditions. The air defense of the Third Reich was not capable of effective action in the presence of passive interference up to the end of the war, which doubtless had some influence on the outcome of the Second World War [1.3].

The examples cited above indicate a definite need for reduction of passive interference of various types in many radar applications. Depending on the kind of passive interference and the purpose of radar it may be useful (for technical and economical reasons) to apply one of the known reduction methods, or it may be necessary to use several methods simultaneously. A discussion of the basic reduction methods for stationary clutter is presented in the following chapter.

2. Review of the basic methods for reduction of stationary clutter.

The present chapter contains a review of the basic methods used in radar devices for detecting desired images against a background of various types of passive interference. The methods described will be discussed in general terms, to familiarize the reader with the basic problems of stationary clutter reduction; questions pertaining to the technical realization will be considered in detail in appropriate chapters of Volume II.

All methods of reducing passive interference relative

to images derived from detected objects are based on taking advantage of the differences between the detected signals and the interference. Depending on the specific requirements, a single most effective method for a given case is used, or several methods have to be used simultaneously. The basic systems and devices used against passive interference may be classified according to differences between the desirable and the undesirable signals.

2.1. Selection by distance

In some cases stationary clutter originates exclusively from surface objects located in the vicinity of the radar, which is supposed to detect only objects located at a distance. Under such circumstances it is possible to mark the signals in such a way as to prevent the signals within the range of stationary clutter from appearing on the screen. In stations having elevated antennas in the form of a single beam this method cannot be used to detect objects against a background of stationary clutter. It prevents unnecessary illumination of the image center. In multiple-beam stations, the situation is more favorable (see Chapter 2.2, Fig. 2.6).

When signals originating from detected objects are expected to be stronger than the stationary clutter, it is more advantageous to apply Sensitivity Time Control (STC) or Swept Gain[1]. This consists in introducing a time-dependent alternating amplification of the detector [2.1;2.2]. Since the reflection amplitude of the nearest surface objects is the greatest, and decreases with distance (cf. Fig.1.1), the sensitivity of a detector equipped with STC is the lowest at small ranges (Fig. 2.1). STC not only eliminates the illumination of the image center, but also prevents oversteering of the detector, making it possible to detect desired objects

when they have a sufficiently large amplitude relative to the stationary clutter.

One of the limitations on the effectiveness of STC is caused by the fact that if stationary clutter occurs with variable intensity in different azimuths, a compromise time characteristic has to be chosen for STC, which will not be optimal for each azimuth.

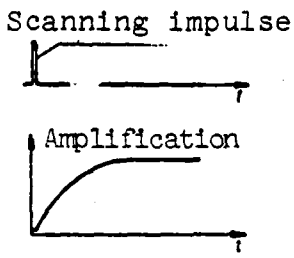

Fig. 2.1. Change in detector sensitivity as a function of time (Sensitivity Time Control)

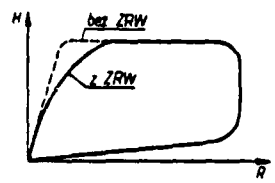

Fig. 2.2. Deformation of the covering diagram caused by the action of STC

The covering diagram for large-elevation angles undergoes a characteristic deformation when STC is applied [2.3; 2.4] (see Fig. 2.2; also text relating to Fig. 2.3).

STC is also used in marine radars, where reflections from waves are approximately the same for every azimuth, and in conjunction with other methods of stationary clutter reduction (see Chapter 2.2)

It should be added here that STC is used in radar stations not only for reasons stated above, but also to eliminate undesirable signals of other types. Since the strength of

---

[1] In English literature the term Swept Gain or Sensitivity Time Control is used (Abbr. STC), In Russian - vary (Vremennaia Automaticheskaia Regulirovka Usileniia).

reflected signals is inversely proportional to the fourth power of the object distance from the radar, objects situated nearby (e.g. birds) may give relatively strong signals, complicating the work of the operator at stations with a high voltage. STC is used to equalize signal amplitudes as a function of distance at stations of this type [2.5].

2.2. Selection by direction

When passive interference occurs in directions different than the direction of the objects to be detected, it is possible to improve the signal to clutter ratio by using appropriate directional characteristics of the antennas. The most typical examples of the application of this method is the reduction of passive interference caused by reflections from surface objects located in the vicinity of the radar which serves to detect aircraft. One of the important parameters here is the radar location. Various methods may be used in selecting the optimal position, at which the interference caused by surrounding objects is the smallest. Thus, one may use sections of the terrain,determined on the basis of topographical maps, take measurements using test installations, or apply a method consisting in making a miniaturized three-dimensional model of the terrain in question and taking photographs under appropriate illumination. The last method gives a good agreement with the results of measurements taken under real conditions [2.45].

In some locations it is possible to reduce the reflections from field objects by placing the antenna low, sometimes even in a recess [2.46], or by surrounding the position of the antenna with an appropriate metal fence [2.47].

In addition, antennas with high obliquity of the lower

of the elevation characteristic of direction are used in order to reduce stationary clutter. It is known that in order to obtain a highly inclined lower slope of the characateristic it is necessary to use antennas with a large (relative to the wavelength) vertical dimension [2.6], which may cause problems when longer wavelengths are used. This method is used, for instance, in airport surveillance radar[1], e.g. in radars operating at a 10cm wavelength (ASR-3 and ASR-4)[2.7], in conjunction with other methods.

When it is difficult, for technical reasons, to obtain an antenna characteristic with a sufficiently sharp lower edge, a modification of the elevation characteristic is also often used to accentuate signals originating from airborne objects situated above the area of stationary clutter; this method is illustrated in Fig. 2.3. Obtaining such an antenna characterisitc does not require any additional increase of the vertical mirror dimensions, and therefore this method is often used in devices operating in the 23cm band as a supplement to other methods of stationary clutter reduction; this type of characteristic also compensates for the unfavorable side effect of the STC system [2.3].

An antenna with a similar form of elevation characterisitic is used e.g. by the air route surveillance radar [2.7][2] ARSR-2 of the Raytheon company (USA)[2.4] and by the station of CR-3 type of the CSF company (France)[2.8;2.9].

In order to achieve a significant reduction of the reflections of field objects, a two-beam system is also used, in which the lower beam serves to detect objects at farther ranges

---

1 In Russian literature - radiolokator zony aerodroma; in English - ASR (Airport Surveillance Radar)

2 In Russian literature - raionnyi radiolokator krugovo obzora; in English - Air Route Surveillance Radar.

and lower altitudes, using scoring or STC in the stationary clutter range; the other beam has a characteristic designed for reducing field clutter (Fig. 2.4). A similar system, in conjunction with e.g. STC systems (cf previous chapter) is used in radar stations which direct and control air traffic and made by "Decca" (Great Britain) [2.8] and by "Thomson-houston" (France)[2.4]; these systems will be described in Chapter 3.

Fig. 2.3 Antenna characteristic facilitating aircraft detection above stationary clutter area.

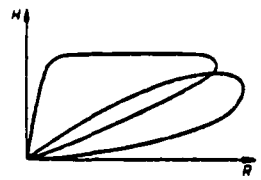

Fig. 2.4 Two-beam antenna system.

Fig. 2.5. shows as an example the photographs of the indicator of a DASR-1 station, which illustrate the operation of a two-beam system under conditions with strong stationary clutter [2.10]. The method described is designated in the English literature by the abbreviation ATI for Air Target Indication [2.11].

Even better results can be obtained by using a multiple-beam elevation characterisitc (see Fig. 2.6 - cf [2.4;2.12]). A similar effect is obtained by programmed gating as a function of the elevation angle (or by STC), used at "three dimensional" radar stations which operate with rapid scanning in elevation by a narrow beam [2.45].

It is not always possible to apply the selection method

by direction; e.g. in the case of intentional passive interference, usually both the aircraft to be detected and the interfering objects are located in the same direction and at a similar distance.

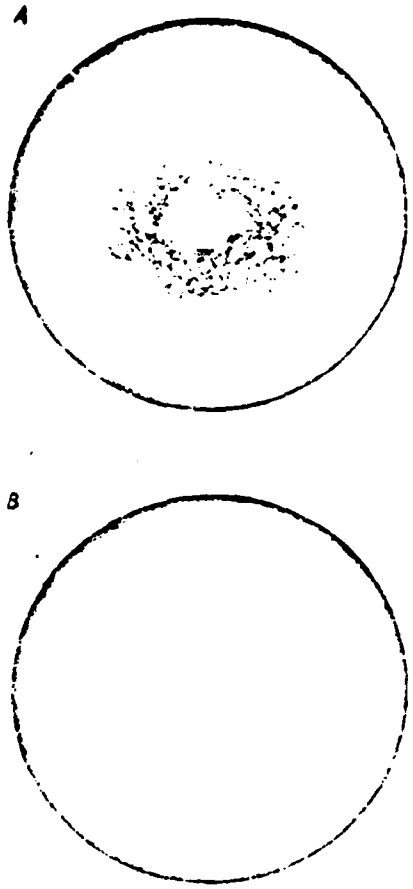

Fig. 2.5. Operation of a two-beam system in the presence of strong stationary clutter. A-photograph of the screen without using the two-beam system; strong stationary clutter is seen. B-photograph of the screen with the two-beam system; stationary clutter practically absent, aircraft previously masked by stationary clutter are seen. Station Decca DASR-1, range 25 mi. (about 46 km) [2.10].

In some cases multiple-beam stations may have an advantage

over systems with an elevation characteristic of the "cosec^2" type. As shown in Fig. 2.7, an airplane located within a cloud of interference will not be detected by either type of station, but an airplane flying above this cloud may be detected in one of the channels of the multiple-beam station without using any other anti-interference methods. Stations with an elevation characteristic of the "cosec^2" type obviously do not have this option.

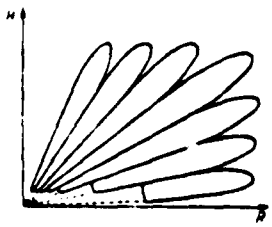

Fig. 2.6. Multiple-beam elevation characteristic of the antenna

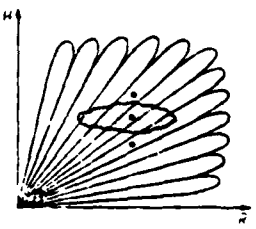

Fig. 2.7. Detectability of objects against a background of passive interference at a multiple-beam station.

2.3. Selection by polarization

In some cases objects which cause passive interference have specific properties with respect to polarization of reflected signals. The most typical example are raindrops, which are essentially spherical. As we know, an electromagnetic wave with circular polarization is reflected from a spherical object with circular polarization, although with opposite twist [2.13;2.14]. Since generally the same antenna is used in radar for emission and reception, when a scanning signal with circular polarization is used, theoretically the signals reflected by spherical objects would not be detected, because they would have the polarization with a twist opposite to that of the receiving antenna. In contrast, airplanes, being objects with a complex shape, reflect a wave with circular polarization in a random fashion, such that there are always

some components of the reflection which will be detected by the receiving antenna. Thus we have the possibility of effective reduction of the interference caused by rain clouds etc., and a relatively smaller loss of the signal to be detected, amounting to 1 - 2 dB[2.10] to 6 - 8 dB [2.15]. According to some authors, the maximum values of effective area (for varying positions of aircraft relative to the radar) are smaller for circular polarization than for linear polarization. For aircraft positions corresponding to the minimum values of effective area for linear polarization, circular polarization gives better results. The effect amounts to a reduced effective clutter fluctuation [2.45].

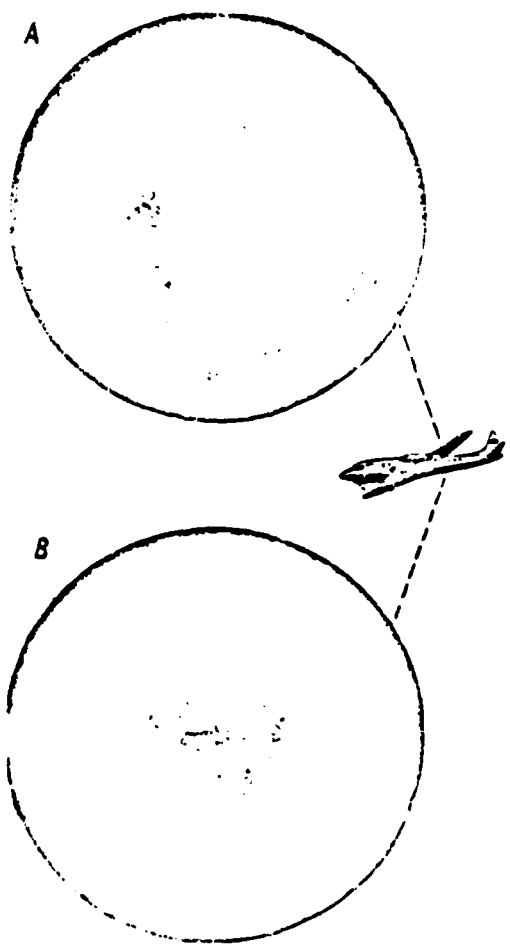

Fig. 2.8. Effect of circular polarization in a station

operating with a 3 cm beam. A-photograph of the screen with linear polarization, during heavy rain. B-photograph for the same conditions, using circular polarization;strong reflections from the aircraft are seen, previously masked by interference. Station Decca 424 Mark II, indicator range 5 mi. (about 9 km) [2.17].

In practice, improvement of the ratio of the signal reflected from the aircraft to the signal reflected by precipitation, with the use of circular polarizaton, amounts to between 8 to 25 dB [2.15; 2.16], and in some cases even 30 dB [2.4].

Fig. 2.8 shows the effect of circular polarization in the system Decca 424 Mark II, working in the 3 cm beam [2.17].

It should be noted here that the usefulness of circular polarization depends on the wavelength of radar operation. Since, as is known [2.16], the signal intensity of reflections from clouds and raindrops is inversely proportional to the fourth power of the signal wavelength, the interference due to meteorological objects is much weaker for a radar operating at longer wavelengths (see Chapter 5). This is illustrated in Fig. 2.9, which shows photographs of two radar screens operating simultaneously. One of them, operating at the 10 cm wavelength, shows strong interference of a meteorological origin; the other, operating at the 50 cm wavelength, gives an image practically free of interference (in both cases linear polarization is used)[2.18].

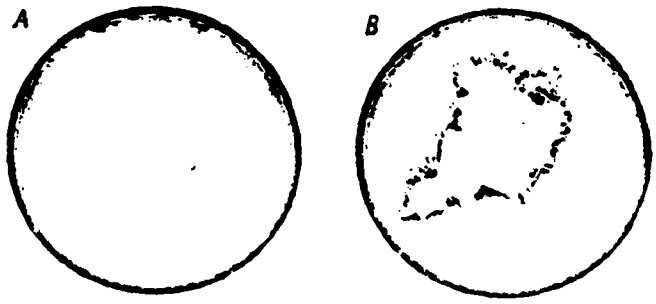

Fig. 2.9. Operation of two different radars of the Marconi

company in identical, severe meteorological conditions (heavy snowfall). A - station working in the 50 cm beam. B - station working in the 10 cm beam [2.18].

In reference to the problems mentioned above, it should also be noted that in order to achieve appropriate contrast, it is necessary to carefully select the operating conditions for the screen imaging lamp [2.20 and 2.21].

2.4. Selection by signal envelope

This chapter will consider those methods of signal reception against a passive interference background which can be used in devices using a noncoherent system, i.e., with detection by amplitude (signal contour).[1]

The application of a visual amplifier with a low time constant of coupling elements, which provides signal discrimination[2], allows in some cases to improve somewhat the visibility against the background of passive interference. Discrimination removes the constant part of the interference, and accentuates the signal to be detected [2.1;2.2]. Discrimination systems cause some loss in the detectability of the signals, which may reach 5 dB. In order to avoid this effect, more complex systems are used with delay lines (with delays on the order of 10 lengths of the scanning pulse), which remove the "constant" component of passive interference [2.50].

We note that all the methods based on the envelope may be applied only when there is no over control of the stages preceding the detector. Since stationary clutter may have a

---

[1] The question of optimal pre-detection filters for individual pulses in the presence of passive interference (Urkowitz filter) will be discussed in Chapter 6.

[2] In English literature this method is also termed FTC (Fast Time Constant)

very high intensity, (see Fig. 1.1) appropriate means should be used to protect the receptor from overcontrol. One of the methods used in this case is the socalled Instantaneous Automatic Gain Control IAGO.[1] This is a fast-acting system of automatic gain control, in which a strong negative reverse coupling is used with a time constant of the same order as the length of the scanning pulse. Thanks to this, the amplitude of the reflection pulses against the background free of interference is negligibly reduced, while in the areas of interference the receptor is protected from overcontrol [2.1;2.2]. Another system used with the same objective (often in conjunction with IAGC) is the so-called detector balance bias [2] [2.1;2.2]. Also, detectors with logarithmic characterisitics are used. Application of such a characterisitic permits to bring the signal fluctuations to the same level, and subsequent dicrimination allows the selection of the desired signal. The question of the effectiveness of the operation of a logarithmic receptor in signal detection against a background of stationary clutter was considered in detail by Croney [2.22]; Fig. 2.10 is (taken from this work) a photograph of the image on radar screen using a logarithmic receptor and discrimination. A discussion of the operating effectiveness of discrimination is also presented in references [2.2 and 2.23].

The use of linear-logarithmic characteristics of the receptor with coherent reception is discussed in Par III.

It should be noted that the means for increasing the dynamics of the receptor are often supplemented by the STC system (of Chapter 2.1).

In detecting objects whose dimensions are small compared to

---

[1] English IAGC (Instantaneous Automatic Gain Control), Russian MARU (Mgnovenna avtomaticheskaia regulaciia usileniia).

[2] English DBB (Detector Balance Bias).

the effective size in space of the scanning pulse[1], it is possible in some cases to take advantage of the fact that stationary clutter usually occupies a considerable area in space. Thus, applying the so-called discriminator of pulse length, which lets through only pulses of length similar to that of the scanning pulse and suppressing longer pulses, it is possible to obtain a certain reduction of stationary clutter (of Fig. 2.11). A pulse length discriminator should be preceded by a receptor which does not restrict the signals, e.g. a logarithmic one [2.24].

Fig. 2.10 Effectiveness of logarithmic amplifier and discrimination. A - imaging obtained with a linear receptor. B - imaging under the same conditions, but using logarithmic amplifier and discrimination [2.22].

The use of pulses with too large a size is not useful in detecting objects in the presence of passive interference, since increasing pulse length leads to (with interfering objects interspersed in space) a decrease in the signal-to-clutter ration, since the number of interfering objects increases and causes possible interference within the area of impulse reflection. Because of this, one should use scanning /23

[1] E. g., at a scanning pulse length of 3 μs, the effective size of the pulse - about 450 m - is considerably larger than an aircraft.

pulses which are as short as possible[1].

The use of such pulses may cause difficulties in reaching the required range, since at peak power, limited for technical reasons, they may not have sufficient energy. In some cases these difficulties may be overcome by applying the method of pulse compression. In some systems operating with a pulse length of 5 μs, the use of linear frequency modulation during the pusle time led to an pulse reflection compressed to an effective length equal to approximately 0.1 μs. This results in a reduction of passive interference from meteorological precipitation of about 17 dB [2.45].

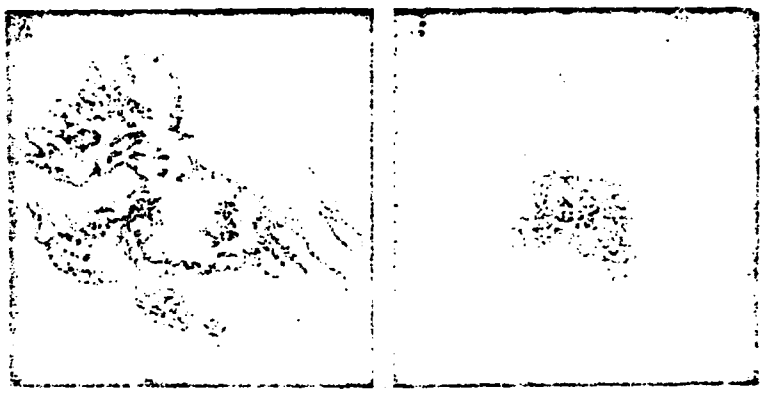

Fig. 2.11. Effect of a pulse length discriminator designed by the Marconi Company. A - imaging without discriminator. B - imaging obtained with discriminator.

The methods described above take advantage of the properties of individual reflections, and not the entire signal reflection, received in the process of space scanning.

---

[1] Radar devices have been constructed which use a pulse negth lower than 1 ns (10^{-9}), working at the 3 cm wavelength [2.48]. Such devices have a range discrimination better than 10 cm, which makes it possible to detect cars in forst [2.49]; however, these radars have a low peak power.

As can be easily noted, a change in the position of an object from pulse to pulse can be detected on the basis of signal envelope displacement only in unusual cases[1], because even for very fast object, this displacement is very small[2]. Thus one should rather consider the possibility to using the change in position between two consecutive cycles of space scanning, e.g. at a station of circular observation, between consecutive revolutions of the antenna.

The simplest method is just to use an imaging lamp with an appropriately long illumination display, which causes moving objects to leave a distinct trace[3]. This allows tracking of moving objects even in areas with numerous but small and isolated stationary clutter (cf Fig. 2.5 B). This property of the display with a long illumination duration gives an additional improvement of the detectability of moving targets in devices for reduction of stationary clutter are used.

---

[1] The envelope of an echo composed of a reflection from the object to be detected and of passive interference may, in contrast, show relatively large fluctuations from pulse to pulse, which are caused by changes in the relative reglection phase. This was used to advantage in the so-called autocoherent system (cf. Chapter 2.5)

[2] E.g., for aircraft velocity of 600 m (about 2M) and repetition frequency of 400 Hz, the displacement from pulse to pulse would only be 1.5 m. This corresponds to a change in delay of 0.01 μs.

[3] E. G., imaging lamps with the luminophore of type P-19 (according to the U.S. nomenclature) (2.6).

The use of two color imaging lamps has been suggested in the past; here one luminophore would show up only after repeated excitation, while the second would show up after a short excitation. In this fashion stationary clutter and moving objects would give rise to imaging in different colors. However, this method has not found general use because of relatively small effectiveness and difficulties in designing luminorphores with good color and memory propertis [2.25]. Recently this method has been considered again in applications to devices with high discrimination, which serve to scan airport surface [2.45].

Considerable system possibilities are opened up if, in addition to imaging lamps with long illumination, special memory lamps are used. It is impossible then to obtain two or three-color imaging [2.26; 2.51], which clearly differentiates moving objects. It is also possible to obtain imaging in which a series of blinking dots moves along the trace of moving objects, thus attracting the operator's attention [2.27;2.52].

It is also possible, using appropriate memory lamps, to produce a system of substracting visual signals between revolutions of the antenna [2.16; 2.28; 2.29]. With appropriate form of the receiving track and selecting radar parameters, this method allows to reduce passive interference and to maintain the imaging of moving object reflections[1]. The detectability of objects against a background of stationary clutter which continuously covers certain area is in this case considerably curtailed because of the stationary clutter fluctuations, which in most cases can be considered noncorrelated from

[1] Since the period of antenna revolution is of the order of seconds in circular observation stations, the aircraft displacement in space during this time is several hundred meters or several km, at aircraft velocities of the order of 1 M - 2 M.

revolution to revolution (see Chapter 5). This method may, /25
however allow detection of objects in the presence of so-called coded passive interference (which consists of individual dipole packets dropped at certain intervals [2.30] and other stationary clutter present in isolated, relatively small area. Selection of moving targets can also be achieved under similar conditions by systems with an automatic numerical measurement of coordinated objects. In such devices, an appropriate computer determines the velocities of all objects being tracked; this method makes it possible to discern between moving and immobile targets. If appropriate extrapolating systems are used in the computer, tracking of moving objects against passive interference may be facilitated when the interference has the form of small isolated "islands". However, it is impossible to detect reflection signals when passive interference exceeds these signals in intensity, and other methods must be used [2.50].

2.5. Selection by Doppler frequency

One of the most effective methods of moving object selections against a background of stationary clutter takes advantage of the differences in the velocity of phase shifts of reflections between desired and unwanted signals. The method is easier to use for a situation in which the reflected signal contains a distinct component with a Doppler frequency. This is why this method is most frequently referred to as being based on the Doppler effect, although in some cases, as will be seen below, this name is not too accurate.

It is know that the frequency of the reflected signal coming from an object moving with respect to the radar station with a radial velocity v differs from the frequency of the scanning signal approximately by $f_D = f_w \cdot \frac{2v}{c}$, (2.5.1)

where f_m -- frequency of the scanning signal; C - velocity of propagation of electromagnetic waves in space. The frequency f_D is often called the Doppler frequency (cf. Chapter 5).

Fig. 2.12 shows the graph of the dependence [2.5.1] which gives an idea of the order of magnitude of Doppler frequencies. Since the objects giving rise to passive interference are usually immobile or move considerably slower than objects to be detected, there is a possibility of their effective differentiation by using appropriate filters.

Radar devices which take advantage of the Doppler effect may be generally classified as belonging to one of three groups (cf.[2.13, Chapter 5; 2.29, Chapter 2]): a. devices emitting a continuous wave; b. devices emitting pulse signals with a high filling coefficient[1]; c. devices emitting a /26
pulse signal with low filling coefficient.

A block diagram of the simplest radar device operating with a continuous wave is shown in Fig. 2.13.

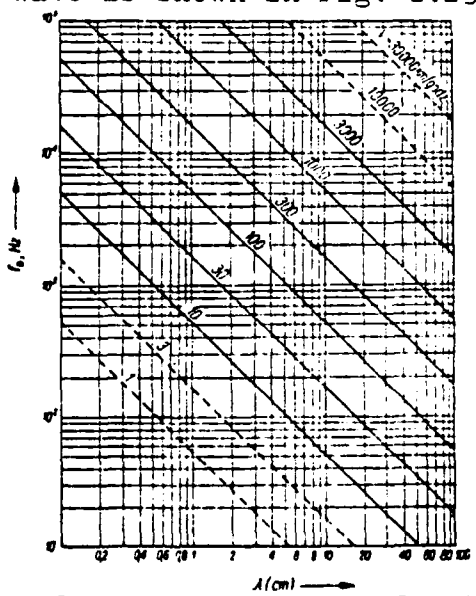

Fig. 2.12. Doppler frequency f_D as a function of the object's radial velocity ν and wavelength λ.

---

[1] Filling coefficient refers to the ratio of pulse length to the repetition period.

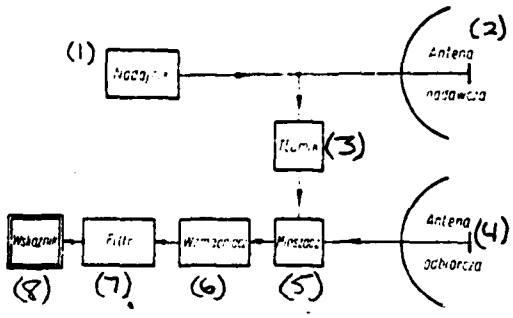

Fig. 2.13. A block diagram of a radar operation with continuous wave. 1. transmitter; 2. emitting antenna; 3. damping unit; 4. receiving antenna; 5. mixer; 6. amplifier; 7. filter; 8. screen.

In practice, amplification occurs at the intermediate rather than the low frequency; this requires an additional local generator , mixer, and intermediate frequency amplifier. However, this does not influence the basis of system operation, and is required only for technical reasons (such as the noise properties of semi-conductor microwave mixers). Therefore the details have been omittted here.

The damp emitting signal with frequency f_w is combined in the mixer with a reflected signal with frequency f_D where $f_w + f_D$,- Doppler frequency for a given object. The generated differential signal is amplified and passed through a filter, in order to separate the low frequency components, which derive from passive interference. The signal frequency f_D at the /27 filter exit is fed to the screen, which may be constricted in various ways, e.g. using deflection, acoustics, etc. As can be seen from Fig. 2.12, Doppler frequencies are found in the range of sound frequencies, and therefore acoustic signal indicators are often used. Instead of a single filter, sometimes systems of narrow band filters are used, which in addition to separating the signal better, also make it possible to determine the Doppler frequency.

The basic problem in constructing these systems is obtaining appropriate stability of the transmitter frequency [2.13, Chapter 5].

Devices of this type (often called - according to the operation principle - Doppler radars) are characterized by simple construction, good detection of moving objects against a background of strong passive interference and by the possibility of measuring the radial velocity of the object. They cannot measure the range to the object, nor do they differentiate between objects with the same radial velocity. Therefore, these devices have limited application, for detecting moving objects and for determining the velocity of individual targets. Examples of the latter application are devices which measure the velocity of missiles or rockets, police radars which measure motor vehicle velocity, etc. [2.16, Chapter 3; 2.31].

In an attempt to remove the imperfections of simple Doppler radars and still maintain good detection against a background of passive interference, various methods of emitter signal modulation have been designed. Of these systems, the most widely used is the so-called pulse-Doppler system, which uses pulses with high filling coefficient. Devices using this method are built in many variations; to illustrate this, Fig. 2.14 shows a block diagram of a typical radar [2.19, Chapter 6].

This system also takes advantage of the Doppler effect. Using a pulse emitter signal, it is possible here (with the use of the NO system) to utilize a common antenna for emission and reception.

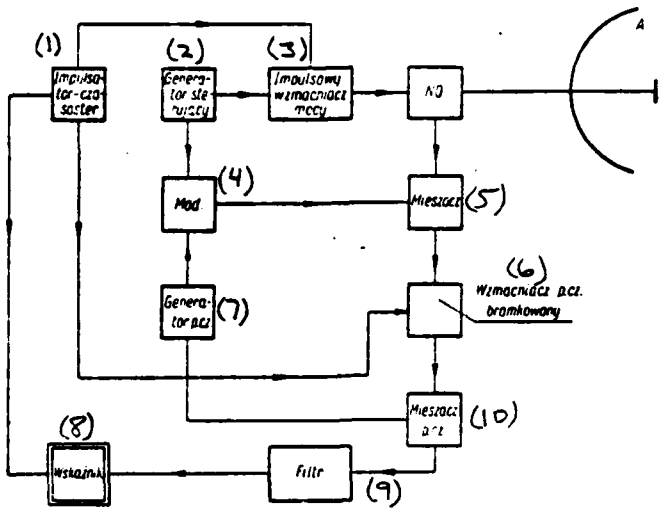

Fig. 2.14. A block diagram of a typical pulse-Doppler radar.
1. pulse-time control; 2. control generator; 3. pulse power amplifier; 4. modulator; 5. mixer; 6. gating amplifier of intermediate frequency; 7. intermediate frequency generator; 8. screen; 9. filter; 10. intermediate frequency mixer.

In this device, the range of detection by distance is subdivided into an appropriate number of gating segments. The output of each of the gating amplifiers is passed onto an appropriate filter system which selects the Doppler frequency; in order to simplify the filters, so-called boxcar demodulators[1] are applied. Thus the range of the object is determined by the gating segment in which the signal appeared, and its Doppler frequency is defined by the filter system [2.16; 2.19; 2.29; 2.32]. In order to improve the efficiency of detection and filtration and to simplify the filter system, a boxcar demodulator is used. Its operation is illustrated in Fig. 2.15. Fig. 2.15a shows a pulse train

[1] In the English literature boxcar demodulator [2.16].

leaving a gating amplifier (i.e., at the input of the boxcar demodulator system).Fig. 2.15b shows the output of this system. As can be seen, the output signal is similar to the modulating pulse series; however, the content of harmonic components with frequencies equal to multiples of the frequency of pulse repetition is rather small. The box car demodulator therefore has the role of demodulating the envelope of pulse series.

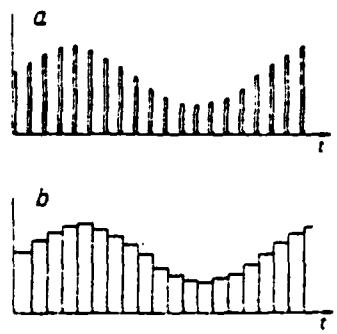

Fig. 2.15. Operation of a boxcar demodulator system: a - input signal; b - output signal.

The pulse-Doppler devices with a high filling coefficient /29 make is possible to measure object range, but they have certain imperfections related to the difficulty in achieving accurate measurements, low capacity for distance differentiation with long pulses. There is also the possibility of ambiguous distance readings. For these reasons they have also a rather low capacity, i.e., they cannot provide imaging of too many targets at once. On the other hand, they are characterized by effective detection against a background of passive interference.

Similar devices have been applied, e.g., as onboard aircraft radars, they are used in some cases for aircraft detection and in detection of moving objects (e.g. soldiers, vehicles) in the battlefield [2.16; 2.19; 2.32-2.35]. Pulse Doppler radars allow in some cases to detect moving objects against

a background of stationary clutter which is stronger by 70 to 90 dB[2.16].

The most commonly used scanning system in various radar devices emit a pulse train with a low filling coefficient, of the order of 10^{-3}. Radars designed on this principle serve to direct and control aircraft traffic , to detect and guide airplanes, to direct the firing of anti-aircraft weapons, as onboard aircraft devices, marine navigation devices, etc. The widespread use of this system is due to its advantages, such as good differentiation and accuracy of range determination, ability to give simultaneous imaging of a large number of targets, and rapid information gathering.

The most effective way of detecting moving objects against a background of passive interference uses the information contained in the phase of the reflected signals. Devices based on this principle are called coherent-pulse. They bring about a reduction of stationary clutter (TES)(MTI)[1][2.13, Chapter 16; 2.16, Chapter 4; 2.29, Chapter 2; 2.36]. Radars of this type can, for present level of technology, detect moving signals against a background of stationary clutter stronger by 20 to 30 dB[2.16].

The operating principle of the TES system will be described first in a simplified manner, to give a general idea of the phenomenon; next, a more detailed discussion of the properties of relevant devices will be given.

---

[1] In English literature - Moving Target Indication MTI); in Russian - Seleksiia Podvizhnih (or Dvizhuhchihsiia) Tzelei (SPTS or SDTS); in French - Elimination d'Echos Fixes (EEF); in German - Standzeichenunterdrückung.

Figure 2.16 shows a (considerably simplified) basic block diagram of a radar station which allows the reduction of stationary clutter. Let us consider the individual stages in this system.

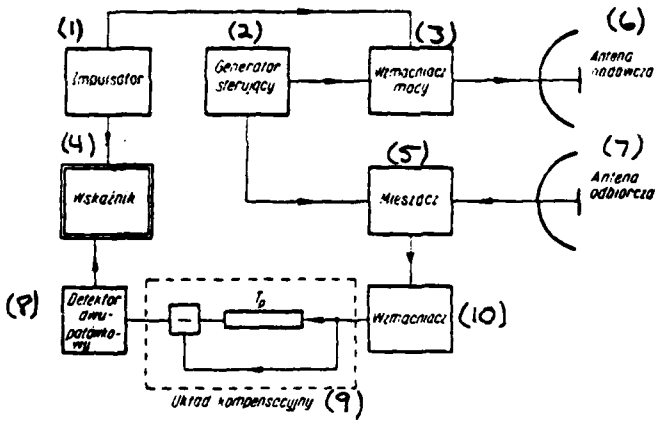

Fig. 2.16 Simplified block diagram of a pulse-coherent radar (working with reduction of stationary clutter).
1. pulser; 2. pilot oscillator; 3. power amplifier; 4. indicator; 5. mixer; 6. emitting antenna; 7. receiving antenna; 8. detector (two-halves); 9. compensating system; 10. amplifier.

The pulser modulates the emitter, which sends high frequency scanning impulses into space. A small part of the emitted pulse power is used to synchronize the so-called coherent oscillator. This oscillator uses a frequency identical to that of the transmitter[1], and is, as mentioned above, synchronized, such that each pulse of the transmitter imposes a defined vibration phase.

---

[1] In actual systems the coherent generator usually uses intermediate frequency, but this does not change the basis of operation, as discussed below.

The pulse reflected by a target is received by a receiving antenna, and then reaches the mixer. Mixing of two vibrations, the continuous wave from the coherent oscillator and the pulse reflected from the target, gives a visual pulse, whose amplitude depends not only on the intensity of the incoming high frequency pulse (as is the case in ordinary radar stations), but also on its phase with respect to COHO[1] vibrations.

For stationary and nonfluctuating objects, the amplitude as well as the phase of reflected pulses remain always the same. Because of the synchronization, the phases of transmitter vibrations and COHO vibrations are identical, and therefore the mixer output always gives a constant reflection from a given stationary object.

The situation is different with a moving object. Even when the amplitude of the reflected signal is constant, the phase changes, since during the time elapsed from the moment of scanning signal emission to the next emission, the distance of the target from the station has changed. This is why the visual pulse output by the mixer will have a different amplitude during each cycle.

These relationships are illustrated in Fig. 2.17a-d. They represent consecutive paths which would be seen on the screen of the indicator A. As can be seen, some reflections are stationary, while others are derived from moving targets. In addition, a difference with respect to the usual image A is seen; with coherent detection, visual pulses may be positive as well as negative.

In fact, because of the human vision inertia, the screen

[1] Abbreviation for coherent oscillator.

of the indicator A shows many paths simultaneously, and thus the image will appear as shown in Fig. 2.18.

The phenomenon described here raises the possibility of differentiating between moving targets and stationary ones. Devices of this type, which make possible the selection of moving targets only, were used in radar stations (e.g., by Germans in the last phase of the war) to make the operator's job easier.

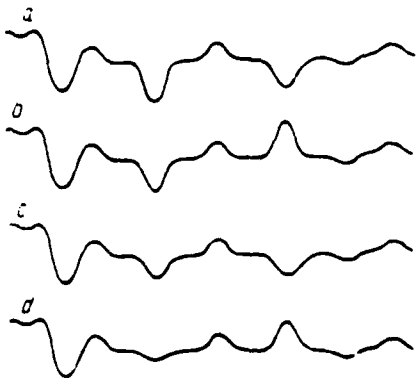

Fig. 2.17. Consecutive images on the indicator A operating coherently.

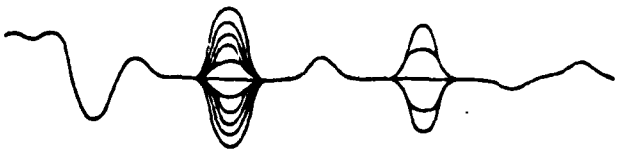

Fig. 2.18. Image obtained on indicator A, operating coherently.

The effectiveness of these devices is limited because stationary clutter remains visible and distracts the operator. In addition, since the image appears only on the indicator A, the station cannot scan the space rapidly, which decreases the tactical value of the method considerably.

Thus it is necessary to use systems which would allow selection and reduction of stationary clutter. The screen of the indicator will only show the signals from moving

targets.

The reduction of stationary clutter is achieved in the following way. Let us draw the paths derived by subtracting the diagrams 2.17a-d, namely: b-a(Fig. 2.19a), c-b(Fig. 2.19b), d-c(Fig. 2.19c). As can be seen, stationary clutter is eliminated, while the oscillating reflection of the moving object remains.

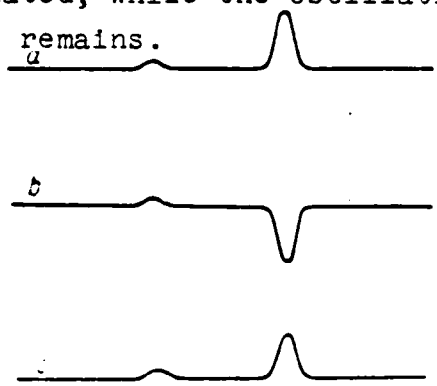

Fig. 2.19. Subtraction of consecutive paths.

The above principle is put into practice by directing the visual signals to the subtracting system using two paths; direct and through a delay line, with a delay equal to the repetition period of the pulses T_p (cf Fig. 2.16). This gives the desired effect, i.e., signals from the previous cycle are subtracted from those received in the current cycle, as in Fig. 2.19.

As a result of subtraction, visual pulses are obtained which may be positive as well as negative, while the indicator is usually designed for work with pulses of one sign. Therefore an appropriate rectifier is introduced between the subtracting system and the indicator; the rectifier transforms a series of negative and positive pulses into a series of pulses of the same sign (Fig. 2.20). These pulses are then passed on to the indicator as in ordinary radar stations.

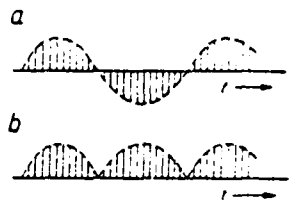

Fig. 2.20. Detection of pulse trains

Now that we realize how a coherent pulse station (MTI) operates, let us go on to define more strictly some relationships. Let us denote the vibrations emitted by the transmitter during the first scanning pulse in the following way:

$$w_1(t) = \begin{cases} 0 & t < 0 \\ a_1 \cos \omega_w t, & 0 \leq t \leq T \\ 0 & T < t \end{cases} \qquad (2.5.2)$$

where T - time of pulse duration.

The vibrations of a coherent oscillator, in accordance with the previous observations, may be expressed as:

$$k_1(t) = a_2 \cos \omega_w t. \qquad (2.5.3)$$

If the reflecting object is small, then the corresponding reflected signal $s_1(t)$ received by the receiver will of course have the form of a pulse of length T, appropriately delayed with respect to the scanning pulse.

It should be noted that even if the object to be detected - e.g., an airplane - flies directly at the radar station with a velocity approaching double the velocity of sound, the change of the object's distance between pulses will be (at typical $T_p = 1000\mu$ sec) only about 60 cm. Let us imagine a pulse reflected from a target shown on the indicator A.

Let us assume, as an example, that the range of the time base is 50 km, and the indicator has an oscilloscope tube with a 5 inch diameter, i.e. the length of time base is about 100 mm. The displacement of the reflection on the screen between pulses for parameters given above would not exceed approximately 0.001 mm. Such an effect would not be noticed. Even using a more extended time base scale, the displacement /34
of the reflection on the indicator would be extremely difficult to detect, since for a typical pulse of length T =1 μS, the displacement between pulses would comprise (with parameters as above) only about 0.004 T. Thus it is clear that the difference in position of the envelope of two consecutive visual pulses of a reflection is practically of no consequence; however, the phase of the signal received (in agreement with the MTI method of system operation described) is important.

Thus we will not use in further considerations the time limits of pulse duration in the form of equation (2.5.2.), which is cumbersome. We should remember, however, that we are dealing with a pulse signal.

Let us assume that the distance of a moving target is defined by the function r(t). Then the reflected signal is delayed with respect to the transmitter signal by $\frac{2r(t)}{c}$. In addition, reflection by a target causes a displacement of the phase by an angle which depends on the object's properties; these properties change with time, so that this angle may change between pulses.

As a result the reflected signal will be expressed by:

$$s_1(t) = a_3 \cos\left\{\omega_w\left[t - \frac{2r(t)}{c}\right] - \varphi_1\right\}. \qquad (2.5.4)$$

The vibrations of the coherent oscillator and the signal are mixed. We assume in these considerations that it is a mixer of multiplicative type, i.e., that the output signal is the product of input signals. As we know, such mixers are designed using appropriate nonlinear elements. In accordance with well known trigonometric formulas, the product of sines (or cosines) is represented as the sum of sinusoidal vibrations with arguments equal to the sum and the difference of the arguments of the product. Because in our case these vibrations have identical or almost identical frequencies, we will obtain a path with a small frequency (Difference of the arguments) and one with a very high frequency (sum of the arguments), The first path corresponds to the visual pulses, which we want to isolate; the second path is filtered out by an appropriate low-capacity filter, as usual in detection.

As a result, a modulated visual pulse will be obtained:

$$u_1(t) = \text{const} \cdot a_2 a_3 \cos\left[\omega_w t - \omega_w\left[t - \frac{2r(t)}{c}\right] + \varphi_1\right] =$$

$$= a_4 \cos\left[\frac{2\omega_w r(t)}{c} + \varphi_1\right]. \qquad (2.5.5)$$

During the second cycle similar events will take place. However, since the second scanning pulse will occur after a time T_p, we have to replace t by $t-T_p$ in the appropriate expressions for s(t) and k(t).

The second visual pulse will thus have the form:

$$u_2(t) = a_4 \cos\left[\frac{2\omega_w r(t)}{c} + \varphi_2\right]. \qquad (2.5.6)$$

Subtracting the first visual pulse, delayed by period T_p, from the second visual pulse, i.e., $u_1(t - T_p)$, one obtains:

$$u_2(t) - u_1(t - T_p) = a_4 \left\{ \cos\left[\frac{2\omega_w r(t)}{c} + \varphi_2\right] + \right.$$
$$\left. - \cos\left[\frac{2\omega_w r(t - T_p)}{c} - \varphi_1\right]\right\}. \qquad (2.5.7)$$

After transformation, we obtain:

$$u_2(t) - u_1(t) = -2a_4 \sin\left\{\frac{\omega_w}{c}[r(t) + r(t - T_p)] + \right.$$
$$\left. - \frac{\varphi_2 - \varphi_1}{2}\right\} \cdot \sin\left\{\frac{\omega_w}{c}[r(t) - r(t - T_p)] - \frac{\varphi_2 - \varphi_1}{2}\right\}. \qquad (2.5.8)$$

Equation 2.5.8 represents the envelope (contour) of the visual pulses at the output of the compensating system. This formula allows to determine the basic properties of a station equipped with a MTI system, and in particular, those characteristics which differentiate it from an ordinary radar station.

To simplify the discussion of eq. 2.5.8, let us consider a simplified case, when $\phi_1 = \phi_2 = 0$, a_4= const, and $r(t) = r_o + vt$. This means that the properties of the target do not change between pulses, and that the target moves with a uniform radial velocity.

In this case $r(t) = r(t-T_p) + vT_p$, and as a result we will obtain:

$$u_2(t) - u_1(t) = -2a_4 \sin\frac{\omega_w}{c}[2r(t) - vT_p] \sin\frac{v\omega_w T_p}{c}. \qquad (2.5.9)$$

that is,

$$u_2(t) - u_1(t) = -2a_4 \sin\left[\frac{2r_0\omega_w}{c} + \frac{2v\omega_w}{c}t + \frac{v\omega_w T_p}{c}\right] \cdot$$
$$\cdot \sin\frac{v\omega_w T_p}{c}. \qquad (2.5.10)$$

Let us note that the quantity $\frac{v\omega_w}{\pi c} = \frac{2v}{c} f_w = f_D$ is the Doppler

frequency for the case of signal reception after reflection by a moving target (see note on Page 82).

Thus, eq. 2.5.10 may be finally written in the form:

$$\Delta u = -\,\mathrm{const}\cdot\sin\left[2\pi f_D\left(t+\frac{T_p}{2}\right)+\varphi_0\right]\cdot\sin(\pi f_D T_p). \qquad (2.5.11)$$

where

$$\varphi_0 = \frac{2r_0\omega_{10}}{c}.$$

In the case of uniform motion of the object, the output of the compensating system will show a series of pulses, modulated in amplitude (Fig. 2.20a), and the modulation frequency is equal to the Doppler frequency defined by eq. 2.5.1.

It should be mentioned that in the literature one often sees explanations of the operation principles of MTI systems, based on the Doppler effect. In practice, the real motion of the target can be taken as uniform, if a short enough time period is considered. However, in discussing the basic characteristics of MTI systems, an interpretation based on the Doppler effect may sometimes lead to paradoxical reasoning because of the pulse character of the signal. This was noticed by Bachmann [2.37], who gave examples of such theoretically possible target motions, which give rise to reflected pulses that will not differ in frequency from emitted signals (and there will be no Doppler effect), but which a MTI system can detect as belonging to a moving object. He also gave examples of motions in which the reflected pulses differ in frequency from those emitted by the Doppler frequency, and still a MTI station reacts as if the target were stationary, i.e., the reflection will be reduced[1]. In

[1] This should not be confused with the so-called "blind" velocities discussed below.

general, it is more useful to apply the approach described above, i.e., consideration of phase relationships.

Let us discuss eq. 2.5.11 introduced above, which describes the output signal of the compensating system. Because of the action of the two-part rectifier [e.g. 2.20], the input signal on the indicator has the form:

$$u_p \doteq \left| \text{const} \cdot \sin\left[2\pi f_D\left(t + \frac{T_p}{2}\right) + \varphi_0\right] \cdot \sin(\pi f_D T_p) \right|. \qquad (2.5.12)$$

As we see, the pulse series reaching the indicator pulsates in time with a frequency corresponding to the /37
Doppler frequency f_D (this is indicated by the first part of the product - $\sin\left[2\pi f_D\left(t + \frac{T_p}{2} + \varphi_0\right)\right]$.

The maximum amplitude of the pulse series depends on the Doppler requency and on repetition period (one should note the second part of the product $\sin \pi f_D T_p$).

It is obvious then, that the MTI station differs from a conventional station in that the visibility of the reflection depends on the radial velocity of the object, among other things.

As has been mentioned above, the maximum amplitutde of the pulse series will be proportional to $\sin(\pi\ f_D T_p)$. A graph of this function is shown in Fig. 2.21. It can be seen that for some velocities the pulse amplitude equals zero. These are the velocities for which the Doppler frequency is equal to an integral multiple of the repetition frequency. It is easy to see that for such Doppler frequencies the consecutive visual pulses at the receiver output have the same amplitudes. Such an object therefore gives stationary clutter which is reduced by the MTI system similar to a non-

moving object.

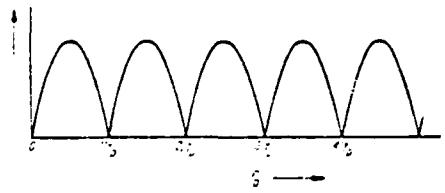

Fig. 2.21. Amplitude of a reflection pulse series at the output of MTI system, as a function of Doppler frequency of the reflection.

This effect may be justified in another , more direct way, using an example. Let us assume that an object moves in such a way that it travels a distance exactly equal to $\frac{\lambda}{2}$ between consecutive pulses. Because the transmission is two-way in radar, the difference in the phases of signals reflected during consecutive impulses will be 360°. As a result we will obtain a reflected vibration indistiguishable from that of a nonmoving object, and such a reflection will be completely reduced. The radial frequency which will cause a signal derived from a moving object to be reduced is called "blind velocity". In agreement with the above remarks, it will be:

$$v_{bl} = n \cdot \frac{\lambda}{2T_p} = n \cdot \frac{\lambda f_p}{2}, \qquad (2.5.13)$$

where n = 1,2,3 ...

The blind velocities may be determined using a nomogram for Doppler frequencies, namely by finding the velocities which correspond to the Doppler frequencies equal to integral multiples of the repetition frequency. /38

The notion of a "blind velocity" obviously makes sense only for reflections with a distinct Doppler component. For objects with strong amplitude fluctuations or random phase fluctuations (cf. consideration of the properties of signals

reflected by objects, in Chapter 5), the effect of blind frequencies is weaker [2.38], but in many practical cases it lowers the sensitivity.

In order to avoid this effect, an alternating repetition frequency[1] is used most often, but this requires a more complicated apparatus (see Chapter 10).

For good functioning of a coherent pulse device, high stability of generation must also be maintained. Figure 2.22 shows a block diagram of a coherent pulse station which assures a high stability of operation[2]. This system is used in the /39 most advanced devices. Previously, when appropriate microwave pulse high power amplifiers were not available, the most wide-spread practical system was one with a coherent oscillator, whose block diagram is shown in Fig. 2.23. This system can use a self-induction transmitter, which is induced from pulse to pulse with a random phase, e.g., magnetron[3]. As the reference vibration one uses the vibration given by the coherent oscillator, which is phased each time by the transmitter pulse, and thus "remembers" the phase of the scanning signal. Otherwise, the principle of operation of this system is identical to the previous one (2.13)

---

[1] This method was proposed by the author, among others, and used in the area control station "Avia" at the Central Airport Warsaw-Okecie (2.39).

[2] The Doppler frequency oscillator G_D allows the compensation of uniform radial object motion; this is important when interfering objects are carried by the wind (this part of the diagram is therefore called the wind compensation system), or when the station itself is in motion.

[3] The requirement of frequency stability during and between pulses is still in effect.

We should mention briefly the so-called autocoherent operation of MTI devices. Such systems do not use the phase of the scanning signal as a reference by the phase of the passive interference itself [2.13]. The reflections from stationary objects play here the role of a coherent /40 oscillator.

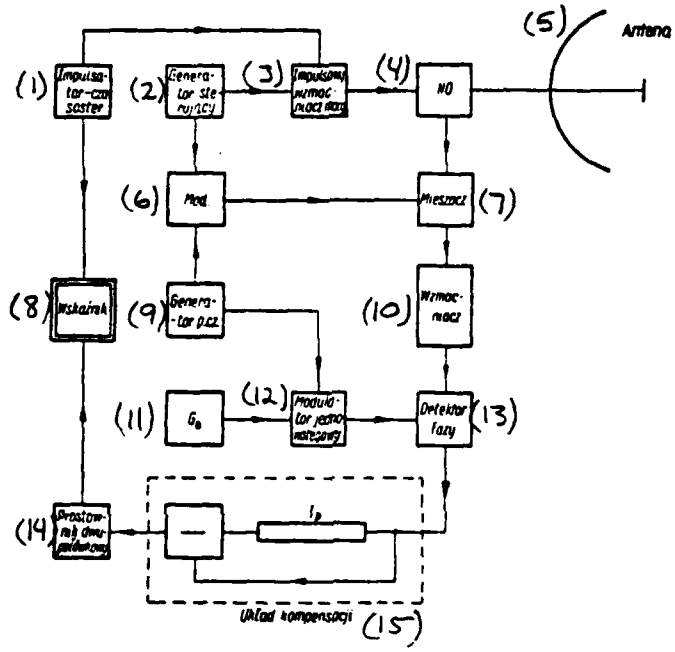

Fig. 2.22. A block diagram of a coherent pulse radar with externally induced transmitter. 1. pulse-time; 2. pilot oscillator; 3. pulse power amplifier; 4. NO; 5. antenna; 6. modulator; 7. mixer; 8. screen; 9. high frequency oscillator; 10. intensifier; 11. G_D; 12. single-band modulator; 13. phase detector; 14. two-part rectifier; 15. compensation system.

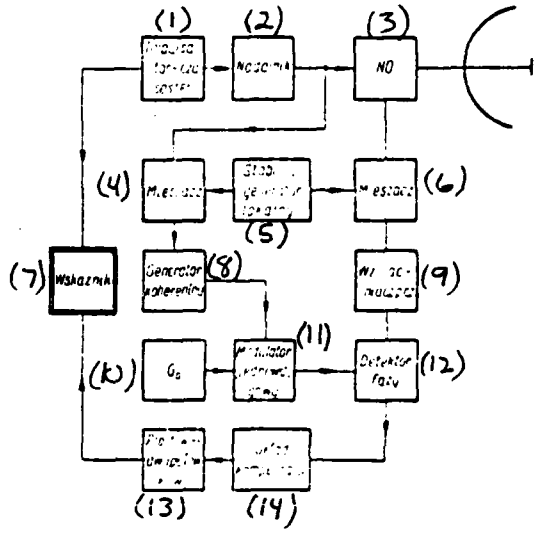

Fig. 2.23. A block diagram of a coherent pulse radar with a self-inducing transmitter and a coherent oscillator. 1. pulse; 2. transmitter; 2. NO; 4. mixer; 5. stable, local oscillator; 6. mixer; 7. indicator; 8. coherent oscillator; 9. amplifier; 10. G_D; 11. single-band modulator; 12. phase detector; 13. full-wave rectifier; 14. compensation circuit.

The station therefore will not have COHO, hence, the (somewhat inaccurate) name for the method. The refelctions from moving objects interfere with stationary clutter and result in a reflection which fluctuates with respect in amplitude between pulses at the position of the moving object. Thus it is sufficient to introduce, after the amplitude detector, a compensating system identical to the one described previously, in order to reduce stationary clutter. The autocoherent system has important advantages in the case when the radar station or the interfering objects are in motion, since it assures automatic compensation of Doppler frequencies for the interference. Its disadvantage is that in areas where there is no passive interference, even the objects to be detected are invisible. This may be circumvented by using a receiving system which uses conventional methods (i. e., with amplitude detection, without reduction of stationary clutter) in areas where passive interference is absent. However, if the intensity of interference exceeds some defined level (within a time interval appropriately longer than the duration of the

refected pulse from a point object), autmatic switching of the receiver to the autocoherent system MTI will occur[1]. Other systems have also been devised, intended to combine the advantages of the coherent and autocoherent systems; not all of them are, however, evident [2.40].

It should be noted that in order to improve the detectability of signals against the background of interference, so-called quadratic reception (described in detail in Chapter 6) may be applied. But this requires, among other things, a doubling of the filtering systems for the signals (compensating system), which causes serious technical problems. Therefore this complication is often avoided in actual radar stations.

The manner of operation of a coherent pulse station described above presents the effects in a simplified fashion. In reality, "stationary clutter" fluctuates considerably, and is modulated because of the movement of the antenna in the course of space scanning; both of these factors strongly influence and lower the effectiveness of object detection against a background of passive interference [2.13; 2.16; 2.41]. Because of this it is necessary to optimize the system taking into account the properties of the signals and the interference using statistical reception methods. This problem is considered in Part II of the present volume.

The coherent pulse method of stationary clutter reduction is one of the most effective methods used to detect objects against a background of stationary clutter.

Fig. 2.24 represents photographs of the screen P of an area control radar station of type S 264 (Marconi Company)[2], which has a high efficiency of stationary clutter reduction

---

[1] In English literature so-called clutter switching [2.45].

[2] This device is described in the next chapter.

using the coherent pulse method. This method is also one of the most effective means of combating man-made passive interference [2.30; 2.42-2.44]. /42

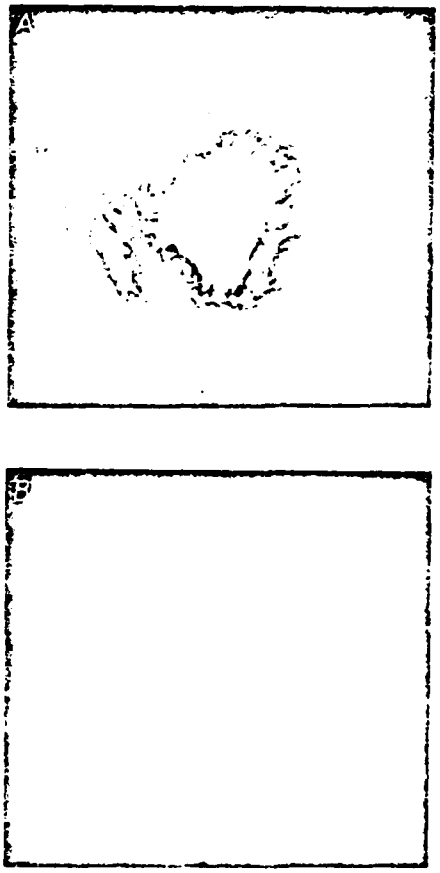

/41

Fig. 2.24. Operation of the MTI system in S 264 type station of the Marconi Company. A - photograph of the screen using the amplitude method; B - photograph of the acreen using MTI systems.

For these reasons this colume considers mainly the pulse coherent system of stationary clutter reduction, called in abbreviation MTI, In particular, the technical aspects of the MTI system are considered in detail in volume II.

REFERENCES

1.1. Kroszczynski, J. :Application of radar in aviation communication

1.2. Wildi, M. Suppression of fixed signals in radar. Radar Bull, SEV 1954 No. 24

1.3. Hoffmann-Heyden. Radio measurement units of the German anti aircraft artillery. Dortmund 1955

2.1 Van Voorhis, S.N. Microwave Receivers. New York,1948

2.2. Lawson, J.L., Uhlenbeck, G.E. Threshold Signals. New York, 1950

2.3. Schrader, W,M, Antenna Considerations for Surveillance Radar Systems. Technical Papers, Seventh Annual East Coast Converence on Aeronautical and Navigational Electronics, 1960.

2.4. Milosevic, L. French solution for the area control radar. (in "Navigation Systems for Aircraft and Space Vehicles, T.G. Thorne, Editor, Pergamon Press, 1962- AGARDograph 55).

2.5. Schrader, W.M. Reducing Clutter in Air Route Surveillance Radar. Electronics, Jan. 26, 1962.

2.6. Silver, S. Microwave Antenna Theory and Design. New York 1949.

2.7. Kroszczyński, J. Applications of radar in communications aeronautics. Przeglad Telekomunikacyjny, No. 7, 1958.

2.8. The CSF radar equipment of the area control center of Orly. L'Electronique, No. 161, 1958.

2.9. Cliquot, R. The band L radars of "type Orly". L'Onde Electrique, May 1961.

2.10. Decca Air Surveillance Radar DASR-1 (Company catalogue).

2.11. Patrick, A.M. (Primary Radar for Flight Control), 1961, Nr. 6

2.12. Gérardin, L. Radar, Navigation and Automation. AGARDograph 55 (see ref. 2.4).

2.13. Ridenour, L.N. Radar Systems Engineering. New York, 1947.

2.14. Offut, W.B. A review of Circular Polarization as a Means of Precipitation Clutter Suppression. Proc. Natl. Electronics Conf., 1955.

2.15. White, W.D. Circular Polarization Cuts Rain Clutter. Electronics, March 1957.

2.16. Skolnik, M.I. Introduction to Radar Systems. New York, 1962.

2.17. Decca Type 424 Mark II Airfield Control Radar (Company project).

2.18. 50cm-A new Concept in Airfield Control Radar (Marconi Company prospectus).

2.19. Povejsil, D.J., Raven, R.S., Waterman, P. Airborne Radar. New York, 1961

2.20. Seifrin, K. S., Kokowin, N.S. Vliianiie osadkov na radiolokatsiinii kontrast. Radiotechnika No. 9, 1959.

2.21. Zelmanowicz, I.L. Yarkostnaia razlicnimost signalov na fone pomeh. Radiotechnika No. 8, 1961

2.22. Croney, J. Clutter on Radar Displays. Wireless Engineer, April 1956.

2.23 Garrett, F.W. A 3-cm Airport Control Radar System. The Marconi Review, 1st Quarter 1958

2.24. Video Pulse Discriminating Unit (Prospectus of the Marconi Company)

2.25. Wildi, M. Suppression of Constant Signals in Radar. Bull. SEV, No. 24, 1954.

2.26. Recent Raytheon Achievement in Radar. Electronics (Engineering issue), Nov. 21, 1958, p. 165.

2.27. Crost, M.E. A Motion - Enhancement Display by Time-Compression IRE Nat. Conv. Record, Part 5, 1962.

2.28. Solomon, K. A double Delay and Subtraction Airborne Clutter Canceller. Proc. Conf. on Military Electronics, 1958.

2.29. Bakulew, P.A. Radiolokatsiinile metodi selektsii dvizhushchihsiia tselei. Moscow, 1958.

2.30. Holahan, J. Tools and Techniques of Electronic Warfare. Space/Aeronautics, April 1960.

2.31. Vinnickij, A. S. Ocherk Osnov radiolokatsee pri neprerivnom izlouchenii radiovoln. Moscow, 1961.

2.32. Sargent, R.S. Moving Target Detection by Pulse-Doppler Radar Electronics, September 1954.

2.33. White, A.S. Application of Signal Corps Radar to Combat Surveillance. IRE Trans. Vol. MIL-4, Oct. 1960

2.34. Goetz, L.P., Algright, I.D. Airborne Pulse-Doppler Radar. IRE Trans. Vol. MIL-5, April 1961.

2.35. Gillespie, N.R., Higley, J.B., Mackimon, N. The Evolution and Application of Coherent Radar Systems. IRE Trans., Vol. MIL-5, April 1961.

2.36. Kroszczynski, J., Grzenkowicz, I. Stationary Clutter Reduction in Radar. Pzheglad Telekomunikacyjny, No. 11 and 12, 1957.

2.37. Bachmann, J.F. MTI in Pulse Radar Systems and the Doppler Myth. Tele-Tech, March 1953.

2.38. Tanter, H. Radar Receiver with Elimination of Fixed-Target Echoes. Electrical Communication, Dece. 1954 (or L'Onde Electrique, Feb. 1953)

2.39 Kroszczanski, J. Radar Station of Aerial Surface Control "AVIA". PIT Works, No. 30, 1960.

2.40 Fowler, C.A., Uzzo, A.P., Ruvin, A.E. Signal Processing Techniques for Surveillance Radar Sets. IRE Trans., Vol. MIL-5, April 1961.

2.41 Kroszczanski, J. Effectiveness of operation of radar stations using stationary clutter reduction. Przeglad Telekomunikacyjny. No. 7, 1958.

2.42. Dax, P.R. ECM vs ECCM in Search Radar. Space/Aeronautics, April 1960.

2.43. Simpson, M. Counter-Countermeasures: Good Design Can Beat the ECM Threat. Space/Aeronautics, April 1960.

2.44. Wolkin, A.N., Janowicz, B.A., Protivoradiolokatsia, Moscow, 1961.

2.45. Electronics Research and Development for Civil Aviation. Materials of the IEE Conference, 2-4th Oct., 1963, London.

2.46. Surveillance Radars for Airports. Télonde, 1962, No. 2

2.47. Carlson, W.D., Cannan, W.W. The High Fences at White Sands, Electronics, Oct. 18, 1963.

2.48. Subnanosecond Radar Shows High Resolutions. Electronics, May 31, 1963.

2.49. Radar Can Pick Out Objects in Clutter. Electronic Design, No. 15, 1963.

2.50. Hubbard, J.V. Digital Automatic Radar Data Extraction Equipment. The Radio and Electronic Engineer, Nov., 1963.

2.51. Cohen, J. Presenting Radar Targets in Color. Electronics, Oct. 18, 1963.

2.52. Doyle, R.J. A Scan Conversion Tube Utilizing Fiber-Optics Photon Transfer. IEEE Trans., ED-10, Nov. 1963.

**

is 265-550 Hz, the width of the beam in azimuth is about 2.1°. /46 A "packet" of echo pulses reflected from a point object thus may consist of about 9 to 19 pulses [3.5]. The effectiveness of stationary clutter reduction of the radar described is illustrated in Fig. 2.24 (also see [3.6]). MTI systems for this station will be described in Part III.

Two devices described above represent different design trends. One of them mainly uses antenna characteristics in elevation for reducing stationary clutter, the second - uses a coherent-pulse system. We will describe a radar which uses both methods simultaneously. This is the ARSR-2 of the Raytheon Company [3.7]. It operates at 23cm wave. The elevation characteristics of the antenna differs from the conventional characteristic of the "cosec^2" type, which leads to an improved target detectability against field reflections and adjustment of the influence of STC (cf. Chapter 2.2, Fig. 2.3). The antenna can operate with linear or circular polarization. The station also uses stationary clutter reduction by the coherent-pulse system.

**
PAGES 44-45 MISSING FROM ORIGINAL

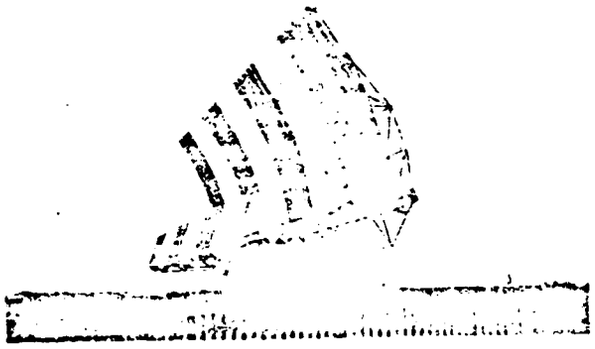

Fig. 3.2. The antenna of the type S 264 radar station of the Marconi Company.

For the final stage in the transmitter, a high power amplitron intensifier has been used. The radar operates with a triple alternating repetition frequency and with a triple compensation system with feedback[1]. Figure 3.3 shows the sequential effect of some systems on the visibility on the screen, under conditions when echoes from both meteorological and field objects are present [3.7]. /47

The antenna of the ARSR-2 radar revolves at 5 RPM, the average repetition frequency is 360 Hz, the width of the beam in azimuth about 1.2°; a "packet" of pulses of the entire echo reflected from a single target thus contains about 14 pulses [3.8]. The MTI systems of this station will be described in somewhat greater detail in vol. II.

A similar approach has been also utilized in the CR-3 station of the CSF Company, which also operates at 23cm; this station differs from the ARSR-2 radar mainly in that it

---

[1] The usefulness of such a system will be clarified in Chapters 7, 8 and 10.

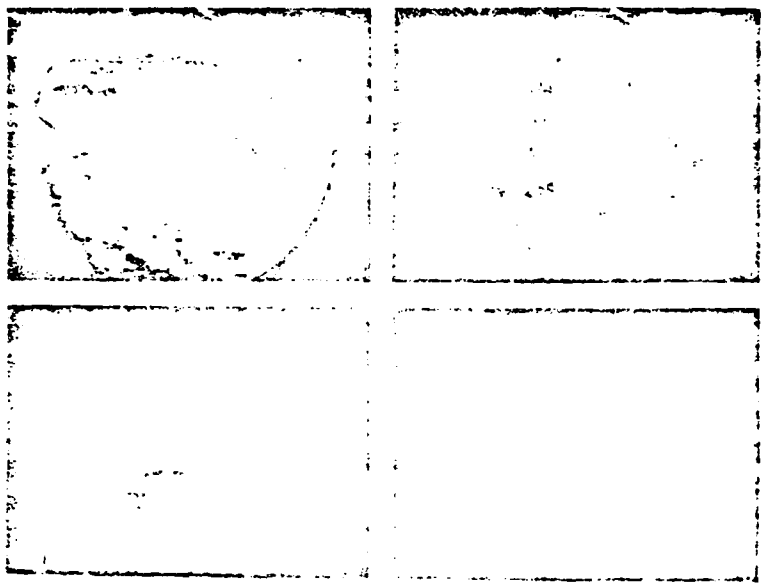

Fig. 3.3 Influence of some counter-interference systems on the visibility on the screen of a ARSR-2 radar station type of the Raytheon Company: A-amplitude operation, severe meteorological conditions; B-circular polarization, same conditions; C-circular polarization and MTI, same conditions; D-circular polarization, MTI and STC, same conditions.

operates with a spectrum of frequencies (diversity) and utilizes an MTI system with double subtraction and modulation of the frequency of pulse repetition. This is possible because memory tubes are used (3.9). The technical solution of MTI systems of this station will also be discussed in part III (volume II).

Over the last few years, so-called "three-dimensional" /49
(3D) radars have found more widespread application. They simultaneously determine the azimuth, distance and altitude of the targets. As mentioned in Chapter 2, in some solutions of such devices the reduction of stationary clutter caused by field objects is made easier because of the high resolution of the antenna system in elevation. We will describe briefly the means of reducing stationary clutter used in one of the newest stations of area control of the AEI Company, type 4502. This

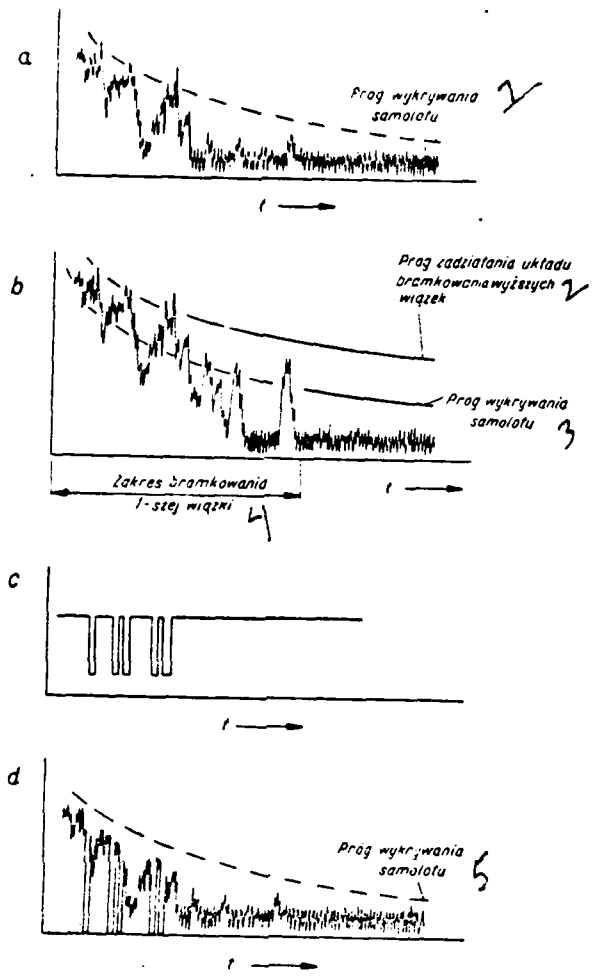

Fig. 3.4 Stationary clutter reduction in lateral lobes of the upper beam of multiple-beam radar: a. visual signal at the output of the receiver of one of the upper beams, b. visual signal at the output of the receiver of the lowest beam, c. gating signal, d. visual signal at the output of the receiver of one of the upper beams (compare with a), after stationary clutter reduction from lateral lobes. 1. threshold of aircraft detection, 2. threshold of operation of the gating system for upper beams, 3. threshold of aircraft detection, 4. range of gating for the 1st beam, 5. threshold of aircraft detection.

is a three-dimensional radar operating at 10cm using a multiple-beam system. A total of 12 beams is used, and each of the 7 lower beams has an elevation width equal to 1°. Because strong stationary clutter penetrates into the receivers of the upper beams through lateral elevation lobes, a special

system has been used to reduce the visual signal at the outputs of the receivers of upper beams, if the signal at the output of the receiver of the lowest beam exceeds a defined threshold (Fig. 3.4).

This radar also uses another means of reducing passive interference, namely pulse compression([3.10]; see also Chapter 4.1). Emitted pulses have a length of 5 μS, but by applying linear frequency modulation during the pulse (with a deviation equal to approximately 10MHz) an effective pulse length of about 0.1 μS can be reached. Thus, a reduction of passive interference by about 17dB is achieved (for uniformly distributed passive interference, such as raindrops or snowflakes). In order to further improve the visibility against a background of reflections from rain, this station also utilizes circular polarization [3.11].

Fig. 3.5. Antenna of the multiple beam radar of type 4502 of the AEI Company (3.13).

The antenna of the radar AEI type 4502 rotates at a speed of 12 rpm, the repetition frequency is 300 Hz, the width of the beam in azimuth is about 0.56°; a "packet" of pulses of the

echo reflected from a point object therefore contains about 2-3 pulses (3.12).

The antenna system of the station described here is shown in Fig. 3.5

References:

3.1 Kroszczynski, J. Radar applications in communications aviation. Pzheglad Telekomunikatsiiny, No. 7, 1958.

3.2 Decca Air Surveillance Radar DASR-1 (company catalogue).

3.3 Patrick, A.M. Primary radar in flight control, No. 6, 1961.

3.4 Milosevic, L. French Solution for regional radar con trol. (in a collection edited by T.G. Thorne: Navigation Systems for Aircraft and Space Vehicles, Pergamon Press, 1962 - AGARDograph 55).

3.5 The Long Clear View. Marconi S264 50cm Radars (Company catalogue).

3.6 Eastwood, E. Blakemore, T.R., Witt, B.J. Marconi Coherent MTI Radar on 50 cms. The Marconi Review, IInd Quarter 1956.

3.7 Schrader. W.M. Reducing Clutter in Air Route Surveillance Radar. Electronics, Jan. 26, 1962.

3.8 Schrader, W.M. Antenna Considerations for Surveillance Radar Systems. Technical Papers, 7th Annual East Coast Conf. on Aeronautical and Navigational Electronics, 1960.

3.9 Cliquot, R. Bande L "Type Orly" radars. L Onde Electrique, May, 1961.

3.10. Cook, C.E. Pulse Compression - Key to more Efficient Radar Transmission, PIRE, March 1960.

3.11. McQueen, J.G., Johnstone, R.M. Stacked Beam Radar Techniques for Air Traffic Surveillance. Electronics Research and Development for Civil Aviation. Materials of IEEE Conf., 2-4th Oct. 1963, London.

3.12. Civil Radar Type 4502. Associated Electrical Industries Ltd. (Company catalogue).

3.13. Interavia, No. 11, 1963.

II. Outline of the theory of signal detection systems /51
operating against a background of correlated interference.

4. Methods of radiolocation systems optimization.

The problem of optimization of the detection process is especially complicated in radar applications because of the various requirements which the radar devices must fulfill simultaneously. The choice of a particular system depends on the requirements on range, resolution, accuracy, quantity of objects detected simultaneously, rate of data gathering, detectability against the background of correlated interference, etc. Reaching an acceptable compromise to satisfy various, often opposing requirements, is a difficult task.

Two groups of problems may be distinguished in this context: first, the problems of optimization of signal gathering, which boils down to designing the scanning signal. The parameters considered here most often include the requirements with respect to the resolution and accuracy of the measurement of coordinates at closer range, which has to be satisfied at a high signal-to-noise ratio. The second group consists of problems arising at low signal-to-noise ratio. A typical question here is the determination of the detection range and its maximization by optimizing reception. These groups of

problems are of course interrelated, but in practice most often (especially when many different requirements must be fulfilled simultaneously) the scanning signal is determined by the resolution and accuracy requirements at a relatively high signal level compared to the noise. The optimization of reception is then carried out for a determined scanning signal.

We will consider here mainly the problem of signal detectability. Because of the problems mentioned above, we will start by discussing the factors which influence the choice of the scanning signal in terms of object resolution. As will be seen below, on the basis of these considerations one can also reach some conclusions about selection of various signals against a background of correlated interference.

4.1 General discussion of the signal selection problem. /52

Various radar systems take advantage of different kinds of scanning signals and are used in practice, as indicated in the previous chapters. This chapter describes the problems of scanning signals. It is presented heuristically, as an introduction to a more detailed analysis of the problem of signal detection against a background of correlated and noncorrelated interference, which will be considered in the following chapters.

As mentioned above, a very important factor in considering scanning signals is the potential resolving power (resolution). This problem will be discussed first with the assumption that the noise is not correlated. In the case of determined signals, the optimal receiver is then a system which calculates inverse correlation function of the received and (appropriately delayed) scanning signals [4.1]. At a high signal-to-noise

ratio the influence of the noise may be neglected. The signal at the output of the optimal receiver thus has a form similar to the autocorrelation function of the scanning signal. One may expect that two signals differing by a delay in time (e.g. echoes from two objects situated at different distances from the radar station) will be distinguished, if the difference in their arrival time $\chi(\tau)$ is large enough to cause the value of the signal autocorrelation function χ (0) [4.2]. A similar situation is found in the difference of Doppler frequencies.[1] Because of this, the resolution of a radar device is related to the two-dimensional autocorrelation function of the scanning signal. If the scanning signal is written in the form $\mathrm{Re}\{w(t)\, e^{j\omega_0 t}\}$, , then this function is defined by:

$$\chi(\tau, \Omega) \stackrel{\mathrm{df}}{=} \int_{-\infty}^{\infty} w(t)\; w^*(t+\tau)\, e^{-2\pi j \Omega t}\, dt, \tag{4.1.1}$$

where w*(t) is a function coupled with w(t). Woodward considered the properties of the function

$$\Psi(\tau, \Omega) = |\chi(\tau, \Omega)|^2, \tag{4.1.2}$$

He showed that [4.2]:

$$\int_{-\infty}^{\infty}\int_{-\infty}^{\infty} \Psi(\tau, \Omega)\, d\tau\, d\Omega = (2E)^2 = \mathrm{const}, \tag{4.1.3}$$

where E - the energy of the scanning signal.

[1] A more general case is discussed in ref. [4.3].

Relationship 4.1.3 indicates that, among other things, /53
it is not possible to obtain simultaneously high resolution with respect to distance and velocity[1], because by narrowing down the function ψ in one axis direction, it will be spread out in the other dimension as follows from 4.1.3. Relationship 4.1.3 is sometimes called the "radar uncertainty principle," and the function ψ the ambiguity function[2]. The constraints on the basic operating properties of some radar devices, described in Chapter 2, are a practical consequence of these properties of the ambiguity function.

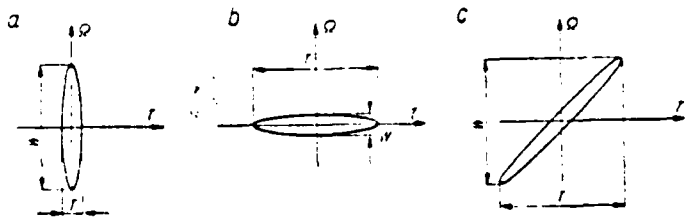

Fig. 4.1. Cross sections of ambiguity functions for a signal in the form of: a-short pulse, b-long pulse, c-long pulse with linear frequency modulation.

The properties of function ψ were considered by Woodward as well as by Siebert [4.4; 4.5] and Lerner [4.6] among others; recently, a certain generalization of this function was presented by Urkowitz, Hauer and Koval [4.3]. As an illustration let us consider the examples shown in Fig. 4.1.

Fig. 4.1a shows a cross section of the ambiguity function (at half-maximum value) for the case of a signal in the form of a short pulse with constant frequency. As we see, for objects (approximately) distant by less than T, the pulse

---

[1] Ω corresponds to the difference in Doppler frequencies, and thus to the difference with respect to the target velocity.
[2] English: ambiguity function.

duration will not be distinguished along the τ axis. On the other hand, objects distant by less than $4\pi/T$ cannot be distinguished along the Ω axis. These relationships are easy to understand on the basis of simple physical interpretations. Fig. 4.1b shows a drawing for a long pulse with constant frequency. As expected, this case gives a poorer resolution in terms of distance, but a better one in terms of frequency. Finally, Fig. 4.1c shows the cross section of the χ function for a long pulse having linear frequency modulation. As we see, in this case it is possible to obtain increased resolution at the cost of spreading out of the signal band. This effect has been utilized in systems with so-called pulse compression [4.7].

Because of the fact that passive interference arises as /54
a result of reflection of scanning signal from objects dispersed in space, one can interpret the problem of useful signal selection against a background of passive interference by analogy, as being related to the resolution problem. Stewart, Westerfield and Prager have analyzed this problem, mainly in the context of applications in sonar ranging, and considered scanning properties for individual pulse signals (4.8; 4.9). These considerations cannot be accepted as a complete discussion of the problem because the influence of noncorrelated interference was omitted, but they lead to an informative presentation of some aspects of the resolution problem in terms of the form of the scanning signal. Therefore below we will discuss in a brief, heuristic manner, the characteristics of detectability of both single- and multiple-pulse signals against a background of passive interference.

As shown by Westerfield, Stewart and Prager (4.9), the signal-to-noise power ratio at the output of an ideally

adjusted filter may be presented in the case under consideration in the form:

$$S_w/N_w = (S_0/N_0)\frac{T\int\limits_{-\infty}^{\infty}\int\limits_{-\infty}^{\infty}E(\tau_0+\tau')\ \Psi(\tau';\Omega')\,d\tau'\,d\Omega'}{\int\limits_{-\infty}^{\infty}\int\limits_{-\infty}^{\infty}E(\tau_0+\tau;\ \Omega_0+\Omega)\ \Psi(\tau;\Omega)\,d\tau\,d\Omega},$$

where

S_0/N_0 - signal-to-noise power ratio at the filter input

$\Psi(\tau;\ \Omega)$	- function defined by eq. 1.3.3;
T	- duration of the scanning pulse;
$E(\tau_0+\tau;\ \Omega_0+\Omega)$	- distribution of the average reflection energy, caused by passive interference, as a function of variables τ and Ω (which correspond to echo delay and Doppler frequency):
$E(\tau_0+\tau)\ \Delta\tau$	- average energy of reflections caused by passive objects located between distances $\frac{c\tau}{2}$ and $\frac{c(\tau+\Delta\tau)}{2}$;
$E(\tau_0+\tau;\ \Omega_0+\Omega)\ \Delta\tau\ \Delta\Omega$	- average energy of reflections caused by these objects, contained within the said layer, whose Doppler frequencies are within the interval between Ω and $\Omega+\Delta\Omega$.

The output ratio of the signal to noise is greatest when the overlap of functions E and Ψ, in the τ, Ω plane is smallest, because of the expressions in the denominator of eq. 4.1.4. This is shown graphically in Fig. 4.2. Fig. /55
4.3 shows the cross sections of the ambiguity function at a defined level for different types of scanning signals: D-for a long pulse; K-for a short pulse; FM-for a long pulse with frequency modulation. Other symbols in the figure: T-effective pulse duration; W-effective width of pulse band. The

shaded area in the same figure represents the cross section of function $E(\tau_0 - \tau; \Omega_0 - \Omega)$ for τ_0, Ω_0 corresponding to coordinates of point A [4.8].

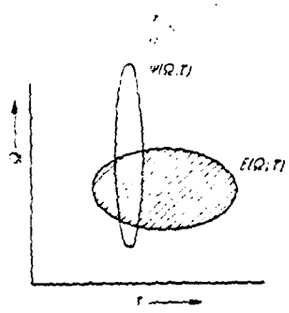

Fig. 4.2. Graph illustrating relation 4.1.4

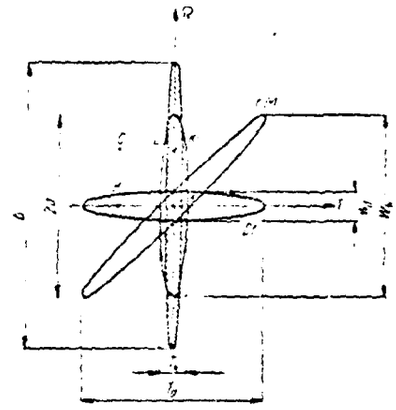

Fig.4.3. Pulse selection at correlated, wide-band interference.

For the case shown in Fig. 4.3 the effective Doppler width of the passive interference band, b, is larger than the resolution in frequency $1/T_d$, attainable when a long pulse is used; whereas the effective time, a, is smaller than the resolution in time (which corresponds to resolution in distance) $1/W_k$, attainable when a short pulse is used. Fig. 4.3 leads to the conclusion that in order to cover the echoes originating from targets B and C, the best pulses are short ones (K) because they allow to distinguish easily the objects beyond the area of interference. The same is true for a pulse with frequency modulation (FM) with a band width identical to that of pulse K. However, if the maximum value of the Doppler frequency for detected targets does not exceed $\pm d$, then the targets situated at the same distance as target A will not be selected (cf. point D). They can only be detected if their reflections are sufficiently large compared with the passive interference. Conclusions concerning the signal-to-noise ratio for various /56

signals may be reached on the basis of a comparison of the cross section area of the interference energy distribution (shaded area in the figure), which is encompassed by the cross-section of ambiguity function [4.8]. In Fig. 4.3 the smallest part of the shaded area is encompassed, in this case the graphs of the long impulse (D) and the pulse with frequency modulation (FM). Thus in order to detect targets situated within the area of passive interference, having a distribution of the type described above, long pulses would be the best. This can be also interpreted in the sense that for distributions with a very long axis b, the character of the interference begins to approach more and more that of white noise, and in this case it is well known that it is advantageous to use long pulses and narrow bands for energy reasons. A mathematical treatment of the signal-to-noise ratio problem using the ambiguity function as outlined above is presented in the cited work of Westerfield, Prager and Stewart [4.9].

Fig. 4.4 represents a situation which occurs with passive interference of a different distribution. The case presented here is typical for radar because passive interference usually extends over large areas, although its fluctuation is relatively narrow-band. For moving target detection it is best then to apply pulses sufficiently long so that for objects with high enough Doppler frequencies (which in this case represent most targets) make it possible to obtain the minimum overlap of functions E and Ψ (cf. Fig. 4.2). This indicates the usefulness of applying Doppler radars (operating in continuous wave) or pulse-Doppler (with long pulse), in this case, which allow target selection thanks to their high resolution in frequency. However, if it is impossible to apply pulses sufficiently long because of requirements with respect to resolving power, then, as shown in Fig. 4.4, the scanning pulse should be relatively short, or an FM pulse with an appropriate

bandwidth should be used. This then gives a relatively small overlap area of functions E and Ψ (although usually larger than in the case of long pulses and high Doppler frequencies, when the functions are "spread out"). This problem is discussed in more detail in refs. [4.9, 4.28].

The advantages of FM signals, resulting, among other things, from the above considerations, have been utilized in radar systems with "pulse compression" mentioned above ([4.7,] (see also Chapter 3).

Up to now we were concerned scanning with individual pulses (or scanning without correlation between pulses). Such a method (as indicated in Chapter 2) is not effective for systems with a low filling coefficient. This is a result of the interrelationships between the values of parameters involved. In order to select an echo pulse of length T_d against a background of passive interference with a Doppler /57 band width b using differences in frequency, the echo signal must have (as shown in Fig. 4.4) a Doppler frequency at least of the order of $(b + 1/T_d)$. In radar, the width of the fluctuation spectra of passive interference are of the order of tens of Hz (cf. Chapter 5), while the Doppler frequencies encountered in practice are usually within the range of sound frequencies. As can be easily noted, in order to satisfy the said condition of selection, the scanning pulses would have to have a duration time of the order of milli-seconds. Pulses of such length may be used only in some pulse Doppler devices. However, scanning pulses of radars operating on a coherent-pulse system usually do not exceed 6μs[1] because of the resolution and accuracy of the measurement. Still, several to several tens of echoes from the target are obtained during the time corresponding to the illumination of a single target

[1]Operating without pulse compression

by this type of radar in the course of space scanning (i.e. during the time corresponding to the displacement of antenna characteristic in space by a bundle width)[2].

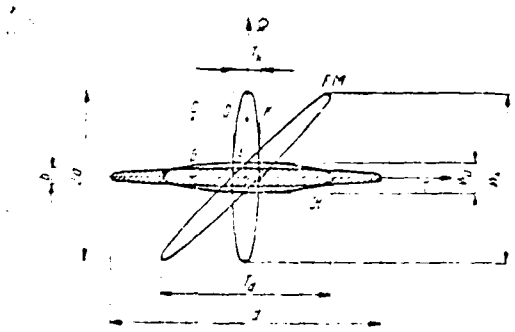

Fig. 4.4. Pulse selection with correlated narrow-band interference.

This fact is used in the pulse-coherent method to obtain signal selection against a background of passive interference; the principle of operation of a similar system has been described briefly from a technical standpoint in Chapter 2, and below we will present an outline of the analysis of this problem using the Woodward ambiguity function, in a manner similar to that presented above for individual scanning pulses.

Figure 4.5b represents a graph of the cross section of the ambiguity function of a modulated series of scanning pulses, i.e. of a pulse "packet" [Fig. 4.5a], which occurs during space scanning in the manner described above (also see Chapter 5). Similarly to Figs. 4.3 and 4.4, the area representing the typical for this case distribution of energy reflected from passive interference has been shaded. As can be seen, the ambiguity function of a pulse "packet" assumes a rather complicated form, which, however, has some specific properties

[2] A typical example for a warning radar: with beam width 1°, repetition frequency 36 Hz and antenna revolution velocity 6 rpm, 10 pulses fall within the beam width; i.e. a single target gives 10 successive echoes.

which facilitate the selection of a signal from passive interference.

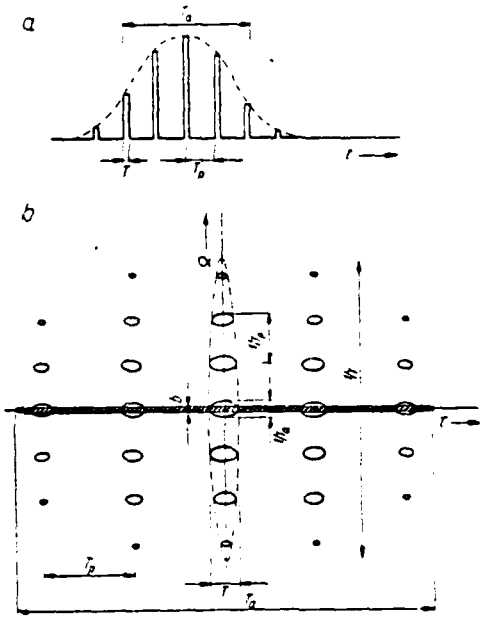

Fig. 4.5. a - envelope of a pulse "packet", b - selection of a pulse "packet" in the presence of correlated narrow-band interference.

The width of individual elliptical cross-sections of the ambiguity function in the domain of frequency is related in this case to the duration time of the entire "packet", in other words - to the number of pulses falling onto the beam width. Since the effective width of an individual cross-section in the frequency domain is of the order of $1/T_a$, where T_a-effective duration time of a pulse "packet" (time during which the antenna revolves by an angle equal to the beam width), in order to select the signal it is sufficient that it have a Doppler frequency different from nT_p (where /59
$n=0,1,2...$, and T_p-repetition frequency) by more than about $b + 1/T_a$). In practice, time T_a is of the order of milliseconds. With narrow-band interference, high repetition of frequencies and long pulse "packets" there exists the possibility of effective selection of most echo signals against a background of passive interference. These conclusions are fully confirmed in practice, where to obtain good detectabi-

lity against a background of passive interference, repetition frequencies as high as possible are used, and the station parameters are chosen such that the highest possible number of pulses falling onto the beam width is obtained.

It should be mentioned that the specific form of the ambiguity function represented in Fig. 4.5, which has many maxima, leads to the possibility of obtaining ambiguous measurements of both the distance and the velocity of the target [4.32].

Concerning the unambiguous measurement of distance, this problem is well known in pulse radars. Ambiguity is avoided by assuming such a repetition frequency that the pulse repetition period is larger than the maximal possible time of e no return (defined by the range of a given device). When the only goal is the detection of object against interference background (in warning devices, serving in air traffic control and direction, guiding, etc.), ambiguity in the coordinate direction is not important, because in this case the velocity of the object is not measured. In some pulse-coherent devices, where an accurate velocity determination is necessary (automatic devices tracking rockets) the ambiguity is eliminated by introducing a two-stage measurement; approximate - on the basis of the change in echo envelope delay (i.e. delay of visual signal) and accurate - using the Doppler effect.

In summary, on the basis of an analysis of the ambiguity function it is possible to reach qualitative conclusions about the resistance of various scanning methods to passive interference, and this analysis provides better insight into the properties of various tracking systems known from practice, and allows to reach conclusions concerning the choice of parameters for a device used for specific purpose.

Obviously, this suggests the future possibility of defining the optimal form of the scanning signal which maximizes detectability against a background of correlated interference for defined conditions for resolving power distance, time of target observation and signal energy. However, this problem is very difficult and so far has been solved only for some simpler cases (see Chapter 4.2).

The considerations contained in this chapter lead to a confirmation of the potential possibility of target detection in the presence of passive interference by using the pulse-coherent system, widely used in radar.

This system provides a high resolution and accuracy of the distance measurement and imaging of a large number of /60 targets. The analysis of the ambiguity function of coherent pulse "packet" indicates, among other things, the necessity of assuring a high enough number of pulses falling onto bundle width in order to obtain good detectability in the presence of stationary clutter. In many important practical situations this is difficult to achieve because of conflicts with the requirements often set for radar devices in terms of the range and rapidity of measurements. The problem of receiving system optimization then becomes even more important.

4.2 Optimization of signal detection

As suggested by the previous considerations, in detection of objects by radar, the finite signal-resolving power of the system must be taken into account. Thus, if the system's resolving power with respect to one of the i parameters characterizing the object equals ξ_i, and the range of values that this parameter may assume is denoted Ξ_i, then, obviously, the maximum number of objects distinguishable on the basis of

this parameter will be $N_i = \Xi_i/\xi_i$. . The total number of objects that can be distinguished (imaged) by a given radar device, therefore does not exceed the number:

$$N = \prod_{i=1}^{I} (\Xi_i/\xi_i),$$

where I - number of all statistically independent parameters of the object, measured by the device.

As an illustration let us consider the example of a radar device serving in control of aerial situation; the resolving power of this device in terms of distance will be ξ_r and in azimuth - ξ_a. With a determined direction of scanning the station cannot of course give imaging of more than $N_r = \frac{R_{max}}{\xi_r}$ objects, where R_{max} - the maximum range of detection.

On the other hand, with a determined distance it is impossible then to obtain imaging of more than $N_a = \frac{2\pi}{\xi_a}$, objects. Stations of this type do not measure the height (elevation angle) of the object or its velocity. Therefore the maximum number of objects that may give unambiguous imaging will be $N = N_r N_a = \frac{2\pi R_{max}}{\xi_r \xi_a}$. .

It should be mentioned with respect to the example above that there is the problem of object displacement. For a typical revolving station the velocity of scanning in azimuth is approximately 5 - 10 rev/min, the width of antenna /61 is 1-2°, and the resolving power in terms of distance is 150-750 m (which corresponds to a pulse length of 1-5 μ S). The time of illumination of a single object equals, for the parameters given, about 0.017 - 0.067 sec. During this time an airplane moving at the velocity of sound will be displaced in space by about 6 - 24 m; thus, the object displacement during the time of its illumination may be ignored, since it is much

smaller than the resolving power in terms of distance.

The problem of object detection by radar methods, considered in the present work, may be therefore reduced to the problem of creating a quantified imaging of the position of these objects.

In this case we have a possibility of reducing the detection problem to a system of N independent decisions which determine if in each of the N segments of the quantified image we should accept the presence or absence of objects; in what follows, it will thus be sufficient to consider the problem of binary decisions with a defined position of the object.

A method based on the theory of statistical decision functions of Wald [4.10][1] is considered the most advanced. This method has found widespread application in problems of signal detection; the optimization criterion is the achievement of minimal loss while making the decision with respect to signal detection (see also: [4.11; 4.1; 4.12; 4.13]).

Definition of decision, loss, risk and formulation of the optimization problem

In every transmitting-receiving system one has to conclude, on the basis of the signal received, what kind of information has been transmitted by the source of information.[2] Because of unavoidable effect of interference this deduction cannot be carried out with absolute certainty. To stress the somewhat

[1] A brief history of the theory of signal detection and the characteristics of its various directions may be found, e.g., in the preface of L.S. Gutkin, contained in a collection of articles: "Priiom signalov pri nalichii shuma", Moscow 1960.

[2] A classification of the kinds of information and a more detailed discussion of their properties can be found in the work of Seidler [4.1].

arbitrary nature of reaching a conclusion in this case, such a conclusion is referred to as decision.

Decisions may be of various types [4.1]. In the present work we will consider a decision the information belonging to the information set X, and denoting it x^*; according to the definition $x^* \in X$.

The principle, according to which every signal received y belonging to the set Y corresponds to a decision from the decision set, is called the decision rule. /62

Since we are dealing with a large variety of decision rules, a basic problem emerges of defining criteria which will allow to accept one rule as being better than another, and in particular will allow to select the best rule from amongst all the possible ones.

Let us note that information is transmitted from the source of information to the destination to cause certain actions by the user of the communications system. If these actions are carried out assuming that information x^* had been transmitted, while in fact information x was transmitted, then the actions will not be the most advantageous, and the user will suffer a loss because of bad operation of the communications system, and this loss may be measured quantitatively. Therefore in principle the user of the communications system should give to the system designer in advance a function of two variables $L(x, x^*)$ which is the loss generated when action is taken as if information x^* had been transmitted, while in fact it was information x that was transmitted. This function will be called, briefly, the loss.

Loss is defined in economic terms and the methods for

determing loss essentially are not part of communications theory. Often, however, the definition of loss is left to the communications system designer and then the choice is made more or less arbitrarily. E.g., for binary information form the set X_2, the loss is defined by four numbers:

$$\begin{matrix} L(x_1, x_1) & L(x_2, x_2) \\ L(x_1, x_2) & L(x_2, x_1) \end{matrix}$$

Information x_1 will be called "lack of alarm" and information x_2 - "alarm".

Number $L(x_1, x_2)$ has the meaning of loss generated in the case when the receiving device gives an alarm signal when it was not in fact transmitted. Therefore it is a loss resulting from a false alarm.

Number $L(x_2, x_1)$ has the meaning of loss resulting from a lack of alarm. Generally one has to assume of course that $L(x_1, x_2) < L(x_2, x_1)$, but one cannot disregard the loss $L(x_1, x_2)$ since false alarms are also to be avoided.

Numbers $L(x_1, x_1)$ and $L(x_2, x_2)$ have the meaning of costs of corrective decisions.

The loss is defined for the decision and for the information in a manner independent of the decision rule. These two notions may be related and lead to an evaluation of the quality of the decision rule. We will consider here one of such possible relations which comes to mind when information and decisions have defined frequencies of occurrence, in other words, if they can be treated as realizations of random variables with defined probability distributions. Then it is natural to assume an average loss to be a measure of the /63 quality of decision rule for all information and all decisions.

Since averaging over decisions is equivalent to averaging over all signals received, this average will be defined by the formula

$$l = \underset{X \times Y}{E}\, L[X, x^*(Y)] = \iint_{X \times Y} L[x, x^*(y)]\, dP_{X \times Y}, \tag{4.2.1}$$

where:

X - random variable or a stochastic process representing informations;

$x^*(y)$ - decision;

Y - random variable or a stochastic process representing signals being received;

E - the averaging operation for all information and signals XxY being received;

$P_{X \times Y}$ - measure of probability in the area XxY of information x and received signals y.

This average will be called the risk.

As an example let us take the case where information, decisions and signals received are one-dimensional and have continuous probability distributions. Then equation 4.2.1 will have the form:

$$l = \int_{-\infty}^{\infty} \int_{-\infty}^{\infty} L[x, x^*(y)]\, p(x, y)\, dx\, dy, \tag{4.2.2}$$

where p(x,y) is the overall probability density for information x and the received signal y ([4.14]; §3.6).

It follows from eq. 4.2.1, and especially from its particular form 4.2.2, that the risk depends on:

1. loss;
2. overall probability distribution for the informations and the signals received;

3. Decision rule.

If the first two functions are given and defined, then the risk depends only on decision rule and the problem of optimization of the decision rule may be formulated as follows:

A decision rule should be found which would entail the minimal risk. Such a rule will be called the optimal rule.

Minimal risk depends on the properties of the signals being transmitted and thus we have to contend with the problem of selecting from a set of signal sets which fulfill certain conditions such a signal set that the risk will be smallest. In other words, this is a problem of optimization of a signal set; problems of this type are the subject of /64 code theory and modulation theory.

The goal of a receiving device is the practical realization of the decision rule. Thus the receiving device is a mathematical machine (computer) carrying out, according to a predetermined rule, decision calculations when a received signal is given.

In many cases of realization of the optimal decision rule, the design difficulties encountered are so serious that practical application of receiving devices making optimal decisions is out of the question. Economic factors related to the cost of realization of the decision rule could be taken into account assuming a linear combination of risk defined by eq. 4.2.1 and of the function describing the cost of realization of the decision rule as an estimate of the quality of the decision rule. The solution to the optimization problem, based on such a criterion is very difficult, and in general practice decision rules are used which are selected in a more or less heuristic manner. Often these rules are such that they allow

one to carry out at least part of the operations related to the calculation of decision using linear quadruples.

Optimal reception according to the method of decision functions.

Using the equation for conditional averages ((4.1.4) Chapter 3.6) we will represent the risk in the form:

$$l = \mathop{E}_{X \times Y} L[X, x^*(Y)] = \mathop{E}_{Y} \left\{ \mathop{E}_{X|y} L[X, x^*(y)] \right\}, \tag{4.2.3}$$

where

$\mathop{E}_{X \times Y}$ - averaging operation for set X Y of information x and received signals y;

$\mathop{E}_{X|y}$ - operation of conditional averaging for set X with a defined received signal y;

$\mathop{E}_{Y}$ - averaging operation for the set of received signals Y.

Let us denote

$$l[x^*(y), y] = \mathop{E}_{X|y} L[X, x^*(y)] \tag{4.2.4}$$

and let us call this quantity the conditional risk for a defined received signal.

In the specific case of binary information

$$l[x^*(y), y] = L[x_1, x^*(y)]\ P(X = x_1 | y) + L[x_2, x^*(y)]\ P(X = x_2 | y), \tag{4.2.5}$$

where $P(X = x_k | y)$ - conditional probability of information x_k k = 1,2 for the defined signal y. /65

In the case when the information is one-dimensional and continuous (forming set X_{C_1}),

$$l[x^*(y),\ y] = \int_{-\infty}^{\infty} L(x, x^*)\ p(x|y)\,dx, \tag{4.2.6}$$

where $p(x|y)$ — - density of conditional probability at point x, for a defined received signal.

From the particular cases (4.2.5) and (4.2.6) it is apparent that when the received signal is defined, the conditional risk depends only on decision x*(y). If we consider various decision rules, the decision is treated as the variable. Let us denote the risk in the form l(x*, y). At a defined received signal it therefore becomes the function (more generally - functional) of the variable $x^* \in X$.

Applying the well known methods of finding function extremes (extremes of functionals) we can find information $x_o^*(y)$ for which the conditional risk for a high received signal is minimal. The information $x_o^*(y)$, treated as a function of the received signal (generally - an operation acting on the received signal) determines the decision rule which minimizes the conditional risk given by eq. (4.2.3). Therefore it is the optimal decision rule.

As mentioned above, decisions have a binary character in the problems considered here. This relates both to detection using simple Doppler systems where the object's distance is not measured, but only its presence is determined, and to detection using pulse-Doppler systems with distance gating, where decisions are made about the presence of a reflected signal within the gate. Also, in a pulse-coherent system with a

small filling coefficient, in spite of simultaneous imaging of many objects, the decision about the existence of an object at a given distance has a binary nature (see also [4.15]). Thus it is only of interest to know whether an object is present at a given distance or not. All other properties of the reflected signal are treated only as passive parameters[1]. This is the reason for considering only binary decisions in the following discussion.

Making the natural assumption that loss caused by a false decision is greater than losses with a correct decision, we will obtain for the function of losses in the binary case:

$$L(x_1, x_2) > L(x_1, x_1),$$
$$L(x_2, x_1) > L(x_2, x_2). \tag{4.2.7}$$

Taking the decision $x^* = x_1$, we will obtain, in accordance with eq.(4.2.5), an average loss with a determined signal y: /66

$$l(y, x^* = x_1) = L(x_1, x_1)\ P(X = x_1 | y) + L(x_2, x_1)\ P(X = x_2 | y), \tag{4.2.8}$$

and, if the decision is $x^* = x_2$, then:

$$l(y, x^* = x_2) = L(x_1, x_2)\ P(X = x_1 | y) + L(x_2, x_2)\ P(X = x_2 | y). \tag{4.2.9}$$

Decision $x^* = x_1$ will be optimal if:

$$l(y, x^* = x_1) \leqslant l(y, x^* = x_2), \tag{4.2.10}$$

[1]Passive parameters are those which determine the shape of the signal, but are not known at the receiving side [4.1].

and this, after substituting relations (4.2.8) and (4.2.9) will give:

$$\frac{P(X = x_2 | y)}{P(X = x_1 | y)} \lessgtr \frac{L(x_1, x_2) - L(x_1, x_1)}{L(x_2, x_1) - L(x_2, x_2)}. \tag{4.2.11}$$

In the case of fulfilment of the opposite inequality the optimal decision will be $x^* = x_2$.

If we introduce the notation:

$$\Lambda = \frac{P(X = x_2 | y)}{P(X = x_1 | y)} \tag{4.2.12}$$

and

$$\Lambda_p = \frac{L(x_1, x_1) - L(x_1, x_2)}{L(x_2, x_2) - L(x_2, x_1)}, \tag{4.2.13}$$

then the optimal decision rule will have the form

$$x_0^*(y) = \begin{cases} x_1, & \text{jeżeli } \Lambda < \Lambda_p, \\ x_2, & \text{jeżeli } \Lambda > \Lambda_p. \end{cases} \tag{4.2.14}$$

The treatment above ascribes a decision to each received signal y, and for each y the conditional risk is minimal. Thus, relationships (4.2.14) represent the solution to the optimization problem.

The probabilities appearing above may be calculated on the basis of the Bayes' equation:

$$P(X = x_k | y) = C \cdot P(X = x_k)\, p(y | X = x_k). \tag{4.2.15}$$

where

$P(X = x_k)$ - a priori probability of signal x_k;

$p(y, X = x_k)$ - conditional probability density of the received signal y for a determined signal x_k;

C - constant which is determined from the normalization condition.

Signals appearing in these applications usually depend on passive parameters, such as e.g., the reflection phase from the object. Passive parameters are treated as random /67 quantities with a defined distribution law. Introducing the optimal decision rule above, we did not make any assumptions about the properties of probabilities. Therefore this rule is optimal both for predetermined signals and for signals dependent on passive parameters. The difference between the two cases consists only of the method of calculation conditional probabilities $P(x_k, y)$.

Let us denote:

ϑ - passive parameter, multidimensional in the general case;

Θ - set of passive parameters;

$p(y, x_k)$ - density of conditional probability of signal y, with the condition that information $X = x_k$ is transmitted;

p_{Θ/x_k} - conditional probability distribution of passive parameter with the condition that information $X = x_k$ is transmitted;

$p\{y, s_k[(\cdot), \vartheta]\}$ - probability density of the signal received with the double condition that information $X = x_k$ is defined and that the passive parameter is defined; these conditions mean that the signal $s_k(t, \vartheta)$ is determined.

It follows from the conditional distribution that ([4.14] Chapter 2.7):

$$p(y|x_k) = \int_{\Omega} p[y|s_k(\cdot), \vartheta]\, dP_{\theta|x_k}. \qquad (4.2.16)$$

As may be seen from these considerations, it is not necessary to operate with the directly received signal y(t) in order to make optimal decisions, but it is sufficient to use quantities $P(X = x_k|y)$. This leads to important design simplifications. Therefore an optimal receiver consists in practice of a device calculating the quantities mentioned above and a device which makes the decision on the basis of these date.

In the following section we will present the application of the principles described to the problem of signal detection in the presence of correlated interference.

Single detection in the presence of correlated interference.

Let us assume that the received signal y(t) is a sum of the signal s(t) and a Gaussian process Z(t), independent of this signal[1].

We assume that signal $s_k(t)$ is related unambiguously to the information x_k (for the case in question - with the presence or absence of the object to be detected). The density of conditional probability $p(y|X = x_k)$ will be obtained immediately because the event whereby the received signal has the

[1] As follows from e.g. Chapter 5, the properties of signals and of interference justify making this assumption.

value y with the condition that information x_K had been transmitted is equivalent to the event $z = y - s_k$. Thus we can write instead of $p(y|X = x_k)$ in this case $p(y|s_k)$, and the probability density $p(y|s_k)$ is defined by a function similar to the one for the process Z(t), but for function $y(t) - s_k(t)$ [4.1].

It is assumed that the average value of the process equals zero:

$$E\{Z(t)\} = 0. \tag{4.2.17}$$

The function of the correlation of the process will be denoted by:

$$R_z(t', t'') = E\{Z(t')\, Z(t'')\}. \tag{4.2.18}$$

We will consider the time interval $\langle t_1, t_2 \rangle$. Let us take into account the random variables $Z[t^{(i)}]$, where $t^{(i)}$ represents the points lying within the interval

$$\langle t_1, t_2 \rangle, \quad i = 1, 2, \ldots n.$$

Making the assumption that the process is Gaussian, the probability density of a multidimensional random variable $Z[t^{(1)}], Z[t^{(2)}], \ldots Z[t^{(n)}]$ at the point $z_1, z_2, \ldots z_n$ is defined by the formula [4.14]:

$$p(z_1, z_2 \ldots z_z) = \frac{|k_{i,j}|^{1/2}}{\sqrt{(2\pi)^n}} \exp\left(-\frac{1}{2} \sum_{i=1}^{n} \sum_{j=1}^{n} k_{i,j} z_i z_j\right). \tag{4.2.19}$$

and the coefficients $k_{i,j}$ are related to the values $R_{i,j} = R_z(t_i, t_j)$ by the matrix equation

$$\|k_{ij}\| \cdot \|R_{ij}\| = \|I\|, \tag{4.2.20}$$

where $\|I\|$ denotes an individual matrix; matrix $\|k_{ij}\|$ is thus the inverse matrix of the matrix $\|R_{ij}\|$ [4.16]. Writing out equation (4.2.20) we obtain:

$$\sum_{j=1}^{n} k_{ij} \cdot R_{j,m} = \begin{cases} 1 & \text{for } i = m, \\ 0 & \text{for } i \neq m. \end{cases} \tag{4.2.21}$$

It can be proven [4.17; 4.18] that with increasing divisions of the interval t_1, t_2 by points $t^{(i)}$ is:

$$\lim_{n \to \infty} \sum_{i=1}^{n} \sum_{j=1}^{n} k_{ij}\, z_i z_j = \int_{t_1}^{t_2}\int_{t_1}^{t_2} K(t', t'')\, z(t')\, z(t'')\, dt'\, dt'', \tag{4.2.22}$$

and function $K(t', t'')$ fulfills the equation which corresponds to (4.2.20), (4.2.21):

$$\int_{t_1}^{t_2} K(t', t'')\, R_z(t'', t''')\, dt'' = \delta(t' - t'''), \tag{4.2.23}$$

where $\delta(t)$ is the Dirac function (see [4.19])[1].

Function $K(t', t'')$ may be interpreted as the nucleus of an integral operator; as follows from eq. (4.2.23), it is an /69 operator opposite to the operator with nucleus $R_z(t'', t''')$. The existence of the opposite operator results from the properties of the correlation function, which is symmetrical and positively determinate [4.20]. Let us introduce the notation:

[1]Consideration of the problems discussed here using matrix methods is presented e.g. in refs. [4.29 and 4.33].

$$\Pi[z(\cdot)] = \int_{t_1}^{t_2}\int_{t_1}^{t_2} z(t')\, z(t'')\, K(t', t'')\, dt'\, dt''. \qquad (4.2.24)$$

By analogy with eq.(4.2.19), the functional

$$p[z(\cdot)] = C_0 e^{-\frac{1}{2}\Pi[z(\cdot)]} \qquad (4.2.25)$$

is treated as the probability density of the process Z(t), calculated for the realization z(t) [4.1; 4.21].

Thus we can write:

$$p(y/s_k) = C_0 \exp\left\{-\frac{1}{2}\Pi[y(\cdot) - s_k(\cdot)]\right\} \qquad (4.2.26)$$

and

$$\Pi[y(\cdot) - s_k(\cdot)] = \int_{t_1}^{t_2}\int_{t_1}^{t_2} [y(t') - s_k(t')]\,[y(t'') - s_k(t'')]\, K(t', t'')\, dt'\, dt''. \qquad (4.2.27)$$

Function K(t', t'') fulfills eq. (4.2.23). Since the correlation function has the property of being symmetrical, $R(t', t'') = R(t'', t')$, and also $K(t', t'') = K(t'', t')$, therefore:

$$\int_{t_1}^{t_2}\int_{t_1}^{t_2} s_k(t')\, y(t'')\, K(t', t'')\, dt'\, dt'' = \int_{t_1}^{t_2}\int_{t_1}^{t_2} s_k(t'')\, y(t')\, K(t', t'')\, dt'\, dt''. \qquad (4.2.28)$$

Denoting

$$s_{fk}(t) = \int_{t_1}^{t_2} K(t', t)\, s_k(t')\, dt', \qquad (4.2.29)$$

eq.(4.2.27) may be represented in the form:

$$\Pi[y(\cdot) - s_k(\cdot)] = \int_{t_1}^{t_2}\int_{t_1}^{t_2} y(t')\, y(t'')\, K(t', t'')\, dt'\, dt'' + 2\int_{t_1}^{t_2} y(t)\, s_{fk}(t)\, dt -$$

$$+ \int_{t_1}^{t_2} s_k(t)\, s_{fk}(t)\, dt. \qquad (4.2.30)$$

After transformations we finally obtain:

/70

$$\ln P(s_k|y) = \ln C + \ln P(s_k) - \frac{1}{2}\int_{t_1}^{t_2} s_k(t)\, s_{fk}(t)\, dt +$$

$$+ \int_{t_1}^{t_2} y(t)\, s_{fk}(t)\, dt. \qquad (4.2.31)$$

The first integral in this formula is proportional to the energy of the signal; therefore the optimal reception algorithm for stationary clutter is defined only by the second integral. Rewriting this integral one can also interpret it as the operation of filtering the received path y(t) by a filter with a pulse response equal to $s_{fk}(t)$ in the interval $\langle t_1, t_2 \rangle$.

$$\int_{t_1}^{t_2} y(t)\, h(t_2 - t)\, dt, \qquad (4.2.32)$$

where

$$h(\tau) = s_{fk}(t_2 - \tau) \quad \text{for} \quad 0 < \tau < t_2 - t_1,$$
$$h(\tau) = 0 \quad \text{for} \quad \tau < 0 \quad \text{or} \quad \tau > t_2 - t_1. \qquad (4.2.33)$$

On the basis of known relationships between the pulse response of the quadruple and its transfer function [4.22] and the properties of the Fourier transform [4.23] it is evident that:

$$F_k(\omega) = \mathcal{F}\{s_{fk}(t)\}^* \cdot e^{j\omega t_2}, \qquad (4.2.34)$$

where $F_k(\omega)$ - transfer function of the optimal filter;
$\mathcal{F}$ - symbol for the Fourier tranform: * - coupled value.

Let us note that $s_{fk}(t)$ can also be obtained directly from the integral equation[1]:

$$\int_{t_1}^{t_2} R(t', t'')\, s_{fk}(t'')\, dt'' = s_k(t'). \qquad (4.2.35)$$

The solution of this equation thus determines simultaneously the algorithm of optimal reception [4.1].

The filter defined by eq. (4.2.32) or (4.2.34)is called <u>fitted filter</u> [4.1; 4.11]. It is easy to see from eqs. (4.2.34) and (4.2.35), in the case of interference in the form of noncorrelated noise, the frequency characteristic of the fitted filter is a function coupled with the signal spectrum.

If the signal is a function of passive parameters, the problem is solved similarly, by introducing appropriate averaging, as shown above (see also [4.1]). We will return to this problem in one of the later chapters. /71

In some cases the signals have a complicated structure, which requires the introduction of many passive parameters in order to obtain an appropriate model representing in adequate approximation the actual signal. However, the increased complications related to the calculation of probability cause the practical usefulness of this method to be rather limited.

It is often possible to treat the signal as a realization of a stochastic process[2]. The receiving device is then optimized assuming that the individual signals transmitted are realizations of a stochastic process with a known correlation

---

[1]This is easy to check by substituting the left side of eq. (4.2.35) into (4.2.29) and using relation (4.2.23)

[2]As will be shown in Ch.5, in many practical cases this approach corresponds to the actual situation in receiving location signals.

function.

This situation corresponds to the following mathematical model. A decision as to the nature of the signal transmitted has to be made on the basis of the signal received $y(t) = z(t) + s_k(t)$, , where $s_k(t)$ is a realization of the process $S_k(t)$, and $z(t)$ - a realization of the Gaussian noise $Z(t)$.

In the binary case the decision depends on the ratio:

$$\frac{P(s_2 \mid y)}{P(s_1 \mid y)};$$

using the equation of Bayes we have

$$\frac{P(s_2 \mid y)}{P(s_1 \mid y)} = \frac{P(s_2)}{P(s_1)} \cdot \frac{p(y \mid s_2)}{p(y \mid s_1)}. \qquad (4.2.36)$$

The ratio of the densities of probabilities appearing in eq. (4.2.36) can be calculated treating (as above) the decisions made on the basis if signal $y(t)$, observed continuously, as the limit case of the decision made on the basis of series of n samples.

It should be noted that if $S_k(t)$ is a Gaussian process, then

$$Y(t) = Z(t) + S_k(t) \qquad (4.2.37)$$

because the sum of Gaussian processes is also a Gaussian process.

Using the formula for a multidimensional Gaussian distribution (4.2.19) it is possible to calculate the logarithm of the

ratio of the probability densities of the samples, and then taking the limit described earlier, it can be shown that [4.24]:

$$\ln \frac{p(y|s_2)}{p(y|s_1)} = C_{1,2} + \int_{t_1}^{t_2}\int_{t_1}^{t_2} K_{1,2}(t', t'')\, y(t')\, y(t'')\, dt'\, dt'', \qquad (4.2.38)$$

where $C_{1,2}$ is a constant which can be expressed by a function called the Fredholm determinant. Function $K_{1,2}(t', t'')$ is determined unambiguously by the correlation function /72
$R_{Y_1}(t', t'')$ with the help of an integral equation similar to eq. (4.2.23) [4.1; 4.24; 4.25].

Only the second component of eq. (4.2.38) depends on the signal received. Let us write it in the form:

$$\int_{t_1}^{t_2} y(t'') \left[\int_{t_1}^{t_2} K_{1,2}(t', t'')\, y(t')\, dt' \right] dt''. \qquad (4.2.39)$$

The expression in square brackets can be interpreted as the intensity at the output of linear quadruple (usually parametric) with a transfer function $K_{1,2}(t', t'')$, , whose input was the signal y(t). It is possible to determine on this basis that the analog system for calculating integral (4.2.39) contains an appropriate filter, which would have the signal y(t) as an input. The output signal of this filter is multiplied by the path y(t), and then integrated within limits from t_1 to t_2.

When $S_1=0$, and Z(t) is white noise, it can be demonstrated [4.24] that integral (4.2.39) can be presented in the form

$$\int_{t_1}^{t_2} [Q_{1,2}(t', t'')\, y(t')\, dt']^2\, dt'', \qquad (4.2.40)$$

and an analog system for calculating the logarithm of the ratio of probability densities contains a linear filter with constant parameters, followed by a synchronized switch, an inertia-free nonlinear quadruple with quadratic characteristic, and by an integrator[1] [4.25].

As shown by Middleton [4.24], the transfer function of this optimal filter is defined by the nonlinear integral equation:

$$\varkappa(t', t'') = \int_{t_1}^{t_2} Q_{1,2}(t''' - t'')\, Q_{1,2}(t''' - t')\, dt''', \tag{4.2.41}$$

and χ (t', t'') is determined from the relation

$$\int_{t_1}^{t_2} [R_s(t, t'') + W_0 \delta(t - t'')]\, \varkappa(t', t'')\, dt'' = R_s(t, t'), \tag{4.2.42}$$

where $t_1 \leqslant t \leqslant t_2,\ t' \leqslant t_2 - t_1;$

R_s - correlation function of the signal;

W_0 - spectrum density of the white noise.

It is not easy to note on the basis of (4.2.41) that by /73
$\varkappa(t', t'')$ it is possible to determine directly the frequency characteristic of the optimal filter, by applying the Fourier transform.

A filter of the type described is a generalization of the notion of a fitted filter for the case of stochastic signals [4.24; 4.25].

Remarks on the optimization of scanning signals.

[1] See Appendix 7.

As is known, in the case of noncorrelated interference the detectability of the signal does not depend on its form (when reception is optimal), but only on the ratio of the signal energy to the spectrum density of interference ([4.1] Ch. 3). In the case of correlated interference the shape of the signals influences significantly their detectability. This problem has been considered e.g. by Nesteruk [4.26]. Making appropriate transformations of the first integral of (4.2.31) and using the properties of the eigenfunctions of integral equations ([4.27]; Appendix 2), he showed that for a predetermined observation time $T_0 = t_2 - t_1$, for the case of correlated interference with autocorrelation function $R(t-t')$, the optimal signal takes the form:

$$S_{opt}(t) = B_k(t), \tag{4.2.43}$$

and $B_k(t)$ is the eigenfunction of the integral equation

$$B(t) = \lambda \int_{t_1}^{t_2} R(t-t')\, B(t')\, dt'; \tag{4.2.44}$$

taking an appropriate value for k, it is possible to obtain the probability of detecting the signal when its energy is predetermined. E.g., if we assume that $R(t-t') = A \cdot \exp[-a(t-t')]$, then [4.26]:

$$s_{opt}(t) = C_k \cdot \sin\left[\omega_k\left(t - \frac{t_2 - t_1}{2}\right) + \frac{k\pi}{2}\right], \tag{4.2.45}$$

where ω_k are the solutions of equation

$$\mathrm{tg}\,\frac{\omega(t_2 - t_1)}{2} = \frac{a}{\omega}. \tag{4.2.46}$$

The effective value of the generalized signal-to-noise ratio

[4.29] at the output of an optimal filter is in this case [4.26]:

$$\rho_1 = \frac{E}{2\pi W(\omega_k)}, \qquad (4.2.47)$$

where

E - energy of the signal;

$W_{(\omega)}$ - spectral density of the power of correlated interference.

Evidently, in the example considered, the optimal signal is a sinusoidal vibration which has an envelope in the shape of a rectangular pulse with length $t_1 = t_2 - t_1$; the carrier frequency of the signal equals ω_k. (4.2.47) indicates that the detectability of the signal improves with increasing carrier frequency ω_k, because the spectrum of correlated interference decreases with frequency[1].

In the case of applications in radar, the carrier freqeuncy of the signal may differ from the carrier frequency of passive interference only when the echo of the signal is derived from a moving object. Then ω_k corresponds to the Doppler frequency and the physical meaning of [4.2.47] is obvious: a Doppler radar detects signals of the echo against a background of correlated interference easier when the Doppler frequency is higher[2]. A theoretical analysis thus confirms relations known from practice.

[1]In the example considered, $W(\omega) = \frac{A}{\pi} \cdot \frac{\alpha}{\alpha^2 + \omega^2}$.

[2]Of course, with a determined carrier frequency of scanning signals. Increasing the carrier frequency of scanning signals a higher Doppler frequency will be obtained for an object moving at a defined velocity, but the spectrum of passive interference will be also appropriately widened (see Ch. 5); therefore no improvement of detectability will be obtained.

The question of signal optimization taking into account the overall conditions influencing the operation of a radar system in the presence of passive interference, especially for pulse radars, is much more complicated and has not been completely resolved to date. Some aspects of this problem, such as e.g., optimization of a pulse packet of predetermined energy in the presence of interference of the type of Markov's process have been considered in ref. [4.30]; some other problems related to the optimization of the signal shape in the presence of correlated interference are discussed in ref. [4.31]. A discussion of the problem of the choice of scanning signals from the point of view of resistance to passive interference is also contained in ref. [4.32]; it is concluded there that an optimal signal should approach as close as possible a path with a discrete spectrum, i.e. periodic or almost periodic path; similar conclusions were reached in ref. [4.34].

References:

4.1. Seidler, J. Statistical theory of signal reception. PWN, 1963.

4.2. Woodward, P.M. Probability and Information Theory, with Application to Radar. London, 1953.

4.3. Urkowitz, H., Hauer, C.A., Koval, J.F. Generalized Resolution in Radar Systems. PIRE, Oct. 1962.

4.4. Siebert, W.A. Radar Detection Philosophy. IRE Trans. IT-2, Sept. 1956.

4.5. Siebert, W. Some Applications of Detection Theory To Radar. IRE Nat. Conv. Rec., Part 4, 1958.

4.6. Lerner, R.M. Signals with Uniform Ambiguity Function. /75 IRE Conv. Rec., Part 4, 1958.

4.7. Cook, C.E. Pulse Compression - Key to More Efficient

Radar Transmission. PIRE, March 1960.

4.8. Stewart, J.L., Westerfield, E.C. A Theory of Active Sonar Detection. PIRE, May 1959.

4.9. Westerfield, E.C., Prager, R.H., Stewart, J.L. Processing Gains Against Reverberation (Clutter) Using Matched Filters, IRE Trans. IT-6, June 1960.

4.10. Wald, A. Statistical Decision Functions. New York, 1950.

4.11. Middleton, D. An Introduction to Statistical Communication Theory. New York, 1960.

4.12. Szulkin, P. Statistical Methods for Determining Parameters of Radar Signals. Warsaw, 1962.

4.13. Gutkin, L.S. Theory of Optimal Radar Reception in the Presence of Fluctuating Noise. Moscow, 1961.

4.14. Fish, M. Probability Calculations and Mathematical Statistics. PWN, 1958.

4.15. Marcum, J.I. A Statistical Theory of Target Detection by Pulsed Radar. IRE Trans. IT-6, April, 1960.

4.16. Cramer, H. Mathematical Methods in Statistics. Warsaw, 1958.

4.17. Davis, R. On the Detection of Sure Signals. Journ. Appl. Phys., Jan. 1954.

4.18. Preston, G. Equivalence of Optimum Transducers and Sufficient and Most Efficient Statistics. J. Appl. Phys., July, 1953.

4.19. Osiowski, J. Significance and Application of Distribution in Circuit Theory. Electronic Discourses, No. 4, 1960.

4.20. Lusternik, L., Sobolev, V. Elements of Functional Analysis. Moscow, 1954.

4.21. Gelfand, I.M., Jaglom, A.M. Integration in Functional Spaces ... Usp. Mat. Nauk, vol. XI, issue 1/67/, 1956.

4.22. Kulikowski, R. Introduction to the Synthesis of Linear Electrical Systems. PWN, 1957.

4.23. Campbell, G.A., Foster, R.M. Fourier Integrals for Practical Applications. New York, 1948.

4.24. Middleton, D. On the Detection of Stochastic Signals ... IRE Trans., IT-3, June, 1957.

4.25. Middleton, D. On New Classes of Matched Filters and Generalizations of the Matched Filter Concept. IRE Trans., IT-6, June 1960.

4.26. Nesteruk, V.F. On the Theory of Signal Reception in the Presence of Correlated Interference. Radiotechnika, No. 6, 1962.

4.27. Davenport, W.B., Root, W.L. An Introduction to the Theory of Random Signals and Noise. New York, 1958.

4.28. Bakulev, P.A. Radiolocation of Moving Targets. Moscow, 1964.

4.29. Vainshtain, L.A., Zubakov, W.D. Signal Selection on the Background of Random Noise. Moscow, 1960.

4.30. Nesteruk, W.F. On the Reception of Pulse Packet in the Presence of Correlated Noise. Radiotechnika, No. 3, 1963.

4.31. Nesteruk, V.F. On the Influence of Signal Shape on its Detection in the Presence of Ordinary Correlated Noise. Radiotechnika i Elektronika, No. 8, 1963.

4.32. Tartakovskii, G.P. et al. Problems of Statistical Radar Theory. Moscow, 1963.

4.33. Kulikowski, J. On some Problems Related to the Calculation of Elements of Inverted Covariance Matrix for Passive Radar Interference. Electrotechnical Discourses, No. 3, 1961.

4.34. Kulikowski, J. Problems of Optimal Detection and Target Selection. Dissertation, Moscow, 1959.

4.35. Fowle, E.N., Kelley, E.J., Sheenan, J.A. Radar System Performance in a Dense-Target Environment. IRE Internat. Conv.., Part 4, 1961.

AD-A098 433 FOREIGN TECHNOLOGY DIV WRIGHT-PATTERSON AFB OH F/G 17/9
REDUCTION OF STATIONARY CLUTTER IN RADAR,(U)
OCT 80 J KROSZCZYNSKI
UNCLASSIFIED FTD-ID(RS)T-0132-80 NL

2 of 4

98 43

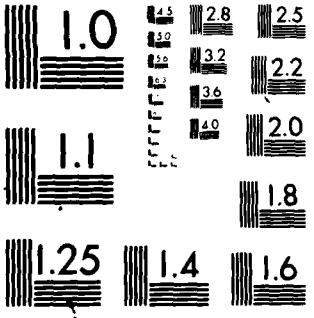

MICROCOPY RESOLUTION TEST CHART
NATIONAL BUREAU OF STANDARDS 1963 A

5. Basic properties of signals and interference. /76

Signals and interference considered in radar technology have specific properties connected both with scanning methods and with the characteristics of detected objects as well as the interfering reflections. In considering the question of optimal reception, knowledge of these properties is indispensable for obtaining results with practical significance. The present chapter contains a brief discussion of phenomena occurring in space scanning and the properties of reflections from objects to be detected and from interfering objects. An exhaustive discussion of this topic, which requires a separate monograph, was not possible within the limitations of a single chapter; we have taken into account mainly those aspects which are necessary to discuss the optimal algorithm for signal detection in the presence of interference.

5.1 Phenomena occuring in space scanning.

The course of events taking place during space scanning by radar or in sonar ranging may be generally presented as follows (Fig. 5.1.1.).

The scanning signals travel in space and are reflected both from objects which are to be detected by the station, and from bodies (stationary or moving) about which information is not required; echoes derived from the latter are the source of interference, making the detection of desired signals more difficult. Because this interference is not actively generated and arises only as a result of reflections of the scanning signals, it is called passive interference to distinguish it from active interference.

The properties of the space being scanned may be generally described by introducing operator V, which transforms

scanning signals w(t) into reflected signals u(t):

$$V\{w(t)\} = u(t). \tag{5.1.1}$$

Assuming linearity of the effect of electromagnetic wave propagation and reflection in space, operator V will be a linear operator. Therefore it is possible, based on the principle of superposition, to write the relation 5.1.1 in a form which shows a separate transformation of the scanning signal, caused by reflection from the object being detected - let us denote the appropriate operator by V_o - and the transformation caused by reflection from objects which are the source of passive interference. The operator of the latter transformation will be denoted V_p.

$$V\{w(t)\} = V_o\{w(t)\} + V_p\{w(t)\}. \tag{5.1.2}$$

The reflected signals u(t) may then be written in the form:

$$u(t) = s(t) + b(t), \tag{5.13}$$

i.e. as the sum of signals derived from objects being detected $s(t) = V_s\{w(t)\}$ - and passive interference - $b(t) = V_p\{w(t)\}$. This form will be useful in later discussion of the properties of signals.

At the input of the receiver, heat noise is added to the reflected signal u(t); their source is both the surrounding space and the receiver itself. As a result we obtain the path y(t), composed of the desired signal, passive interference and heat noise

$$y(t) = s(t) + b(t) + n(t), \tag{5.14}$$

where n(t) - heat noise.

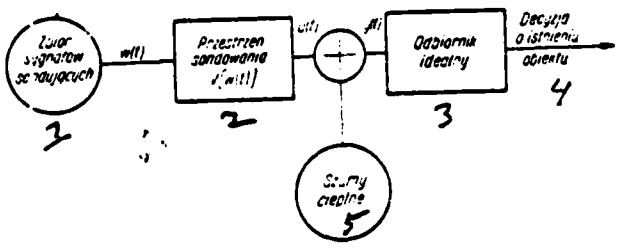

Fig. 5.1.1. Generation and reception of radar signals. 1. set of scanning signals, 2. space being scanned, 3. ideal receiver, 4. decision about the object's existence, 5. heat noise.

An ideal reception algorithm should assure an optimal detection (in the sense of considerations contained in Ch. 1.3 of the object on the basis of knowledge of path y(t). In order to define the optimal way to receive the signals it is necessary to know the appropriate characteristics of signals and of the interference.

As mentioned above, these characteristics are related to the methods of space scanning by directional antennas, characteristic for a location. In systems problems in location it is assumed as a rule that the system "transmitting antenna - space being scanned - receiving antenna" can be replaced by an equivalent separable quadruple with variable parameters [Fig. 5.1.2], thanks to which a signal reflected from a stationary, nonfluctuating point object may be presented in the form:

$$u_p(t) = k(t)\, g_n\left(t - \frac{2r}{c}\right) g_o(t)\, w\left(t - \frac{2r}{c}\right), \tag{5.1.5}$$

where

$k(t)$	- attenuation of signal along the path: transmitting antenna-object-receiving antenna, determined by the radar range; equation (5.1).
g_n and g_o	- functions related to the directional characteristics of the transmitting and receiving antennas, respectively;
r	- distance of the object;
c	- velocity of signal propagation in the environment being scanned[1].

In pulse radar devices the same antenna is most often used to transmit and receive the signals. In addition, the parameters of the device are chosen such that an individual object will give rise to a signal composed of several to several tens of pulses (see Ch. 2). Thus we will have in this case $g_n(t) = g_o(t) = g(t)$, and in addition we can assume approximately that $g(t) \cong g\left(t - \frac{2r}{c}\right)$, because the antenna revolves during a time equal to $\frac{2r}{c}$ by an angle which is small compared to the width of the antenna beam. We can then write:

$$u_p(t) = k(t) \cdot G(t)\, w\left(t - \frac{2r}{c}\right), \qquad (5.1.6)$$

where $G(t) = g^2(t)$.

It is easy to note that $G(t)$ is related to the directional power gain characteristics of the antenna $G(\varphi)$ in a manner similar to the relationship between $g(t)$ and the directional amplitude characteristic.

As could be expected, it follows from (5.1.6) that the echo signal received from a point target is reduced and delayed

[1]Derivation of (5.1.4) is discussed in Appendix 1.

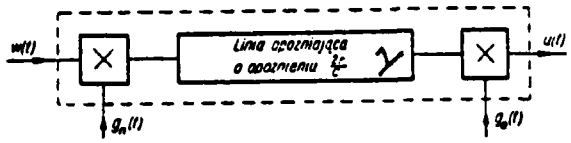

Fig. 5.1.2. Equivalent system of transmitting antenna, space being scanned and receiving antenna. 1. delay line, with a delay of $\frac{2r}{c}$.

by the echo return time of the scanning signal, which is modulated in the scanning process by the path corresponding to the directional antenna characteristic.

This relation is easily illustrated for the case when space scanning takes place with a constant velocity in one plane; this is a situation often encountered in radar - e.g., antennas of warning stations, area control stations, airspace control stations, etc. revolve with a constant azimuth velocity. Then $G[\varphi(t)] = G(\gamma t)$, , where γ - angular velocity of antenna revolutions. Fig. 5.1.3 the signals reflected from a point object when the scanning signal is a series of pulses with repetition frequency $f_p = 1/T_p$. This kind of signal is often called a "pulse packet" in radar.

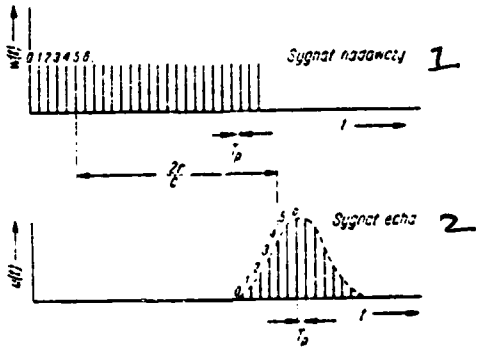

Fig. 5.1.3. Generation of pulses in the form of pulse "packet" during reflection from a point object. 1. transmitting signal, 2. echo signal

5.2 Reflection properties of detected objects.

The objects detected may be usually considered to be points, since their dimensions are small compared to the effective range of the scanning signals[1]. The characteristic attributes of reflections generated by actual objects detected are the following: Doppler frequency, caused by the object's motion, and the fluctuation in amplitude. The problem of electromagnetic wave reflection from moving objects has been discussed e.g., by Cole [5.2]; see also [5.3]. For the purposes of this work it is sufficient to use (5.1.5), /80 taking into account $r = r(t) = r_0 + vt$, , where v - radial component of the object's velocity. In this case

$$s_v(t) = k(t) \cdot G(t) \cdot w\left(t - \frac{2r_0}{c} - \frac{2vt}{c}\right). \tag{5.2.1}$$

Comparing (5.16) and (5.2.1) we obtain:

$$s_v\left[t\left(1 - \frac{2v}{c}\right)\right] = s(t), \tag{5.2.2}$$

or

$$s_v(t) = s\left[t\left(1 + \frac{2v}{c}\right)\right]. \tag{5.2.3}$$

During reflection from a moving ojbect the reflected signal is, so to speak, "stretched" or "compressed" in time (depending on the magnitude and sign of radial velocity, i.e. depending on whether the object is moving closer or away). This can be interpreted to mean that the path s(τ) is transformed into

[1] e.g. at typical scanning pulse lengths between 1-5 μ S the effective range will be 150-750m, much greater than dimensions of an airplane. This is even more evident in terms of angular coordinates; e.g. at a distance of 100km the beam width of 1° corresponds to the effective width of about 2000m.

path $s_v(t)$ by the following operation:

$$s_v(t) = s[\beta(t)]. \tag{5.2.4}$$

This kind of operation has a simple geometrical interpretation (Fig. 5.2.1) [2.4].

In agreement with relations (5.2.2) and (5.2.3) we have

$$\beta(t) = \left(1 + \frac{2v}{c}\right)t. \tag{5.2.5}$$

As known, a harmonic vibration modulated in frequency can be written in the form:

$$y(t) = A \sin \int_0^t \omega(\tau)\, d\tau, \tag{5.2.6}$$

where ω - instantaneous pulsation (5.5).

In this particular case we thus have:

$$\beta(t) = \frac{1}{\omega_0} \int_0^t \omega(\tau)\, d\tau. \tag{5.2.7}$$

If, according to (5.2.7) we transform the complex vibration represented by the Fourier series

$$Y(\tau) = \sum_{k=-\infty}^{\infty} \dot{S}_k \exp(j\omega_k \tau), \tag{5.2.8}$$

then the transformed path can be presented in the following /81
form, which demonstrates the modulation of frequency of the individual components of the echo signal, caused by the

object's motion:

$$s_v(t) = \sum_{k=-\infty}^{\infty} S_k \exp\left\{j\omega_k \int_0^t \left[1 + \frac{2v(\tau)}{c}\right] d\tau\right\}. \qquad (5.2.9)$$

In the general case the components of the scanning signal are thus modulated with unequal deviations during reflection from a moving object. This effect is sometimes called "Doppler dispersion" [5.6].

However, since signals used in detection have as a rule a small bandwidth relative to the carrier frequency (e.g., the bandwidth of such signals is of the order of a megaherz, and carrier frequencies - of the order of 10^3MHz [5.1],) we can usually assume that $\omega_k \approx \omega_0$.

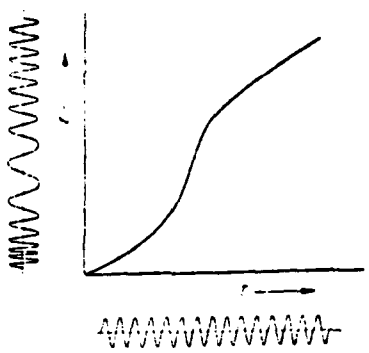

Fig. 5.2.1 Geometric interpretation of relation 5.2.4

As follows from (5.2.9), all components of the spectrum will then be subject to the same transformation. The physical interpretation of this relationship is particularly clear for the case of constant radial velocity v; with the assumption, justified above, that $\omega_k \approx \omega_0$. We can then say that the spectrum of the echo signal is displaced along the frequency axis by

$$f_D = f_w \cdot \frac{2v}{c}. \qquad (5.2.10)$$

Frequency f_D is the known Doppler frequency for the case of reflected signals [5.1]. This frequency is one of important properties which distinguishes echoes derived from objects to be detected from amongst interfering reflections.

As an example, for an object moving with velocity v = 1000km/hr and a scanning signal having a carrier frequency of 1000MHz, f_D is approximately 1850Hz (cf. Fig. 2.12)[1]. /82

In some very special cases the Doppler frequency for a given object may be known, but in general it is a passive parameter of the signal. Making certain assumptions as to the probable velocities and directions of the objects' motions within the space being scanned, it is possible to determine the probability density function $p(f_D)$ ([5.1], p. 127-128). However, the correctness of such assumptions depends on specific conditions; for air communications using defined air corridors and utilizing airplanes with known velocities such a method would be justified. For the detection of airplanes of unknown type which could arrive from any direction, obviously the usefulness of determining $p(f_D)$ could be questioned. The problem is somewhat simplified when considering typical signals in radar stations serving for target detection, i.e., series of short pulses with relatively small repetition frequency. The bandwidth of the possible Doppler frequencies is then usually much larger than the pulse repetition frequency f_p, but considerably smaller than the width of the spectrum of an individual pulse. Since for the type of signal mentioned above it is practically impossible to distinguish (see Ch. 4.1) an echo signal with a Doppler frequency f_D from a signal

[1]Taking into account conclusions of relativity theory, we obtain a more accurate formula for Doppler frequency. But the relativistic aspect of the effect may be omitted here even for satellite velocities (of the order od 2.10^{-5}.c), e.g. for f_W=1000 MHz the difference in f_D values obtained using relativistic formula and (5.2.10) is only appr. 0.5Hz [5.7; 5.8; 5.9].

with a Doppler frequency equal to $f_D + kf_p$ (where k = 1,2, 3...), a certain "averaging" of the effective probability density of this passive parameter takes place. Therefore, it is often possible to assume a uniform distribution of the probability density $p(f_D)$ in appropriate interval.

We will now discuss a typical property of reflections from real objects, such as airplanes, namely strong random fluctuations.

Because an airplane is usually an object with dimensions much greater than the wavelength of scanning signal, it is usually assumed that reflections occur independently at many points on its surface. Because of the constant change in the airplane's position in space, its vibration, etc., there are constant fluctuations of phase and amplitude of these primary reflections. It is most often assumed that following reflection the sine and cosine components of narrowband signal become independent and approach stochastic process (which may be considered stationary within the time interval considered in detection problems), which are Gaus- /83
sian according to the central limit theorem. This indicates that the instantaneous amplitude distribution of such a signal is determined by Rayleigh's law, and the phase distribution is uniform (cf. Appendix 2) [5.3; 5.10-5.12].

For instance, Fig. 5.2.2 shows the results of experimental studies of the probability distribution of the echo signals amplitudes, derived from a two-engine jet plane of the type B-45. The measurements were taken simultaneously at wavelengths of appr. 3, 10 and 25 cm [5.112].

Concerning data about the variability of aircraft reflections in time, it can be generally said that for propeller planes fluctuations between pulses can be expected, while for

jet planes there exist strong fluctuations between pulse "packets", but within such a "packet" the reflected signals are strongly correlated [5.18][1].

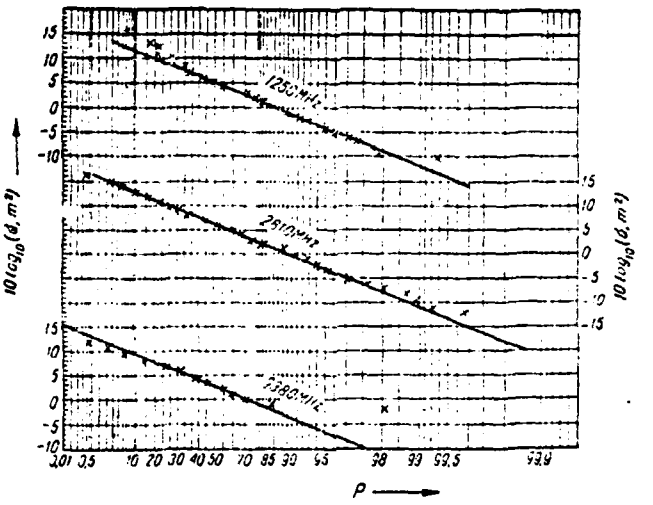

Fig. 5.2.2. Graph of the probable reflection area of a jet plane of type B-45. Points x - experimental data; solid line denotes the theoretical relationship for Rayleigh's distribution (5.11).

On the basis of these considerations it is possible to represent the received echo signal, originating from space scanning by a narrow-band coherent signal, in the following way: /84

$$s(t;\, \vartheta_1;\, \vartheta_2;\, f_D) = \vartheta_1(t)\, A(t) \sin(2\pi f_s t) + \vartheta_2(t)\, A(t) \cos(2\pi f_s t). \qquad (5.2.11)$$

[1]Extensive literature on the problem of the properties of echo fluctuation is cited in one of the previous works by the author [5.13]. Specific theoretical considerations of the form of reflected signals in more general cases can be found in ref. [5.14].

$\vartheta_1(t)$, $\vartheta_2(t)$ - Gaussian stochastic processes, which determine signal fluctuation; for fluctuation "between packets" we can simple write ϑ_1, ϑ_2 - random variables with normal distribution, which determine the influence of signal fluctuation;

A(t) - envelope of the echo signal in the case of non-fluctuating reflection from an object with an equivalent effective reflecting surface;

f_s - carrier frequency of the echo signal, and $f_s = f_w \pm f_D$, where f_w - carrier frequency of the transmitted (scanning) signal;

f_D - unknown Doppler frequency.

For instance, if we consider a panoramic station scanning the azimuth with a uniform angular velocity, and the scanning signal is a series of periodically repeating pulses with period T_p and the envelope of individual pulse $A_s(t)$, then

$$A(t) = G(\gamma t) \sum_{n=-\infty}^{\infty} A_s(t - nT_p) \qquad (5.2.12)$$

(cf. Fig. 5.1.3).

(5.2.11) may be written in the equivalent form (see Appendix 3):

$$s(t; \vartheta_3; \vartheta_4; f_D) = \vartheta_3(t)\, A(t) \cos\left[2\pi f_s + \vartheta_4(t)\right], \qquad (5.2.13)$$

where

$\vartheta_3(t)$ - a process with Rayleigh distribution, determining the amplitude fluctuation of the signal; for fluctuation "between packets" we can take simply ϑ_3 - random variable with Rayleigh distribution ;

$\vartheta_0(t)$ - a process which determines the phase function of the signal, with a uniform distribution within the interval $<0,2_\pi>$; for fluctuation "between packets" we can write ϑ_v - random variable with an analogous distribution.

In the case when the scanning signal is noncoherent or when the reflection shows fluctuations "between packets", the signal can be represented in the form:

$$s(t;\vartheta_1;\vartheta_2) = \vartheta_1(t)\,A(t)\sin(2\pi f_0 t) + \vartheta_2(t)\,A(t)\cos(2\pi f_0 t), \qquad (5.2.14)$$

where $\vartheta_1(t), \vartheta_2(t)$ — - Gaussian stochastic processes whose correlation time is much smaller than the pulse repetition period (but longer than their duration).

When the signal shows this type of phase fluctuation, /85
and it is practically impossible to select the regular component due to the Doppler effect, it can be generally assumed that $f_v \cong f_0$.

Depending on the particular case it may be more useful to assume a model of the echo signal. There may also be some intermediate situations. In Ch. 6 it will be shown what form is assumed by the optimal receiving system depending on the signal model accepted.

5.3 Properties of passive interference.

It is known that passive interference is the result of reflection of the scanning signal from many objects, whose detection is not required in a given radar application. Thus for a radar device to detect airplanes, passive interference will include reflections from surface objects, clouds, rain or artificial obstacles in the form of a cloud of dipoles tuned

to the radar wavelength.

As in the previous paragraph we will limit ourselves to a brief description of the basic properties of passive interference based on published literature. An extensive bibliography on this subject is contained in one of the earlier works by the author [5.13].

Fluctuations of passive interference.

A basic property of passive interference is the fact that usually the effective volume of the scanning pulse (see note in the previous chapter) contains an enormous quantity of elementary reflecting objects. Therefore the applications of the central limit theorem to the resultant reflected signal leads to the conclusion that the signal fluctuations must have the characteristics of a Gaussian process. This conclusion is confirmed experimentally with a relatively high accuracy [5.15-5.17].

Aside from individual motions of individual reflecting particles giving rise to fluctuations of passive interference, all particles may also have a common motion component. This occurs e.g. in clouds, moving as an entity due to winds. The reflected signal then undergoes Doppler displacement, similar to the events described in the previous chapter.

The influence of the movement of the cloud as an entity (or, equivalently, the possible movement of the radar device with respect to interfering objects) can be compensated for by using approrpiate systems in the location device (see Ch. 2). Therefore it will be often assumed below that Doppler displacement does not occur for passive interference.

Reflections from objects such as clouds or artificial /86
obstacles do not have a constant component (nonfluctuating component). In contrast, reflections from ground objects may have such a component due to reflection from a large smooth object (rock, large building) or from a group of such objects. In this case the amplitude probability distribution of the reflected signal takes on the form of a generalized Rayleigh distribution [5.15, 5.16].

As shown by Veinshtein and Zubakon [5.3], passive interference can be treated as a narrow-band stationary process for problems considered here. Therefore they can be represented in the form (cf. Appendix 2):

$$B(t) = P(t)\cos\omega_s t + Q(t)\sin\omega_s t. \tag{5.3.1}$$

As suggested in Ch. 4.2 in considering signal detection problems against a background of interference it is necessary to know, among other things, the appropriate correlation functions.

The spectrum of passive interference is usually symmetrical with respect to the carrier frequency of the reflected signal. Thus if we take $f_s = f_w + f_D$, then the mutual correlation function of processes P and Q, $R_{PQ}(\tau) = 0$. If the frequency f_w of the scanning signal is taken as the reference frequency, then the mutual correlation function R_{PQ} for passive interference is not zero (see Appendix 2). As mentioned above, the displacement of the central frequency of the interfering echo, due to the Doppler effect, can be compensated for by appropriate systems.

The correlation properties of passive interference are conveniently represented by dividing the autocorrelation

function into two parts, namely, the autocorrelation function $R(\tau)$ depending on the scanning signal and on the properties of the reflecting objects. In order to stress the latter we can interpret the effect in such a way that first, an autocorrelation function will be found for the case when the scanning signal is a continuous wave. Such a function distinguishes only the correlation properties of the reflections from interfering objects. It will be denoted $R_p(\tau)$. It is easy to note that, given $R_p(\tau)$, it is easy to find the complete autocorrelation function $R(\tau)$ for each scanning signal with constant carrier frequency. This is because the scanning signal is treated as a continuous wave signal modulated by the envelope of the scanning signal. Then, in agreement with the relationship defining the autocorrelation function of a process modulated in amplitude [5.18]:

$$R_P = R_Q = R_p R_w, \tag{5.3.2}$$

which gives

$$R(\tau) = R_w(\tau)\ R_p(\tau) \cos(2\pi f_s \tau), \tag{5.3.3}$$

where $R_w(\tau)$ - autocorrelation function of the envelope of /87
transmitted (scanning) signal; see also Appendix 5.

Considering the general problem of electromagnetic wave dissipation in a non-uniform fluctuating environment, Gorelik [5.10] has demonstrated that autocorrelation functions R_p have in this case the characteristics similar to function $e^{-\alpha\tau}$ or $e^{-\beta\tau^2}$. In radar applications a Gaussian shape is most often assumed for the autocorrelation function R_p, and therefore a Gaussian shape is assumed for the spectrum of fluctuation power [5.15, 5.16, 5.20, 5.21].[1]

[1] In some problems of circuit synthesis it is more useful to use the trigonometrical-exponential approximation (5.14).

In refs. [2.18, 2.19[the spectrum approximation $W_p(f) = \mathcal{F}\{(R_p \cos 2\pi f_s \tau)\}$ is substituted by a Gauss function:

$$W_p(f) = W_p(f_s) \exp\left[-a\left(\frac{f}{f_s}\right)^2\right], \qquad (5.3.4)$$

where f_s - carrier frequency, a - coefficient dependent on the object. Here are several typical values of this coefficient:

1. Reflections from ground objects (little vegetation, no wind) $a=(3 - 5)\cdot 10^{19}$
2. Reflections from ground objects (dense trees, windy) $a=(2 - 3)\cdot 10^{17}$
3. Artificial obstacles $a=$ appr. 10^{16}
4. Rain clouds $a=(2 - 3)\cdot 10^{15}$

Fig. 5.3.1 gives typical examples of the approximation of spectra of passive interference by formula (5.3.4).

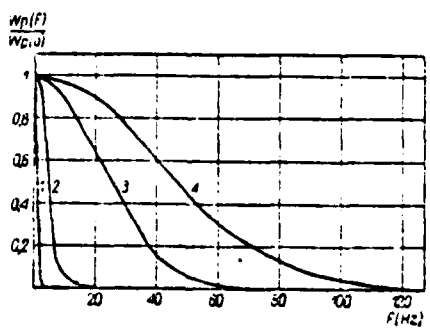

Fig. 5.3.1. Spectra of correlated interference for various objects, calculated according to formula 5.3.4.

In practice, especially when air whirlpools are possible etc., the spectra of passive interference may differ from the shape defined by formula (5.3.4). Fig. 5.3.2 shows the spectra of passive interference measured experimentally (on the basis of ref. [5.17].

Concerning the spatial properties of passive interference, there is a lack of specific experimental data in the published literature. Assuming, as Emslie and McConnell had done ([5.23], Ch. 16), the most unfavorable case of passive interference from point objects distributed in space randomly, it is possible by analogy with formula (5.1.6) to represent the effect in the following way. At a constant distance r and antenna revolution speed γ, the envelope of the ouptut signal will be obtained by putting a signal with the characteristics of white noise through a hypothetical quadrupole with a pulse response in the form of the directional antenna characteristic $G(\phi)$ (cf. Ch. 5.1 and Appendix 1). This signal will have the power spectrum

$$W_A(\omega) = [\mathcal{F}\{G(\gamma t)\}]^2. \tag{5.3.5}$$

On the basis of the Wiener-Chinchin theorem and because of the properties of the Fourier transform [5.24, 5.25] we obtain, after appropriate transformations, an autocorrelation function $R_A(\tau)$ in the form:

$$R_A(\tau) = \mathcal{F}^{-1}\{W_A(\omega)\} = G(\gamma t) * G(\gamma t), \tag{5.3.6}$$

where * represents the operation of convolution[1].

Finally, treating the influence of space scanning as a modulation of reflected signals by a process with the correlation function $R_A(\tau)$ (cf. Ch. 5.1 and Appendix 1 and 5), we can write

[1] As known, convolution of functions $f_1(t)$ and $f_2(t)$ is defined as: $f_1(t) * f_2(t) = \int_{-\infty}^{\infty} f_1(t) f_2(\tau - t)\, dt.$

the autocorrelation function of the signal derived from passive interference in the form: /89

$$R(\tau) = R_w(\tau)\, R_p(\tau)\, R_A(\tau) \cos \omega_0 \tau. \qquad (5.3.7)$$

From (5.3.7) (on the basis of the Wiener-Chinchin theorem [5.24]) we find an equivalent relationship for the passive interference power spectrum:

$$W(\omega - \omega_0) = W_w(\omega) * W_p(\omega) * W_A(\omega). \qquad (5.3.8)$$

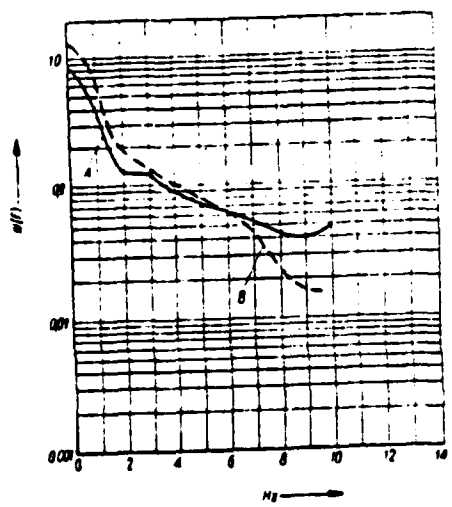

Fig. 5.3.2. Results of measurements of the spectrum of passive interference in the form of a dipole cloud [5.17].

Intensity of passive interference.

Considering the problems related to the detection of objects in the presence of passive interference we should realize the possible range of values for the interfering signals.

For dipole interference, we can cite as an example the data contained in ref. [5.17]. It describes the properties of interfering dipoles tuned to a wavelength of appro. 20cm. A packet of such dipoles weighed 4.5kg and contained $3.75 \cdot 10^6$ dipoles. Fig. 5.3.3 represents the effective area of the packet as a function of time; it indicates that the orientation of dipoles in space is not completely random - the effective area depends on signal polarization. However, the difference is not too great and amounts to about 2.5 dB. Evidently, immediately after dropping, the effective area of the packet is smaller, which is understandable because the dipoles have not moved away from each other yet. After several minutes, when the dipoles are sufficiently dispersed, the effective area stabilizes. The diameter of a dipole cloud derived from a 4.5kg packet was 1800-2700m^2 (in the horizontal projection) in the studies described[1]. The falling velocity was 30 to 60m/min. The width of the fluctuation spectrum[2] was (depending on wind velocity, 6 to 32km/hr) between 6 and 15Hz [5.17].

Special attention should be given to a large effective surface of interference, which totals 500-100 m^2/kg in the case described. Present-day jet fighters, for example, are known to have an effective surface on the order of 1 m^2.

Modern means thus allow to create very strong passive interference and aircraft detection in its presence may be a difficult task.

We should mention briefly the relationship between the detected signal - passive interference ratio and the pulse length and the width of the beam of antenna characteristic. The effective range in space of the radar pulse of duration /90
time T is, $\frac{cT}{2}$ (where c - velocity of light) and for detection devices is greater than the dimensions of an airplane. Thus the effective area of an airplane may be assumed to be independent of pulse length. In contrast, the interfering dipoles

[1] In the work discussed [5.17] the typical shapes of dipole clouds were also given.

[2] At the level of 0.05 power.

may be, as suggested by the results of experiments described above [5.17] dispersed over a large area. The combined power of passive interference is directly proportional to the quantity of dipoles [5.17], and therefore - because of their uniform distribution in space it is proportional to the effective pulse length. This indicates that the signal-to-noise ratio in this case is inversely proportional to pulse length. This is reflected in the manner of defining the quantity of dipoles necessary to achieve a predetermined noise-to-signal ratio with a known effective area of the aircraft and radar pulse length. The dipoles weight corresponding to an element of distance resolution of the radar is determined.

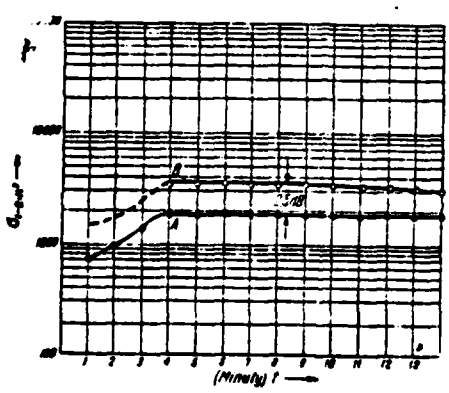

Fig. 5.3.3. Intensity of passive interference in the form of dipole cloud depending on wave polarization [5.17].

The dependence on antenna characteristics can be presented approximately as follows[1]. If the interference occupies a small part of the bundle cross-section[2], then the signal-to-noise

[1]A more detailed analysis of this problem is found in refs. [5.15] and [5.26].

2) To fill bundles with a width of 1° at a distance of 100 km, for example, dipoles must have a diameter of approx. 2 km.

ratio is independent of bundle width. However, if interference is present over large areas, completely filling the bundle, then there is a dependence on bundle width.

As follows from the radar range formula [5.1], the echo signal is: /91

$$P_e = \frac{P_s}{r^4} \cdot \frac{G^2\lambda^2}{(4\pi)^3} \cdot \sigma, \qquad (5.3.9)$$

where

P_s - power of scanning signal;

r - distance of reflecting object;

σ - wavelength;

G - antenna gain;

λ - effective area of reflecting object.

It can be assumed that $G = k_1/\Theta_a\Theta_e$, where $\Theta_a; \Theta_e$ - widths of the antenna characteristic (at the half-power level) in azimuth and elevation [5.27]. If it is assumed that for a unit volume of a cloud there are n objects with an average effective area σ_0[1], then the interference power received will be:

$$P_z = \frac{P_s}{r^2} \cdot \frac{k_1\lambda^2}{(4\pi)^2\Theta_a\Theta_e} \cdot \frac{cT}{2} \cdot n\sigma_0, \qquad (5.3.10)$$

and therefore the signal-to-noise ratio will be:

$$\frac{P_e}{P_z} = \frac{1}{r^2} \cdot \frac{2}{cT} \cdot \frac{1}{\Theta_a\Theta_e} \cdot \frac{\sigma}{n\sigma_0}. \qquad (5.3.11)$$

[1]for a half-wave dipole, the effective surface depends on its orientation in space relative to radar station. The maximum value of this surface is $0.86\lambda^2$ assuming that all dipole positions in space are equally probable, the averaged value σ_0 is appr. $0.11\lambda^2$ (5.28, p. 36-38).

As evident from (5.3.11)(in the case where interference fills the beam) the signal-to-noise ratio is inversely proportional to the solid angle of the beam. If, for instance two stations have identical antenna characteristics in the vertical plane, then the greater the beam width in azimuth, the smaller will be the resistance to passive interference ranging over large areas.

Similar relationships also hold for interference caused by rain, snow, etc. As we know, the effective area of a raindrop depends on the drop diameter D [5.15].

$$\sigma_k = \frac{\pi^5 |k|^2 D^6}{\lambda^4}, \qquad (5.3.12)$$

where $k = \frac{\varepsilon - 1}{\varepsilon + 2}$, , and ε - coupled dielectric constant; in practice, for wavelength range of 3 - 23 cm it may be assumed /92 that $|k|^2 \cong 0{,}93$ [5.29]. It is assumed that $D \ll \lambda$.

Because of the strong dependence of D an exact determination of the power of interference is not possible, because of the possibility of varying size distribution of the drops. An estimate of the effective surface is possible because of some empirically observed relationships between the average drop size and the intensity of rainfall, expressed in mm/hr [5.1, p. 538-543; 5.30; 5.31]. Fig. 5.3.4 represents the graphs taken from ref. [5.31] of the average effective area (related to unit volume) of rain, snow and clouds, for several typical wavelengths used in radar.

This graph gives an idea of the order of magnitude of passive interference caused by the aforementioned meteorological factors; a more detailed discussion of this problem may be found in literature cited.

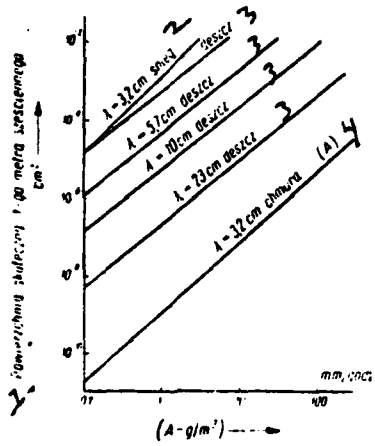

Fig. 5.3.4. Average effective area (related to unit volume) of rain, snow and clouds [5.31]. 1. effective area of the 1st cubic meter, 2. snow, 3. rain, 4. cloud.

Concerning passive interference caused by field reflections, a theoretical evaluation of its intensity is obviously difficult because of the possible considerable variability in the surface both as a function of azimuth and of distance. An example is Fig. 1.1 (see also [5.32]). In the following we will limit ourselves only to presenting some characteristic general properties of this type of interference; a more detailed discussion of this problem may be found in refs. [5.1] p. 522-534, [5.11, 5.15, 5.16, 5.23, 5.33-5.36].

As is known, reflections from the earth's surface cause the elevation characteristic of an antenna above this surface to have lobe character. If the reflecting object is within the lower part of the lowest lobe, then the power of echo signal P_e is inversely proportional to r^8 (where r - distance of the object). Such a situation is present for the more distant objects situated on the ground. For nearer distances the object may be within an entire lobe or even several lobes; then $P_e \sim \frac{1}{r^4}$, as in free space [5.11, p. 212]. In pulse

radar devices the effective reflection area from the ground is approximately proportional to the distance because of the increase of the geometrical field area which gives rise to the reflections. Therefore at nearer distances the power of the echo signal generated by a given object located on the earth's surface shoudl decrease inversely to r^3, whereas at larger distances - inversely to r^7.

Fig. 5.3.5 shows the results of measurements where echoes were caused by reflections from sea waves ([5.11], p. 212). The results indicate the agreement of the character of the phenomenon with the simipified theoretical model presented above.

To evaluate approximately the intensity of stationary clutter, caused by reflections from ground objects, Shrader [5.37] used the following simplified model (which takes into account the curvature of the earth's surface). Let us assume that the average height of reflecting objects is h_z. The height of that part of the reflecting object which is visible above radar horizon depends on the effective height of the radar antenna h_a. As an approximation, the geometric area of reflecting objects A may be taken $A(r) = r\Theta_a h_z$ up to the limit of the radar horizon (i.e. for $r < \sqrt{2h_aR}$, where R=2/3 of the earth's radius. At larger distances we will have $A(r) = r\Theta_a\left[h_z - \frac{1}{2R}(r - \sqrt{2h_aR})^2\right]$.

Assuming that the minimum signal power detected by a given device is P_o we will thus obtain;

$$\frac{P_z}{P_0} = \left(\frac{G_0}{G_{\max}}\right)^2 \cdot \frac{r^4_{\max}}{\sigma} \cdot \frac{k_z \cdot A(r)}{r^4};$$

$$A(r) = \begin{cases} r\Theta_a h_z, & \text{gdy} \quad r < 2h_aR \\ r\Theta_a\left[h_z - \frac{1}{2R}(r - \sqrt{2h_aR})^2\right], & \text{gdy} \quad r \geq 2h_aR. \end{cases}$$

(5.3.13)

where

G_{max} - antenna gain in the direction of maximum radiation,

r_{max} - maximum range of a device for a detected object with effective area σ,

G_o - antenna gain in horizontal direction (i.e. for an elevation angle equal zero),

r - distance of the reflecting area,

k_z - coefficient of reflection, which is the ratio of effective and geometrical areas of the interfering object [5.37].

/94

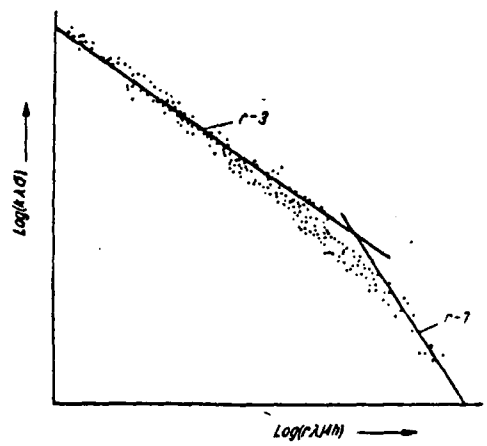

Fig. 5.3.5. Results of intensity measurements for reflections from sea waves [5.11].

Fig. 5.3.6 gives the results of calculations (curve A), /95
carried out with the following parameters:

$$G_{max} = 34 \text{ dB}; \quad G_0 = 31 \text{ dB}; \quad \Theta_a = 1{,}2^\circ; \quad r_{max} = 315 \text{ km};$$
$$\sigma = 2{,}25 \text{ m}^2; \quad h_a = 23 \text{ m}; \quad h_z = 12.2 \text{ m}; \quad k_z = 0{,}05.$$

These parameters correspond to a radar station of ARSR-2 type, used in the U.S. to direct and control air traffic, described in Ch. 3. The actual intensities of stationary clutter, measured at two stations, are given by curves S and O in Fig.

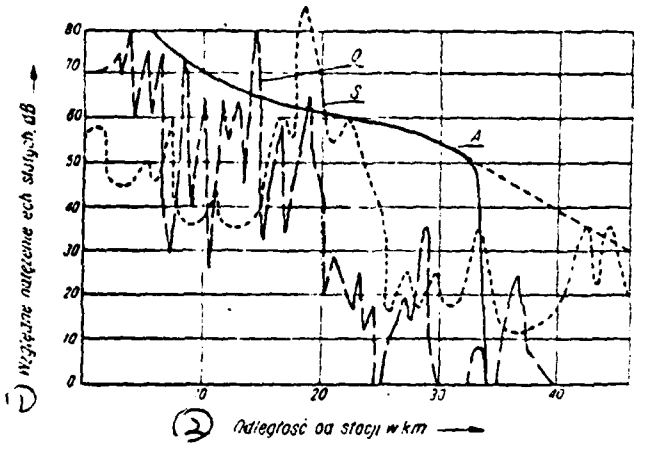

Fig. 5.3.6. Intensity of passive interference caused by reflections from field objects, as a function of distance from the radar station. A - theoretical curve, S and O - results of measurements at two different locations [5.37]. 1 - relative intensity of stationary clutter, 2 - distance from station, km.

5.3.6. In Seattle the terrain was hilly; whereas in Oklahoma City (curve 0) it was relatively flat [5.37]. It is self-evident that in mountainous regions there may be very strong stationary clutter even at large distances; ref. [5.32] gives the appropriate data for a radar installed in the Alps.

Passive interference in moving radar devices.

In the case when the radar station is in motion (i.e. when it is located aboard a ship or a plane) the reflections from stationary objects have a radial velocity component with respect to the station. Aside from the aforementioned factors - i.e. internal fluctuations of interference and the modulation caused by space scanning - which influence the structure of passive interference, the effect of the movement of the device with respect to reflecting objects must also be taken into account.

When objects causing passive interference are in the same plane as the radar station (which is approximately correct, e.g. in the case of devices located aboard ships), the radial velocity component of the object v_r is related to the station velocity v_{st} by a simple formula:

$$v_r = v_{st} \cos \alpha \tag{5.3.14}$$

(see Fig. 5.3.7).

In the case when the station is located aboard a plane, and stationary clutter from field objects is considered, the relative radial velocity of objects is defined (fig. 5.3.8) by the relation:

$$v_r = v_{st} \cos \alpha \cos \beta = v_{st} \cos \Theta. \tag{5.3.15}$$

/96

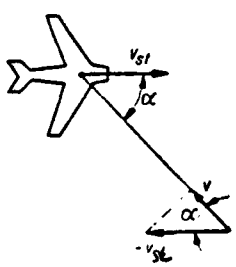

Fig. 5.3.7. Determination of radial velocity component of the object with respect to a moving radar station.

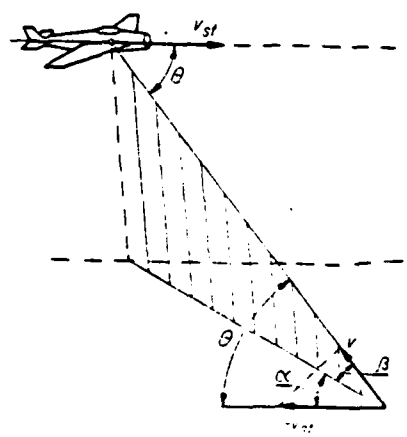

Fig. 5.3.8. Determination of the radial velocity component of the object with respect to a radar station moving in a different plane.

The radial velocity component of interfering objects can be compensated for by introducing an appropriate signal of

Doppler correction, or by using an autocoherent system (see Ch. 2.5 and [5.1, 5.23, 5.38].

The effect of the movement of the station itself is also evident in the form of a modification of the interference spectrum. We will explain this using the example of an air station. Because of the finite width of the beam of directional antenna characteristic and because of the finite pulse length, the surface area illuminated by the scanning signal where reflected interference originates, also has finite dimensions. Therefore individual points on this surface will have slightly different radial velocities with respect to the radar station, and this different Doppler frequencies. As an example let us consider the influence of beam width. If the beam axis is directed at the angle Θ, then the radial velocity component is defined by formula 5.3.15, and the Doppler frequency at the beam axis is

$$f_D = \frac{2v_{st}}{\lambda}\cos\Theta, \qquad (5.3.16)$$

where λ - wavelength of the radar station.
For narrow beams we can write an approximate formule for the /97
width of beam "scatter" of Doppler frequencies in the form:

$$\Delta f_D = \Theta_0 \cdot \frac{d}{d\Theta}\left(\frac{2v_{st}}{\lambda}\cos\Theta\right) = \frac{2v_{st}\Theta_0}{\lambda}\cdot\sin\Theta, \qquad (5.3.17)$$

where Θ_0 - beam width.

The spectrum of interference is widest when the antenna is directed at a 90° angle with respect to airplace path [5.1, 5.39].

However, passive interference also enters the receiver through the side lobes of the antenna. Moreover, the spectrum of passive interference in the beam takes on a characteristic form. It can be determined by the method given in reference [5.40].

Let us note, on the basis of (5.3.15), that the geometric location of points with the same relative radial velo-

city with respect to the moving radar station is the surface of a cone with angle Θ. Therefore the surface of the terrain which reflects signals with Doppler frequencies between f_D and $f_D + \Delta f_D$, is limited by two parabolas; the participation of reflections from this surface in the spectrum of passive interference is represented by the shaded area in Fig. 5.3.9.

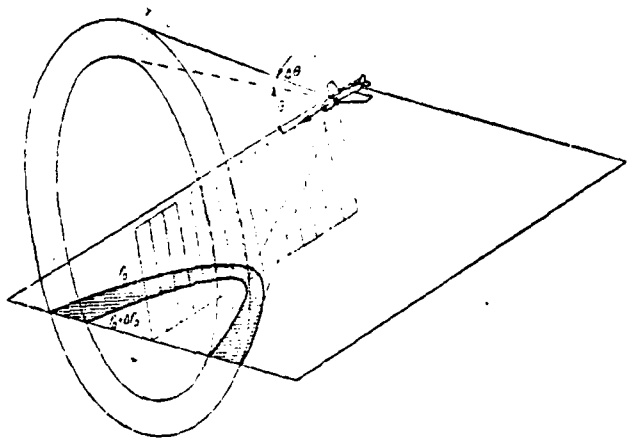

Fig. 5.3.9. Geometric location of reflecting points, giving a spectrum component with frequencies between f_D and $f_D + \Delta f_D$.

Starting from simple geometric relations and using the radar range formula, it is possible to calculate the shape of the spectrum of passive interference derived from field reflections. In order to do this it is necessary to know the antenna characteristic and reflection coefficient which defines the relation between geometrical and radar reflecting surface [5.40]. For a dry area the reflection coefficient is practically independent of the angle of radiowave incidence because of the scattered character of the reflection. In contrast, at the sea surface this coefficient depends strongly on the angle of incidence, as well as on the state of sea surface. Fig. 5.3.10 shows typical averaged graphs of the reflection coefficient; a more detailed discussion of this problem may be found in refs [5.1, 5.11, 5.15, 5.40-5.46]. /98

A typical shape of the spectrum of passive interference resulting from the motion of radar station with respect to interfering objects is shown in Fig. 5.3.11. As can be seen, the total spectrum width is $\frac{4v_{st}}{\lambda}$; ; the maximum spectrum den-

corresponds to the interference originating from the main leaflet of antenna characteristic [5.39].

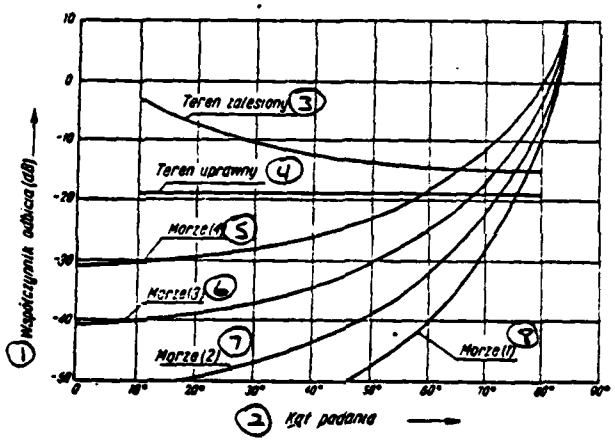

Fig. 5.3.10. Averaged graphs of the coefficient of reflection from terrain (state of the sea according to the scale of Douglas [5.11]. 1 - coefficient of reflection (dB), 2 - angle of incidence, 3 - forest area, 4 - cultivated area, 5 - sea (4), 6 - sea (3), 7 - sea (2), 8 - sea (1).

These remarks indicate the difficulties in obtaining effective reduction of stationary clutter in radar devices which are in motion. A more detailed analysis of the problem, contained in the works of George, Dickey and Urkowitz [5.47-5.49], allows to determine the theoretical effectiveness of MTI systems under these conditions. Fig. 5.3.12 represents a graph of theoretical stationary clutter reduction by an on-board aircraft radar station with the following parameters: width of antenna beam - 3°; antenna revolution rate - 12/min; /99
pulse length - 0.75μs; repetition frequency - 2kHz; flight altitude - appr. 6100m; velocity - appr. 460km/hr; MTI system with a single subtracting system. As seen from the figure,

the effectiveness of reduction depends largely on the direction, and varies by appr. 24dB (from 12dB to 36dB) [5.48].

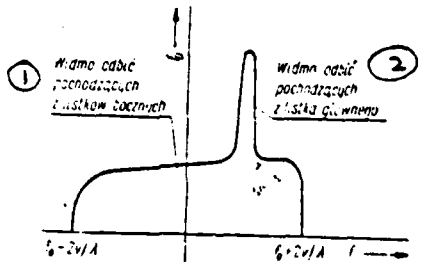

Fig. 5.3.11 Typical shape of the spectrum of passive interference caused by the movement of radar station with respect to the reflecting objects [5.39]. 1-spectrum of reflections from lateral lobes, 2-spectrum of reflections from the main lobe.

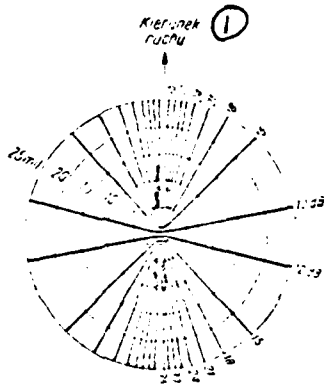

Fig. 5.3.12. Graph of stationary clutter reduction for an on-board radar station [5.48]. 1-direction of motion.

References.

5.1. Skolnik, M.I., Introduction to Radar Systems. New York, 1962.

5.2. Cole, C.F. Characteristics of Electromagnetic Wave Reflected from Moving Objects. J.Franklin Inst., June 1958.

5.3. Veinshtein, L.A., Zubakov, V.D. Signal selection on the background of random noise. Moscow, 1960.

5.4. Kroszczanski, J. Notes on some generalizations on modulation theory. Seminar given at the Inst. of El. Theor. IPPT PAN, 3/14/1955.

5.5. B.v.d. Pol, The Fundamental Principles of Frequency Modulation. JIEE, May 1946, Part IIIA.

5.6. Rubin, W.L., DiFranco, J.V. The Effect of Doppler Dispersion on Matched Filter Performance, PIRE, Oct. 1962.
5.7. Landau, L., Lifshitz, E. Field Theory. Moscow, 1951.
5.8. Temes, C.L. Relativistic Considerations of Doppler Shift. IRE Trans., ANE-6.
5.9. Bakulev, P.A. Radiolocation of Moving Targets. Moscow, 1964.
5.10. Swerling, P. Probability of Detection for Fluctuating Targets. IRE Trans., IT-6, April 1960, No. 2.
5.11. Povejsil, D.J., Raven, R.S., Waterman, P. Airborne Radar. New York, 1961.
5.12. Perov, V.P. Calculation of Radar Tracking Systems with Consideration of Random Actions. Leningrad, 1961.
5.13. Kroszczynski, J. On the Optimal Algorithm of Signal Reception in Correlated Interference. PIT Works, 1962, No. 37.
5.14. Kulikowski, J. Problems of Optimal Target Detection and Selection. Cand. Dissert., Moscow, 1959.
5.15. Kerr, D.E. Propagation of Short Radio Waves. New York, 1951.
5.16. Lawson, J.L., Uhlenbeck, G.E. Threshold Signals. New York, 1950.
5.17. Bauer, L.H., Sharp, C.E., Herring, R. Feasibility of study of chaff communication. IRE Intern. Conv. Rec., Part 8, 1962.
5.18. Zadeh, L.A., Correlation Functions and Power Spectra in Variable Networks. PIRE, Nov. 1950.
5.19. Gorelik, G.S. On the Theory of Radio Wave Dissipation in Wandering Nonuniformities. Radio Technika i Elektronika, No. 6, 1956.
5.20. Barlow, E.J. Doppler Radar. PIRE, April, 1949.
5.21. Grisetti, R. Santa, M.M., Kirkpatrick, G.M. Effect of Internal Fluctuations and Scanning on Clutter Attenuation in MTI Radar. IRE Trans., ANE-2, March, 1955.

5.22. Kroszczanski, J. Effectiveness of Radar Station Operation Reducing Stationary Clutter. Przeglad Telekomunikacyjny No. 7, 1958.
5.23. Ridenour, L.N. Radar System Engineering. New York, 1947.
5.24. Davenport, W.B., Root, W.L. An Introduction to the Theory of Random Signals and Noise. New York, 1957.
5.25. Campbell, G.A., Foster, R.M. Fourier Integrals for Practical Applications. New York, 1948.
5.26. Propert-Jones, J.R. The Radar Equation in Meteorology. Q.J. Roy Met. Soc., Oct. 1962.
5.27. Hall, W.N. Prediction of Pulse Radar Performance. PIRE, Feb. 1956.
5.28. Sajbel, A.G. Principles of Radar. Moscow, 1961.
5.29. Gunn, K.L.S., East, T.W.R. The Microwave Properties of Precipitation Particles. Q.J. Roy. Met. Soc., Oct. 1954.
5.30. Battan, J.J. Radar Meteorology. Univ. of Chicago Press, 1959.
5.31. Rider, G.D. Weather and Radar. The Marconi Review, Vol. XXVI, No. 149, II quarter 1963.
5.32. Wildi, M. Supression of radar fixed signals. Bull. SEV, No. 24, 1954.
5.33. Herold, H. Increasing noise separation in radar devices. NTZ, NTF-2, 1955.
5.34. Clapp, R.E. A Theoretical and Experimental Study of Radar Ground Return. MIT Rad. Lab. Rep., No. 1024, 1946.
5.35. Taylor, R.C. Terrain Return Measurements at X and K Band. IRE Natnl. Conv. Rec., Vol. 7, Part 1, 1959.
5.36. Peake, W.H. Theory of Radar Return from Terrain. IRE Natnl. Conv. Rec., Vol. 7, Part 1, 1959.
5.37. Shrader, W.M. Antenna Considerations for Surveillance Radar Systems. Technical Papers of the Seventh Annual East Coast Conf. on Aeronautical and Navigational Electronics, 1960.

5.38. Bakulev, P.A. Radar Methods of Selection of Moving Targets. Moscow, 1958.

5.39. Maguire, W.W. Application of Pulsed Doppler to Airborne Radar Systems. Proc. Natnl. Conf. on Aeronautical Electronics, 1958.

5.40. Coleman, S.D., Hetrich, G.R. Ground Clutter and its Calculation for Airborne Doppler Radar. Proc. 5th Conf. on Military Electronics, 1961.

5.41. Wiltse, J.C., Schlesigner, S.P., Johnson, C.M. Back-Scattering Characteristics of the Sea in the Region /101
from 10 to 50 kmc. PIRE, Feb. 1957.

5.42. Berger, F. The Design of Airborne Doppler Velocity Measuring Systems. IRE Trans., Vol. ANE-4, No. 4.

5.43. Grant, C.R., Yaplee, B.S. Back-Scattering from Water and Land at Centimetre and Millimetre Wavelengths. PIRE, July 1957.

5.44. Fried, W.R. Principles and Performance Analysis of Doppler Navigation Systems. IRE Trans., Vol. ANE-4, Dec. 1957.

5.45. Taylor, R.C. Terrain Return Measurements at X and K Band. IRE Natl. Conv. Rec., Part 1, 1959.

5.46. Peake, W.H. Theory of Radar Return from Terrain. IRE Natl. Conv. Rec, Part 1, 1959.

5.47. George, T.S. Fluctuations of Ground Clutter in Airborne Radar Equipment. Proc. IEE, Vol. 99, Part IV, No. 2, April 1952.

5.48. Dickey, F.R. Theoretical Performance of Airborne Moving Target Indicators. IRE Trans. PGAE-8, June 1953.

5.49. Urkowitz, H. Extension to the Theory of Performance of Airborne Moving Target Indicators. IRE Trans. Vol. ANE-5, Dec. 1958.

5.50. Mooney, D., Ralston, G. Performance in Clutter of Airborne Pulse MTI, CW Doppler and Pulse Doppler Radar. IRE Intern. Conv. Rec., Part 5, 1961.

6. The optimal reception algorithm. /102

On the basis of previous chapters we can begin to define the optimal signal location algorithm in the presence of passive interference. The optimization of reception is considered here in terms of making binary decisions, in accordance with the mathematical model discussed in Ch. 4.2.

One of the most important problems in this case in the determination of the structure of the optimal filter, defined by the integral equation (4.2.35) or (4.2.41) and (4.2.42).

Thus we will begin the consideration of the problem of the optimal reception algorithm by discussing methods, which may lead to an effective solution of the appropriate integral equations.

6.1 Solution of the basic integral equation.

As follows from considerations in Ch. 4., in considering the optimal reception algorithm it is important to obtain effective solutions of integral equations of the kind:

$$a(t) = \int_{t_1}^{t_2} \Gamma(t, t')\, g(t')\, dt'. \tag{6.1.1}$$

This is the so-called Fredholm equation of the first kind [6.1]. Before considering in more detail the optimal reception algorithm, we should spend some time on the outline of the methods for solving such equations.

An integral equation of this type may be solved by the general expansion method, using orthogonal function systems or orthogonalized function systems [6.1], or by other methods. E.G., for kernals $\Gamma(t,t')$ belonging to a certain higher class

of functions. A method is used which consists simply of solving some differential equation related to the initial equation [6.2, 6.3][1]. We will use here the method of orthogonal expansions, which simplifies the proof of the theorem of displacement for integral equations, and makes it possi- /103 ble to obtain simplified solutions. An outline of the method of solving integral Fredholm equations of the first kind with the help of orthogonal expansions is given in Appendix 3. In the applications described here, the kernals $\Gamma(t,t')$ are the autocorrelation functions of stationary stochastic processes. Taking advantage of the properties of the autocorrelation functions it is possible, as indicated in Appendix 3, to solve the basic integral equation using one of the best known orthogonal expansions, namely the Fourier expansion.

Equation (4.2.35) may also be rewritten in the equivalent form (cf. D.3.15):

$$\int_{-\infty}^{\infty} R(t-t')\, s_f^T(t')\, dt' = s(t-t_0), \tag{6.1.2}$$

where

$$0 < t < T, \quad T = |t_1 - t_2|,$$

$$s_f^T(t') = \begin{cases} s_f(t') & \text{dla } 0 < t' < T \\ 0 & \text{for other values of } t'. \end{cases}$$

Using Fourier transformation, we obtain the solution (see D.3.16-D.3.22):

$$s_f^T(t) = \int_{-j\infty}^{j\infty} S(p)\, e^{pt} \frac{dp}{2\pi j}, \tag{6.1.3}$$

where

[1] It should be mentioned that special computers have been constructed which allow the analog solution of similar equations [6.4], Ch. VII, §18).

$$S(p) = \frac{2S_r(p)}{W(p/2\pi j)} + 2\frac{X^{(+)}(p) + X^{(-)}(p)}{W(p/2\pi j)}, \qquad (6.1.4)$$

and $S_r(p) = \mathcal{F}\{s_r\}$; S_r is the so-called expanded function $s(t-t_o)$ - see D.3.16; W(p) is the spectral power density, corresponding to the autocorrelation function ($R(t-t')$, and functions $X^{(+)}$ and $X^{(-)}$ are defined by eqs. D.3.19, D.3.23 and D.3.24.

An effective solution of (6.1.2) using the method given above may be tedious because of the necessity of determining the functions $X^{(\pm)}$. Therefore it is worth exploring the possibility of finding simplified solutions. We consider below two methods which simplify the solution of this type of equations. One of them allows using the solutions for some functions in the case when we deal with narrow-band paths with envelopes having the form of these functions; the second method takes advantage of the special properties of the signals generated in the process of space scanning in order to obtain a simplified solution of (4.2.35).

The first of the methods described is of practical importance because the signals in radio- and sonar location represent narrow-band paths. Most often, they are pulse /104 series with carrying frequency f_o (see Ch. 1.2). A certain theorem can be proven, which simplifies the solution in the case of narrow-band paths, if the solution of the corresponding integral equation for the envelope is known. This dependence will be called the theorem of displacement for integral equation, formulated in the following way:

If s_f^T is a solution of the integral equation

$$\int_{-\infty}^{\infty} R(t-t')\, s_f^T(t')\, dt' = s(t-t_0), \tag{6.1.5}$$

then the integral equation

$$\frac{1}{2}\int_{-\infty}^{\infty} R(t-t')\cos\omega_0(t-t')\, s_{f0}^T(t')\, dt' = \\ = s(t-t_0)\,[A\cos\omega_0 t + B\sin\omega_0 t] \tag{6.1.6}$$

has a solution in the form

$$s_{f0}^T = s_f^T(t)\,[A\cos\omega_0 t + B\sin\omega_0 t] + \Delta(t), \tag{6.1.7}$$

where

$$\Delta(t) = \mathcal{F}^{-1}\{2(A-jB)\left[\frac{X^{(+)}(p+p_0)\,X^{(-)}(p+p_0)}{W(f-f)} + \right. \\ \left. + \frac{X^{(+)}(p-p_0)+X^{(-)}(p-p_0)}{W(f+f_0)}\right]. \tag{6.1.8}$$

The proof of the theorem of displacement is given in Appendix 4.

Dependence [6.1.7] should be discussed further. Except for the term $\Delta(t)$, this relation would mean simply that the modulation of signal $s(t)$ by a harmonic vibration results in a modulation of the transformed signal $s_f(t)$ with the same vibration. Since we are dealing here with narrow-band paths, one might think that the expression of the type $X^{(\pm)}(p\pm p_0)/W(f\mp f_0)$ can be approximately taken equal to zero. In the general case the appropriate terms of the solution $s_f^T(t)$ may, contain functions δ or their derivatives [6.4], and therefore the spectra $X^{(\pm)}(p)$ are not narrow-band.

The presence of the term $\Delta(t)$ in (6.1.7) can be easily interpreted as follows. If this term were absent, then the solution of (6.1.6) would not depend on the phase of the carrier vibration which corresponds to the integration limits. However, as seen from examples shown in Fig. 6.1.1, there may be boundary conditions very different from each other. Since expressions $X^{(+)}$ and $X^{(-)}$ appearing in the solution of the integral equation take into account precisely the effect of boundary conditions, the form of solution (6.1.7) becomes /105 understandable. We should add that in some practical applications (e.g. in pulse signals with duration time appropriately shorter than T) the effect of boundary conditions may be omitted and the term $\Delta(t)$ will then be absent.

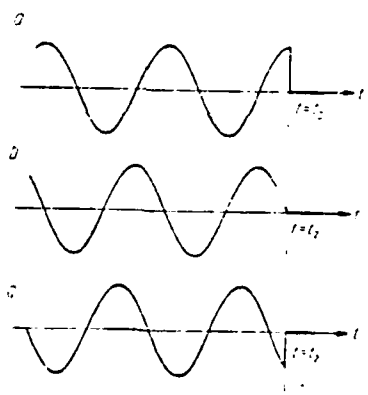

Fig. 6.1.1. Examples of changes of boundary condition at $t=t_2$, depending on the phase of the carrier vibration.

The theorem of displacement, proven above, has an important physical interpretation. It is related to the justification for using the so-called quadrature reception, utilized in technical signal detection systems with correlated interference. Quadrature reception consists in applying two receiving channels and a local generator, which gives two vibrations differing in phase by $\frac{\pi}{2}$. Considerations of the paths shown in Fig. 6.1.1 have a physical interpretation in

the form of transition states, which appear in systems of signal displacement to the zero frequency. The question of quadrature reception will be considered below in Ch. 7, where realization of optimal reception systems is discussed.

Now we will turn to the discussion of the solution of the basic integral equation using the specific properties of the signals generated in the course of space scanning.

In the preface to this chapter (and in Ch. 4) we assumed a finite interval $t_2 - t_1 = T$. This is related to one of the basic difficulties in solving the basic integral equation, namely determination of the appropriate functions $X^{(+)}$ and $X^{(-)}$ (see Appendix 3).

However, as follows from Ch. 5.1., in the case of location, the reception of signals from detected objects occurs in a manner defined by the characteristics of the directional beam, which scans the space being scanned. The echo signal then has the form shown in Fig. 6.1.2, i.e. the infinite series of scan- /106
ning pulses is "modulated" by a function defined by the directional characteristic of the antenna (see 5.1.6). In system considerations we usually assume an approximation of this function using a Gauss function [6.5-6.8].

This may be interpreted as if signal reception took place for infinite limits, but with a weight function (imposed by the characteristics of scanning) of such a character that in many cases a finite time of echo duration is assumed.

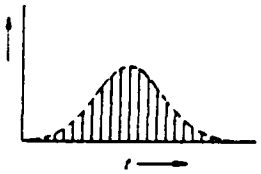

Fig. 6.1.2. Echo pulses reflected form object.

Fig. 6.1.3. Perpendicular pulse "packet".

Thus it is often assumed in the literature that the shape of the echo signal envelope is simplified, and corresponds to the sectional directional antenna characteristic [Fig. 6.1.3]. This simplifies certain considerations, since all pulses then have the same amplitude. A notion of the effective quantity of pulses is also applied in this connection, i.e. a number of pulses with the same amplitude, which is equivalent to a signal with a shape similar to that shown in Fig. 6.1.2 (cf. [6.5]).

Undoubtedly a more realistic model of the signal will be obtained, by taking into account the shape of the echo signal envelope resulting from the continuous scanning process.

Thus if we denote this type of signal by $s_a(t-t_o)$, the integral equation in question may be written as follows:

$$\int_{-\infty}^{\infty} R(t-t')\, s_{fa}(t')\, dt' = s_a(t-t_0). \qquad (6.1.9)$$

Using the Fourier transformation on both sides of (6.1.9) we will obtain:

$$S(f) = \frac{S_s^*(f)}{W(f)} e^{-j(2\pi f t_0)}, \qquad (6.1.10)$$

where $S(f) = \mathcal{F}\{s_{fa}(t)\}$, $S_s(f) = \mathcal{F}\{s_a(t)\}$, $S_s^*(f)$ - spectrum coupled with $S_s(f)$.

Relation (6.1.10) directly defines the characteristic of an optimal filter, as shown in Ch. 1.3. This relation has a similar form as that for a "matched filter" (Ch. 4.2.); we /107 should remember, however, that $s_a(t)$ is not an individual echo pulse, but a series of such pulses (Fig. 6.1.2).

We should mention briefly the problem of the physical realizability of the filter defined by (6.1.10). It is easy to see that for $t_o=0$ such a filter cannot be realized, because its

pulse response would not be zero for $t < 0$[1]. However, by selecting appropriately large values for t_o it is possible to approach the realization of optimal filter characteristics using systems that are physically feasible. There is some formal similarity with the method of Bode-Shannon, used in problems of filtration and prediction [6.9], which involves solving a similar equation. However, using filters with a very large delay would not be useful in filtration and prediction, because in systems of automatic regulation this could cause de-actualization of data. In contrast, in systems of signal selection with passive interference, the situation is usually different. The delay time t_o in this case has a concrete physical interpretation. Since passive interference is usually strongly correlated, the filters used in appropriate detection systems are most often composed of delay lines, with the delay equal to the period of repetition of the scanning pulses (see 2.5 and Ch. 8). Approximation of a given characteristic by systems of delay elements in general requires the use of a greater number of such elements for more accurate approximations [6.11]. Use of a greater number of delay lines causes an appropriate increase of the overall delay introduced by the system. This results in the requirement for introducing an appropriately long time t_o in ideal approximation of filter characteristic by physical systems.

We may add that in devices used in detection it is usually not important if there are delays between the echo signal arri-

[1]This is because both $S_s(f)$ and $W(f)$ are usually symmetrical functions, and the pulse response of the filter is defined by an inverse Fourier transform to (6.1.10). Of course, a condition of filter realizability could be imposed by requiring appropriate transfer functions without poles in the right half of complex plane (as in optimal filtration theory, see 6.10). This would probably be an indirect method, apparently not having any advantage compared to solving the integral equation directly; see also below concerning specific properties of filters realized using delay elements.

val and its imaging, as long as the delay is of the order of 1 sec. There are devices that consciously use this fact, large screen projectors, which display the image-using film; these devices introduce a delay of 5 sec or more ([6.5, 6.12]). Meanwhile, modern technology allows the use of at most 2-3 delay elements in filter systems [6.13 - 6.15]. Thus, the /108 overall delay of practical filters t_{po} is smaller than several times the repetition periods of scanning pulses. In radar detection devices the pulse repetition period is of the order of 1-10mS, and therefore t_{po} would be of the order of several to several tens of milliseconds. Even for airplanes with velocities of 2500km/hr the interval traveled in the time t_{po} would thus be of the order of 1-10 m, while the accuracy of distance measurement by stations for target detection is of the order of 1 km.

As indicated by the above considerations, the method discussed in this chapter leads to a considerable simplification of the solution of the basic integral equation, and its assumptions are justified by the properties of the process of space scanning, used in location. Equation (6.1.10) is of course especially useful when we are interested primarily in the filter characteristic as a function of frequency.

Let us consider in more detail relation (6.1.10). Spectrum W(f) is composed of a spectrum of heat noise with a constant spectral density W_o and of a spectrum of passive interference $W_p(f)$. The latter depends, as described in Ch. 5, both on the properties of the scanning signal and on the reflecting objects which are the source of passive interference.

As shown in Ch. 5.3, the autocorrelation function of passive interference $R(\tau)$ is defined by the formula:

$$R(\tau) = R_s^0(\tau) \cdot R_A(\tau) \cdot R_p(\tau) \cdot \cos(2\pi f_s \tau). \qquad (6.1.11)$$

where $R_s^0(\tau), R_A(\tau), R_p(\tau)$ are autocorrelation functions of: envelope of the scanning signal, modulation of the echo signal resulting from space scanning by the directional antenna, fluctuation of passive interference, respectively (cf. eq. 5.3.7). Denoting the product of functions R_s^0 and R_A by R_s, we can write:

$$\mathcal{F}\{R(\tau)\} = \mathcal{F}\{R_s(\tau)\, R_p(\tau)\} = \mathcal{F}\{R_s(\tau)\} * \mathcal{F}\{R_p(\tau)\}, \qquad (6.1.12)$$

where sign * denotes the operation of convolution[1]. Further, on the basis of the theorem of Wiener-Chinchin [6.4] we have:

$$\mathcal{F}\{R(\tau)\} = W(f), \qquad (6.1.13a)$$
$$\mathcal{F}\{R_s(\tau)\} = W_s(f), \qquad (6.1.13b)$$
$$\mathcal{F}\{R_p(\tau)\} = W_p(f), \qquad (6.1.13c)$$

where $W_p(f)$ denotes the power spectrum of fluctuations of passive interference.

Substituting (6.1.12) and (6.1.13 abc) into (6.1.10) we obtain:

$$S_{opt}(f) = \frac{S_s^*(f)}{W_0 + W_s(f) * W_p(f)} \cdot e^{-j2\pi f t_0} \qquad (6.1.14)$$

This relation defines the characteristic of the optimal filter /109
(with assumptions given above) under conditions of both correlated and non-correlated Gaussian interference. (6.1.14) will be used below as one of the basic relations in determining the characteristics of ideal filters in the case of coherent signals (see Ch. 7.3).

Analogous considerations concerning the simplified method

[1]See footnote to (5.3.6).

of solution may be also applied to (4.2.41) (the case of stochastic signals; cf. relation (6.2.19) below).

6.2. Optimal algorithm of signal reception for correlated interference.

Based on previous considerations, it is possible to determine the optimal algorithm of signal reception in the presence of correlated interference. An interesting aspect of this question will be the structure of the optimal receiver realizing the appropriate signal processing.

We will first consider the echo signal represented as follows:

$$s(t; \vartheta_1; \vartheta_2; f_s) = \vartheta_1 A(t) \cos(2\pi f_s t - \vartheta_2). \tag{6.2.1}$$

In this equation A(t) is the function describing the envelope of an echo pulse packet; ϑ_1, ϑ_2 are passive parameters which take into account the effect of signal fluctuation. It is assumed that the fluctuations are sufficiently slow to be taken as occurring between packets[1] (see Ch. 5). These assumptions are usually justified in the case of echoes for which the duration time of a packet is smaller than the correlation time of the reflected signal, e.g., for echoes from small jet planes.

Thus in this case we can talk of a coherent pulse packet. In terms of detection this is a typical example of a signal with passive parameters. Such parameters are here: ϑ_1, ϑ_2 and f_s. The last quantity is a passive parameter in the sense

[1] We consider the optimalization of a pulse packet reception, but not the reception between packets. The latter problem is related to different problems than the ones considered here. They are connected with the methods of so-called track while scan, TWS [6.17].

$f_s = f_w + f_D$, where f_w is the known carrier frequency of scanning signals, and f_D is the Doppler frequency which in most radar applications must be considered unknown.

Let us assume for a moment that f_D is known. In this case we deal with reception of a coherent pulse packet with an unknown initial phase, with the possibility of fluctuation between packets.

As represented in Ch. 4, in order to define the optimal algorithm for receiving signals with passive parameters we /110
determine the conditional probability:

$$P[s(\Theta_1; \dots \Theta_k \dots \Theta_n)|y] = \int_{\Theta_1} \dots \int_{\Theta_k} \dots \int_{\Theta_n} p[s(\vartheta_1; \dots \vartheta_k \dots \vartheta_n)|y], \\ dP_{\Theta_1} \dots dP_{\Theta_k} \dots dP_{\Theta_n}, \qquad (6.2.2)$$

where

$P[s(\Theta_1 \dots \Theta_k \dots \Theta_n)|y]$ - probability that signal s with unknown parameters $\vartheta_1 \in \Theta_1 \dots \vartheta_k \in \Theta_k \dots \vartheta_n \in \Theta_n$ was transmitted;

$P[s(\vartheta_1 \dots \vartheta_k \dots \vartheta_n)y|]$ - probability that signal s with defined values of parameters $\vartheta_1 \dots \vartheta_k \dots \vartheta_n$ was transmitted;

P_{Θ_k} - probability distribution of parameter ϑ_k in space Θ_k .

At the start we will determine the relationships for the case of signals with a defined amplitude and frequency, which may be written as follows:

$$s(t; \vartheta_2) = A(t) \cos(2\pi f_s t + \varphi + \vartheta_2). \qquad (6.2.3)$$

In accordance with Ch. 5. it is assumed that:

$$p(\vartheta_2) = \begin{cases} \frac{1}{2\pi}, & 0 \leqslant \vartheta_2 \leqslant 2\pi \\ 0, & \vartheta_2 < 0, \vartheta_2 > 2\pi. \end{cases} \qquad (6.2.4)$$

As shown in Ch. 4 (4.2.31):

$$\ln P(s \mid y) = \ln C + \ln P(s) - \frac{1}{2}\int_{t_1}^{t_2} s(t)\, s_{f0}(t)\, dt + \int_{t_1}^{t_2} y(t)\, s_{f0}(t)\, dt, \tag{6.2.5}$$

and the first integral in this equation is proportional to the signal energy. The optimal reception algorithm with interference is thus defined only by the second integral. We have used the notation s_{f_0} because the signal is narrow-band, with known carrier frequency (see previous chapter). From the assumption of narrow-band nature of the signal and because of the theorem of displacement (6.1.7, see also Appendix 4) it follows that:

$$s_{f0}(t) = s_f(t) \cos(2\pi f_s t + \varphi + \vartheta_2), \tag{6.2.6}$$

where s_1 - solution of the basic integral equation for the envelope. Since ([6.18], eq. 6.4.11):

$$\frac{1}{2\pi}\int_0^{2\pi}\left\{\exp\left[\int_{t_1}^{t_2} y(t)\, s_f(t) \cos(2\pi f_s t + \varphi + \vartheta_2)\, dt\right]\right\} d\vartheta_2 = I_0[\eta(y)], \tag{6.2.7}$$

where I_0 denotes the modified Bessel function of the zeroth /111
order, and

$$\eta(y) = \sqrt{\mu_c^2(y) + \mu_s^2(y)}, \tag{6.2.8}$$

$$\mu_c(y) = \int_{t_1}^{t_2} y(t)\, s_f(t) \cos(2\pi f_s t)\, dt, \tag{6.2.9a}$$

$$\mu_s(y) = \int_{t_1}^{t_2} y(t)\, s_f(t) \sin(2\pi f_s t)\, dt, \tag{6.2.9b}$$

Because of the unequivocal relation between echo signal and information (see remarks before (4.2.17)) we obtain as a result:

$$\ln P(x_2 \mid y) = \text{const} + \ln I_0[\eta(y)]. \tag{6.2.10}$$

Since function ln I_o is monotonic, the problem of optimal reception is reduced mainly to the calculation of functional [6.19].

On the basis of these considerations, especially eqs. (6.2.8), (6.2.9 ab) and (6.2.10), it is possible to define a system realizing the optimal reception algorithm in the case of a signal of the type (6.2.3). A diagram of such a system is shown in Fig. 6.2.1.

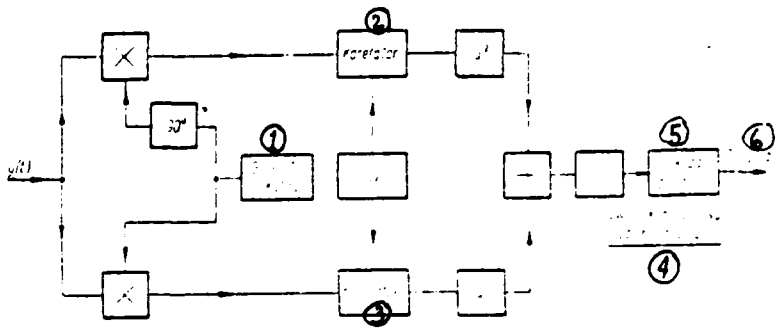

Fig. 6.2.1. Optimal receiver with known f_D. 1 - Local generator, 2 - Correlator, 3 - Correlator, 4 - Nonlinear quadrupole (without inertia), 5 - Threshold system, 6 - Decision.

The correlators appearing in this system may be replaced, in accordance with the considerations at the end of Ch. 4.2, by appropriate linear filters. We will then obtain an equivalent optimal system in the form shown in Fig. 6.2.2.

These systems are called quadrature signal reception systems, since signals differing by 90° in phase (quadrature signals) or two-channel systems [6.20] are used. A third system, equivalent to the previous ones, can also be presented. This system is shown in Fig. 6.2.3. It differs from the system in Fig. 6.2.2 in that the role of quadrature terms, two visual filters, and systems adding the squares of signals originating /112

from each channel is carried out by a single filter and an envelope detector. But this filter differs from filters in Fig. 6.2.2 because it is a high-frequency filter. Its characteristic is defined by (6.1.13). In addition, the characteristics of filters in Fig. 6.2.2 are displaced to the zero frequency by the characteristics of filter in Fig. 6.2.3.

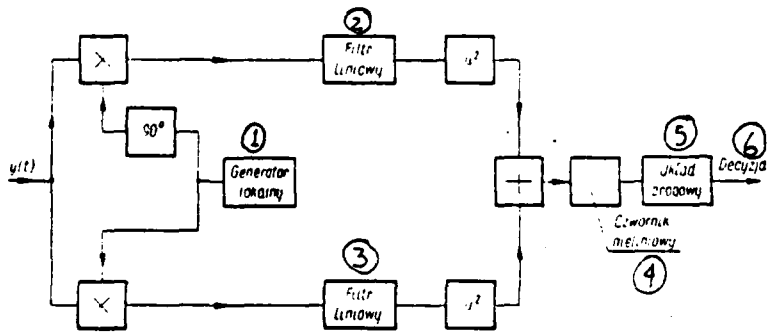

Fig. 6.2.2. Equivalent realization of optimal receiver with known f_D. 1. Local generator, 2. Linear filter, 3. Linear filter, 4. Nonlinear quadruple, 5. Threshold system, 6. Decision.

The diagram shown in Fig. 6.2.3 corresponds in practice to the so-called system of stationary clutter reduction at the intermediate frequency.

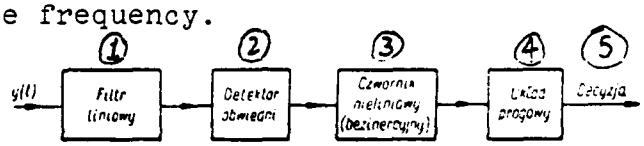

Fig. 6.2.3. Equivalent form of systems from Figs. 6.2.1. and 6.2.2. 1. Linear filter, 2. Envelope detector, 3. Nonlinear quadruple (without inertia), 4. Threshold system, 5. Decision.

In the case when the signal exhibits amplitude fluctuations in addition to phase fluctuations, it may be represented in the form:

$$s(t;\, \vartheta_1;\, \vartheta_2) = \vartheta_1 A(t) \cos(2\pi f_0 t + \varphi + \vartheta_2). \qquad (6.2.11)$$

Taking the assumptions which follow from Ch. 5, the random variables ϑ_1 and ϑ_2 will be defined as follows:

1. random variable ϑ_1 has the Rayleigh distribution:

$$p_1(\vartheta_1) = \begin{cases} \frac{1}{\sigma^2} \exp\left(-\frac{\vartheta_1^2}{2\sigma^2}\right), & \vartheta_1 \geq 0 \\ 0 & \vartheta_1 < 0 \end{cases} \tag{6.2.12}$$

2. Random variable ϑ_2 has the uniform distribution

$$p_2(\vartheta_2) = \begin{cases} \frac{1}{2\pi}, & 0 \leq \vartheta_2 \leq 2\pi \\ 0, & \vartheta_2 < 0;\ \vartheta_2 > 0. \end{cases} \tag{6.2.13}$$

The mean value of signal amplitude fluctuations is equal in this case to $\sigma\sqrt{\frac{\pi}{2}}$.

On the basis of (6.2.2) and (6.2.5), using (6.2.7) and substituting (6.2.12) and (6.2.13), we can write:

$$\ln P(x_2, y) = \text{const} - \int_0^\infty \frac{\vartheta_1}{\sigma^2} e^{-\frac{\vartheta_1^2}{2\sigma^2}} \cdot I_0(\vartheta_1 y)\, d\vartheta_1. \tag{6.2.14}$$

The integral appearing in the above formula is the so-called Weber integral; using its known solution [6.21], we finally obtain:

$$\ln P(x_2, y) = \text{const} - C[\eta(y)]^2, \tag{6.2.15}$$

where C denotes a constant proportional to the mean signal energy, while $\eta(y)$ has a meaning analogous to that in (6.2.8) [6.19, 6.20].

Comparing (6.2.10) and (6.2.15) we can note that the

systems realizing the optimal signal reception algorithm in the form (6.2.11) are similar to those considered previously for a signal of type (6.2.3); the difference is only in a different nonlinear treatment. Thus the systems of optimal reception of signals with phase and amplitude fluctuations can be represented in a form similar to Fig. 6.2.1-6.2.3. In the system corresponding to Fig. 6.2.3 we can assume in this case that the detector has a characteristic of type u^2 (cf. also [6.20].

This difference is not very important in the case of weak signals because, as we know [6.18]:

$$\ln I_0(x) = \frac{x^2}{4} - \frac{x^4}{64} + o(x^6), \quad x < 1.$$

We should mention that in practice often systems are introduced in which the characteristics of some elements differ from the optimal; this is caused by attempts to simplify the device. Of course this leads to some decrease of detectability. An analysis of a suboptimal system in which one channel of the quadrature system has been omitted, was given by Veinshtein and Zubakov [6.20]. Such systems have been used in the first devices which used the correlation of passive interference for detecting signals in its presence [6.5, 6.22, 6.23].

The case of replacing the optimal addition of quadrature /114
signals by modulus addition was considered by Mitiashev [6.24].

If $f_s = f_w \pm f_D$ is also a passive parameter, then according to (6.2.2) and utilizing (6.2.10) and (6.2.15), the conditional probability should be averaged according to f_D, creating expressions like:

$$\int_{\Omega_D} p(f_D) \exp[\lambda(\eta)] d\Omega_D, \tag{6.2.16}$$

where

$p(f_D)$ - probability that a signal with Doppler frequency f_D had been transmitted;

Ω_D - set of possible Doppler frequencies, and

$$\lambda(\eta) = \begin{cases} I_0[\eta(y)] & \text{for signals of given amplitude} \\ C[\eta(y)]^2 & \text{for fluctuating signals} \end{cases} \tag{6.2.17}$$

The question of determining expressions of type (6.2.16) is difficult. The kind of functions appearing here does not allow to reduce such an expression to a form permitting a simple technical realization; it is only possible to model operation (6.2.16) approximately with the help of appropriate systems ([6.25,] p. 151; see also [6.26]). It is easy to grasp the essence of these problems by considering the case when f_D can have a finite number of values: $f_D = f_1, f_2, \dots f_k, \dots f_n$. The probability distribution $p(f_D)$ is then of discontinuous type. Therefore we have finite probabilities $p_1 = p(f_D = f_1), p_2, \dots p_k = p(f_D = f_k), \dots p_n$. It is easy to note that averaging according to f_D consists of generating an appropriate sum of terms similar to those in the case of known Doppler frequency, but with weights $p_1, \dots p_k, \dots p_n$ [6.25]. In the case of uniform distribution of Doppler frequency probabilities in some interval (the justification of such an assumption is discussed in Ch. 5), $p_1 = p_k = p_n$. Then averaging according to f_D is obviously reduced systematically to appropriate parallel combination of terms, each of which would represent a system similar to that of Fig. 6.2.1 (or its equivalent - as in Fig. 6.2.2 or 6.2.3), optimal for the appropriate Doppler frequency f_k. We will obtain in this case a system shown in Fig. 6.2.4.

An important aspect of this diagram is the parallel connection of elements, consisting of linear filter and nonlinear element connected in series. The possibility of ideal replacement of this sytem by a simpler substitute diagram, composed of

one linear filter with "average" frequency characteristic and one nonlinear element is not known [6.25]. What remains then is the option of optimizing the number of parallel channels of filters and their appropriate formation. Similar questions have been raised in the literature [6.27-6.30, 6.37].

In some practical realizations there is a possibility of /115
reducing the number of filters by using sequential systems [6.31].

A method of multichannel coherent detection approximation was given by Reed and Swerling [6.38]. In this system it is theoretically possible to obtain an arbitrarily close approximation by using iteration methods. The corresponding reception system does not contain a set of narrow-band filters, but many multiplying and delay systems. Their number increase for the more accurate approximation of coherent detection desired [6.38][1].

The optimization of reception systems for signals between the coherent and noncoherent class, i.e. for signals with some phase fluctuations, was considered (for the case of known frequency of the scanning signal) in Kulikowski's work [6.32]. For noncorrelated phase fluctuations such systems may be realized in a finite form, containing quadrature systems and some correction terms.

In the case of correlated phase fluctuations in finite form it is possible only to realize reception systems for weak phase fluctuations [6.32].

Let us now consider the case when the echo signal has random phase fluctuations, among which it is impossible to select

[1]Some other possibilities of realization were also mentioned in Ch. 10.3.

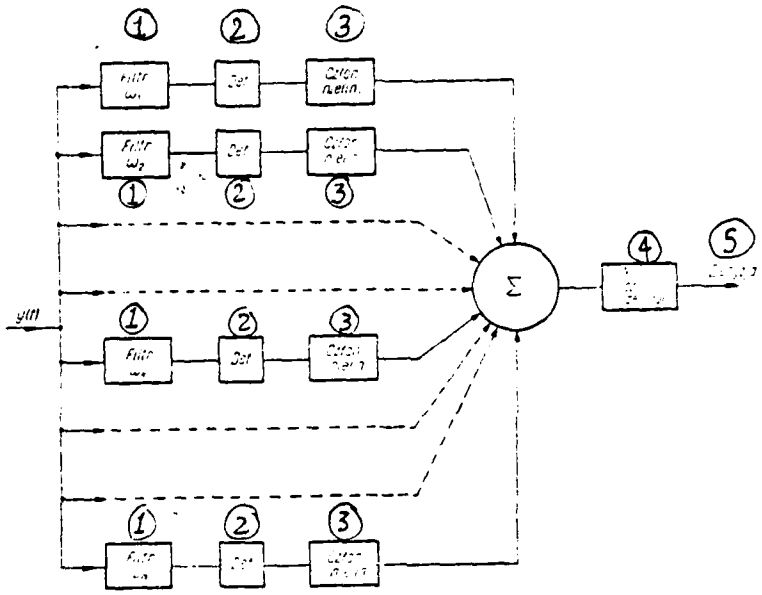

Fig. 6.2.4. Optimal reception system with unknown f_D. 1. Filter, 2. Detector, 3. Nonlinear term, 4. Nonlinear decision term, 5. Decision.

a regular component caused by the Doppler effect[1]. Such signals, as mentioned above (see Ch. 4 and 5), may be considered as a realization of a general signal representing a stochastic process, using the methods described in Ch. 4.2 for optimization of reception systems.

In considering this question we will use the method where the filter "whites out" the interference spectrum, which allows utilizing the results obtained with the assumption that interference has the form of white noise. This method consists in determining the characteristic of the filter correcting the power spectrum of real interference such that it becomes a spec-

[1]Note that this applies only to the detected signal and is caused by the reflecting properties of objects considered here. In contrast, further considerations assume a coherent scanning signal, which is related to appropriate characteristics of passive interference.

trum with a uniform density (and therefore identical to the spectrum of white noise). It is possible in turn to use the methods and results of determination of the optimal reception algorithm in the presence of white noise[1].

As is easily seen, in the case considered, the modulus of the frequency characteristic of the "whiting out" filter is defined by the relation:

$$F_w(f) = \left| \frac{W_0}{W_0 + W_z(f)} \right|^{1/2}, \tag{6.2.18}$$

where

W_0 - spectral density of noncorrelated noise;

$W_z(f)$ - spectral density of correlated interference.

It should be remembered of course that the "whiting out" filter also modifies the signal spectrum, which will be taken into account in later considerations.

The system realizing the optimal reception algorithm may be represented in this case, in accordance with Ch. 4.2 and the above remarks, in the form shown in Fig. 6.2.5[2]. The characteristic of the second linear filter remains to be determined here. As shown in Ch. 4.2, it is possible to determine it with the help of appropriate integral equations.

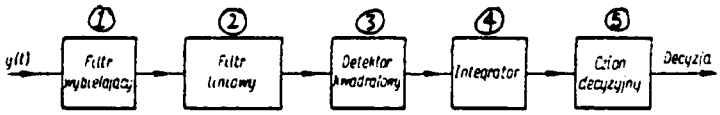

Fig. 6.2.5. Optimal receiver for stochastic signals. 1. whiting out filter; 2. linear filter; 3. quadratic detector; 4. integrator; 5. decision term; 6. decision.

---

[1]The justification of the method of "whiting out" filter is given in Chapter 3 of the book by Gutkin [6.33].

[2]Some specific aspects of integrator operation in this system are described in Appendix 7.

Taking into account the specific properties of the paths /117
that have to be considered in location problems, we can introduce simplifying assumptions, identical to those described in the previous chapter. Equation (4.2.42) can then be rewritten in the form:

$$\int_{-\infty}^{\infty} [R_s'(t - t'') + W_0\delta(t - t'')]\varkappa(t' - t'')\,dt'' = R_s(t - t'), \qquad (6.2.19)$$

where R_s' - autocorrelation function of the signal at the output of the "whiting out" filter.

Using the Fourier transform on both sides of the above equation, we will obtain:

$$\mathcal{F}\{\varkappa(\cdot)\} = \frac{W_s'(f)}{W_0 + W_s'(f)}, \qquad (6.2.20)$$

where $W_s(f)$ - power spectrum of the signal after passing through the "whiting out" filter.

Since, as indicated by (4.2.41) (see also [6.34]):

$$|F_{opt}^{(2)}(f)|^2 = \mathcal{F}\{\varkappa(t' - t'')\}, \qquad (6.2.21)$$

finally, the modulus of the transfer function of the second filter will have the form:

$$|F_{opt}^{(2)}(f)| = \left\{\frac{W_s'(f)}{W_0 + W_s'(f)}\right\}^{1/2}. \qquad (6.2.22)$$

On the basis of these considerations it is thus possible to determine the modulus of the effective transfer function of an optimal filter, for conditions where both correlated and non-correlated interference is present, when a stochastic signal is being detected.

This filter includes (Fig. 6.2.6) two serially connected filters: a "whiting out" filter and an optimal filter for reception in noncorrelated interference, so that the modulus of its transfer function can be defined by the formula:

$$|F_{opt}(f)| = |F_w(f)| \cdot |F^{(2)}_{opt}(f)| \qquad (6.2.23)$$

Because $W'_s(f) = W_s \cdot |F_w(f)|^2$, substituting (6.2.18) and (6.2.22) into (6.2.23) we will obtain:

$$|F^{(2)}_{opt}(f)| = \sqrt{\frac{W_0}{W_0 + W_z(f)}} \sqrt{\frac{W_s(f) \dfrac{W_0}{W_0 - W_z(f)}}{W_0 + W_s(f) \dfrac{W_0}{W_0 + W_z(f)}}} \qquad (6.2.24)$$

PAGES 118 and 119 MISSING FROM ORIGINAL

References /120

6.1. Morse, P.M., and Feshbach, H. Methods of Theoretical Physics New York, 1953.

6.2. Davenport, W.B., Root, W.L. An Introduction to the Theory of Random Signals and Noise. New York, 1958.

6.3. Zadeh, L., Ragazzini, J.R. An Extension of Wieners Theory of Prediction. Journ. Apply. Phys., July, 1950.

6.4. Solodovnikov, V.V. Statistical Dynamics of Linear Systems of Automatic Tracking. Moscow, 1960.

6.5. Ridenour, L.N. Radar System Engineering. New York, 1947.

6.6. Blake, L.V. The Effective Number of Pulses per Beamwidth for a Scanning Radar. PIRE, June 1953.

6.7. Enstrom, R.A. The Effects of Noise on a Stacked Beam Height Finding Radar. IRE Conf. Proc. on Military Electronics, 1959.

6.8. Levine, D. Maximum Antenna Gain of Shaped Beams. J. Franklin Inst., March 1961.

6.9. Bode, H.W. A Simplified Derivation of Linear Least-Square Smoothing and Prediction Theory. PIRE, April, 1950.

6.10. Kulikowski, R. Introduction to the Synthesis of Linear Electric Systems. PWN, 1957.

6.11. Urkowitz,H. Analysis and Synthesis of Delay Line Periodic Filters. IRE Trans. on Circuit Theory, June 1957.

6.12. Kelvin-Hughes: Rapid Processing Photographic Projector (prospectus, 1960).

6.13. White, W.D., Rubin, A.E. Recent Advances in the Synthesis of Comb Filters. IRE Conv. Rec. Part 2, 1957.

6.14. Moltz, K.F. AN/FPN-34 Air Traffic Control Radar. Proc. of the 5th East Coast Conf., 1958.

6.15. Shrader, W.N. Reducing Clutter in Air Route Surveillance Radar. Electronics, 26th Jan. 1962.

6.16. Kroszczanski, J. Effective operation of radar stations reducing stationary clutter. przeglad Telekomunikacyjny, No. 7, 1958.

6.17. Clergue, J. Automatic Tracking System for Discontinuous Informations. L'onde Electrique, No. 386, May 1959.

6.18. Rizhik, I.M. Tables of Integrals, Sums, Radii. Moscow, 1951.

6.19. Seidler, J. Statistical Theory of Signal Reception. PWN, 1963.

6.20. Veinshtein, L.A. Zubakov, V.D. Signal Selection Against a Background of Random Noise. Moscow, 1960.

6.21. Lebedev, M.N. Special Functions and Their Applications. Moscow, 1953.

6.22. Kroszczanski, J., Grzenkiewicz, I. Reduction of Stationary Clutter in Radar. Przeglad Telekomunicacyjny, No. 11, 1957.

6.23. Bakulev, A. Radolocation of Moving Targets. Moscow, 1964.

6.24. Mitiashev. B.N. On the Resistance to Noise of Two Methods of Pulse Signal Reception. Radiotechnika i Electronika, No. 5, 1961.

6.25. Falkovich, C.E. Reception of Radar Signals Against a Background of Fluctuating Noise. Moscow, 1961.

6.26. Drenick, R.F., Gartenhouse, S., Nesbeda, P. Detection of Coherent and Non-coherent Signals. IRE Conv. Rec., Part 4, 1955.

6.27. Miller, K.S., Bernstein, R.I. Analysis of Coherent Integration and its Application to Signal Detection. IRE Trans., IT-3, Dec. 1957.

6.28. Galejs, J., Cowan, W.M. Interchannel Correlation in a Bank of Parallel Filters. IRE Trans., IT-5, Sept. 1959.

6.29. Brookner, E., Flink, J. Coherent Enhancer for Pulse Radar Applications. IRE Conv. Rec., Part 8, 1960. /121

6.30. Tartakowski et al. Problems of Statistical Radar Theory. Moscow, 1963.

6.31. Galvin, A.A. A Sequential Detection System for the Processing of Radar Returns. PIRE, Sept. 1961.

6.32. Kulikowski, J. On the Optimal Method of Reception in the Presence of Phase Interference. PIT Works, No. 34, 1961.

6.33. Gutkin, L.S. The Theory of Optimal Radar Reception Methods in Fluctuating Noise. Moscow, 1961.

6.34. Middleton, D. On the Detection of Stochastic Signals in Additive Normal Noise. IRE Trans. on Inf. Theory, IT-3, June 1957.

6.35. Slepian, D. Some Comments on the Detection of Gaussian Signals in Gaussian Noise. IRE Trans. on Inf. Theory, IT-4, March 1958.

6.36. Middleton, D. On Singular and Nonsingular Optimum (Bayes) Tests for the Detection of Normal Stochastic Signals in Normal Noise. IRE Trans. on Inf. Theory, IT-7, April 1961.

6.37. Lerner, R.M. A Matched Filter Detection System for Complicated Doppler Shifted Signals. IRE Trans., IT-6, June 1960.

6.38. Reed, I.S., Swerling, P. Filterless Approximations of Kth Order to Coherent Detection. IRE Trans., IT-8, April 1962.

7. Characteristics of optimal filters. /122

In previous chapters we have defined the optimal algorithm for reception of fluctuating signals with correlated interference and we have presented the systems realizing optimal reception. As indicated by the considerations above, an important role is played in these systems by the nonlinear predetection filter. We will discuss below the characteristics of such filters in detail; in order to determine their characteristics we have to consider the spectra of signals and of interference.

7.1. Signal and interference spectra.

The signal in radar applications is usually a series of short pulses (cf. Ch. 2 and 3). Let us denote the spectrum of an individual scanning pulse by $S_1(f)$. As we know, the spectrum of a coherent series of such pulses, repeating periodically, is represented in the form of a sum of the Dirac function δ ([7.1], [7.2], Ch. 5):

$$S_0(f) = \frac{1}{T_p} \sum_{n=-\infty}^{\infty} S_1(f)\, \delta(f - nf_p), \tag{7.1.1}$$

where T_p - period of pulse repetition; $f_p = \frac{1}{T_p}$ [1].

If, in turn, the series of pulses is modulated by the path corresponding to the directional antenna characteristic in the course of space scanning, then we can write the following on the basis of the theorem of modulation [7.3].

[1] It is easy to see that (7.1.1) represents a Fourier series for an infinite series of periodically repeating pulses, written in a manner stressing the relation with the spectrum of an individual pulse.

$$S_e(f) = \sum_{n=-\infty}^{\infty} S_A(f - nf_p)\, S_1(nf_p) \qquad (7.1.2)$$

where $S_A(f)$ denotes the modulation spectrum generated by space scanning using an antenna with directional characteristic (see Ch. 5.2.).

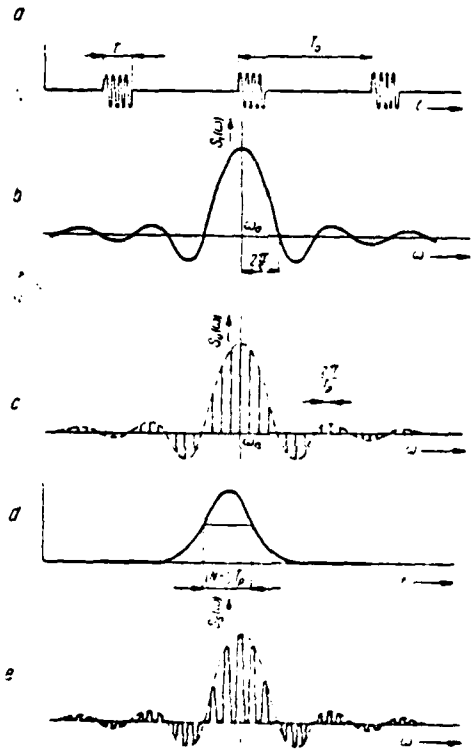

Fig. 7.1.1. Formation of the signal spectrum structure: a-pulse series in time; b-spectrum of individual pulse; c-spectrum of pulse series; d-function modulating pulse series in the process of space scanning; e-spectrum of the received (modulated) pulse series.

The relationships described above are illustrated in Fig. 7.1.1 where the formation of the structure of echo signal spectrum is shown.

It should be noted that in practical applications some of

the quantities appearing in (7.1.2) are usually of different order. Thus in radar the width of pulse spectrum $S_1(f)$ is usually of the order of 10^{-1} - 10 MHz, repetition frequency f_p is (in detection devices) of the order of hundreds of Hz, while the width of spectrum $S_A(f)$ is usually of the order of several to several tens of Hz. This is why we can write approximately:

$$S_s(f) \cong S_1(f) \sum_{n=-\infty}^{\infty} S_A(f - nf_p). \qquad (7.1.3)$$

(7.1.3) indicates that the spectrum of echo signal is the /124
product of the periodic factor in frequency domain (with period f_p) and a non-periodic factor (see Fig. 7.1.1).

In the case of stochastic signals, their spectral density (power spectrum) has to be determined (cf. Ch. 6.2). In radar there is a frequent situation when amplitude and phase fluctuations are present with weak correlation between pulses. Such a signal, as mentioned in the previous chapters, is conveniently represented in the form:

$$s(t; \vartheta_1; \vartheta_2) = \vartheta_1(t)\, A(t) \sin(2\pi f_s t) + \vartheta_2(t)\, A(t) \cos(2\pi f_s t). \qquad (7.1.4)$$

As we know, (cf. Ch. 5.3 and Appendix 2), the autocorrelation functions of processes $\vartheta_1(t)$ and $\vartheta_2(t)$ are equal:

$$R_I(\tau) = R_{II}(\tau) = R_0(\tau), \qquad (7.1.5)$$

and the autocorrelation function of signal $s(t; \vartheta_1, \vartheta_2)$ is determined by the formula:

$$R(\tau) = R_0(\tau)\, R_A(\tau) \cos(2\pi f_s \tau), \qquad (7.1.6)$$

where $R_A(\tau)$ - autocorrelation function of the envelope of signal A(t).

Assuming that the signal fluctuations have an effective correlation time much longer than the duration time of a pulse, but considerably shorter than the pulse duration time, we will obtain:

$$\rho_s(\tau) \cong \rho_1(\tau), \tag{7.1.7}$$

i.e., the normalized signal autocorrelation function then has a form approximately similar to the normalized autocorrelation function on an individual pulse[1].

On the basis of the Wiener-Chinchin theorem [7.1] of course the normalized power spectrum of such a signal will also have a form analogous to the normalized power spectrum $W_1(f)$:

$$\frac{W_s(f)}{W_s(0)} \cong \frac{W_1(f)}{W_1(0)}. \tag{7.1.8}$$

The interference spectrum $W_z(f)$ is composed of the spectrum of noncorrelated white noise with uniform spectral density W_o (generated e.g. by thermal noise) and of the spectrum of correlated interference $W_k(f)$:

$$W_z(f) = W_0 + W_k(f) \tag{7.1.9}$$

Spectrum $W_k(f)$ can be determined using (5.3.8):

$$W_k(f) = W_s(f) * W_\Delta(f) * W_p(f). \tag{7.1.10}$$

Sometimes it is more convenient to use the equivalent relation /125
(in accordance with the Wiener-Chinchin theorem):

[1]Autocorrelation function of an individual pulse is defined here as in ([7.20], p. 162).

$$W_k(f) = \mathcal{F}\{R_s(\tau)\, R_\Delta(\tau)\, R_p(\tau)\}, \qquad (7.1.11)$$

ere

$R_s(\tau), R_\Delta(\tau), R_p(\tau)$ - autocorrelation functions of the transmitted signal, fluctuations caused by space scanning, and fluctuations of passive interference, respectively;

$\mathcal{F}$ - Fourier transform.

Denoting by $W_f(f)$ the spectrum of fluctuations caused by both space scanning and by the variability of passive interference,

$$W_f(f) = W_\Delta(f) * W_p(f), \qquad (7.1.12)$$

it is possible on the basis of the theorem on modulation of stationary stochastic processes, proven previously by the author, ([4.4], Appendix 5) to write the power spectrum $W_k(f)$ in the form:

$$W_k(f) = \sum_{m=-\infty}^{\infty} W_f(f - nf_p)\, W_{1n}(mf_p), \qquad (7.1.13)$$

where $W_{1n}(f) = S_{1n}(f)|^2$ and $S_{1n}(f) = S_1(f)/S_1(0)$. Similarly, (see eqs. 7.1.2 - 7.1.3) we can write approximately:

$$W_k(f) \cong W_{1n}(f) \sum_{m=-\infty}^{\infty} W_f(f - mf_p). \qquad (7.1.14)$$

The spectrum of correlated interference may also be divided into two factors, one of which is periodic in frequency domain, and the other is non-periodic. It is seen from (7.1.14) that the non-periodic factor is determined by the properties of the transmitted signal (as in eq. 7.1.3), but the periodic factor is

determined by the properties of signal fluctuations and the pulse repetition frequency.

On the basis of these relationships we can consider the specific frequency characteristics of optimal filters.

7.2. Optimal filter for stochastic signals.

In this chapter we will consider the characteristics of optimal filter appearing in the system shown in Fig. 6.2.5. As derived previously (Ch. 6.2, eq. 6.2.26), the modulus of the transfer function of this filter is defined by the formula:

$$|F_{\text{opt}}(f)| = \frac{\sqrt{W_0 W_s(f)}}{W_0 + W_s(f)}. \tag{7.2.1}$$

As shown in the preceding chapter, for the case in question, i.e. /126
a signal with fluctuations practically independent between pulses, $W_s(f) \cong W_1(f)$. Using (7.1.13) we will obtain:

$$|F_{\text{opt}}(f)| = \frac{\sqrt{W_0 W_1(f)}}{W_0 + \sum_{m=-\infty}^{\infty} W_f(f - mf_p)\, W_{1n}(mf_p)} \tag{7.2.2}$$

Because of (7.1.14), we can write:

$$|F_{\text{opt}}(f)| \cong \frac{\sqrt{W_0 W_1(f)}}{W_0 + W_{1n}(f) \sum_{m=-\infty}^{\infty} W_f(f - mf_p)} \tag{7.2.3}$$

In order to stress the structure of the filter, (7.2.3) can be transformed as follows:

$$|F_{\text{opt}}(f)| = \frac{\sqrt{W_0 W_1(f)}}{W_{1n}(f)\left[\frac{W_0}{W_{1n}(f)} + \sum_{m=-\infty}^{\infty} W_f(f - mf_p)\right]}. \tag{7.2.4}$$

Since $W_1(f) = |S_1(f)|^2$, we will finally obtain:

$$|F_{opt}(f)| = \sqrt{W_0} \cdot \frac{1}{|S_1(f)|} \cdot \frac{W_1(0)}{\frac{W_0}{W_{1n}(f)} + \sum_{m=-\infty}^{\infty} W_1(f - mf_p)}. \qquad (7.2.5)$$

It is easy to note that in the case when noncorrelated noise may be omitted (i.e. when $W_0=0$), the optimal filter contains two serially connected filters. The first, with a transfer function defined by the first term in (7.2.5) is the so-called Urkowitz filter [7.5, 7.6]. The second filter has a transfer function which is periodic in frequency domain; it is the so-called periodic filter [7.7]. The Urkowitz filter carries out "intra-periodic" filtration, i.e., filtration of individual pulses; the periodic filter carries out the "inter-periodic" filtration, using the correlation of passive interference (Fig. 7.2.1). It should be noted that the Urkowitz filter is not very effective in terms of signal detection against a background of correlated interference, but is extremely sensitive to noncorrelated noise, i.e., it worsens signal detectability in thermal noise [7.19]. Thus the optimal receiver (in the case discussed here) carries out effective signal detection primarily thanks to the operation of the periodic filter.

In the case when passive interference, $W_k=0$, can be omitted, then, as expected, the optimal filter takes the form of a filter matched to the spectrum of an individual pulse, /127
i.e., $|F(f)| \cong |S_1(f)|$ (cf. (7.2.1).

In most practical cases the passive interference, when present, has an intensity much higher than thermal noise[1]. The

[1] e.g. stationary clutter in radar devices may exceed the level of noise by several tens of dB; in some cases the relative level of stationary clutter reaches even 100dB (see Ch. 5 and [7.8, 7.9].

optimal filter thus approaches the form shown in Fig. 7.2.1, and the filter of correlated interference has a characteristic approaching closely periodic. We will consider the characteristics of such a filter below. As indicated by the name, in order to know the characteristic of a periodic filter it is sufficient to determine its path within the limits of a single period. Because the width of both spectra $S_1(f)$ and $W_1(f)$ are in practice about 10^3 times greater than f_p (which is the period of the frequency characteristic of the filter), the variability of $S_1(f)$ and $W_1(f)$ may be omitted[1] within this period. Thus, on the basis of (7.2.5) and the above considerations, we can write the formula determining the transfer function of the periodic filter within a single period:

$$F^{\circ}_{opt}(f) = \frac{\text{const}}{W_0 + W_f(f)}; \quad nf_p \le f \le (n+1)f_p \tag{7.2.6}$$

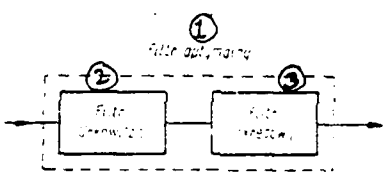

Fig. 7.2.1. Realization of an optimal filter by connecting in series an Urkowitz filter and a periodic filter. 1. optimal filter, 2. Urkowitz filter, 3. periodic filter.

Fig. 7.2.2 represents the normalized graphs of the modulus of the transfer function for a periodic filter $|F^{\circ}_{opt}(f)|$ for various spectral widths $\Delta_f = 2\delta_f$, assuming a Gaussian shape of $W_f(f)$; (cf. Ch. 5). Because of the symmetry (Fig. 4.2.2a), the exact graph 4.2.2b shows only the path within half of the period. In calculations the ratio of the maximum spectral density

[1]Cf. text between (7.1.2) and (7.1.3). Of course, omitting the variability in $S_1(f)$ and $W_1(f)$ refers only to the characteristics of the periodic filter, and does not imply discarding the serially connected filter for individual pulses.

of correlated interference $W_f(f=f_p)$ to the spectral density of noncorrelated interference W_o was assumed to equal 30 dB[1].

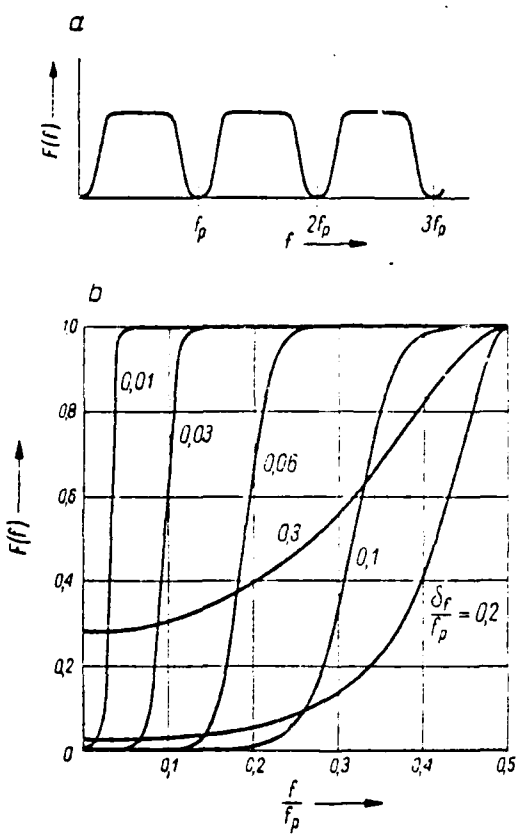

Fig. 7.2.2. a - modulus of the transfer function of an optimal periodic filter; b - transfer function of an optimal periodic filter at various spectrum widths of correlated interference (Gaussian interference spectrum).

In order to illustrate better the character of relationship (7.2.6) Fig. 7.2.3 shows a three-dimensional graph of the

[1]In considering Fig. 7.2.2 one should remember the definition of the ratio of intensities of the correlated and non-correlated interference assumed here, because in practice different definitions may be encountered, leading to ambiguities.

normalized moduli of transfer function $|F^{o}_{opt}(f)|$ as a function of two variables: f/f_p and δ_f/f_p .

The relations allowing to determine the spectrum width Δ_f for known properties of interference and parameters of space scanning are presented in Appendix 6.

For clarification we have shown: in Fig. 7.2.4 - the width of spectrum Δ^p_f as a function of carrier frequency of /130
the scanning signal and the coefficient a, characterizing the properties of passive interference; in Fig. 7.2.5 - normalized width of spectrum Δ^A_f/f_p and the width as a function of the number of echo pulses N, falling within the beam width, in Fig. 7.2.6 - the total width of the correlated interference spectrum Δ_f as a function of the widths Δ^p_f and Δ^A_f.

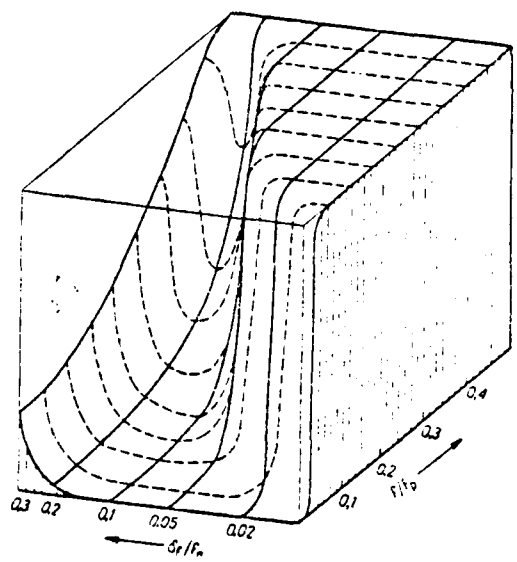

Fig. 7.2.3. Three-dimensional graph of the characteristics of an optimal periodic filter (Gaussian interference spectrum).

As an example, for a radar device operating at a wavelength appr. 23 cm with a pulse repetition frequency of 400Hz, with antenna beam width 1.2° and the velocity of scanning in azimuth equal to 6 rpm, we will have:

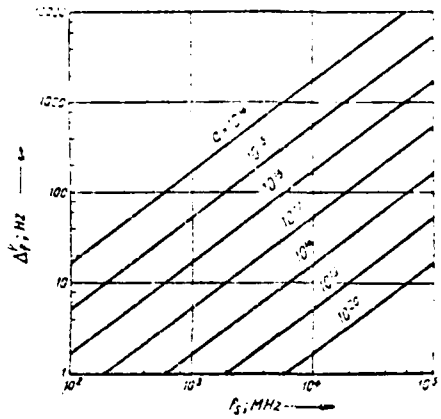

Fig. 7.2.4. Width of spectrum Δ_f^p as a function of carrying frequency f_z.

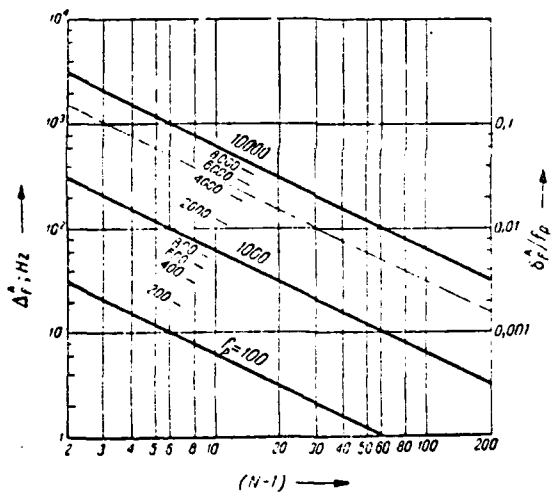

Fig. 7.2.5. Δ_f^A and δ_f^A/f as functions of the number of pulses falling within beam width.

Δ_f^p - assuming on the average for reflections from ground objects coefficient $a=10^{18}$ (see eq. 5.3.4), $\Delta_f^p \cong 2$Hz (from Fig. 7.2.4);

Δ_f^A - for the parameters given above, $N \cong 13$, and $\Delta_f^A \cong 21$Hz, (from Fig. 7.2.5).

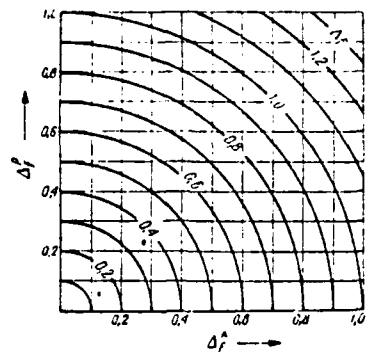

Fig. 7.2.6. Auxiliary normogram for determination of Δ_f when Δ_f^A and Δ_f^p are known.

As a result, the total width of correlated interference spectrum Δ_f is about 21Hz (from Fig. 7.2.6), i.e., $\Delta_f/f_p \cong 0.05$. As can be seen, the main factor is in this case the effect of space scanning. If a = 10^{16} is assumed (which corresponds to e.g., man-made dipole interference), then we have $\Delta_f^p \cong 20$ Hz and $\Delta_f = 29$ Hz, i.e., $\Delta_f/f_p \cong 0.07$. In this case the effects of interference fluctuation and space scanning are approximately the same.

The practical significance of the results obtained should be discussed further. As we know, the simplest periodic filter used in stationary clutter reduction systems is the so-called single compensation system, composed of a delay line with a delay time T_p and a subtracting system (Fig. 7.2.7 a) [7.8]. The frequency characteristic of such a filter is represented by curve $\beta=0$ in Fig. 7.2.8. The signal compensation system is similar to the optimal filter only in terms of the position of the minima and maxima of the characteristic, whereas the path of this characteristic itself is significantly different from the shape obtained for the optimal filter, for any δ_f/f_p.

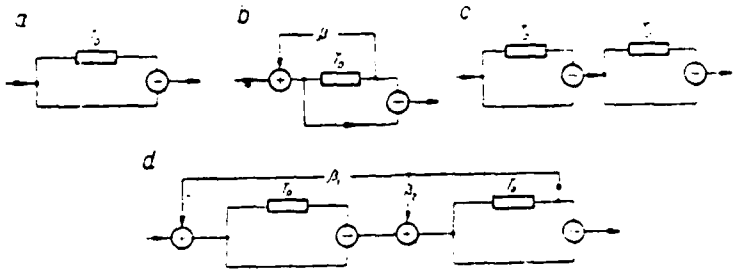

Fig. 7.2.7. Block diagrams of simple periodic filters: a - single subtraction system; b - single subtraction system with feedback; c - double subtraction system; d - double subtraction system with double feedback.

Characteristics approaching the optimal ones can be obtained in practice with the help of more complicated systems with delay lines. For a value of δ_f/f_p of about 0.2, the characteristics approaching optimal can be obtained using a single compensation system with negative feedback (Fig. 7.2.7 b). The characteris- /132 tics of such a system for various values of the feedback coefficient β are shown in Fig. 7.2.8 [7.10]. Observations and measurements in practical situations have confirmed the better effectiveness of stationary clutter reduction using appropriate feedback, compared to operation without such feedback.

For small values of δ_f/f_p it becomes necessary to use a greater number of delay elements in the periodic filter. The double compensation system (Fig. 7.2.7 c) has a characteristic shown in Fig. 7.2.9, curve C [7.11, 7.12]. Such systems are most often realized using memory tubes [7.13]. A better approximation to optimal characteristics can be obtained, using a double system with double feedback (Fig. 7.2.7 d). In this system it is possible to obtain the characteristics shown in Fig. 7.2.9 [7.14, 7.15]. It is evident that by using such a system a relatively good approximation of the optimal filter for various values of

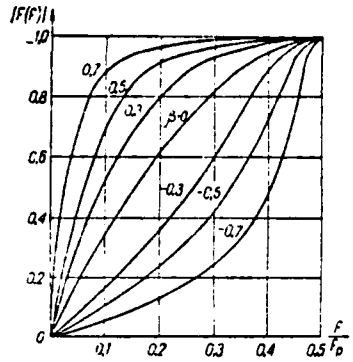

Fig. 7.2.8. Transfer function of the filter shown in Fig. 7.2.7. b for various values of the feedback coefficient β.

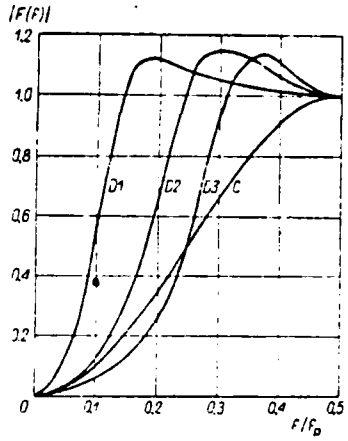

Fig. 7.2.9. Transfer function of the filter shown in Fig. 7.2.7 c (curve C) and transfer functions of the filter shown in Fig. 7.2.7. d (curve D1, D2, D3).

δ_f/f_p is possible. This is also in agreement with the general theory of periodic filter synthesis, which leads to the conclusion that an approximation of a given characteristic is better when an increased number of delay elements is used in the approximating system [7.7, 7.15][1].

However, for technical reasons the use of a larger number of delay elements is difficult. In practice, periodic filters are rather complicated devices. In addition, there are difficulties in accurate adjustment of the delay of individual delay elements. For these reasons there are many descriptions in the literature of practical realization of systems of the type shown in Fig. 7.2.7. d [7.16, 7.17]. The use of more complicated systems would allow a closer approximation to the optimal characteristics, in particular, the improvement of the /134

[1]An outline of the theory of periodic filters is contained in Ch. 8.

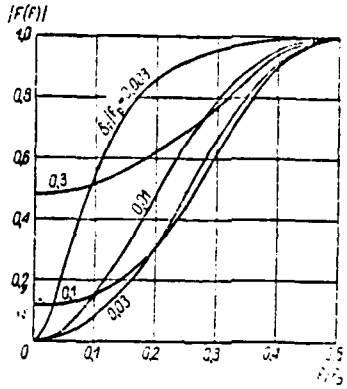

Fig. 7.2.10. Transfer function of an optimal periodic filter at various widths of the correlated interference spectrum

(interference spectrum of the type $\frac{1}{a^2 + \omega^2}$)

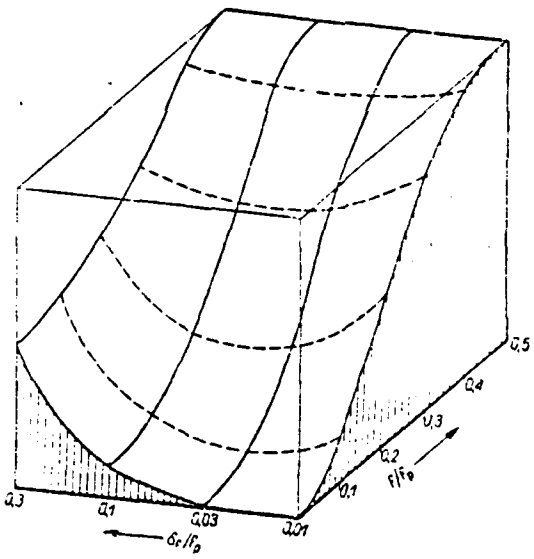

Fig. 7.2.11. Three-dimensional graph of the characteristics shown in Fig. 7.2.10.

effectiveness of reducing narrow-band passive interference, but it would require further technical improvements.

In the case when the autocorrelation function of the interference is exponential (i.e., the interference spectrum is proportional to $\frac{1}{a^2+\omega^2}$; see Ch. 5.3), the modulus of the normalized transfer function of an optimal filter assumes the shape shown in Fig. 7.2.10. Similar to the previous analysis, Fig. 7.2.11 shows a three-dimensional graph of normalized transfer functions as a function of two variables: f/f_p and δ_f/f_p.

7.3. Optimal filter for signals with a distinct Doppler component.

As shown in Ch. 6.2, in the case of signals with a distinct Doppler component, unknown a priori, the optimal reception algorithm is realized with the help of a multichannel receiving system (Fig. 6.2.4). The optimization of such a system in a real situation must take into account many additional factors, such as interchannel correlation, partial overlapping of channel characteristics, usefulness of introducing simplified, linearized characteristics for nonlinear elements, etc. Therefore it is not practically possible to represent in general the characteristics of the appropriate filters in the form of a graph similar to Fig. 7.2.2. It is necessary to make calculations for specific assumptions. However, one may consider the relationships which encompass some general asymptotic properties of the optimal multichannel system.

The transfer function of an optimal filter appearing in the k-th channel of the system is defined by the formula (cf. eq. 6.1.10):

$$F_k(f) = \frac{S_k^*(f)}{W_z(f)} \cdot e^{-j(2\pi f t_0)} = \frac{S_k^*(f)}{W_0 + W_k(f)} \cdot e^{-j(2\pi f t_0)}, \qquad (7.3.1)$$

and $S_k(f)$ - spectrum of an echo pulse signal at Doppler frequency equal to f_k.

Substituting the relations in (7.1.2) and (7.1.13) in /135
(7.3.1) we obtain:

$$F_k(f) = \frac{\sum_{l=-\infty}^{\infty} S_A(f - lf_p - f_k) S_1(lf_p - f_k)}{W_0 + \sum_{m=-\infty}^{\infty} W_f(f - mf_p) W_{1n}(mf_p)} \cdot e^{-j(2\pi f t_0)}. \tag{7.3.2}$$

Using relation (7.1.3) and(7.1.14) we can write:

$$F_k(f) \cong \frac{S_1^*(f - f_k) \sum_{l=-\infty}^{\infty} S_A^*(f - lf_p - f_k)}{W_0 + W_{1n}(f) \sum_{m=-\infty}^{\infty} W_f(f - mf_p)} \cdot e^{-j(2\pi f t_0)}. \tag{7.3.3}$$

In order to stress the structure of the filter we will transform (7.3.3):

$$F_k(f) \cong \frac{S_1^*(f - f_k)}{W_{1n}(f)} \cdot \frac{\sum_{l=-\infty}^{\infty} S_A(f - lf_p - f_k)}{\frac{W_0}{W_{1n}(f)} + \sum_{m=-\infty}^{\infty} W_f(f - mf_p)} \cdot e^{-j(2\pi f t_0)}. \tag{7.3.4}$$

In the case when the interval of possible Doppler frequencies is much smaller than the spectrum width of an individual pulse[1], we can assume $S_1(f - f_k) \cong S_1(f)$, obtaining:

$$F_k(f) \cong \frac{W_1(0)}{S_1(f)} \cdot \frac{\sum_{l=-\infty}^{\infty} S_A(f - lf_p - f_k)}{\frac{W_0}{W_{1n}(f)} + \sum_{m=-\infty}^{\infty} W_f(f - mf_p)} \cdot e^{-j(2\pi f t_0)}. \tag{7.3.5}$$

[1]This is a situation typical for the majority of pulse radar stations for detection, where f_D are of the order of 10^2 - 10^3 HZ, and spectrum widths are of the order of 0.1 - 10MHz.

As it is easy to see, the optimal filter $F_k(f)$ is composed of a serially connected Urkowitz filter (cf. Ch. 7.2) and a periodic filter, whose characteristics are defined by the second term of (7.3.5). Intra-periodic filtration (by the Urkowitz filter) may be common to all channels (Fig. 7.3.1).

An important question is the study of filter structure depending on f_k, especially if large values of k are possible, i.e., a large number of channels. The large number of channels is related to use of a signal with narrow spectrum, where a large number of pulses fall within the antenna beam width. The /136 width of the band of a single channel is then small, which results also from the relations given above.

Assuming that the width of the band of echo signal spectrum Δ_s and the width of the spectrum of correlated fluctuations Δ_f is small in comparison with the repetition frequency f_p $(\Delta_s \ll f_p; \Delta_f \ll f_p)$, we can write the formula for the modulus of the transfer function of the periodic filter $F_k^o(f)$ within a single period as:

$$|F_k^o(f)| = \text{const}\,\frac{|S_k^*(f-f_k)|}{W_0 + W(f)}, \qquad (7.3.6)$$

where $nf_p \leqslant f \leqslant (n+1)f_p;\ f_k \leqslant f_p.$

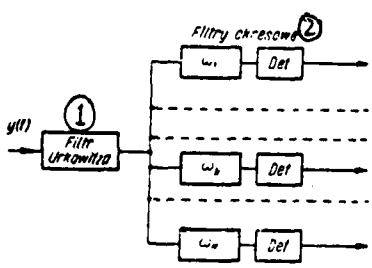

Fig. 7.3.1 A system of filters with common intra-periodic filtration. 1 - Urkowitz filter, 2 - periodic filters.

With the assumptions introduced here, the maxima of the characteristics of narrow-band filters will be at $f \cong f_k$. Thus we can write:

$$\mathrm{Max}\,\{|F_k^0(f)|\} = \frac{\mathrm{const}}{W_0 + W_f(f)}. \qquad (7.3.7)$$

This relation has an interesting interpretation, which allows us to understand the general structure of a multichannel filter system. Comparing (7.3.7) and (7.2.6) we can see that the envelope of the maxima of transfer characteristics of narrow-band periodic filters of a multichannel system has the same shape as the modulus of the transfer characteristic of an optimal periodic filter in the case of stochastic pulse signals (see preceding chapter). This is illustrated in Fig. 7.3.2.

This conclusion is of considerable practical importance because it allows rapid orientation in the structure of a multichannel filter system and facilitates approximate estimates of the requirements which should be fulfilled by such filters.

The above result may also be presented in a different manner. The system shown in Fig. 6.2.5 does not use completely the information related to the Doppler displacement of signal frequency, while the system in Fig. 6.2.4 utilizes the information about the existence of such a displacement. It may be noted that both systems filter the spectrum of the arriving /137 signals similarly in the sense of general utilization of the appropriate spectrum ranges. However, in the first case one stops at the reduction of those fragments of the spectrum which contain especially passive interference, using subsequently the so-called noncoherent signal integration. In contrast, in the second case we use a more subtle filtration within the non-reduced portions of the spectrum. It is easy to see that it is equivalent to the coherent signal integration.

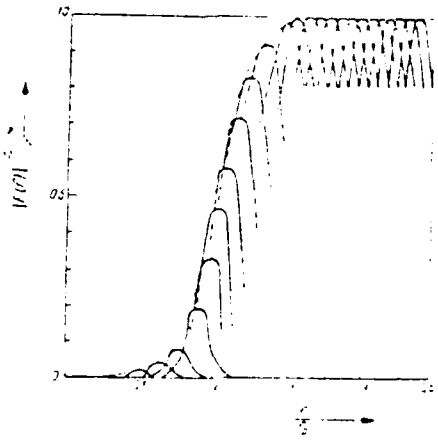

Fig. 7.3.2. Envelope of the transfer function of the filters of an optimal multichannel receiving system (with Gaussian spectrum of correlated interference).

We should add that the two optimal reception systems mentioned represent two extreme cases, related to extreme signal models. In practice, depending on the target properties within a given frequency range, either system described may be more appropriate; also, intermediate situations are possible (see previous chapter)[1]. The interpretation of the optimal process of signal reception mentioned above may have other practical consequences also.

A multichannel system is much more complicated and more difficult to realize than systems represented in Fig. 6.2.5 /138 or 6.2.7. Even by using such solutions as a common delay line for several channels [7.18], the multichannel system will be

[1]We should note that there are also possibilities of future use of systems which automatically match the properties of interference. E.g., when only matching with the spectrum of passive interference fluctuation is needed; it is easy to imagine a modification of the multichannel filter system by using some automatic regulation of intensification in individual channels. Matching different types of detected signals would require more complicated systesm.

very complex. Therefore it may sometimes be justified to purposely give up information about the existence of Doppler displacement of signals. At the cost of a possible decrease in detectability, one obtains a simpler receiver system. The usefulness of such an approach obviously depends on the specific requirements in any given situation.

In summary, this chapter has presented the methods for calculating the characteristics of optimal filters for detection of location signals in the presence of correlated and non-correlated interference, as well as a discussion of the practical realization of such filters taking into account the state of technology in this area at present. Numerous graphs were included to facilitate planning of various devices.

The following chapters will describe (based on the above results) the problems of the realization of the given characteristics of periodic filters and the problem of the signal detection effectiveness in the presence of correlated and non-correlated interference.

References

7.1. Levin, B.P. The theory of random processes and its application in radio technology. Moscow, 1957.

7.2. Lighthill, M.J. An Introduction to Fourier Analysis and Generalised Functions. Cambr. Univ. Press, 1959.

7.3. Kroszczanski, J. On Some Properties of Modulation. Pzheglad Telekomunikacyjny, No. 11, 1954.

7.4. Kroszczynski, J. On the Modulation of Stationary Stochastic Processes, PIT Works, No. 35, 1961.

7.5. Urkowitz, H. Filters for Detection of Small Radar Signals in Clutter. J. Appl. Phys., No. 8, 1953.

7.6. Kulikowski, J. Problems of Optimal Detection and Target Selection (Dissertation). Moscow, 1959.

7.7. Urkowitz, H. Analysis and Synthesis of Delay Line Periodic Filters. IRE Trans., ANE-4, June 1957.

7.8. Kroszczanski, J. Stationary Clutter Reduction in Radar. Przeglad Telekomunikacyjny, No. 11, 1957.

7.9. Herold, H. Increasing Noise Separation in Radar Units. NTZ, NTF-2, 1955.

7.10. Kroszczynski, J. Radar Station of Air Control "Avia". PIT Works, No. 30, 1960.

7.11. Kriszczynski, J. Effectiveness of Stationary Clutter /138
Reduction in a Simple and Double Compensation System. PIT Works, No. 24, 1958.

7.12. Kroszczynski, J. Effective Operation of Radar Stations Reducing Stationary Clutter. Przeglad Telekomunikacyjny, No. 7, 1958.

7.13. Cliquot, R. Les Radars Bande "LP, Type Orly. L'Onde Electrique, May 1961.

7.14. White, W.D., Rubin, A.E. Recent Advances in the Synthesis of Comb Filters. IRE Conv. Rec., Part 2, 1957.

7.15. Linden, D.A., Steinberg, B.D. Synthesis of Delay Line Networks. IRE Trans., ANE-4, March 1957.

7.16. Moltz, K.F. AN/FPN-34 Air Traffic Control Radar. Proc. of the 5th East Coast Conference.

7.17. Shrader, W.M. Reducing Clutter in Air Route Surveillance Radar. Electronics, 26th January 1962.

7.18. Brookner, E., Slink, J. Coherent Enhancer for Pulse Radar Application. IRE Conv. Rec., Part 8, 1960.

7.19. Veinshetein, L.A., Zubakov, V.D. Signal Selection on the Background of Random Noise. Moscow, 1960.

7.20. Middleton, D. An Introduction to Statistical Communication Theory. New York, 1960.

8. Outline of the theory of intermittent (periodic) filters. /140

Some properties of certain periodic filters were mentioned in the preceding chapter, but this problem requires a more detailed discussion. For the sake of clarity we will first present in this chapter an analysis of the properties of less complicated systems, using simple methods. Next, we will discuss more advanced theoretical methods, especially useful in considering periodic filters, both in terms of analysis and synthesis of such filters. Because of space limitations, all questions cannot be discussed at length; more detailed information concerning many points may be found in the references cited.

8.1. Transfer functions of some intermittent (periodic) filters:

The simplest periodic filter applied in stationary clutter reduction is (as mentioned in the preceding chapters) a system composed of a delay line with a delay equal T_p and a subtracting system (Fig. 8.1.1)[1].

The transfer function of such a system can be calculated from the relation [8.1]:

$$F(\omega) = \frac{S_w(\omega)}{S_e(\omega)}, \qquad (8.1.1)$$

where $S_e(\omega)$ - signal spectrum at filter input; $S_w(\omega)$ - signal spectrum at filter output.

Because the signal at the output of an ideal delay line is delayed by a time T_p by the input signal

$$u_1(t) = u_e(t - T_p), \qquad (8.1.2)$$

[1]To facilitate our discussion, we assume in Fig. 8.1.1 a notation for the subtracting system which shows the signs of the signals being subtracted.

in accordance with the theorem of displacement in the time domain ([8.1], Ch. 1.3.2, [8.2]), we have:

$$S_1(\omega) = S_e(\omega)\, e^{-j\omega T_p}. \tag{8.1.3}$$

As indicated by Fig. 8.1.1, /141

$$S_w(\omega) = S_e(\omega) - S_1(\omega). \tag{8.1.4}$$

Substituting (8.1.3) and (8.1.4) into (8.1.1) we obtain:

$$F_1(\omega) = 1 - e^{-j\omega T_p}. \tag{8.1.5}$$

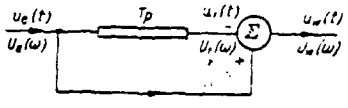

Fig. 8.1.1. Single subtracting system.

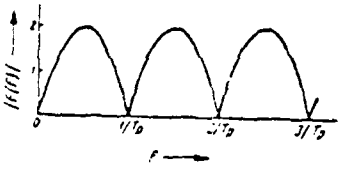

Fig. 8.1.2. Modulus of transfer function of a single subtraction system.

After simple transformations, we can write the modulus of the transfer function of a single subtracting system:

$$|F_1(\omega)| = 2 \sin \frac{\omega T_p}{2}, \qquad F_1(f) = 2 \sin (\pi f / f_p). \tag{8.1.6}$$

Fig. 8.1.2 illustrates the relation obtained above[1].

[1] A more accurate graph, for $0 \leqslant f/f_p \leqslant 0.5$, is shown (in normalized form) in Fig. 7.2.8, curve $\beta = 0$.

A double subtracting system (Fig. 8.1.3) is a serial connection of two single systems. Because the resultant transfer function of a chain of quadrupoles is equal to the product of the transfer functions of its elements, we can obtain the transfer function of a double subtraction system by taking a square of the righthand side of (8.1.5):

$$F_2(\omega) = (1 - e^{-j\omega T_p})^2 = 1 - 2e^{-j\omega T_p} + e^{-j2\omega T_p}. \qquad (8.1.7)$$

It is easy to note that on the basis of the above relation the double subtraction system is theoretically equivalent to the systems shown in Fig. 8.1.4. It should be mentioned, however, that from a technical point of view the double system (Fig. 8.1.3) has certain advantages. This is easy to illus- /142
trate by assuming that at the input of the systems being compared there is an ideally constant echo. In the case when the amplitude of one of the signals being subtracted in the first subtracting systems in Fig. 8.1.3 (e.g., as a result of a change in line reduction, or enhancement of one of the intensifiers), the interfering signal will be reduced by the second system. However, if the amplitude of one of the delayed signals changes

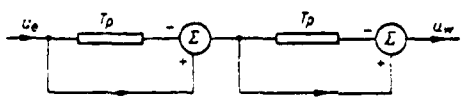

Fig. 8.1.3. A double subtracting system.

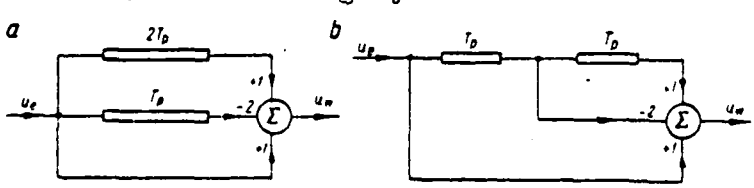

Fig. 8.1.4. Systems equivalent to a double subtracting system.

in the systems shown in Fig. 8.1.4, the uncompensated difference will appear at the output. The problem of the optimal system configuration will be discussed in more detail in Ch. 8.4.

From (8.1.7) we can determine the modulus of the transfer function of a double subtracting system [8.3]:

$$|F_2(\omega)| = 4\sin^2\frac{\omega T_p}{2}.$$

$$|F_2(f)| = 4\sin^2(\pi f/f_p). \qquad (8.1.8)$$

Fig. 8.1.5 illustrates this relation[1].

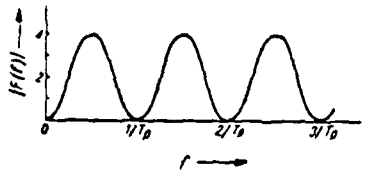

Fig. 8.1.5. Modulus of the transfer function of a double subtraction system.

Analogously, for the L-fold subtraction system (Fig. 8.1.6) we can write:

$$F_L(\omega) = (1 - e^{-j\omega T_p})^L, \qquad (8.1.9)$$

and

$$|F_L(\omega)| = \left|2^L\left(\sin^L\frac{\omega T_p}{2}\right)\right| = |2^L[\sin^L(\pi f/f_p)]|. \qquad (8.1.10)$$

Of course, the system of L-fold cascade subtraction corresponds to equivalent systems with modified configuration, as discussed in comments to (8.1.7). /143

As mentioned in Ch. 7 additional possibilities of trans-

[1]A more accurate graph, for $0 \leq f/f_p \leq 0.5$, is shown (in normalized form) in Fig. 7.2.9, curve C.

fer function formation result from the use of feedback.

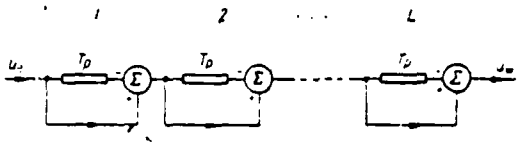

Fig. 8.1.6. L-fold subtraction system.

Let us consider the simplest system of this type (Fig. 8.1.7). As is easy to see:

$$S_i(\omega) + \beta S_u(\omega) e^{-j\omega T_p} = S_u(\omega), \tag{8.1.11}$$

where β - feedback coefficient.

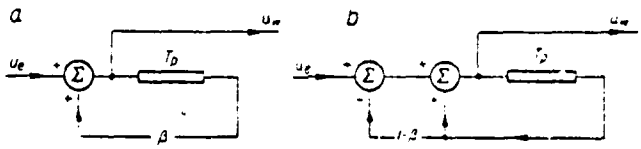

Fig. 8.1.7. System with feedback (integrator).

The transfer function of the system shown in Fig. 8.1.7 therefore has the form (see 8.1.1):

$$F_\beta(\omega) = \frac{1}{1 - \beta e^{-j\omega T_p}}, \tag{8.1.12}$$

and its modulus is defined by the formula:

$$|F_\beta(\omega)| = \frac{1}{\sqrt{1 - 2\beta \cos \omega T_p + \beta^2}}. \tag{8.1.13}$$

Fig. 8.1.8 illustrates relationship (8.1.13). In order for the system to be stable, condition $|\beta| < 1$ must be fulfilled. As is known, the system of the type described is used as an approximation of the ideal summator (e.g., in systems similar to that shown in Fig. 6.2.7); it is also frequently

called an integrator ([8.4], Ch. 4; [8.5]). In this application the feedback coefficient approaches unity as the number of /144 pulses to be summed increases. In the system shown in Fig. 8.1.7 it is difficult to achieve stable operation for $\beta > 0.9$. Often a somewhat modified system is applied (Fig. 8.1.7. b), which is theoretically equivalent to the previous one, but - as is easy to see, this allows a more stable operation for β close to unity. It is possible to achieve $\beta \cong 0.98$ in such a system [8.5]. Furthermore, cascade connection of integrators is possible, which has some advantages. Since the main topic in this chapter concerns periodic filters used in systems of stationary clutter reduction, integrators with feedback will not be considered in detail here. A more detailed discussion of their properties may be found e.g., in refs. [8.6 - 8.8].

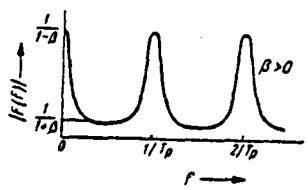

Fig. 8.1.8. Modulus of transfer function of the system shown in the preceding Figure.

Let us consider now a single subtraction system with feedback (Fig. 8.1.9). It is easy to see that:

$$S_e(\omega) + \beta S_2(\omega) = S_2(\omega)\, e^{j\omega T_p}, \tag{8.1.14}$$

(see also Fig. 8.1.7 and eq. 8.1.11). In analogy to (8.1.4) we can also write:

$$S_{ie}(\omega) = S_2(\omega)\,(e^{j\omega T_p} - 1). \tag{8.1.15}$$

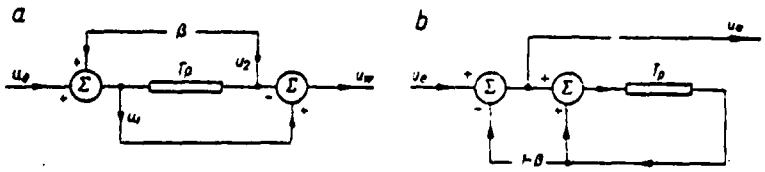

Fig. 8.1.9. Subtraction system with feedback.

As follows from (8.1.1), (8.1.14) and (8.1.15),

$$F_{1\beta}(\omega) = \frac{e^{j\omega T_p} - 1}{e^{j\omega T_p} - \beta}. \tag{8.1.16}$$

Comparing (8.1.16), (1.5) and (8.1.12) we find that $F_{1\beta}(\omega) = F_1(\omega) \cdot F_\beta(\omega)$, , i.e., the transfer function of a single subtraction system with feedback is a product of the transfer function of a single subtraction system and an integrator with feedback. The modulus of the transfer function of the system in question is determined by the formula: /145

$$|F_{1\beta}(\omega)| = \frac{2\left|\sin\frac{\omega T_p}{2}\right|}{\sqrt{1 - 2\beta\cos\omega T_p + \beta^2}}. \tag{8.1.17}$$

Fig. 8.1.10 illustrates relation 8.1.17[1].

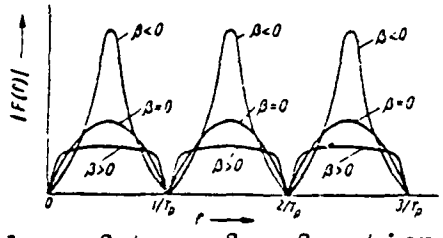

Fig. 8.1.10. Modulus of transfer function of a single subtraction system with feedback.

Using similar methods it may be possible to determine the transfer function of a double subtracting system with feedback (see Fig. 7.2.7. d) of even more complicated systems. By using elementary methods in considering these problems the solutions become more difficult and less clear as the systems get more complex. Therefore certain theoretical methods have been developed which considerably facilitate the analysis and allow a

[1]A more accurate graph for $0 \leq f/f_p \leq 0.5$ is shown (in normalized form) in Fig. 7.2.8.

practical synthesis of periodic filters systems. These problems will be discussed below.

8.2. The transformant and its application in the analysis of periodic filters.

In considering the problems related to periodic filters which contain delay lines, a useful method is the application of the so-called transform z.

As we know, the transfer function of a linear quadrupole refers to the voltage at the output of this quadrupole, generated by the application at the input of the voltage in the form of an individual pulse (Dirac function) $\delta(t)$ [8.1]. The transition function $h(t)$ and the transfer function $F(\omega)$ (see eq. 8.1.1) are related by the known relationships [8.1]: /146

$$F(\omega) = \mathcal{F}\{h(t)\} = \int_{-\infty}^{\infty} h(t)\, e^{-j\omega t}\, dt, \tag{8.2.1A}$$

$$h(t) = \mathcal{F}^{-1}\{F(\omega)\} = \frac{1}{2\pi} \int_{-\infty}^{\infty} F(\omega)\, e^{j\omega t}\, d\omega. \tag{8.2.1B}$$

As follows from (8.2.1B), the periodic transfer function corresponds to the transition function in the form of a sum of individual pulses, occurring at constant time intervals [8.9]:

$$h(t) = \sum_n h_n \delta(t - nT_p), \tag{8.2.2}$$

and $T_p = \frac{2\pi}{\omega_p}$, where ω_p is the period of the transition function.

It is easy to see on the basis of Fig. 8.1.1 that the pulse response of a single subtracting system has the form:

$$h_1(t) = \delta(t) - \delta(t - T_p); \tag{8.2.3}$$

for a double system we will have:

$$h_2(t) = \delta(t) - 2\delta(t - T_p) + \delta(t - 2T_p) \tag{8.2.4}$$

etc.

Ch. 7 indicates that if only the filtration between pulses is considered, the shape of the pulse is not important, and the input voltage may also be represented in the form of individual pulses. In considering signals of this type it is convenient to use the Laplace transforms. As we know ([8.1], [8.10]),

$$\mathcal{L}\{\delta(t)\} = 1 \tag{8.2.5}$$

and

$$\mathcal{L}\{u(t - T_p)\} = \mathcal{L}\{u(t)\} \cdot e^{-pT_p}. \tag{8.2.6}$$

Since the transition function h (t) and the operator transfer function F(p) are related by relations analogous to (8.2.1):

$$F(p) = \mathcal{L}\{h(t)\}, \tag{8.2.7A}$$

$$h(t) = \mathcal{L}^{-1}\{F(p)\}, \tag{8.2.7B}$$

it is evident that both the operator transfer function F(p) and the Laplace transform of the signal in question may be represen- /147
ted in the form of a sum of terms of the type e^{-npT_p}.

Transform z consists in applying the substitution

$$z = e^{pT_p}. \tag{8.2.8}$$

Therefore, the operator transfer function of a periodic filter F(z) has the form:

$$F(z) = \sum_n f_n z^{-n}; \tag{8.2.9}$$

and similarly, the transform z of the input signal consisting of a series of individual pulses is

$$U_e(z) = \mathcal{Z}\{u_e(t)\} = \sum_n e_n z^{-n}. \tag{8.2.10}$$

The Laplace transform of the output signal is defined by the formula:

$$U_w(p) = U_e(p) \cdot F(p), \tag{8.2.11}$$

and thus we can write:

$$U_w(z) = U_e(z) \cdot F(z) \tag{8.2.12}$$

Transform z of the output signal may also be represented in the form of the sum:

$$U_w(z) = \sum_n W_n z^{-n}. \tag{8.2.13}$$

The coefficients W_n can be obtained by substituting (8.2.9) and (8.2.10) into (8.2.12) and by carrying out appropriate algebraic calculations, or by taking advantage of the relation:

$$W_n = \frac{1}{2\pi j} \int U_w(z) z^{n-1} dz, \tag{8.2.14}$$

and keeping in mind that the integration envelope encompasses all zeros and poles of function $U_W(z)$ [8.11-8.13]. Table 8.1

gives the z transforms of some signals.

The transform z transforms (cf. eq. 8.2.8) the left half-plane of the variable $p=\sigma + j\omega$ into the area contained within a circle with unit radius (see Fig. 8.2.1). More precisely, this transformation is not unambiguous, namely the inside of the circle corresponds to each strip of the left half-plane p, for which $n\frac{2\pi}{T_p} < \omega < (n+1)\frac{2\pi}{T_p}$, where n = 0, ± 1, ± 2 ... (Fig. 8.2.2). The axis $\sigma = 0$ is transformed into the circumference of a unit circle on the plane $z=x+jy$.

Table I

Lp.	$f(t)$	(1) Obwiednia $f(t)$	$\mathcal{L}\{f(t)\}$	$\mathcal{Z}\{f(t)\}$
1	$\delta(t)$	$\delta(t)$	1	1
2	$\sum_{n=0}^{\infty}\delta(t-nT_p)$	$1(t)$	$\frac{1}{1-e^{-pT_p}}$	$\frac{z}{z-1}$
3	$\sum_{n=0}^{\infty}k^n\delta(t-nT_p), \quad k<1$	$e^{-\alpha t}, \quad t>0$ $\alpha = -\frac{1}{T_p}\ln k$	$\frac{1}{1-ke^{-pT_p}}$	$\frac{z}{z-k}$
4	$\sum_{n=0}^{\infty}n\delta(t-nT_p)$	$t, \quad t>0$	$\frac{e^{-pT_p}}{(1-e^{-pT_p})^2}$	$\frac{z}{(z-1)^2}$
5	$\sum_{n=0}^{\infty}(-1)^n\delta(t-nT_p)$	$\cos\frac{\pi t}{T_p}$ $t>0$	$\frac{1}{1+e^{-pT_p}}$	$\frac{z}{z+1}$
6	$\sum_{n=0}^{\infty}\frac{1-k^{n+1}}{1-k}\delta(t-nT_p)$	$\frac{1}{1-k}(1-ke^{-\alpha t})$ $t>0$	$\frac{1}{(1-e^{-pT_p})(1-ke^{-pT_p})}$	$\frac{z^2}{(z-1)(z-k)}$

1 - envelope

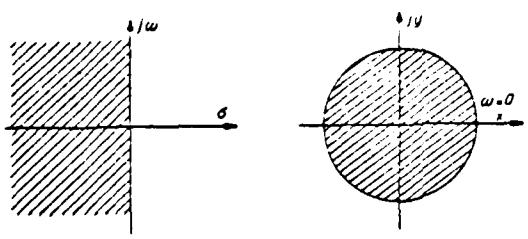

Fig. 8.2.1. Transform $z=e^{pT_p}$

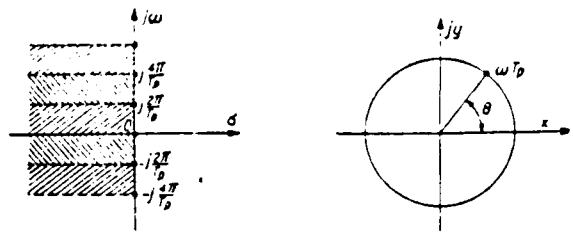

Fig. 8.2.2. Properties of the z transform.

These properties of the z transform can be interpreted /149
to mean that the application of this transform allows to consider only the variability within the period in the case of periodic transfer functions (or signals); whereas the periodicity is taken into account by the form of the transform itself. This facilitates algebraic operations and discussion of some properties of the systems as will be shown.

In general, the transfer function F(z) will have the form of a rational fraction

$$F(z) = \frac{a_n z^n + a_{n-1} z^{n-1} + \ldots + a_0}{b_m z^m + b_{m-1} z^{m-1} + \ldots + b_0}, \qquad (8.2.15)$$

which may also be written in the form:

$$F(z) = K \left[\frac{(z - z_{01})(z - z_{02}) \ldots (z - z_{0n})}{(z - z_{p1})(z - z_{p2}) \ldots (z - z_{pm})} \right] \qquad (8.2.16)$$

which shows the zeros and poles of the function F(z). Both the zeros and poles must be real quantities, or complex. The condition of system stability is to have the poles of F(z) situated within the unit circle; the position of zeros is not restricted.

To illustrate the kind of relationship between F(z) and F(ω) let us note that in (8.2.16) both the numerator and the denominator contain the product of com lex vectors, which are the distances of a point (corresponding to a given value ω) along the circumference of a unit circle from the appropriate zero or pole of function F(z). Therefore:

$$F(\omega) = \frac{\text{product of all distances from given point at the circumference of unit circle to zeros of function } F(z)}{\text{product of all distances from given point at the circumference of unit circle to poles of function } F(z)} \qquad (8.2.17)$$

The above relationship is illustrated in Fig. 8.2.3. Let us note that the peculiar point at the system origin does not influence the modulus of the transfer function because the corresponding distance is always equal to unity [8.14].

As an example, let us consider the single subtracting system (cf. Fig. 8.1.1). On the basis of (8.1.5) we have:

$$F_1(z) = 1 - z^{-1} = \frac{z-1}{z}. \qquad (8.2.18)$$

The transfer function $F_1(z)$ has a pole at the system origin and a zero at z=1 (Fig. 8.2.4). In Fig. 8.2.4 the distance from a point at the circle circumference to the point z-1 is:

$$r = 2 \sin \frac{\omega T_p}{2},$$

so that we obtain for $F|(\omega)|$ an expression identical to (8.1.6).

The values of F(z), F(ω) and sketches of the position of the poles and zeros for several systems of periodic filters are given in Table 8.II. Using Tables 8.I and 8.II and (8.2.12)

it is possible, if needed, to determine the signals at the output of periodic filters([8.14] Appendix I).

/150

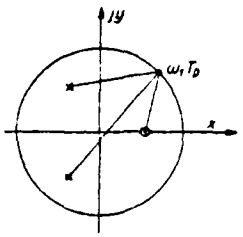

Fig. 8.2.3. Illus ration of the relationship (8.2.17)

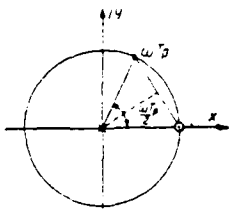

Fig. 8.2.4. Graph of the properties of a single subtracting system in plane z.

8.3. Synthesis of periodic filters.

By the synthesis of periodic filters we mean the design of the electric system and the values of its component elements on the basis of filter characteristics [8.1].

In the case when the operator transition function F(z) of the filter is given (see previous chapter), it is possible to consider the question of synthesis using various methods. For the simpler cases it is sufficient to simply compare the given transfer function with the known (cf. Table 8.II) functions F(z) or to recognize the system structure by simple algebraic transformations. As an example let us consider the synthesis of a filter realizing the transfer function

$$F(z) = \frac{z^2}{(z - z_1)(z - z_2)}. \qquad (8.3.1)$$

AD-A098 433 FOREIGN TECHNOLOGY DIV WRIGHT-PATTERSON AFB OH F/G 17/9
REDUCTION OF STATIONARY CLUTTER IN RADAR,(U)
OCT 80 J KROSZCZYNSKI
UNCLASSIFIED FTD-ID(RS)T-0132-80 NL

3 OF 4
AD
A098433

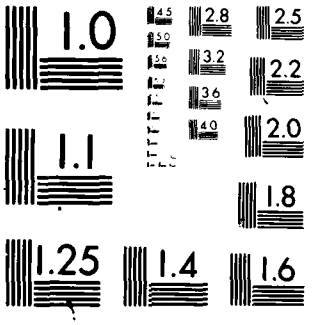

MICROCOPY RESOLUTION TEST CHART
NATIONAL BUREAU OF STANDARDS 1963 A

Transforming (8.3.1) we will obtain:

$$F(z) = \frac{1}{1 - (z_1 + z_2)/z + z_1 z_2/z_2}. \qquad (8.3.2)$$

Because of (8.2.12) we will have:

$$U_e(z) = U_w(z)\,[1 - (z_1 + z_2)/z + z_1 z_2/z^2]. \qquad (8.3.3)$$

The realization of (8.3.3) will be assured by a system of summator whose input will be appropriately the signals representing individual components of the equation (Fig. 8.3.1). Further, /151 it is easy to recognize that these components may be generated by an appropriate joining of delaying lines (whose operator transfer function is equal, as shown in the preceding chapter, to 1/z). As a result, we will obtain a system represented in Fig. 8.3.2 [8.13]. By placing the output of the system at point A, it is possible to realize with its help the transfer function as well

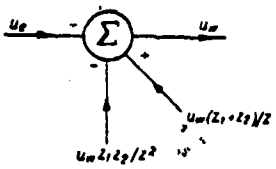

Fig. 8.3.1. Geometric interpretation of (8.3.1).

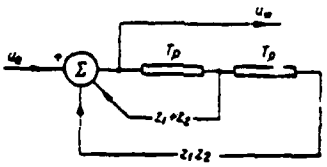

Fig. 8.3.2. System realizing the transfer function given by (8.3.1)

$$F(z) = \frac{z^2}{(z - z_1)(z - z_2)} \cdot \frac{1}{z} = \frac{z}{(z - z_1)(z - z_2)}, \qquad (8.3.4)$$

and placing the output at point B- the function

$$F(z) = \frac{1}{(z - z_1)(z - z_2)}. \qquad (8.3.5)$$

The transfer functions, defined by more complicated expressions, may be represented in the general form as a proper fraction (see (8.2.15):

$$F(z) = \frac{a_n z^n + a_{n-1} z^{n-1} + \ldots + a_0}{b_m z^m + b_{m-1} z^{m-1} + \ldots + b_0}. \qquad (8.3.6)$$

Every expression of this type may be generally realized in a canonical system represented in Fig. 8.3.3 [8.12, 8.15] . Since in the cases considered here the coefficients a and b are real, the roots of both numerator and denominator are either real or complex. It follows that the numerator and denominator of expression (8.3.6) can be represented in the form of the ratio of factors appearing at most in the second power. This is an important property because it means in terms of the system that any transfer function of the type (8.3.6) with real coefficents can be realized by connecting systems serially, with each system having at most two delay lines; also, the feedback loops encompass no more than two delay lines [8.12, 8.15] . /152

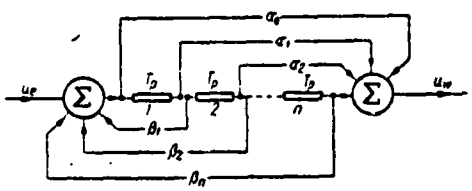

Fig. 8.3.3. Canonical system system of a periodic filter.

Therefore we should consider the properties of the "basic blocks" containing one or two delay lines. The canonical form of a system containing one delay line is shown in Fig. 8.3.4, and one with two lines is shown in Fig. 8.3.5. The transfer function of both systems is given in Table 8.II.

Various system configurations are possible, as mentioned previously, which have the same transfer function. Linden and Steinberg [8.15] have applied the theory of flow graphs to the configuration problem of periodic filters. We will not present

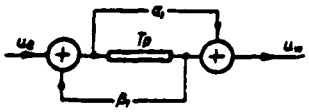

Fig. 8.3.4. Canonical form of a system with one delay line.

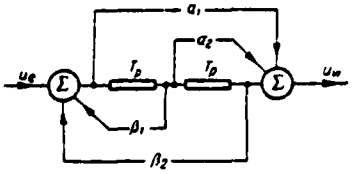

Fig. 8.3.5. Canonical form of a system with two delay lines.

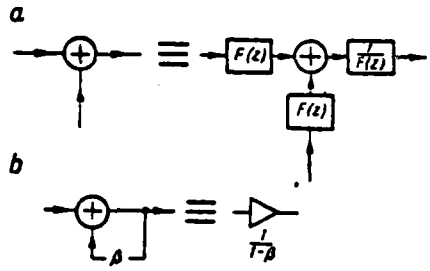

Fig. 8.3.6 System identities resulting from the theory of flow graphs.

this theory in detail here, because in the cases of interest it is sufficient to utilize only two simple identities resulting from it. These are represented in Fig. 8.3.6. A reader more interested in this problem may find more detailed information in the literature [8.16-8.19]. Fig. 8.3.7. shows equivalent configurations of a single subtracting system with feedback, /154 resulting from the identities mentioned above [8.15].

Up to now our considerations indicate that the number of delay lines in a system which synthesizes a given characteristic is equal to the number of poles not situated at the system origin, or to the number of zeros - depending on which number is greater. Any transfer function have n poles[1] or n zeros may be

[1]Obviously, obeying the stability condition $|z_p|<1$ (cf. Ch. 8.2).

Table II /153

1-filter system; 2-position of zeros and poles.

Układ filtru 1	F(z)	Położenie zer i biegunów 2
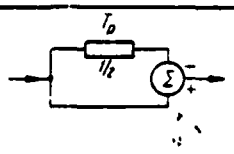	$\frac{z-1}{z}$	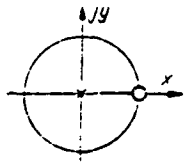
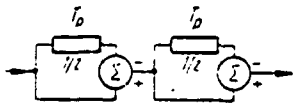	$\left(\frac{z-1}{z}\right)^2$	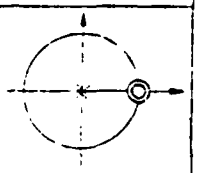
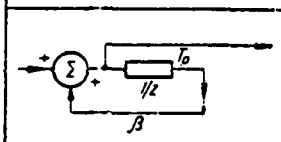	$\frac{z}{z-\beta}$	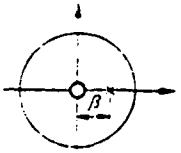
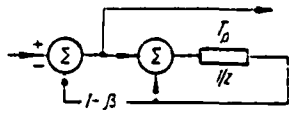	$\frac{z-1}{z-\beta}$	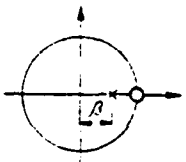
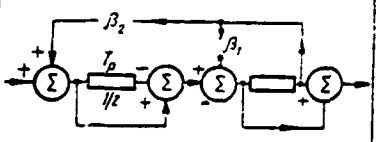	$\frac{(z-1)^2}{z^2-(\beta_1+\beta_2)z+\beta_2}$	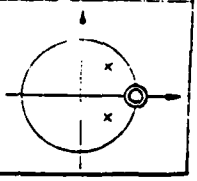

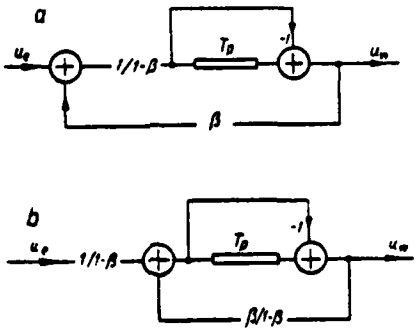

Fig. 8.3.7. Equivalent configurations of a single subtracting system with feedback.

realized in a system containing n delay lines [8.15].

In the case when there is no given direct transfer function F(z) and a synthesis is desired of a system which approximates a defined function $F(\omega)$, we use the transform p* [8.12]. The results of the synthesis of filters with upper- or lower passband in order to obtain the given transfer functions of periodic filters.

The transform p* transforms the circumference of a circle of unit radius in plane z onto the imaginary axis in plane p*. In other words, the consecutive use of transforms z and p* transforms a strip of the plane p (cf. Fig. 8.2.2) into a half of plane p*. In this way the determination (by defining the zeros and poles) of the characteristic of a filter with upper- or lower passband in plane p* leads to the determination of the appropriate characteristic of a periodic filter; this problem will be explained below.

The transform p* is defined by the equations:

$$z = \frac{\Omega + p^*}{\Omega - p^*}, \tag{8.3.7 A}$$

$$p^* = \Omega \frac{z-1}{z+1}. \tag{8.3.7 B}$$

The transform p* may be used directly in the synthesis /155
of periodic filters which reduce stationary clutter if we are using the characteristics of filters with upper passband, or in the synthesis of systems of protection integrators using the characteristics of filters with lower passband.

However, if we want to synthesize a periodic filter for reducing stationary clutter by using the characteristics of filters with lower passivity, or in the synthesis of systems of protection integrators using the characteristics of filters with upper passbank; we should apply the transform p*, similar to transform p*, and defined by equations:

$$z = \frac{q^* + \Omega}{q^* - \Omega}, \tag{8.3.8 A}$$

$$q^* = \Omega \frac{z+1}{z-1}. \tag{8.3.8 B}$$

In both cases Ω is a coefficient which allows to guage the transformation appropriately, thus allowing to obtain an appropriate width of the passbank and reduction bands of the filter [8.12].

Equations (8.3.7) and (8.3.8) are similar to the expressions defining the impedance as a function of reflection coefficient[1]. Therefore, in considering the synthesis of systems using the method described graphic methods are also used, taking advantage of the Smith graph known in microwave technology [8.20]. The application of transform p* will be best illustrated by the example of the synthesis of a triple subtracting system with feedback, given below [8.12].

Example of the synthesis of a periodic filter.

---

[1] If the complex reflection coefficient is denoted by ϱ and the impedance by Z_k, then: $\varrho = \frac{Z_k - Z_0}{Z_k + Z_0}$,

where Z_0 - characteristic impedance [8.20], Ch. 9. Substituting q* for Z_k and Ω for Z_0 we obtain (8.3.8A) and by substituting p* for Z_0^k and z for ϱ, we obtain (8.3.7A).

In order to reduce stationary clutter we need a filter which has a maximum effective reduction at points = 0, $\pm\omega_p, \pm 2\omega_p \ldots$ where $\omega_p = \frac{2\pi}{T_p}$), , and a possible flat course of the transfer function in the band $\theta_0 < \omega T_p < 2\pi - \theta_0$ (smaller than 1 dB). In other words, the value F(z) should be almost constant (smaller than 1 db) for the values of z on that part of the circumference of a unit circle $ze^{j\theta}$, where $\theta_0 < \theta < 2\pi - \theta_0$. /156
In the vicinity of point z=1, F(z) should assume a minimal value.

Let us assume that we will accept as the model nonperiodic filter a filter with lower passband. Using the method described we can use the data of Butterworth, Bessel, Chebyshev and others [8.1]. In the present example we will assume a transfer function of the Chebyshev type.

Based on relationships (8.3.8 B) the requirements for F(z) correspond to the condition of obtaining a transfer function with a variation smaller than 1 dB in the passband[1]:

$$-\Omega \operatorname{ctg}\frac{\theta_0}{2} < \omega^* < \Omega \operatorname{ctg}\frac{\theta_0}{2}; \qquad (8.3.9)$$

at the same time, the transfer function should assume minimal values for $\omega^* = \infty$.

By choosing appropriately Ω, it is possible to consider the model filter with the condition

$$-1 < \omega^* < 1; \qquad (8.3.10)$$

[1]Inequality (8.3.9) follows directly from (8.3.8 B) on the basis of relationship $\operatorname{ctg}\frac{\theta}{2} = j\frac{e^{j\theta}+1}{e^{j\theta}-1}$.

It is easy to see that in order to accomplish this we have to take $\Omega = \mathrm{tg}\frac{\Theta_k}{2}$.

The solution of the problem of the synthesis of a filter with lower passband and with the above transfer function is discussed in detail e.g., in refs. [8.21, 8.22]. The position of the poles is calculated from the formula:

$$q_k^* = \sinh\gamma\cos\Theta_k + j\cosh\gamma\sin\Theta_k, \qquad (8.3.11)$$

where

Θ_k $\quad -\frac{\pi}{2}\cdot\frac{N+1-2k}{N}; \quad k = 1, 2, 3 \ldots N$

N - number of poles

$(N\gamma)$ $\quad -\frac{|F(\omega)|_{max}}{|F(\omega)|_{min}}$, , i.e., the variation of the transfer function in the passband.

For the case in question, i.e., for N=3 and the variation 1 dB, we obtain from the tables contained in refs [8.21, 8.22:]

$$q_1^* = -0{,}2471 + j\,0{,}9659, \quad q_2^* = -0{,}4942,$$
$$q_3^* = -0{,}2471 - j\,0{,}9659. \qquad (8.3.12)$$

The position of these poles in plane q* is shown in Fig. 8.3.8. /157 The transfer function of a model filter with lower passband, obtained as the result of this synthesis, is shown in Fig. 8.3.9.

Going from the model filter (with lower passband) to the periodic filter using the method described above, we utilize (8.3.8 a). For $\theta_0 = 45^\circ$ we obtain:

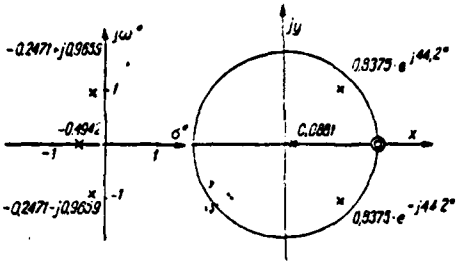

Fig. 8.3.8. Position of poles of the synthesized transfer function for a filter with lower passband in plane q.

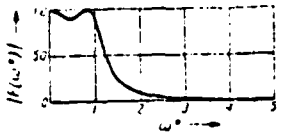

Fig. 8.3.9. Transfer function of a filter with lower passband which is the model for the synthesis of a periodic filter.

$$z_1 = 0{,}8379 \cdot e^{ja}, \quad z_2 = 0{,}0881, \quad z_3 = 0{,}8374 \cdot e^{-ja}, \quad a = 44{,}2^\circ. \qquad (8.3.13)$$

These values may also be determined graphically using the Smith graph. In order to do this we must first calculate the normalized values $-q_k^*$, i.e. $\mathrm{tj.}\ \dfrac{-q_k^*}{\mathrm{tg}\,\dfrac{\Theta_0}{2}}$:

$$-\frac{q_1^*}{\Omega} = 0{,}597 - j\,2{,}332, \quad -\frac{q_2^*}{\Omega} = 1{,}194, \quad -\frac{q_3^*}{\Omega} = 0{,}597 + j\,2{,}332. \qquad (8.3.14)$$

These values should be placed on the Smith graph; the modulus and the argument z_k may then be found graphically, as shown in Fig. 8.3.10[1].

Finally, the transfer function F(z) of the filter being synthesized may be written in the form:

[1] A detailed discussion of this problem is contained in ref. [8.23].

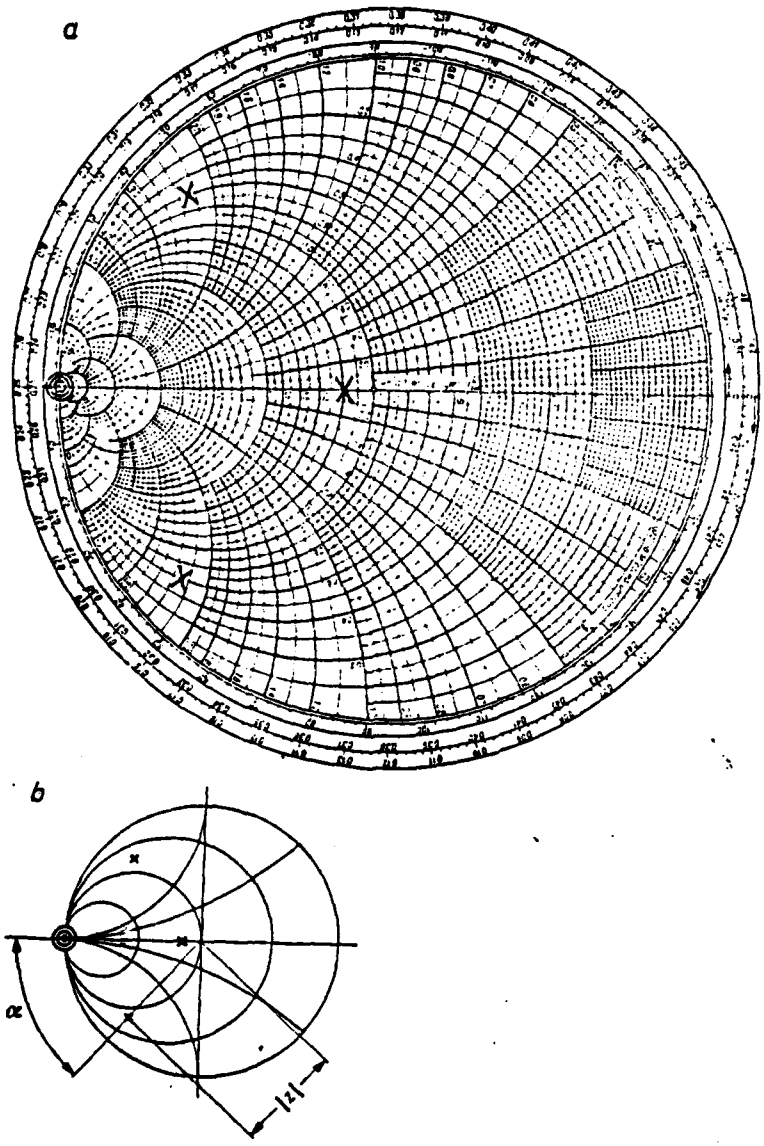

Fig. 8.3.10. Position of singular points of the transfer function on a circular graph.

$$F_3(z) = \frac{(z-1)^3}{(z-z_1)(z-z_2)(z-z_3)} =$$

$$= \frac{(z-1)^3}{(z-0{,}0881)(z^2-1{,}2001z+0{,}7012)}. \qquad (8.3.15)$$

The filter is composed of two sections: the first is /159
a single subtracting system with feedback (β=0.0881), while the second is a double subtracting system with feedbacks (Fig. 8.3.11). The transfer function of this filter is shown in Fig. 8.3.12.

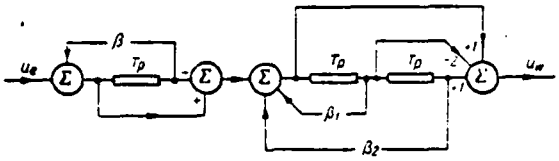

Fig. 8.3.11. Realization of the synthesized periodic filter.

The second section of the filter, shown in Fig. 8.3.11 in the canonical form, may also be realized in another config- /159
uration (cf. Table 8.II), possessing some practical advantages (cf. CH 8.1).

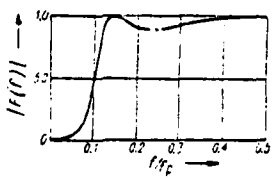

Fig. 8.3.12. Transfer function of a periodic filter, based on the characteristic shown in Fig. 8.3.9.

The appropriate system is shown in Fig. 8.3.13. On the basis of (8.3.15) and Table 8.II, for the case in question, we find β_1=0.4909, β_2=0.7012.

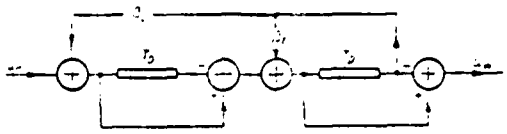

Fig. 8.3.13. A variation of the configuration of the second section of the filter shown in Fig. 8.3.11.

To illustrate the dependence of the shape of transfer function on the value taken for θ_o, Fig. 8.3.14 shows (taken from ref. 8.23) F(f) for three values of θ_o[1].

In some cases it is useful to make the assumption that /160
the zeros of the transfer function lie on the circumference of a unit circle at some relatively small distance from the point z=1.

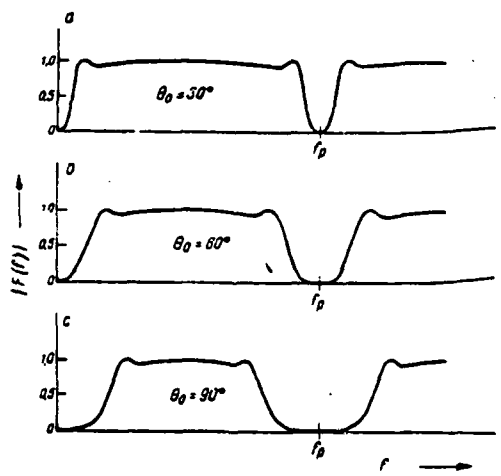

Fig. 8.3.14. Dependence of the shape of transfer function on the assumed value of θ_o.

[1]Similar to this case, the transfer functions shown in Fig. 8.3.14 were synthesized for N=3 and Chebyshev's characteristics, but with the inequality in the lower passband assumed to be 0.5 dB rather than 1 dB.

The system realizing a double subtracting system with the zeros "spread out" is shown in Fig. 8.3.15 [8.12]. Such a system can be regulated more easily than a corresponding canonical system. The reason is that each of the subtracting systems can be regulated (when we set $\beta_0=0$) for minimum output signal; the regulation of the value of β_0 then determines the separation of the zeros. The transfer function of such a system has the form [8.12, 8.23].

$$F_2(z) = \frac{z^2 - (2-\beta_0)z + 1}{z^2 - (\beta_1 + \beta_2)z + \beta_0}. \tag{8.3.16}$$

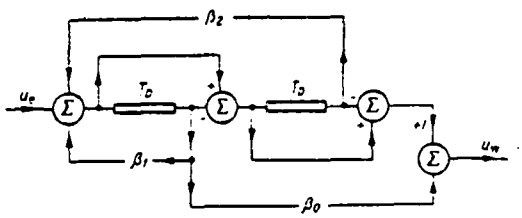

Fig. 8.3.15. A double subtracting system with feedback, having "spread-out" zeros.

References /161

8.1. Kulikowski, J. Introduction to the synthesis of linear electrical systems. PWN, 1957.

8.2. Kroszczynski, J. A simple method for the calculation of the spectra of pulse paths. PIT works, No. 10, 1953.

8.3. Kroszczynski, J. Effectiveness of stationary clutter reduction in a simple and double compensation system. PIT works, No. 24, 1958.

8.4. Seidler, J., Editor. An outline of statistical telecommunication theory. Warsaw, 1964.

8.5. Skolnik, M.I. Introduction to Radar Systems. New York, 1962.

8.6. Cooper, D.C., Griffiths, J.W.R. Video Integration in Radar and Sonar Systems. Journ. BIRE, May 1961.

8.7. Lezin, J.S. Optimal Filters and Collectors of Pulse Signals. Moscow, 1963.

8.8. Finkelshtein, M.I. On Multiple Synchronous Collection of Pulse Signals. Radiotechnika, No. 10, 1963.

8.9. Lighthill, M.J. Introduction to Fourier Analysis and Generalized Functions. Cambridge, 1963.

8.10. Wegrzyn, S. Operator Calculus Applied to the Calculation of undetermined Paths in Linear Systems with Focused Constants. PWN, 1960.

8.11. Solodovnikov, V.V. Statistical Dynamics of Linear Systems of Automatic Guiding. Moscow, 1960.

8.12. White, W.D., Rubin, A.E. Recent Advances in the Synthesis of Comb Filters. IRE Conv. Record, Part 2, 1957.

8.13. Tamburelli, G. Some New Properties of the Z-Transform. Alta Frequenza, Vol. XXXII, English Issue, No. 1, 1963.

8.14. Urkowitz, H. Analysis and Synthesis of Delay Line Periodic Filters. IRE Trans., CT-4, June 1957.

8.15. Linden, D.A., Steinberg, B.D. Synthesis of Delay Line Networks. IRE Trans., ANE-4, March 1957.

8.16. Mason, S.J., Feedback Theory - Some Properties of Signal Flow Graphs. PIRE, Sept. 1953.

8.17. Mason, S.J. Feedback Theory - Further Properties of Signal Flow Graphs. PIRE, July 1956.

8.18. Mason, S.J., Zimmermann, H.I. Electronic Circuits , Signals and Systems. New York, 1960.

8.19. Konorski, B. The Method of Flow Graphs. Przeglad Elektrotechniczny, No. 8, 1963.

8.20. Bronwell, A.B., Beam, R.E. The Theory and Application of Microwaves. PWT, 1951.

8.21. Weinberg, L. Modern Synthesis Network Design from Tables. Electronic Design, Sept. 15, Oct. 1, 15, 1956.

8.22. Weinberg, L. Network Design by Use of Modern Synthesis Techniques and Tables. Proc. Natl. Electronics Conf., Vol. XII, Chicago, 1956.

8.23. White, W.D. Synthesis of Comb Filters. Proc. Natl. Conf. on Aeronautical Electronics, 1958.

8.24. Ignatiev, I.K. Frequency Characteristics of Comb Filters. Nauch. Dokl. Wyssh. Shkoly, Radiotech. and Electronika series, No. 2, 1959.

8.25. MacFarlane, A.G.J. An Analysis of a Type of Comb Filter. PIEE, Part B, Jan. 1960.

8.26. Kulikowski, J. On Some Problems Related to the Calculation of the Elements of an Inverted Covariance Matrix... Electrotechnical Discourses, No. 3, 1961.

9. EVALUATION OF THE DETECTABILITY OF SIGNALS AGAINST AN INTERFERENCE BACKGROUND. /162

For practical applications it is important not only to determine the structure of the optimal receiver systems, but also to evaluate the quality of the decisions made with the use of optimal and suboptimal systems. This problem, which may also be called the problem of evaluation of the signal detectability against the background of interference, will be briefly discussed in the present chapter.

9.1. Calculation of the quality of optimal decisions in the binomial case.

As had been shown in Ch. 4.2., the optimal binary decision rule has the form:

$$x_0^*(y) = \begin{cases} x_1, \text{ jeżeli } \dfrac{P(X = x_2|y)}{P(X = x_1|y)} \leqslant \Lambda_p \\ x_2, \text{ jeżeli } \dfrac{P(X = x_2|y)}{P(X = x_1|y)} > \Lambda_p \end{cases} \tag{9.1.1}$$

(cf. eqs. 4.2.12-4.2.14).

In order to determine the quality of the decisions made on the basis of this rule, we have to calculate, according to the definition (Ch. 4.2 and [9.1] Ch. I), the average risk:

$$l = \mathop{E}_{X \times Y} L[X, x^*(Y)] \tag{9.1.2}$$

taking the decision rule given by (9.1.1) for x*(.). As in the derivation of the optimal rule, it is convenient to calculate the average encompassing the information and signals trans-

mitted as the average of the conditional average. We can write:

$$l = \underset{X \times Y}{E} L[X, x^*(Y)] = \underset{X}{E} \left\{ \underset{Y|x}{E} L[X, x^*(Y)] \right\}, \qquad (9.1.3)$$

where $\underset{Y|x}{E}$ denotes the averaging operation encompassing the set Y of signals received for the information x. We will define /163 the conditional risk:

$$l[x^*(\cdot)\ x] = \underset{Y|x}{E} L[x, x^*(Y)], \qquad (9.1.4)$$

for a defined transmitted signal. Let us assume that information $X=x_1$ is transmitted. The conditional risk is:

$$\begin{aligned} l[x(\cdot)|x_1] = L(x_1, x_1)\, P[x^*(Y) = x_1 | X = x_1] + \\ + L(x_1, x_2)\, P[x^*(Y) = x_2 | X = x_1], \end{aligned} \qquad (9.1.5)$$

where $P[x^*(Y) = x_m | X = x_1]$ denotes the conditional probability of decision $x^*(Y) = x_m$ with the condition that information $X=x_1$ is transmitted.

When the loss is defined, the conditional risk depends only on the probabilities in (9.1.5). They have the meaning of decision error probabilities. Let us denote:

$$\begin{aligned} a_{2|1} &= P[x^*(Y) = x_2 | X = x_1], \\ a_{2|1} &= P[x^*(Y) = x_1 | X = x_2]. \end{aligned} \qquad (9.1.6)$$

Obviously,

$$\begin{aligned} P[x^*(Y) = x_1 | X = x_1] &= 1 - a_{2|1}, \\ P[x^*(Y) = x_2 | X = x_2] &= 1 - a_{1|2}. \end{aligned} \qquad (9.1.7)$$

The calculation of conditional risk is reduced to the calculation of the probabilities of errors $a_{2/1}$ and $a_{1/2}$.

In the detection problems considered here, the information x_1 corresponds to a lack of signal, and information x_2 - to its presence. It is accepted in radar to define the quality of decision by giving the probability of signal detection

$$D = 1 - a_{1/2} \tag{9.1.8}$$

for a defined probability of a false alarm

$$F = a_{2/1} \tag{9.1.9}$$

and for a defined signal-to-noise ratio at the input of the receiving system. Let us note that we are then treating the information (and therefore the transmitted signal) as being defined, and the signal received as being random[1].

As an example we will give the relations for the case of optimal detection of coherent signals with unknown phase and unknown phase and amplitude, on the background of white noise /164 (9.1, 9.3[2]). In both cases the signal frequency is known; thus detection takes place in the system shown in Fig. 6.2.1 or an equivalent one. As a consequence of (6.2.8-6.2.10), the probability distribution of the normalized variable (i.e., the path at the input of the decision system in Fig. 6.2.1), i.e.,

---

[1]We should remind the reader that optimization of reception in the sense of the Neymann-Pearson criterion, i.e., maximization of D at defined value of F, leads to an identical receiver structure as that defined by the criterion of averaged risk. The value of a decision threshold is determined here by the given probability of false alarm [9.2].

[2]Assumptions concerning the signal probability distributions are identical to those in Ch.6; see (6.2.4) and (6.2.13, 6.2.1).

$$\eta'(Y) = \frac{1}{\sqrt{W_0 E_0}}\,\eta(Y) \tag{9.1.10}$$

(cf. eq. 6.2.8), has the form of the Rice distribution:

$$p(\eta' | x_0) = \eta' \cdot \exp\left[-\frac{1}{2}(\eta'^2 + \rho_0^2)\right] I_0(\eta'\rho_0), \tag{9.1.11}$$

where the signal-to-noise ratio is

$$\rho_0 = \sqrt{\frac{E_0}{W_0}}, \tag{9.1.12}$$

and E_0 - signal energy, W_0 - spectral noise density [9.1].

In the case of no signal, distribution (9.1.11) becomes the Rayleigh distribution:

$$p(\eta' | x_1) = \eta' \exp\left[-\frac{1}{2}\eta'^2\right]. \tag{9.1.13}$$

On the basis of these relations, the probability of false alarm F in the case of a signal with unknown phase is:

$$F = \int_{\eta_p}^{\infty} p(\eta' | x_1)\, d\eta' = e^{-\frac{\eta_p^2}{2}}, \tag{9.1.14}$$

where η_p - normalized detection threshold (9.1, Ch.III; 9.3, §33). On the other hand, the probability of signal detection is defined by the formula:

$$D = \int_{\eta_p}^{\infty} p(\eta' | x_0)\, d\eta' = \int_{\eta_p}^{\infty} \eta' \cdot \exp\left[-\frac{1}{2}(\eta'^2 + \rho_0^2)\right] I_0(\eta'\rho_0)\, d\eta'; \tag{9.1.15}$$

the methods for calculating this integral are discussed e.g., in §33 of ref.[9.3] and in ref.[9.4]. Fig. 9.1.1 shows $D(\rho_0)$ (dashed line) for various values of F, calculated according to relation (9.1.15) [9.5].

In the case when amplitude fluctuations are also present, /165
the relation between D, F and $\bar{\rho}$ assumes the following well-known and simple form [9.2] (§34):

$$D = F^{\frac{1}{1+\bar{\rho}^2}} \tag{9.1.16}$$

where

$$\bar{\rho} = \sqrt{\frac{\bar{E}}{W_0}}, \tag{9.1.17}$$

and

$$\bar{E} = \frac{1}{2} E \int_{t_1}^{t_2} \vartheta^2 A^2(t)\, dt \tag{9.1.18}$$

is the average signal energy ([9.1], Ch. III). Relationship (9.1.16) is shown in Fig. 9.1.1 (solid line).

In the case when the signal is composed of a coherent pulse packet, the above equations may also be applied, because we have not made any restrictions as to the shape of the envelope A(t). Since the energy of a pulse series is equal to the sum of the energy of individual pulses

$$E = \sum_i E_i, \tag{9.1.19}$$

it is easy to determine the values E_0 or E, which should be sub-

stituted into (9.1.12 or 9.1.17). If we assume that the packet is "rectangular", i.e., contains N pulses with the same signal-to-noise ratio ρ_1, then we can write:

/166

$$\rho_0 = \rho_1 \sqrt{N},$$
$$\bar{\rho} = \bar{\rho}_1 \sqrt{N}. \qquad (9.1.20)$$

These relations are characteristic of coherent detection.

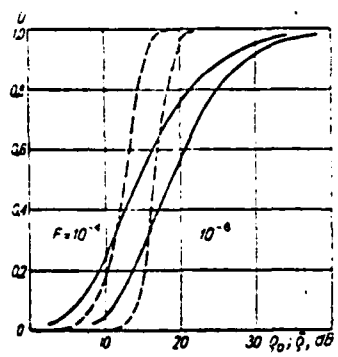

Fig. 9.1.1. Characteristic of detection of signals with unknown phase (dashed lines) and with unknown phase and amplitude (solid lines) [9.3].

The determination of the decision quality for a multichannel system (i.e., with signals of unknown frequency) and for systems designed for detection of noncoherent signals are against a background of strongly correlated interference are much more complicated problems. These will be discussed below.

9.2. Evaluation of the detectability in a multichannel system.

As shown in Ch. 6, the optimal receiver realizing the reception of coherent signals with unknown frequency is a multi-

channel system shown in Fig. 6.2.4[1]. For this system, as follows from Ch. 4.2 and 6.2, the probability ratio (for interference with uniform spectral density W_o) is:

$$\frac{P(x_2|y)}{P(x_1|y)} = \frac{1}{M} \cdot \frac{P(x_2)}{P(x_1)} \cdot \exp\left(-\frac{E}{2W_o}\right) \cdot \sum_{m=1}^{M} \exp\left(\frac{\mu_m}{W_o}\right), \qquad (9.2.1)$$

where M - number of channels, and

$$\mu_m = \int_{t_1}^{t_2} s(t, f_m)\, y(t)\, dt. \qquad (9.2.2)$$

Let us define

$$\Lambda(y) = \sum_{m=1}^{M} \exp\left(\frac{\mu_m}{W_o}\right); \qquad (9.2.3)$$

This is the only factor dependent on the signal received, in (9.2.1). The otpimal binary decision rule is thus equivalent to the rule:

$$x^*(y) = \begin{cases} x_1, & \text{if } \Lambda < \Lambda_p \\ x_2, & \text{if } \Lambda > \Lambda_p \end{cases} \qquad (9.2.4)$$

where Λ_p - threshold of detection (cf. [9.1], p. 142).

In order to calculate the error probability of the rule (9.2.4), we have to calculate the probability density of the random variable $\Lambda(Y_1)$ where Y_1 is a process representing the signals received with the assumption that information $x=x_1$ /167
had been transmitted. This variable is the sum of random variables exp $[\mu_m(y)/W_o]$. They are the so-called logarithmically-

[1]Realization of an equivalent system by other methods is described in Ch. 10.3.

normal variables ([9.6], §17.5). Because of their special character, an accurate calculation of the probabilities of errors meets with considerable difficulties [9.1].

Let us consider certain optimal decision rules, simpler than the rule (9.2.4), namely:

$$x^*(y) = \begin{cases} x_1, & \text{if} \quad \mu_m(y) < \mu_p; \quad m = 1,2 \ldots M \\ x_2, & \text{if} \quad \mu_m(y) > \mu_p; \quad m = 1,2 \ldots M. \end{cases} \tag{9.2.5}$$

Rule (9.2.5) means that if the decision threshold has not been exceeded in any of the individual channels, a decision for no target is made. However, if the decision threshold is exceeded, in at least one of M channels, a decision for presence of the target is made.

The calculation of the errors probability of rule (9.2.5) consists in calculating the joint probability of events

$$\mu_m(Y_i) > \mu_p; \quad m = 1,2 \ldots M, \tag{9.2.6}$$

with the condition that the signal transmitted is defined as $s_i[(\cdot); f_m]$.

If we assume the orthogonality of signals (which is the case here), then the variables μm(Y) become independent and the calculation of probabilities is considerably simplified.

Let us assume that the probabilities of a false alarm and of correct detection are identical for each channel (taken individually):

$$F_1 = F_2 = \ldots = F_M; \quad D_1 = D_2 = \ldots = D_M. \tag{9.2.7}$$

In the case when we assume the detection of a single object, the signal may appear only in one of the channels. The probability of a false alarm for the entire system realizing rule (9.2.5) may be written in the form:

$$F_M = 1 - (1 - F)^M. \qquad (9.2.8)$$

Analogously, the probability of detection will be:

$$D_M = 1 - (1 - D)(1 - F)^{M-1}. \qquad (9.2.9)$$

For sufficiently small F we can set

$$F_M \approx MF \qquad (9.2.8\ A)$$

and

$$D_M \approx D. \qquad (9.2.9\ B)$$

As indicated by the above formulas, the probability of detection in a multichannel system (i.e., with unknown frequency) is approximately identical to that in a single-channel system (i.e., with known frequency), in which an M-fold increase of the pro- /168 bability of a false alarm has been allowed. This can also be interpreted as meaning that to assure certain probability of detection in a multichannel system when the probability of a false alarm is given, it is necessary to determine in each of the individual channels an M-fold lower probability of a false alarm than in the entire system. This relation is discussed and utilized in many publications [9.3, § 57; 9.7, § 3.4].

Let us use these relationships to determine the minimal signal detected in the case of a multichannel system, designed for reception of coherent signals with unknown phase, amplitude, and frequency. As indicated by the preceding chapters, and in

particular by Ch. 9.1, for each individual channel we have the following relationship fulfilled in this case:

$$D = F^{\frac{1}{1+\bar{\rho}^2}}. \tag{9.2.10}$$

where $\bar{\rho}$ – the signal-to-noise ratio for an individual channel (see (9.1.16)).

Thus it follows from (9.2.8 A, 9.2.9) and 9.2.10) that:

$$\bar{\rho}_M^2 = \frac{\ln \frac{1}{F_M} + \ln M}{\ln \frac{1}{D_M}} - 1; \tag{9.2.11}$$

this equation can be written in the form:

$$\bar{\rho}_m^2 = \bar{\rho}_1^2 + \frac{\ln M}{\ln \frac{1}{D_M}}, \tag{9.2.12}$$

where $\bar{\rho}_1$ - the signal-to-noise ratio be necessary to assure identical probability of a false alarm in a single-channel system as in the M-channel system considered here.

In the case of a signal with unknown phase and frequency the relationships are somewhat more complicated and these derivations will not be presented. For D_M=0.5, however, a similar formula is obtained

$$\rho_M^2 = \rho_1 + 2 \ln M \tag{9.3.12}$$

(see [9.3], §57).

As seen from the formulas above, the increase of the signal power, necessary for M-channel detection of the same quality as in single-channel detection, depends approximately on the logarithm of the number of channels M.

A completely accurate comparison of an optimal system /169
operating according to rule (9.2.4) with a suboptimal system operating according to rule (9.2.5) is extremely difficult for reasons described above. However, for large signal-to-noise ratios [9.1], and for small F, these systems can be considered practically equivalent in most cases [9.3, §57, 9.8, 9.9]. The problems related to the questions discussed here are also described in refs. [9.7, 9.10-9.16].

The relationships described above demonstrate the character of the detection process using a multichannel receiver. For a more accurate evaluation of a specific system it is necessary to carry out a more detailed analysis. We have to consider here such problems as the choice of the shape of the transfer function of individual filters[1], their number, positioning, etc. The appropriate considerations require very tedious calculations. Because of space limitations we will not discuss these detailed questions, and will limit ourselves to a summary of certain conclusions.

If the time duration of a signal is denoted by T, and the range of unknown frequencies by B, then the number of the narrow-band filters M should be: $M=(2-3)BT$ [9.9, 9.17]. Reference [9.17] contains numerous graphs of detection probability of a signal in a multichannel system with coherent integration as a function of F, ρ and M. However, the effect of inter-channel correlation was omitted [9.17]. The latter problem is discussed in refs. [9.9, 9.15 and

[1]The optimal shape of transfer function of an individual filter is defined by (7.3.2), but in practice matched filters are usually not used because of practical difficulties, and simple narrow-band filters are used.

9.18]. The last reference also contains many graphs for practical applications. The effect of the positioning of the filter bands (disposition) is discussed in refs. [9.7,], p.234 and (9.9; 9.17.]

Fig. 9.2.1. shows the detection characteristics for the case BT=60, with $F-10^{-4}$. The curves correspond to: A-multichannel receiver with optimal number of channels with rectangular transfer functions; B - a similar case, filters in the form of resonant circuits; C - wide-band receiver with non-coherent integration [9.9]. It is evident that the multichannel receiver gives a distinct improvement relative to the wide-band receiver for both types of characteristics.

In some cases, in individual receiving channels, sub-optimal systems are used which consist of a pre-detection filter, detector and a non-coherent integrator. The detection characteristics for radar devices of this type are presented in the form of five graphs (for $F-10^{-4}$ - 10^{-8}) in the paper of Bussgang et al. [9.19].

The above considerations referred to the detection of signals against the background of white noise. The practical solution of analogous problems for detection against the background of strongly correlated passive interference has not been published /170 to date. Therefore we will discuss some possibilities of utilizing the results obtained for white noise for an approximate evaluation of detectability against the background of passive interference.

When correlated interference has a narrow fluctuation band with a Gaussian shape, the envelope of the maxima of the absolute values of the transfer function for narrow-band filters in a multichannel system has a flat apex within a rather large frequency range [cf. eq. 7.3.7 and Figs. 7.2.2 and 7.3.2). In contrast, within the reduction band, the envelope of the transfer function has

a value near zero, whereas between the base and the apex the transition is very steep (cf. also Fig. 9.4.3).

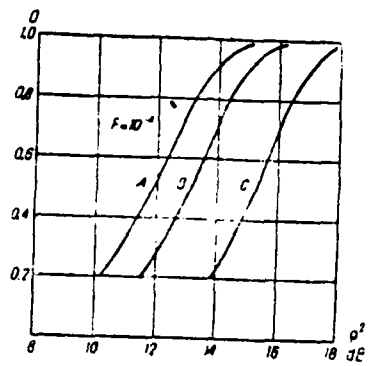

Fig. 9.2.1. Characteristics of detection: A-of a multichannel receiver with an optimal number of channels with rectangular transfer functions; B-as above, filters in the form of resonant circuits; C-of a wide-band receiver with non-coherent integration [9.9].

As follows from this, in this instance the multichannel system may consist of identical channels positioned only within the pass band; whereas the reduction band simply lacks the appropriate channels[1].

The system created in this way may be considered similarly to the previous one, i.e., assuming that within the passband range we are dealing with multichannel detection against the background of white noise. We should, however, in determining the averaged detection characteristic take into account the lowering of the overall detection probability which follows from the fact that in the reduction band, the signal is not detected at all. With the assumption that the probability distribution of occurrence of a given frequency within the range of possible Doppler frequencies is uniform, the detection probability would thus decrease according to

[1]The problem of the decreased influence of the "blind velocities" ranges, generated in this way, is discussed in Ch. 10.

the ratio of the width of transfer band (covered by the multichannel filter system) to the width of the band of possible Doppler /171 frequencies.

In the case when the envelope of the transfer function cannot be approximated by a rectangular function (cf. e.g. Fig. 7.2. 10), the problem becomes very complicated. When the band widths of individual channels are small, it is possible to ignore the variability of the spectral density of interference within the channel's transfer function ([9.2], p.286), which corresponds to approximating the envelope of the transfer function by a step function. Then one could calculate D and F for each channel. In an approximate way, one can match the numerical result with the assumptions, by the method of trial and error. It is easy to see, however, that such a procedure would be extremely tedious and not very accurate. It seems that both because of the calculation difficulties and the large number of parameters which would have to be taken into account, the question of signal detectability against a background of strongly correlated interference using multichannel systems can be effectively considered only with the use of appropriate modeling systems or computers. Similar approaches are used more and more commonly in detection problems [9.20-9.22].

9.3. Passage of signals and interference through optimal and non-optimal filters.

In analyzing the systems for signal detection against the background of correlated interference, the concept of the reduction effectiveness of the filter is often used. This effectiveness is defined as the ratio of the average power of correlated interference at the filter input to the average power of the remains of this interference at the output [9.23-9.25]. It is easy to note that reduction effectiveness cannot be taken as the only

criterion for evaluating the detection systems; e.g., by closing the filter output we will easily obtain an infinitely large reduction of correlated interference, but we will certainly not achieve any improvement of signal detectability. However, as will become evident below, assuring an appropriate effectiveness of reduction of correlated interference is one of the necessary conditions for obtaining good decision quality (see Ch. 9.4). Analysis of the reduction of interference and of the signal also allows us to better understand the operating mechanism of optimal and non-optimal receiver systems. Therefore we will consider this problem in swmewhat more detail here.

In accordance with the definition given above, the reduction effectiveness ; can be written as follows:

$$\zeta = \frac{\int_{-\infty}^{\infty} W_k(f)\, df}{\int_{-\infty}^{\infty} W_k(f) \cdot |F(f)|^2\, df}, \qquad (9.3.1)$$

where

W_k (f) - spectral density of correlated interference; /172

F (f) - transfer function of the filter.

In the case when it is more convenient to use the autocorrelation function rather than spectral densities, we can write the equivalent relation:

$$\zeta = \frac{R_e(0)}{R_k(0)}, \qquad (9.3.2)$$

where

R_e (τ) - autocorrelation function of interference at the filter input;

$R_W(\tau)$ - autocorrelation function of the remaining interference at the output.

As before, we will start by considering the simplest systems. The reduction effectiveness of a single subtracting system (Fig. 8.1.1) can be calculated by substituting (8,1.6) into (9.3.1), or by determining $R_W(\tau)$ and then using (9.3.2).

On the basis of Fig. 8.1.1 we can write:

$$R_w(\tau) = \lim_{T\to\infty} \frac{1}{2T} \int_{-T}^{T} [u_e(t) - u_e(t - T_p)] \cdot [u_e(t + \tau) - - u_e(t + \tau - T_p)]\, dt, \qquad (9.3.3)$$

where $u_e(t)$ is the realization of a stationary stochastic process, representing correlated interference.

After transformation we obtain:

$$R_w(\tau) = 2R_e(\tau) - R_e(\tau + T_p) - R_e(\tau - T_p). \qquad (9.3.4)$$

The reduction effectiveness of a single subtracting system can be therefore written in the form:

$$\zeta_1 = \frac{R_e(0)}{2[R_e(0) - R_e(T_p)]} = \frac{0.5}{1 - \rho_e(T_p)}, \qquad (9.3.5)$$

where $\rho_e(\tau)$ - normalized autocorrelation function of the interference.

We should note the interpretation of (9.3.5). Let us draw the normalized autocorrelation function $\rho_e(\tau) = R_e(\tau)/R_e(0)$. The quantity proportional to the remaining (i.e. not reduced) interference can be read directly from the graph in Fig. 9.3.1.

This gives a graphic picture of the dependence of the reduction on the parameters considered.

Similarly, for a double system (cf. Fig. 8.1.3), we will have [9.24]:

$$R_w(\tau) = 2\left[3R_e(\tau) - 2R_e(\tau + T_p) - 2R_e(\tau - T_p) + \right.$$
$$\left. + \frac{1}{2} R_e(\tau + 2T_p) + \frac{1}{2} R_e(\tau - 2T_p)\right], \qquad (9.3.6)$$

and from this:

$$\zeta_2 = \frac{0.5}{3 - 4\rho_e(T_p) + \rho_e(2T_p)}. \qquad (9.3.7)$$

Various periodic filters have different values of the maxima of transfer function, which should be taken into account in considering reduction. This can be done e.g. by calculating ζ . for normalized transfer functions[1]; then we will be using the notation ζ_n .

For the case of Gaussian shape of the fluctuation spectrum (cf. eq. 5.3.4) we can specifically determine the reduction effectiveness depending on the type of interference. For instance, substituting (5.3.4) and (8.1.6) or (8.1.8) into (9.3.1), we obtain for the single subtracting system[2]:

$$\zeta_{1n} = \frac{2}{1 - \exp\left[-\frac{1}{a}(\pi f_p T_p)^2\right]}; \qquad (9.3.8)$$

[1]This corresponds to the assumption of the same system dynamics following periodic filter.

[2]In substitutions to (9.3.1) the following relation was used [9.26]:

$$\int_0^\infty e^{-px^2} \cdot \cos qx \, dx = \frac{1}{2}\sqrt{\frac{\pi}{p}} \cdot e^{-\frac{q^2}{4p}}.$$

while for the double system we will have [9.24]:

$$\zeta_{2n} = \frac{8}{3 - 4\exp\left[-\frac{1}{\alpha}(\pi f_p T_p)^2\right] + \exp\left[-\frac{4}{\alpha}(\pi f_p T_p)^2\right]}. \qquad (9.3.9)$$

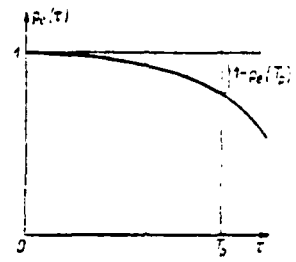

Fig. 9.3.1. Geometrical interpretation of (9.3.5).

The graphs of relations (9.3.8) and (9.3.9) for a wide range of parameters (for normalized transfer functions) are given in ref. [9.24]. In order to simplify the discussion let us introduce coefficient k, equal to the ratio of the spectrum width (at the /174
half-power level) Δ_f to the repetition frequency f_p (cf. Fig. D 6.1):

$$k = \frac{\Delta_f}{f_p} = \Delta_f T_p. \qquad (9.3.10)$$

This coefficient indicates the part of the period of the periodic filter's transfer function which is "filled" by the fluctuation spectrum of passive interference. It is easy to see that the greater the coefficient k, the more difficult it becomes to obtain significant reduction of correlated interference using simple filters.

Substituting (9.3.10) in (9.3.8) or (9.3.9) we will obtain for the case of interference with a Gaussian spectrum:

$$\zeta_{1n} = \frac{2}{1 - \exp(-3{,}56k^2)}, \tag{9.3.11}$$

$$\zeta_{1n}(\mathrm{dB}) = 3 + 10\log[1 - \exp(-3{,}56k^2)]^{-1}, \tag{9.3.11A}$$

and

$$\zeta_{2n} = \frac{8}{3 - 4\exp(-3{,}56k^2) + \exp(-14{,}24k^2)}, \tag{9.3.12}$$

$$\zeta_{2n}(\mathrm{dB}) = 9 + 10\log[3 - 4\exp(-3{,}56k^2) + \exp(-14{,}24k^2)]^{-1}. \tag{9.3.12A}$$

These relations are illustrated in Fig. 9.3.2. For most practical applications the coefficient k lies in the range 0.01-0.1.

For the case of interference with a spectrum of type $a/(a^2 + \omega^2)$, i.e. with a correlation function $p(\tau) = \exp(-a\tau)$, it is easy to calculate the reduction using (9.3.2). After transformations we obtain:

$$\zeta_{1n} = \frac{2}{1 - \exp(-\pi k)}, \tag{9.3.13}$$

$$\zeta_{1n}(\mathrm{dB}) = 3 + 10\log[1 - \exp(-\pi k)]^{-1} \tag{9.3.13A}$$

and

$$\zeta_{2n} = \frac{8}{3 - 4\exp(-\pi k) + \exp(-2\pi k)}, \tag{9.3.13}$$

$$\zeta_{2n}(\mathrm{dB}) = 9 + 10\log[4 - 3\exp(-\pi k) + \exp(-2\pi k)]^{-1}. \tag{9.3.14A}$$

A graph of these relationships is shown in Fig. 9.3.3; for this type of interference the reduction effectiveness of both systems is similar and smaller than for interference with a Gaussian spectrum.

When the interference is strongly correlated, the auto- /175
correlation function decreases slowly and the exponential terms in the above equations are smaller than unity. We can say then, approximately, that the reduction effectiveness for interference with Gaussian spectrum is inversely proportional to k^2 for the single, and to k^4 - for the double subtracting system (cf. Fig. 9.3.2). Similarly, for interference with an autocorrelation function of the type $e^{-a\tau}$ the reduction effectiveness is approximately inversely proportional to k for both single and double subtracting systems[1] (cf. Fig. 9.3.3). These relationships give a graphic comparison of the systems discussed in terms of reduction of correlated interference.

Similar methods as the ones above may be used to determine reduction of L-fold subtracting systems.

In the case of more complicated systems (especially when they contain feedback circuits), the z-transform may also be used (cf. Ch. 8). The periodic spectrum of correlated interference at the filter input can be represented [9.27] in the form:

$$W_e(z) = \sum_{q=-\infty}^{\infty} R_e(qT_p)\, z^{-q}. \qquad (9.3.15)$$

[1]These conclusions may be reached by replacing the exponential terms by the first terms of their expansion into a power series in the reduction equations.

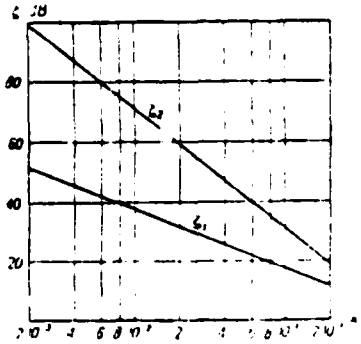

Fig. 9.3.2. Reduction effectiveness of correlated interference in a single and double subtracting system (interference with Gaussian spectrum).

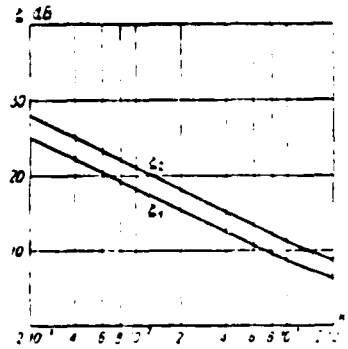

Fig. 9.3.3. Reduction effectiveness of correlated interference in a single and double subtracting system (interference with exponential autocorrelation function).

The interference spectrum at the filter output when the filter has an operator transfer function F(z) can be therefore determined from the formula: /176

$$W_w(z) = F(z)\,F(1/z)\,W_e(z). \tag{9.3.16}$$

The autocorrelation function of interference at the output of a periodic filter is obtained from the relationship (cf. eq. 8.2.14).

$$R_w(rT) = \frac{1}{2\pi j}\oint F(z)\,F(1/z)\,W_e(z)\,z^{r-1}\,dz. \tag{9.3.17}$$

As shown by Urkowitz (9.27), it follows from the above equation that:

$$R_w(rT) = R_e(0)\left\{\sum_n h_n h_{n+|r|} + \sum_{q=1}^{\infty} \rho_e(qT)\left[\sum_n h_n h_{n+|r-q|} + \sum_n h_n h_{n+|r+q|}\right]\right\}, \tag{9.3.18}$$

where h_n has a meaning identical to that in (8.2.2); in the formula above $h_i=0$ for $i < 0$.

The average power of interference at the output is therefore:

$$R_w(0) = R_e(0)\left[\sum_n h_n^2 + 2\sum_{q=1}^{\infty} \rho_e(qT) \sum_n h_n h_{n+q}\right]. \qquad (9.3.19)$$

On the basis of the above equations we can determine the reduction effectiveness of systems whose operator transfer function or the pulse response are given. For instance, for a single subtracting system with feedback (Fig. 8.1.7) we have:

$$\zeta_\beta = \frac{0{,}5(1+\beta)}{1-(1-\beta)\sum_{m=1}^{\infty} \beta^{m-1} \rho_e(mT)} \qquad (9.3.20)$$

and

$$\zeta_{\beta a} = \frac{2}{(1+\beta)\left[1-(1-\beta)\sum_{m=1}^{\infty} \beta^{m-1} \rho_e(mT)\right]}. \qquad (9.3.21)$$

We will now discuss the example of an optimal periodic filter, of the type described in Ch. 6.2, whose transfer function modulus is defined by (7.2.6). As the transfer function is matched to the properties of interference (cf. Fig. 7.2.2 and 7.2.10). Let us consider a typical case, when the interference spectrum has a Gaussian shape, the average power of correlated interference is greater by 40 dB than the average power of non-correlated noise, and k=0.06. This corresponds to the ratio of the maximal /177 spectral density of correlated interference to the spectral density of noncorrelated noise being equal to appr. 55 dB (see Appendix 6). Fig. 9.3.4 represents the modulus of the normalized transfer function of an optimal filter for this case[1].

[1]Because of the symmetry, the figure shows only the graph in the range of frequency from 0 to $f_p/2$.

Unfortunately, for the case in question it has not been possible to find an exact general expression of reduction effectiveness. This reduction was calculated using approximate methods.

As indicated by the calculations, a filter having the modulus of the transfer function shown in Fig. 9.3.4 reduces correlated noise by about 64 dB. One should note that at a given ratio of the maximal spectral density of passive interference fluctuation C to the spectral density of noncorrelated noise W_n, the reduction by the optimal filter [illegible] is, within a wide range, independent of the coefficient k because of the characteristic flat course of the upper part of the filter transfer characteristic (cf. Fig. 9.3.4).

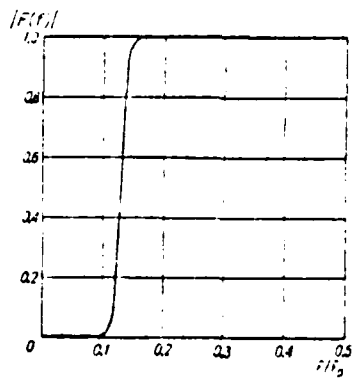

Fig. 9.3.4. Transfer function of the optimal filter for k=0.06

For instance, in the present case the reduction would be effectively independent of k starting at very low values of k up to [illegible].

Fig. 9.3.5 shows the function [illegible] and the spectrum of correlated noise at the output of the optimal filter for the parameters accepted above. At the output of an optimal filter the greatest spectral density of correlated interference falls within

the region of the maximal inflection of the filter's transfer function F(f).

Next, we consider the possible reduction of the detected signal during its passage through the periodic filters discussed here. Since, as shown in Ch. 7, the power spectrum of the signal has a shape similar to the power spectrum of a single pulse in the cases considered here (cf. eq. 7.1.8), it may be assumed with sufficient approximation to be constant within a single period of the periodic filter characteristic. Therefore, the reduction of such a signal in a periodic filter will be identical to the reduction of white noise. For a single and double subtracting system it can be easily calculated, assuming that $k \to \infty$. The value of the exponential terms in the equations then approaches zero and we obtain as a result for a single subtracting system a signal reduction equal 3 dB, and for a double system - about 4.3 dB[1]. For optimal filters, obviously, the signal reduction depends on the value of the coefficient k, which determines the shape of the optimal filter characteristic.

For the case C/W_0=55 dB (i.e., as in example described above), the signal reduction as a function of coefficient k is shown in Fig. 9.3.6.

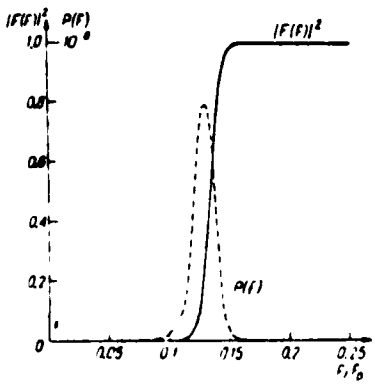

Fig. 9.3.5. Graph of function $|F(f)|^2$ and the spectrum of correlated noise at the output of a periodic filter.

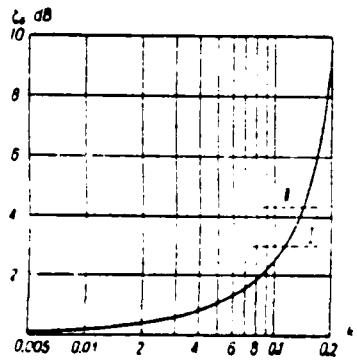

Fig. 9.3.6. Reduction of signal (by an optimal filter with transfer function as in Fig. 9.3.4) as a function of coefficient k.

[1] Of course, for normalized characteristics.

The optimal filter in question is characterized by a considerable reduction of correlated interference and relatively small signal loss. In the example cited the reduction of correlated interference was more than twice the ratio of the power of average correlated and noncorrelated interference. In terms of the reduction of correlated interference, the optimal filter has better properties than single or double subtracting systems at relatively greater values of coefficient k. For instance, for /179
k=0.1 the optimal filter reduces the interference with a Gaussian spectrum by about 47 dB more effectively than the single system and by about 33 dB for the double subtracting system. Although these systems show good reduction for very narrow-band interference, they cause greater signal losses than the optimal filter[1] within this range.

The optimal filter, in contrast with the simple subtracting systems, has a characteristic which depends on the given interference spectrum. It is easy to see the result of the interference spectrum at the input of such a filter. It is significantly different from the spectrum assumed. Let us denote the value of coefficient k assumed in defining the characteristics of the optimal filter by k_o. Such a filter will reduce more strongly the correlated noise with a narrower band (i.e., with $k<k_o$), but it will not be optimal in this case because it will not utilize the possibilities of decreasing signal losses. In contrast, when $k>k_o$, the reduction of the filter (because of the specific shape of characteristic - see Fig. 9.3.4) will decrease considerably. Since the signal losses change relatively little depending on the accepted value of k_o, a highly negative effect on signal detectability is pro-

[1]A simple physical interpretation is easy for the effect of strong reduction of subtracting systems, if we deal with very narrow-band interference. For interference with "infinitely narrow" spectrum the path within each pulse repetition period would be effectively the same, and thus their elimination would be achieved even by a single subtracting system.

duced by the appearance of correlated interference with a wider band than the one assumed for the given optimal filter. In contrast, narrow-band noise is in this case less adverse.

In summary, the optimization of the transfer function of a periodic filter becomes all the more necessary when the relative bandwidth of the fluctuation spectrum of correlated interference increases. Thus such an optimization is especially important in modern radar devices characterized by rapid scanning of space and operating with small numbers of reflections from a single object.

9.4. Evaluation of the detectability of noncoherent signals.

In order to evaluate the quality of decisions made by a receiving system it is necessary to define the probability of correct signal detection for a given probability of a false alarm (see Ch. 9.1). It is well known that this requires the knowledge of appropriate distributions of probability densities at the input of a threshold decision system.

For the case of a receiver of noncoherent signals the problem of finding these distributions is rather difficult even /180 when only noncorrelated noise is present, because of nonlinear transformation effected by the detector. For the case of a quadratic detector (cf. Fig. 6.2.6), this problem is solved, but complicated expressions are obtained (9.3, 9.29-9.31). Their application in specific calculations is tedious. Swerling's work [9.31] considers e.g., the problem of signal reception in the form of a pulse packet, characterized by fluctuation between pulses, with noncorrelated noise, quadratic detector characteristic and application of post-detection summation[1]. For such signals, with

[1]For signals of the type considered, i.e., pulse series with low filling coefficient, we may assume the operation of summation approximately equivalent to integration.

with the distribution of fluctuation probability according to Rayleigh's law, the dependence of the probability of correct detection D as a function of the averaged signal-to-noise ratio $\bar{\rho}$ is the following [9.31]:

$$D = 1 - I\left[\frac{\Lambda_p}{(1+\bar{\rho}^2)\sqrt{N}}, N-1\right] \tag{9.4.1}$$

where

I - incomplete function gamma [9.32];

N - number of pulses per packet;

Λ_p - decision threshold.

Ref. [9.31] contains many graphs which allow easy determination of D(F) for various N and $\bar{\rho}$.

In the case of correlated noise the problem is incomparably more complex, since we cannot use the assumption of statistical independence of noise for the consecutive pulses within the packet received, which contains N pulses. One should find here the appropriate multidimensional probability distributions for signals and noise, at the output of optimal filters described previously. Then, one should find the multidimensional probability distributions after passage of the paths described through the nonlinear element - the detector - and then take into account the transformation carried out by the integrator, to finally obtain the probability distributions for signal and noise at the input of the decision system.

The problem of determining the probability distribution for a stochastic process generated from the correlated Gaussian process by detection (however, with a linear detector characteristic) was considered by Hoffman [9.33], but the expression he obtained is complex. The problem of the probability distribution at the output of a system consisting of a serial connection of a

linear filter, quadratic detector, and a second linear filter, was considered by Mayer and Middleton and, from a somewhat different point of view, by Emerson ([9.34, 9.35). These references use complicated mathematical methods and achieve solutions for simple filter characteristics. For periodic filters this problem has not been solved to date, especially the shape of optimal filters. An exact solution of the problem of determining the decision quality for the case in question must therefore be seen as a very difficult numerical problem. A practical utilization of the solution, even if it were obtained, would require numerical calculations even more complicated than those contained in refs. [9.30, 9.31]. They would also be very extensive because of the considerably greater number of variables involved in the problem of detection in the presence of noncorrelated interference (the bandwidth of correlated noise, shape of the autocorrelation function, ratio of the power of correlated and noncorrelated noise, etc.). This question could be approached using the methods of analog modeling or computers [9.20, 9.36], which would require rather extensive programs. No results of such investigations for the case of correlated interference have been published so far. /181

In this situation it becomes particularly important to find methods which allow to solve the problem in question in an approximate manner, but simply. It seems that for the range of questions considered in the present work there are possibilities of an approximate evaluation of the decision quality for parameters encountered in practice using certain special properties of the transfer function of optimal periodic filters.

In the case of correlated interference with a relatively narrow band of Gaussian shape, its reduction by an optimal filter is very strong. E.g., in the example considered in Ch. 9.3. The difference between the power levels of correlated interference and noncorrelated noise was 40 dB and the reduction of correlated interference was about 64 dB. In contrast, the reduction of non-

correlated noise by the same filter is rather small and in the case considered was only about 1.4 dB. Evidently, the interferences at the output of a periodic filter are derived almost entirely from the noncorrelated input noise. However, it differs from white noise because in the characteristic of the optimal filter there exist bands of strong reduction in the regions of multiple repetition frequency f_p. But these bands are relatively narrow. Outside of these the characteristic of the optimal periodic filter is completely flat (Fig. 9.3.4).

In summary, it seems justified to consider the problem of the decision quality in the system considered by an approximate method, by determining the reduction of the noise and signal by an optimal pre-detection filter, and then treating the quantities obtained as the input to the "quadratic detector + linear summator" system with the assumption that the noise at the input of the quadratic detector already has an approximately noncorrelated charac- /182
ter. We can use in this case the solutions of the problem of the decision quality in the "quadratic detector + linear summator" system [9.31], and in particular (9.4.1).

Fig. 9.4.1 shows the probability of correct detection of signal D as a function of the averaged ratio of the signal to correlated interference $\overline{\rho}^2$, with $k = \frac{\Delta f}{f_p} = 0{,}06$ (calculated with the simplifying assumptions as above) and with correlated interference stronger by 40 dB from noncorrelated noise (the optimal periodic filter has a characteristic shown in Fig. 9.3); the detected signal contains ten pulses[2] and the number of false alarms is $n-10^8$ [1].

[1]The false alarm number is a way of determing the probability of false alarm accepted in refs.[9.30,9.31], which is convenient in some applications. $n=T_{fa} \cdot f_p \cdot \nu$, where T_{fa} - time of false gating alarm, f_p - frequency of repetition, ν - the number of spaces for detection, falling within a single repetition period.

2) A correction of 1.6 dB has been introduced in the plot of graph 9.4.1, in order to make allowance for the nonrectangular shap of the pulse packet [9.30; 9.37].

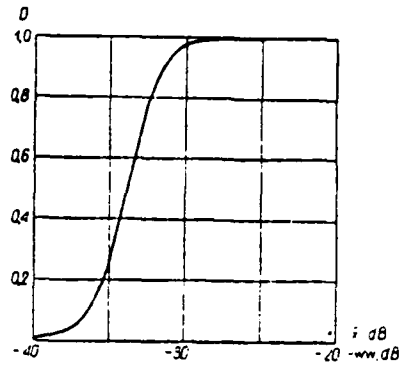

Fig. 9.4.1. Probability of signal detection against the background of correlated noise (with an optimal filter having a transfer function as in Fig. 9.3.4).

In evaluating the signal detectability in correlated noise, the notion of the so-called visibility coefficient[1] is used in practice; this coefficient will be denoted by WW.

The visibility coefficient is defined as the ratio of the levels of passive interference and the echo signal (usually expressed in dB), at which the signal is still detected[2]. Thus, if one detects a signal weaker by e.g. 25 dB than the passive interfer- /183

[1]English: Subclutter Visibility, SVC (cf. e.g. [9.25]).

[2]This definition is used e.g., in refs. [9.25] and [9.39]. We should note that there are also other ways of defining visibility. E.g., in ref. [9.40] SCV is defined as the ratio of the passive interference to the level of such a signal with optimal Doppler frequency, at which the ratio of the power of signal to noise at the output of a periodic filter is 2. ESCV (Expected SCV) is similarly defined there, and averaged assuming uniform probability distribution of Doppler frequencies. The visibility coefficient may also be defined as the ratio of signal level detectable in the presence of passive interference without using counter-noise systems to the signal level detectable in the presence of the same interference with the use of such systems [9.41].

ence, then we say that the visibility coefficient for this example equals 25 dB. The graph shown in Fig. 9.4.1 gives the values of WW for a given detection probability. E.g., the value of WW at D=0.5 (denoted by $WW_{0.5}$) is about 34 dB; $WW_{0.9}$= 31.5 dB, etc. These values are higher than those usually obtained in practice under condition corresponding to the assumptions made; this problem will be discussed below.

In order to make some comparisons, let us estimate WW for some suboptimal receptor systems, such as the single and double subtracting systems mentioned above. We should mention that the following considerations should be treated as a completely approximate estimate; but they allow to understand better some aspects of the physical interpretation of optimal reception in correlated interference.

At k=0.06 (i.e. at k identical as in the example of the optimal filter considered previously), the reductions for correlated interference with Gaussian spectrum have the following values for the single and double subtracting systems, ζ_1=22 dB, ζ_2=40 dB, respectively (cf. Fig. 9.3). The signal reduction is 3 dB for the single system, and about 4.3 dB for the double system. With noncorrelated interference weaker by 40 dB than the correlated interference (as assumed in preparing Fig. 9.4.1), the interference at the output of the periodic filter will therefore be derived, mainly from the correlated interference in contrast to the situation in the optimal filter. The summator system gives an improvement of signal detectability for signals composed of N pulses primarily in the presence of noncorrelated interference. Noting again that the present analysis is a very rough estimate, we can expect that for a suboptimal filter, i.e., with strong remaining noise at the output of periodic filter, the signal detected would be of a similar order as for the case of lack of integration in the worst case i.e., for N=1. Therefore we can

estimate $WW_{0.5}$ as approximately equal 20 dB for a double system, and only several dB for a single subtracting system. For more narrow-band interference, already at k=0.01 we have ζ_1=37 dB and ζ_2=71 dB. Therefore, for k=0.01 WW could be estimated close to the optimal WW when a double subtracting system is used. In contrast, for a single subtracting system, $WW_{0.5}$ at k=0.01 may be roughly estimated to be about 20 dB[1].

Evidently, when the suboptimal system has a periodic filter, with smaller correlated noise reduction than an optimal filter, it leads to a decrease in detectability for two reasons; first, correlated interference is reduced less effectively; second, there is a decrease in the effectiveness of post-detection integration. The examples considered show that in some cases post-detection integration practically would be almost unnecessary. We should mention that experience confirms this conclusion and in practical applications one usually does not find any special integration systems (aside from the indicator screen) in receivers where simple periodic filters are used in the form of single or double subtracting systems. /184

Our estimates also suggest that for very narrow-band passive interference with a Gaussian spectrum, the double subtracting system could have properties similar to an optimal filter. This would apply to the rather rare cases, since even omitting their own fluctuations for passive interference, such a situation would only occur at N>60 (cf. Appendix 6).

In summary, we can state that the advantages of optimal filters are most apparent in detection of signals with correlated interference having a large relative bandwidth. Compared to the

[1]When systems of non-quadratic reception are used (which is often the case in practice), WW will decrease. This problem will be considered below.

single or double subtracting systems, the optimal filters then allow a considerable improvement of signal detectability. This also indicates the practical usefulness of using filters which better approximate the optimal characteristics, e.g., double subtracting systems with double feedback.

The problem of the detection effectiveness when a single subtracting system is used, has been considered in the literature from a somewhat different standpoint, namely assuming a [illegible]ent echo signal. Bailey [9.38] has estimated the detectabili[illegible] of a coherent pulse signal with unknown carrier frequency, using a single subtracting system with phase detection and post-detection summation[1]. Fig. 9.4.2 (taken from the reference cited) shows the detection probability of a packet composed of 30 coherent pulses (at $F=10^{-6}$), as a function of the reduced signal-to-noise ratio $\rho_r^2 = \rho^2/\zeta$, where ρ - the signal-to-noise ratio at the receiver input, and ζ - reduction (non-normalized) of correlated interference in the periodic filter[2].

Evidently, for the detection probability d=0.5, in this system the visibility coefficient $WW_{0.5}$ is smaller by about 5 dB than ζ - reduction of correlated interference. Similarly, $WW_{0.9}$ /185
$WW_{0.9}$ (dB) $\cong \zeta$(dB) $-$ 19 dB [9.38], Fig. 8.

Vainshtein and Zubakov [9.3] also considered the detectability of a coherent signal against a background of correlated interference using a receiver equipped with subtraction systems. They assumed that such a receiver is, approximately equivalent to the optimal receiver for highly correlated interference. Fig.

[1]In ref. [9.38] it was also assumed that the interference at the summator input (i.e. at the output of subtraction and detector systems) may be considered noncorrelated. The appropriate integrals were calculated numerically, since exact solution could not be found.

[2]It is easy to note that ρr^2 is the ratio of signal power to interference at the output of subtraction system.

9.4.3 (taken from the reference cited) shows the detection probability of a nonfluctuating coherent signal with unknown frequency, at $F-10^{-5}$. For the receiver signal subtraction was used without post-detection summation. Curve A refers to the case of a quadratic (two-channel) system, B - the single-channel system. This figure illustrates the effect of omitting one channel on the decrease in detection effectiveness ([9.3], Fig. 3.9). The authors also discussed the problem of detectability of a fluctuating echo, using a receiver with a single subtracting system without post-detection summation, and included an example of a graph for a specific case.

The questions related to the detectability of coherent signals using subtraction systems (including multiple systems) has been also considered at length in the work by Tartakowski et. al. [(9.7, Ch. 4).

As indicated by the above, the signal detectability against a background of correlated interference is related to the effectiveness of its reduction ζ. Knowing ζ, it is possible to reach certain approximate conclusions about the visibility coefficient WW

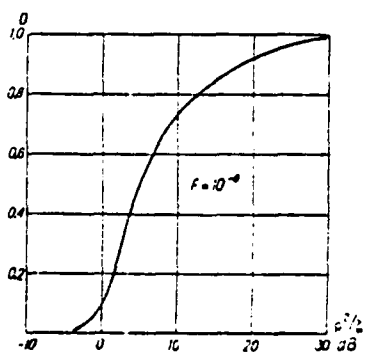

Fig. 9.4.2. Detection probability of a pocket of coherent pulses, with a single subtracting system with phase detection and without post-detection integration [9.38].

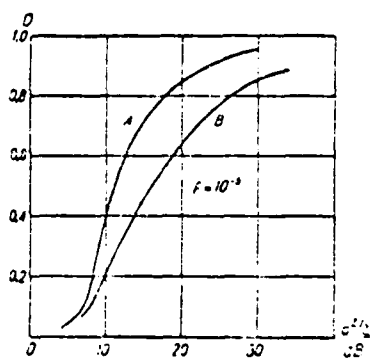

Fig. 9.4.3. Detection probability of a coherent signal using a two-channel system (curve A) and a single-channel system (curve B); single subtraction.

(of course remembering the assumptions restricting such an approach). Let us denote by P_k the average power of correlated interference, and by P_n - the average power of noncorrelated noise. /136
For the range of parameters seen in practice, usually $WW < 1$ and $WW < P_k/P_n$. The visibility coefficient thus depends approximately on the reduction of correlated interference ζ, or on the ratio of the power of correlated interference to the noncorrelated noise P_k/P_n, namely on the smaller of the two values. A more exact estimate of the visibility coefficient can be obtained by the methods described above.

References.

9.1. Seidler, J. Statistical Theory of Signal Reception. PWN, 1963.

9.2. Gutkin, L.S. The Theory of Optimal Radar Methods in Fluctuating Noise. Moscow, 1961.

9.3. Vainshtein, L.A., Zubakov, V.D. Signal Selection Against a Background of Random Noise. Moscow, 1960.

9.4. Bunimovich, V.I. Approximate Expression of the Probability of Correct Detection with Optimal Reception of Signal with Unknown Phase. Radiotechnika i Elektronika, No. 4, 1958.

9.5. Shirman, J.D., Golikov, V.N. The Principles of the Detection Theory of Radar Signals and of the Measurement of their Parameters. Moscow, 1963.

9.6. Cramer, H. Mathematical Methods in Statistics. PWN, 1958.

9.7. Tartakowski, G.P. et al., Problems of the Statistical Radar Theory. Moscow, 1963.

9.8. Dobrushin, R.L. A Statistical Problem of the Detection Theory of Signal against the Background of Noise in Multi-channel System, Which Leads to Stable Distribution Principles. Probability Theory and Its Applications. No. 2, 1958.

9.9. Cherniak, J.B. Detection of Signal with Unknown Frequency and Arbitrary Leading Phase against the Background of White Noise. Radiotechnika i Elektronika, No. 3, 1960.

9.10. Peterson, W.W., Birdsall, T.G., Fox, W.C. The Theory of Signal Detectability. IRE Trans. on Inform. Theory, PGIT-4, Sept. 1954 RCA Review, No. 3, 1955.

9.11. Benner, A., Dreniek, R. On the Problem of Optimum Detection of Pulsed Signals in Noise. RCA Review, No. 3, 1955.

9.12. Middleton, D., Van Meter, D. On Optimum Multiple-alternative Detection of Signals in Noise. IRE Trans. on Inform. Theory, IT-1, January 1955.

9.13. Filipov, L.I. Potential Resistance to Interference in Pulse Signal Reception. Radiotechnika, No. 10, 1955.

9.14. Siebert, W. A Radar Detection Philosophy. IRE Trans. on Inform. Theory, IT-2, Sept. 1956.

9.15. Cherniak, J.B. An Approximate Method for the Calculation of Detection Characteristics of Mulitple-Channel Systems in Correlated Interference with Amplitude Selection According to the Highest Value. Radiotechnika i Elektronika, No. 2, 1960.

9.16. Fine, T.L., Levin, M.J. Extreme-Value Theory Applied to False-Alarm. Probabilities. IRE Trans. on Inform. Theory, IT-8, April 1962, p. 250.

9.17. Miller, K.S., Bernstein, R.I. An Analysis of Coherent Integration and Its Application to Signal Detection. IRE Trans. on Inform. Theory, IT-3, December 1957.

9.18. Galejs, J., Cowan, W.M. Interchannel Correlation in a Bank of Parallel Filters. IRE Trans. on Inform. Theory, IT-5, Sept. 1959.

9.19. Bussgang, J.J., Nesbeda, P. Safran, H. A Unified Analysis /187
of Range Performance of CW, Pulse, and Pulse Doppler Radar. PIRE, Oct. 1959. Correction, PIRE, May 1960, p. 931.

9.20. Lambert, J., Heidrich, A. Radar Systems Simulation Techniques. IRE Nat. Conv. Rec., Part 4, 1959.

9.21. Meltzer, S.A., Thaler, S. Detection Range Predictions for Pulse Doppler Radar. IRE Inten. Conv. Rec., Part 4, 1960.

9.22. Wishner, R. P. Distribution of the Normalized Periodogram Detector. IRE Trans. on Inform. Theory, IT-8, October 1962.

9.23. Grisetti, R.S., Santa, M.M., Kirkpatrick, G.M. Effect of Internal Fluctuations and Scanning on Clutter Attenuation. IRE Trans. ANE-2, March 1955.

9.24. Kroszczynski, J. Stationary clutter Reduction Effectiveness in A simple and Double Compensation System. PIT Works, No. 24, 1958.

9.25. Skolnik, M.I. Introduction to Radar Systems. New York, 1962.

9.26. Ryzyk, I.M., Gradshtein, I.S. Tables of Integrals, Sums, Radii and Derivatives. Moscow, 1951.

9.27. Urkowitz, H. Analysis of Periodic Filters with Stationare Random Inputs. IRE Trans. on Circuit Theory. IT-6, Dec. 1959.

9.28. Helstrom, C.W. Statistical Theory of Signal Detection. New York, 1960.

9.29. Stone, W.M. On the Effect of Integration in a Pulsed Radar, Randomly Modulated Carrier. Journ. Appl. Phys., Dec. 1954.

9.30. Marcum, J.I. A Statistical Theory of Target Detection by Pulsed Radar. IRE Trans., IT-6, April 1960. No. 1.

9.31. Swerling, P. Probability of Detection for Fluctuating Targets. IRE Trans, IT-6, April 1960, No. 2.

9.32. Jahnke, E., Emde, F. Table of Higher Functions. Leipzig, 1952.

9.33. Hoffman, W.C. Joint Distribution of n Successive Outputs of a Linear Detector. Journ. Appl. Phys., August 1954.

9.34. Mayer, M.A., Middleton, D. On the Distribution of Signals and Noise after Rectification and Filtering. Journ. Appl. Phys., August 1954.

9.35. Emerson, R.C. First Probability Densities for Receivers with Square Law Detectors. Journ. Appl. Phys., Sept. 1953.

9.36. Buslenko, N.P., Shreider, J.A. The Method of Statistical Trials (Monte Carlo) and Its Realization on Computers. Moscow, 1961.

9.37. Blake, L.V. The Effective Number of Pulses ... PIRE, June 1953.

9.38. Bailey, F.B. A Method for Calculating the Probability of Detection for a Coherent (AMTI) Radar Unit with Phase Cancellation. Journ. of the Franklin Inst., Vo. 275, April 1963.

9.39. Feiner, A., Diamond, F.I. A Three-Dimensional Aircraft Visibility Diagram. IRE Conf. Rec., Part 8, 1956.

9.40. Rees, F.L., Thomas, G.F. A Frequency-Domain Approach to Sub-Clutter Visibility Limitations...IRE Wescon Conv. Rec., Part 5, 1959.

9.41. Banks, L.E. A Review of Anti-Clutter Facilities for Primary Surveillance Radar. Electronics Research and Development for Civil Aviation. Conf. Record, London, 2-4, Oct. 1963.

9.42. Steinberg, B.D. Receiver Sensitivity and Design Curves for Radar Pulse Integration. PIEEE, April 1964, p. 437.

10. SOME METHODS FOR IMPROVING THE DETECABILITY OF SIGNALS /188

In optimizing the receiving systems in preceding chapters certain assumptions were made which can be fulfilled in practice more or less exactly. Since under real conditions we encounter objects with various properties, the system applied may in some cases be close to the optimal, and in others (i.e., for an object with different properties) it may not operate adequately. Therefore it is necessary to consider certain technical methods which allow to improve the detectability of certain types of signals, which differ from those assumed in optimization [1].

Another problem is the possibility of using more complex system than the ones considered in the preceding chapters (e.g., devices operating with the use of more than one high frequency channel). This permits to decrease the negative effect of some factors restricting the detectability, but at the cost of complicating the device.

This chapter will consider some systems of this type; we will also discuss some development prospects.

10.1. Decrease of the influence of "blind velocities"

In coherent systems operating on the principle of the Doppler effect it is of course impossible to select the objects whose radial velocity equals zero. The objects moving in the direction perpendicular to the line connecting this object with the radar station (operating on the above principle) will not be detected.

---

[1]This chapter contains a system approach, with a special consideration of MTI systems; ref. [10.1] contains a general discussion of the possibility of dropping some assumptions about signals and interference.

For devices which operate by reducing stationary clutter using periodic filters and using a scanning signal in the form of a coherent pulse series with repetition frequency f_p, it is also not possible to detect objects moving with certain radial /189 velocities called "blind velocities". As mentioned in preceding chapters, these are velocities for which the Doppler frequency equals a multiple of the repetition frequency. It is therefore defined by the formula (cf. Ch. 2.5):

$$v_n = n \cdot \frac{\lambda}{2T_p} = n \cdot \frac{\lambda f_p}{2}; \quad n = 1, 2, 3, \ldots \tag{10.1.1}$$

With noncoherent signals whose spectral density has a shape similar to the spectrum of a single pulse (cf. Ch. 7.1), the phenomenon of "blind velocities" should not occur. However, if the optimal (or approximately optimal) receiving system designed for detection of such signals against the background of correlated interference is utilized in a radar device, a situation may develop in which objects giving approximately coherent echoes will appear within the range of the device. Since periodic filters are also present in the system discussed (see Ch. 6 and 7), the phenomenon of "blind velocities" will be present for these objects[1].

Obviously, the problem of reducing the effect of "blind velocities" is important in radar. We will discuss below some basic methods allowing more or less effective solution of this problem:

A. Selection of the parameters of the device. As seen from

[1]We should mention that we are referring to systems where scanning signals are coherent (or the reception system has a phased coherent generator - see Ch. 2.5). Therefore the spectrum of passive interference has a "line" shape; the noncoherence of detected signal is due only to the rapid and strong fluctuations of the object's reflection.

(10.1.1), by appropriately selecting long waves or an appropriately high repetition frequency it is possible to achieve a displacement of the first blind velocity (n=1) beyond the range of the velocities which can be reached by the objects detected. It is easy to note that the possibilities are rather limited here. In order to achieve v_{b1}=800m/sec at n=1, with f_p providing an unequivocal distance reading within the range up to 250km, we must use a device operating on the wave length of appr. 3m. At this wavelength there are of course difficulties in achieving an appropriate discrimination in azimuth angle, which causes a decrease in detectability against passive interference scattered over larger areas.

The reduction of the maximal pulse repetition frequency, originating from the condition of unequivocal distance measurement, may be omitted by using a special scanning system. In this system the scanning signal is transmitted with a repetition frequency similar to that of the conventional radar stations. However, this signal consists of two rather closely spaced pulses. If the interval between them is denoted by T_r, we can say that this system corresponds to a system with a repetition frequency equal $1/T_r$ /190 with respect to blind velocities. For instance, the first blind velocity could then increase severalfold compared to a conventional station operating at the same λ and f_p. Of course, the receiving systems are constructed here somewhat differently than in a conventional station. This method, beside its advantages, has also some specific drawbacks. A more detailed analysis may be found in Ch. 2.8 of the book by Carpentier [10.2][1].

[1]Other possibilities have also been proposed, e.g., the realization of the principle of stationary clutter reduction using additional coherent modulation by a vibration with frequency much lower than the carrier frequency, chosen with blind velocities in mind. For the parameters mentioned above the scanning pulse (of appropriate lengths) would have to be modulated by a sinusoidal vibration with frequency of about 100MHz. Realization of such a system would be difficult for both basic and technical reasons. In addition, because of the spacing of the lateral bands of the scanning signal, this system would not have any advantage in the range of microwave frequencies compared to the one described in C. Certain technical advantages would be present in its application to devices operating in the visible range [10.39].

B. Operation with variable repetition period. On the basis of (10.1.1) we see that the value of blind velocities depends on the repetition period T_p. By altering T_p it is possible to decrease the effect of blind velocities. The variation of the period may be carried out basically in various ways: between periods, every few periods, between antenna revolutions, finally, in a slow manner, corresponding to the "scanning" of the range of Doppler frequencies. In practice, the method most often used is variation between periods. This method is also called the method of operation with variable repetition period or with variable repetition frequency.

This method is one of the simplest and effective in terms of decreasing the effect of blind velocities. It is applied in many radar stations (cf. Ch. 3). Therefore, we will discuss it further in this chapter.

C. Operation at several carryier frequencies. Blind velocities also depend on λ (see eq. 10.1.1), but a rapid change of wavelength (e.g. between pulses) would make the operation of the MTI system practically impossible. What remains is the possibility of switching the carryer frequency at greater time intervals (e.g., between antenna revolutions), which would involve some inconvenience, or the possibility of simultaneous operation at several carrying wavelengths. Already at two wavelengths (with appropriate difference) the signal detectability in correlated interference may be better than in a single channel system with a variable repetition period (cf. [10.3], Ch. 4.11). This is because, aside from the "effacing" effect of blind velocities there is an effect similar to that seen in operation with frequency spacing[1] (cf. [10.4,] Ch. 4), which gives a significant improvement of detectability, especially at high detection probabilities [10.16]. The system in question has important advantages, but is is more complex, which entails increased cost and other complications. /191

[1]A system with frequency spacing is also known as the system of "frequency diversity" [10.5].

D. Use of several separate radar stations. By using three stations, situated on earth's surface at some distance from each other, the radial velocity of the object may not be equal to zero for each of these stations when objects move in a plane. This is the only method allowing to avoid the first effect listed at the beginning of this chapter, i.e., the disappearance of objects having a radial frequency equal to zero when using a coherent MTI system. In the case considered all three radial velocities cannot be identical either. It is possible to have a situation when these velocities are different, but each of them is "blind" (i.e., corresponds to a different value of n); with the increase of the number of stations, the areas where this phenomenon may occur is diminished.

Obviously, this is the most expensive method of all those discussed. In addition, we have here the problems of cooperation between stations, transmission of output signals over large distances, utilization of information etc. [1]. It should rather be considered from the point of view of a system of radar stations (together with transformation and information use systems), which control a certain area, rather than from the point of view of a single radar system.

Of the approaches mentioned, the most widely used is the system of variable repetition frequency. We will consider it in somewhat more detail later on in this chapter.

Operation with variable pulse repetition frequency

Variability of the period between pulses means the technical realization of a periodic filter with variable parameters. In devices using memory tubes [10.5 - 10.7], the variation of the

[1] In the case when the use of the principle of bistatic radar is desired, there are additional problems.

period within rather wide limits does not require additional system equipment [10.5]. But when delay lines are used, the variation of the period cannot be done arbitrarily because it requires switching of the systems of delay lines, each of which has a defined, constant delay[1] [10.8, 10.9]. Therefore, in stations having MTI systems with delay lines we use only double or at most triple the repetition period [10.10-10.12]. In stations using memory tubes the variation of the period can be carried out by continuous modulation (so-called period wobbulation) [10.5].

Let us consider the case of double repetition period. /192 If we denote by $F_1(\omega)$ the transfer function of a periodic filter in the case of the shorter period, and if for the longer period it is $F_2(\omega)$, then the decrease of the effect of blind velocities can be estimated from the function [10.13]:

$$F_{\text{sr}}(\omega) = \frac{1}{\sqrt{2}} \cdot \sqrt{F_1^2(\omega) + F_2^2(\omega)}. \qquad (10.1.2)$$

Fig. 10.1.1 shows $F_{\text{sr}}(\omega)$ for the case of the single subtracting system, for $T_1/T_2=2/3$ and $T_1/T_2=7/8$. Because of symmetry, only one period $F_{\text{sr}}(\omega)$ for each case is shown. The first blind velocity at $T_1/T_2=m/n$ is defined by the formula:

$$v_{\text{sl}}\Big|_{T_1/T_2} = \frac{\lambda}{2nT_1} = \frac{\lambda}{2mT_2}. \qquad (10.1.3)$$

The larger m and n, the larger will be the first blind velocity, but at the same time the greater will be the gaps in the averaged transfer function [10.8]. With the shaped transfer functions (e.g., when the periodic filter is a double subtracting system with feedback -see Ch. 7 and 8), it is possible to obtain

[1]We do not discuss the details of realization in this chapter; these system problems will be considered in detail in Vol. II.

better gap filling [10.11]. Ref. [10.14] describes the method of simplified determination of function $F_{\Delta}(\omega)$ and the evaluation of the signal-to-noise ratio at the output of periodic filters with variable repetition frequency.

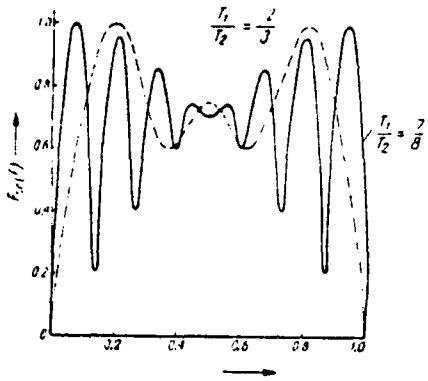

Fig. 10.1.1. Average-quadratic transfer characteristic of a system with single subtraction with variable repetition periods [10.13] (normalized); abscissa - normalized Doppler frequency.

The necessity of using variable repetition frequency is present especially when high detection probabilities are desired. This may be illustrated by the following reasoning. Let us /193 assume that a nonfluctuating coherent signal without interference is to be detected. In the case of reception with conventional amplitude detection, in this case obviously D=0 when the signal amplitude U is lower than the threshold value U_0, and D=1 when $U>U_0$ (curve A in Fig. 10.1.2).

In the case of coherent reception with phase detection and a periodic filter in the form of a single subtracting system, we have the following for a signal with uniform distribution of the probability of the radial velocity (and therefore of the Doppler frequency) ([10.15], p.651):

$$D = \frac{\frac{\pi}{2} - \arcsin \frac{U_n \sqrt{2}}{U}}{\frac{\pi}{2}}. \qquad (10.1.4)$$

The graph of this relation is shown in Fig. 10.1.2, curve B. Detection of objects in the presence of passive interference occurs at the cost of decreased detectability in this case. The signal must have a high amplitude especially with respect to high probabilities of detection.

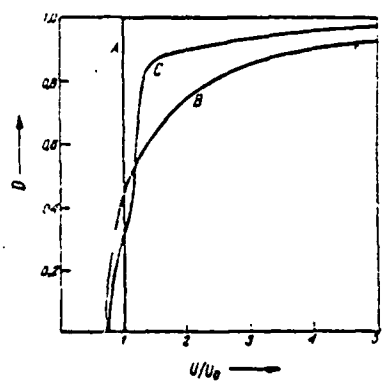

Fig. 10.1.2. Detection probability of a signal with known amplitude and unknown Doppler frequency: A-in amplitude detection; B-for operation with a single subtracting system; C-for operation with a single subtracting system and variable repetition period (T_1/T_2=2/3) [10.13].

In contrast, the analogous graph for the case of variable repetition frequency has a better shape, approaching curve A. This makes it possible to obtain high detection probabilities. E.g. during operation with variable frequency at T_1/T_2=2/3 (curve C in Fig. 10.1.2), in order to detect the signal with a probability of D-0.8, a signal amplitude equal to one half of that with constant average repetition frequency is sufficient[1] [10.13]. /194

[1]I.e. repetition frequency $f_p = \frac{2}{T_1 + T_2}$.

When periods T_1 and T_2 are not very different, the reduction of correlated interference can be calculated as in the case of operation with nonvariable period $T=(T_1+T_2)/2$. When the difference is greater, a more detailed analysis is required [10.13, 10.14]. The problem of signal detectability for variable repetition frequency is considered in more detail in Ch. 4.11 of ref. [10.3]. Some problems related to the operation with variable repetition frequency are also considered in refs. [10.7] and [10.17].

10.2. Decrease of the influence of the modulation arising in the course of space scanning.

In the course of space scanning using directional antennas the echo signals undergo modulation because of the displacement of the antenna characteristic (see Ch. 5 and Appendix 1). Thus the pulses reflected from the object have in this case a variable amplitude even when this object does not fluctuate. As follows from Ch. 7 and 9, this factor may - in some applications - constitute the basic restriction of the detection effectiveness for correlated interference, especially in devices where a small number of pulses falls within a beam width.

As a result of this modulation, the spectrum of correlated interference becomes wider. If we use an optimal filter, or a filter approximating the optimal one rather closely, it is possible to obtain good reduction of correlated interference[1], but at the cost of narrowing the filter passbands. This leads to a decrease in signal detectability. In contrast, when nonoptimal filters (e.g. single subtracting systems) are used, it is very difficult to obtain good reduction effectiveness with widening of the interference spectrum because of the modulation caused

[1] E.g., transfer functions of a double subtracting system with feedback, shown in Fig. 7.2.9 assure the reduction of 30dB with the number of pulses falling within the beam width N=17 (D1); 9(D2); 6(D3), for a nonfluctuating object [10.18].

by antenna revolution [10.19].

Therefore, various systems have been proposed which allowed to decrease the influence of the phenomenon described. One of the methods uses discontinuous motion of the antenna, i.e., operation during M repetition periods with a defined antenna direction, followed by a discontinuous displacement of the radiation characteristic by some angle, operation during the next M periods etc. Realization of this system would require the application of one of the known methods of electronic steering of the beam motion. Because of the manner in which compensation systems operate, appropriate blanking out of the output signal would have to be used at the start and the end of each beam, in order to avoid noncompensated first and last echoes [10.20]. The disadvantage of this /195 system is of course the lengthening of the scan time or the decrease of the accuracy in azimuth measurement and the signal losses caused by blanking out. These losses can be avoided by using a system in which the first of M pulses of an echo generated by a given object are delayed by a time equal to $(M-1)T_p$, the second by a time $(M-2)T_p$ etc. At the outputs of all delay system one would thus obtain simultaneously the echo pulses corresponding to the given object. Subtracting consecutively the output pulses corresponding to the echoes generated by the first and second, second and third, ... (M-1) and M scanning cycles, and adding up the squares of these differences, one would thus obtain a reduction of correlated interference without signal loss caused by blanking out.

Another method for decreasing the effect of modulation caused by space scanning was proposed in ref. [10.21]. The operation principle here is the introduction of additional antennas with directional characteristics formed according to consecutive derivatives of the directional characteristic of the main antenna. The signals obtained in this manner serve to compensate

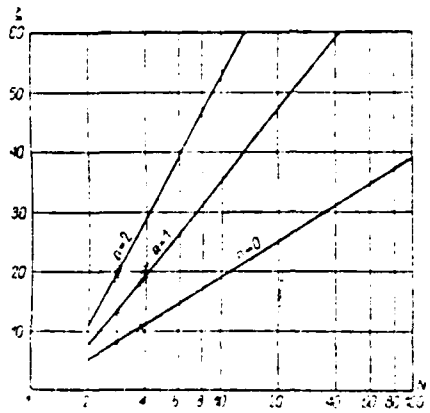

Fig. 10.2.1. Effectiveness of reduction as a function of the pulse number N, falling within the beam width; n=0 - reduction of a single subtracting system; n-1,2 - reduction with a single subtracting system and correction antennas [10.21].

for the remainder generated by the modulation caused by the antenna revolution. The system proposed was for the case of a system equipped with a single subtracting system. With respect to the reduction effectiveness (in considering only the effect of antenna's revolution, i.e., for nonfluctuating objects), we can say approximately that taking into account the characteristics up to the n-th derivative theoretically makes it possible to obtain the reduction $\zeta_{(dB)} = (n+1)\zeta_{1(dB)}$ (Fig. 10.2.1) [10.21] in this system. Thus, if for some pulse number falling within the beam width the reduction obtained with a single subtracting system /196
ζ_1 is 10 dB, then taking into account two correction antenna characteristics would theoretically give a reduction of about 30 dB. In this system it would be necessary to maintain a constant antenna revolutions rate. With periodic filters having a larger number of delay lines, the device would also have to contain further antennas and other systems.

Another system for compensating of the effect of space scanning was proposed by the author in 1956[1]. In order to explain

[1]Similar ideas were also proposed in refs. [10.22; 10.23].

its operation let us assume for a moment that the transmitting antenna has a beam so wide that directional characteristics are determined entirely by the receiving antennas. The conceptual diagram of the receiving part of the station is shown in Fig. 10. 2.2.

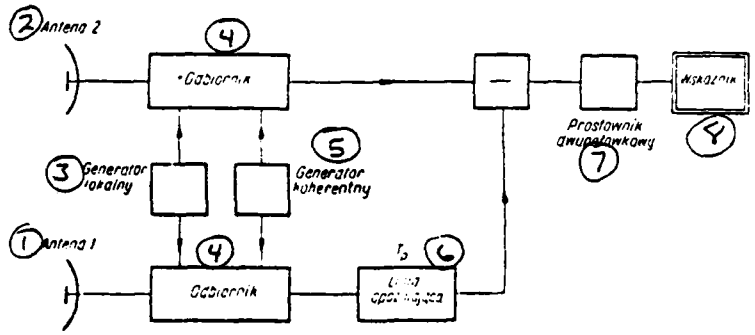

Fig. 10.2.2. Block diagram of the receiving part of a device operating with the system of compensation for antenna revolution. 1-Antenna 1, 2-Antenna 2, 3-local generator, 4-receiver, 5-coherent generator, 6-delay line, 7-two-part rectifier, 8-display.

Both receiving antennas have identical directional characteristics, but displaced in the plane of revolution by the angle $\Delta\varphi = \gamma T_1$, where γ - angular velocity of antenna. Between pulses the antenna system thus moves by an angle equal to the angular displacement of the antenna characteristics. Thus antenna 2 assumes in space the same positions as antenna 1 had during the previous scanning cycle. Because the signals received by antenna 1 are directed into a delayed channel, and those received by antenna 2 - into the direct channel of the subtracting system, the signals are completely compensated. This can be easily illustrated for the case of an echo derived from a point stationary object. In Fig. 10.2.3. the curve B represents the envelope of the pulse series received by antenna 1 and curve A the envelope of pulses received by antenna 2. Curve C is the envelope-delayed by time T_p - of the pulse train received by antenna 1, with the /197 sign changed. It is easy to note that the sume of curves A and C equals zero.

One could also imagine a variation of this system, where subtraction of the high frequency signals occurs (similarly to the mono-pulse systems [10.9]) and the difference signal is given as the correction signal to the subtracting system (Fig. 10.2.4).

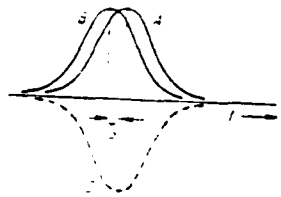

Fig. 10.2.3 Operating principle of the compensation system for antenna revolution.

In the method described, the total compensation occurs at a constant angular velocity γ. The dependence of the reduction effectiveness on the tolerance of the velocity of antenna revolutions is shown in Fig. 10.2.5 (for a Gaussian shape of the antenna characteristic).

The use of a transmitting antenna with a wide beam would obviously cause a loss of range. The transmitting antenna may have a characteristic identical to that of the receiving antennas. Let us denote the directional characteristic of the transmitting antenna by $g_n(\psi)$ and let us assume that the receiving antennas have identical directional characteristics, but displaced by angle $\delta\psi$:

$$g_{10} = g_n(\psi + \delta\psi); \quad g_{20} = (\psi - \delta\psi). \qquad (10.2.1)$$

Thus the receiving antennas have characteristics situated symmet- /198
rically with respect to the characteristic of the transmitting antenna (Fig. 10.2.6). The pulse envelopes will be proportional to:

$$u_{10} = g_n(\psi)\, g_n(\psi + \delta\psi); \quad u_{20} = g_n(\psi)\, g_n(\psi - \delta\psi). \qquad (10.2.2)$$

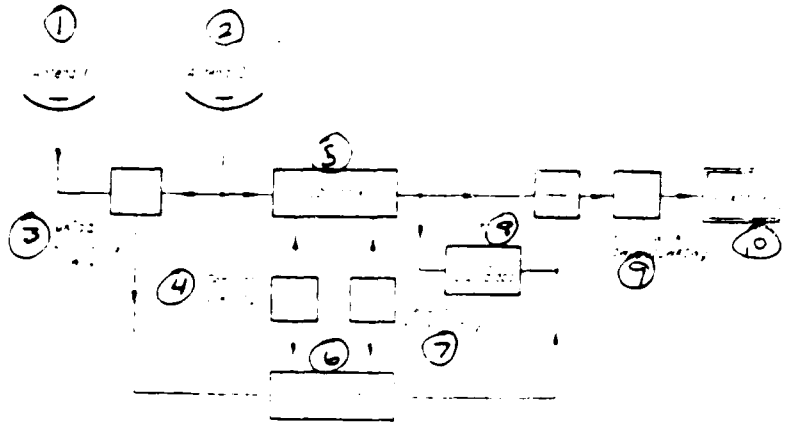

Fig. 10.2.4. A different realization of the receiving part of a device operating by the system of compensation of antenna revolution. 1-antenna 1, 2-antenna 2, 3-subtracting system in time, 4-local generator, 5-receiver, 6-receiver, 7-coherent generator, 8-delaying line, 9-two-part rectifier, 10-indicator.

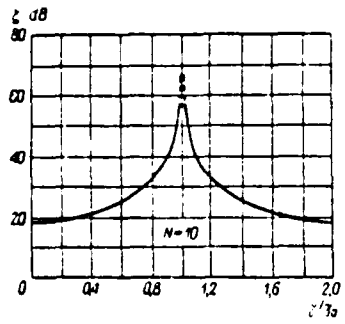

Fig. 10.2.5 Effect of tolerance of the antenna revolution rate on the compensation effectiveness in systems shown in Fig. 10.2.2 and 10.2.3.

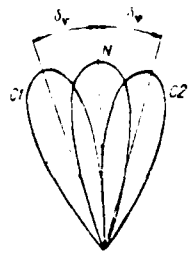

Fig. 10.2.6 Respective position of directional characteristics of the transmitting antenna and of receiving antennas in the compensation system for antenna revolution.

The envelope of pulses at the output of the subtracting system will have the form[1]:

$$
\begin{aligned}
u_r(\gamma t) &= u_{10}[\gamma(t - T_p)] - u_{20}(\gamma t) = \\
&= g_n(\gamma t - \gamma T_p)\, g_n(\gamma t + \delta\psi - \gamma T_p) - \\
&- g_n(\gamma t)\, g_n(\gamma t - \delta\psi).
\end{aligned}
\tag{10.2.3}
$$

As can be seen, if $\delta\psi = \gamma T_p$, i.e. if $\delta\psi = \Delta\psi$, then in a three-beam system (with identical beams) we will also obtain complete compensation of the effect of antenna revolution.

The above was concerned with a case when the device is equipped with a periodic filter in the form of a single subtracting system. If systems of multiple subtraction (or systems with feedback) are to be used, multiple-beam systems would have to be applied, which would complicate the device.

In the system described it would be possible to obtain deflected beams by appropriate shaping of illuminating systems, while the antenna mirror could be common. We should note, however, that at $\gamma = 60°/\text{sec}$ (10 rpm) and $f_p = 400$ Hz, $\Delta\psi = 0.15°$; the realization of the appropriate illumination systems entails some technical difficulties.

In general it may be said that compensating systems for the effect of antenna revolution, operating on the principle of using additional receiving channels are rather complicated and their application does not pay off as long as the number of pulses falling within the beam width is not very small.

10.3. Some prospects of development.

---

[1] At a constant angular velocity $\gamma_1 = \gamma t$ (cf. Ch. 5.1).

We often mentioned in the previous chapters that the approximation of the optimal receiver characteristics in practice entails some difficulties, caused by the limited possibilities of realization of the appropriate systems. Therefore it seems appropriate to discuss certain development prospects existing in this area.

With respect to systems containing periodic filters with designed characteristics (cf. Ch. 6.2 and 7.2), one of the main difficulties in realization is the problem of obtaining a larger number of delay channels and maintaining strict time tolerance and the equality of transfer functions. This problem is related both to the properties of the memory elements themselves and to the cooperating systems. There is continuous progress in this area [10.24]. In particular, delay lines of melted silicates are made for ever wider bands. Lines have been developed with many branches and continuous delay regulation. A survey of the most recent advances in this area is contained e.g. in ref. [10.25][1]. Other types of memory elements are also being developed [10.38].

There are also other technological possibilities here, namely giving up the analog use of the distance coordinate and introducing its discontinuity. In such a system the distance range is divided into a large number of sections with the length approximately equal to the discrimination of the device in distance. Windowing systems are used successively, so that each distance element corresponds to an appropriate filtering system. This system usually contains a boxcar generator[2], and therefore the filters can be realized as simple systems of elements with focused con-

---

[1]The realization problems of MTI systems will be discussed in more detail in Vol. II; in the present chapter we will only list some more important problems, related to the developmental prospects of the devices.

[2]In English literature, boxcar generator (cf. Fig. 2.15).

stants. Of course, it is easier in such a system to obtain a good approximation of the optimal transfer function for the filter, although at the cost of a significant complication of the system as a whole. However, in the age of transistors and miniaturization this is not the principal obstacle. The results obtained with this system are better than in systems with delay lines [10.9], Ch. 4.4.

Work is also going on concerning the application of numerical signal processing; some authors believe that appropriate /200 systems will be more suitable for mass production ([10.24],10.40). In order to obtain a reduction of the order of 40 dB, the signal at the output of phase detector has to be quantized, and the number of the quantization levels should be about 100. The signal generated in this way is coded appropriately, and then processed in a computer (operating with the required speed) [10.41].

Regarding systems designed for reception of coherent signals, one of the main difficulties here is both the approximation of the optimal expression [6.2.16], and the realization of the appropriate systems.

The approximation of an algorithm of type [6.2.16] can be implemented not only with a multichannel filter system, as described in Ch. 6. In some cases it is possible to use the principle of scanning the range of Doppler frequencies [10.26, 10,27]. Also, iteration methods have been proposed, which make it possible to approximate coherent integration without multichannel filters, using a large number of multiplying systems and delay systems [10.28].

The problem of approximation is related in this case to the analog or discrete use of the distance coordinate. When using purely electrical systems and an analog distance coordinate, a multichannel filter system must be used. These systems can also

be realized with the help of wide-band delay lines or branched delay lines [10.29, 10.30]. In the cases of interest to us, the filters should be periodic.

With a discrete distance coordinate, i.e. using appropriate systems of sequential windowing and large numbers of filter systems, various solutions are possible. We can also use multichannel filters, which may be simpler in this case (non-periodic)[1]. Thus we have in this case also a discretization according to Doppler frequency. On the other hand, we can use analog systems in the form of so-called memory filters[2]. Such a system consists of a delay line and a feedback loop containing a mixer and a local generator. The frequency of the local generator exactly equals the inverse of the delay time of the line. One can prove that after appropriate processing of the signal in the system described, the signal at the output has the shape analogous to the spectrum of the input signal [10.31-10.35].

New possibilities in the area of signal processing are opened up by the systems of optical filtration. In some solutions they make possible the two-dimensional filtration, giving in this way one more degree of freedom than electrical filtrations. Optical systems are particularly suitable for algorithm realization in cases with integral transformations [10.36, 10.37].

A more detailed discussion of many problems mentioned above is contained in ref. [10.38]. In general, we can state /201
that with progress of systems-realization technology it becomes possible to approximate the optimal receiver characteristics ever more accurately. Systems of signal processing used in radar stations are expanding.

[1]E.g. progress in the area of quartz filters allowed their widespread use.

[2]Eng. Coherent Memory Filter, abbr. CMF

References.

10.1. Kulikowski, J. Survey of new developmental directions in the technology and theory of signal reception in interference. PIT Works, No. 45, 1964.

10.2. Carpentier, M. Radars, modern theories. Paris, 1963.

10.3. Tartakowski, G.P. et al. Problems of statistical radar theory, vol. 1. Moscow, 1963.

10.4. Seidler, J. et al. Outline of a statistical telecommunications theory. Warsaw, 1964.

10.5. Cliquot, R. L-band radars, "type Orly" L'Onde Electrique, May 1961.

10.6. Kroszczynski, J., Grzenkiewicz, I. Reduction of stationary clutter in radar. Przeglad telekomunikacyjny, No. 11/12, 1957.

10.7. Bakulev, P.A. Radar location of moving targets. Moscow, 1964.

10.8. Fowler, C.A., Uzzo, A.P., Ruvin, A.E. Signal Processing Techniques for Surveillance Radar Sets. IRE Trans. on Mil. Electronics, Mil-5,.April 1961.

10.9. Skolnik, M.I. Introduction to Radar Systems. New York, 1962.

10.10. Kroszczynski, J. Radar Area Control Station AVIA. PIT Works, No. 30, 1960.

10.11. Molz, K.F. AN/FPN-34 Air Traffic Control Radar. Proceedings of the 5th East Coast Conference, 1958.

10.12. Snrader, W.M. Reducing Clutter in Air Route Surveillance Radar. Electronics, 26 Jan. 1962.

10.13. Perlman, S.E. Staggered Repetition Rate Fills Radar Blind Spots. Electronics,Nov. 21, 1958 (Engineering Issue).

10.14. Rees, F.L., Thomas, G.F. A Frequency Domain Approach to Sub-Clutter Visibility Limitations...IRE Wescon Conv. Rec., Part 5, 1959.

10.15. Ridenour, L.N. Radar System Engineering. New York, 1947.

10.16. Leger, J. Surveillance Radar; Theoretical Study of the Frequency Diversity. Revue CFTH, No. 39, Dec. 1963.

10.17. Kulikowski, J. On Some Problems Related to the Calculation of Elements of Inverted Covariance Matrix of Passive Radar Interference. Electrotechnical Discourses, No. 3, 1961.

10.18. White, W.D., Rubin, A.E. Recent Advances in the Synthesis of Comb Filters. IRE Natl. Conv. Record, Part 2, 1957.

10.19. Kroszczynski, J. Operation Effectiveness of Radar Stations which Reduce Stationary Clutter. Przeglas Telekomunikacyjny, No. 7. 1958.

10.20. Zetterberg, L.H. Detection of Moving Radar Targets in Clutter. Information and Control, No. 1, 1958.

10.21. Grisetti, R.S. et al. Effect of Internal Fluctuations and Scanning on Clutter Attenuation in MTI Radar. IRE Trans., ANE-2, March 1955.

10.22. Ameliorations des dispositifs de EEF. French patent, cl. 12.4 No. 1145633 of Oct. 28, 1957.

10.23. Anderson, D.B. A Microwave Technique to Reduce Platform Motion and Scanning Noise in Airborne MIT Radar. IRE Wescon Conv. Record, Part 1, 1958.

10.24. Wilcox, J., Thompson, R. Recent Advances in Delay-Line /202
Data Processors. Proc. Conf. Mil. Electronics, 1959.

10.25. Hammond, V.J. Quartz Delay Lines, the State of the Art, British Communications and Electronics, Feb. 1962.

10.26. Applebaum, S. Frequency Scanning Filter Principles. Proc. Conf. Mil. Electronics, 1959.

10.27. Howells, P.W. Frequency Scanning Filter Applications. Proc. Conf. Mil. Electronics, 1959.

10.28. Reed, I.S., Swerling, P. Filterless Approximations of K-th Order to Coherent Detection. IRE Trans. on Information Theory, IT-8, April 1962.

10.29. Brookner, E., Flink, J. Coherent Enhancer for Pulse Radar Applications. IRE Conv. Record, Part 8, 1960.

10.30. Lerner, R.M. A Matched Filter Detection System for Complicated Doppler Shifted Signals. IRE Trans. on Information Theory, IT-6, June 1960.

10.31. Temes, C.L. Implementation of the Ideal Radar Receiver using the Coherent Memory Filter. 7th East Coast Conf. on Aeronautical and Navigation Electronics.

10.32. Bickel, H.J., Brookner, E. A Delay Line Synthesized Filter Bank with Electronically Adjustable Impulsive Response. Proc. Conf. Mil. Electronics, 1960.

10.33. Baumann, R.H. Transposition Time-Frequency for Measuring an Unknown Frequency. Annales de Radioelectricite, Oct. 1960.

10.34. Brookner, E. Synthesis of an Arbitrary Bank of Filters by Means of a Time-Variable Network. IRE Conv. Record, Part 4, 1961.

10.35. Capon, J. High-Speed Fourier Analysis with Recirculating Delay-Line-Heterodyner Feedback Loops. IRE Trans. I-10, June 1961.

10.36. Hoefer, W.G. Optical Processing of Simulated IF Pulse Doppler Signals. IRE Trans. on Mil, Electronics, MIL-6, April 1962.

10.37. Cutrona, L.J. et al. Optical Data Processing and Filtering Systems. IRE Trans. on Information Theory, IT-6, June 1960.

10.38. Mintzer, A.I. Advanced Radar Signal and Data Processing. Space/Aeronautics, No. 6, 1962; No. 1, 4, 5, 1963.

10.39. Hankin, R.B., Todd, A.C. A High-Resolution Microwave Modulated Optical Doppler Radar. IEEE Int. Conv. Rec., Pt. 7, 1964.

10.40. Krantz, F.H., Murray, W.D. A Survey of Digital Methods for Radar Data Processing. Proc. East Joint Computer Conf., Dec. 13-15, 1960.

10.41. Brandsell, P. MTI, Survey of Developments since 1948. 8th AGARD Avionics Panel Symposium, Sept. 1964.

THE FORM OF SIGNALS REFLECTED IN THE COURSE OF SPACE SCANNING

Fig. D.1.1 represents a substitute diagram of the system transmitting antenna-space with the object contained in it-receiving antenna. With the previously mentioned assumption of linearity of the phenomena of reflection and dispersion of electromagnetic waves, the system shown in the figure will be a linear system. Thus various reflecting objects may be represented, including appropriate representative quadrupoles parallel to the center quadrupole, as shown by the broken line in Fig. D.1.1, which represents a system with time variable parameters with respect to the effect of space scanning, reflection fluctuations, etc. Its properties will be considered using general

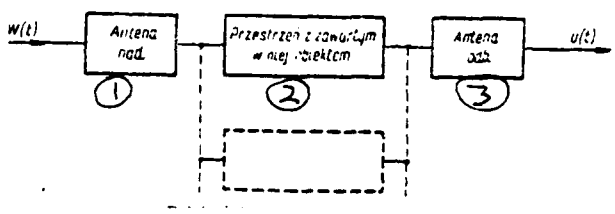

D.1.1. Substitute diagram of the system: transmitting antenna-space being scanned - receiving antenna. 1-transmitting antenna, 2-space with the object contained in it, 3-receiving antenna.

methods for linear systems with variable parameters [D.1.1, D.1.2].

The properties of the quadrupoles representing appropriate elements of the actual system will be defined in this case by their pulse responses h(t, t´), and - as is known [D.1.1.] - an equivalent pulse response h_V of the entire system represented in Fig. D.1.1 can be written in the form:

$$h_V = h_{A_n} * \left[\sum_{m=1}^{M} h_{E_m} \right] * h_{A_0}, \qquad \text{(D.1.1)}$$

where

h_{A_n}, h_{A_o} - pulse responses of the quadrupoles representing the transmitting and receiving antenna;

h_{E_m} - corresponding pulse response of the m-th reflecting object (in other words - this is the pulse echo originating from this object);

* - symbol of the twist operation.

The signal u(t) will thus be defined by the relation:

$$u(t) = \int_{-\infty}^{\infty} h_v(t, t')\, u(t')\, dt'. \qquad (D.1.2)$$

Let us consider the problem of the pulse response of the antenna. The antenna systems used in radar can be represented in an idealized form as apertures whose linear dimensions are large compared to the scanning signal wavelength. For a /204 uniformly illumined aperture of width D (where $D \gg \lambda$), with a linear polarization, the field intensity in plane ψ in the far range (Fraunhofer range) is defined by the relation:

$$E_{A_n}(\omega, d) = \frac{\text{const}}{r} \cdot j\omega \cdot \frac{\sin \omega d}{\omega d} \cdot e^{-j\omega r/c}, \qquad (D.1.3)$$

where: ω - pulsation of the vibration feeding the antenna;

$d = \frac{D \sin \psi}{2c}$, and c - velocity of wave propagation in space;

r - distance from antenna [D.1.3].

By analogy, the expression (D.1.3) may be treated as the characteristic of a hypothetical quadrupole, whose input receives the scanning signal, and whose output signal is defined as proportional to the appropriate component of vector $\vec{E}$ (D.1.4). On the basis of known relations between the frequency characteristic and the pulse response of the quadrupole we have:

$$h_{A_n} = \mathcal{F}^{-1}\{E_{A_n}(\omega)\}, \qquad (D.1.4)$$

where $\mathcal{F}^{-1}$ denotes inverse Fourier transform. Considering the terms on the right-hand side of (D.1.3) we can note that a. Multiplication by $j\omega$ in the frequency domain corresponds to taking the differential in the time domain; b. on the basis of theorem about displacement for Fourier transformations the exponential term corresponds to the delay in time domain by a quantity equal to $\frac{r}{c}$ (D.1.5).

Thus, we can write:

$$h_{A_0} = \frac{d}{dt}\left[\mathcal{F}^{-1}\left\{\frac{\sin \omega d}{\omega d}\right\}\right]_{t-\frac{r}{c}}. \qquad \text{(D.1.5)}$$

For the direction of radiation corresponding to the electrical axis of the antenna, $\psi=0$, we will therefore obtain[1]:

$$\left[h_{A_0}\right]_{\psi=0} = \delta\left(t-\frac{r}{c}\right). \qquad \text{(D.1.6)}$$

For $\psi \neq 0$ we will have:

$$h_{A_0} = \delta\left(t-\frac{r}{c}+d\right) - \delta\left(t-\frac{r}{c}-d\right). \qquad \text{(D.1.7)}$$

Similarly we can find the pulse response of the antennas for other functions of aperture illumination (D.1.4), but the general character of the phenomenon is not altered here, and therefore the consideration of this problem is not necessary.

The physical interpretation of (D.1.9) and (D.1.10) should be considered. As we know (D.1.6),

[1]To simplify notation we will assume the normalized form of the pulse response, omitting constant coefficients.

$$\int_{-\infty}^{\infty} x(t)\,\delta'(t-a)\,dt = x'(t-a). \qquad \text{(D.1.8)}$$

We should note, however, that in the problem considered in the present work, the scanning signals are narrow-band signals, thus a scanning pulse contains a large number (on the order of 10^3-10^4) periods of carrier vibration. Therefore such a signal can be represented in the form:[1]

$$w(t) = A(t)\sin(\omega_0 t + \varphi), \qquad \text{(D.1.9)}$$

where

A(t) - envelope of the scanning pulse; /205

ω_0 and ϕ - pulsation and initial phase of the carrier vibration.

Then

$$w'(t) = A(t)\,\omega_0\cos(\omega_0 t + \varphi) + A'(t)\sin(\omega_0 t + \varphi); \qquad \text{(D.1.10)}$$

When A(t) is a pulse with a slope that is not too steep and with duration time much longer than the period of the carrier vibration (as mentioned above), the second term of (D.1.12) can be omitted. In this case the operation of the substitute quadrupole of the transmitting antenna would be reduced to the appropriate delay of the scanning pulse and the phase displacement of its carrier vibration.

It should be noted that in practical problems it is not important to know the absolute phase of the reflected signal, since this is a random value, e.g. because of the properties of reflecting objects (D.1.7); only the relative phase dependencies are of interest. If the constant phase displacement, intro-

[1]See Appendix 2.

duced by the substituting quadruple of transmitting antenna is omitted, one can assume a simplified form of the pulse response h_{A_n}, important for narrow-band signals:

$$\left[h_{A_{nm}}\right]_{\psi=0} = \delta\left(t - \frac{r}{c}\right). \qquad \text{(D.1.11)}$$

The assumption of this form of the pulse response can be also interpreted as the assumption that in the band occupied by the scanning signal the frequency characteristic of the antenna is constant, which occurs approximately in most practical cases[1].

When $\psi=0$, the scanning signal is transformed by the antenna in a more complicated manner. The problem of undefined states in the antennas was considered in detail by Polk (D.1.8), who also took into account the effect of lateral lobes. However, for signal analysis in the present context, even in this case certain simplifying assumptions can be made. As follows from (D.1.7), if the scanning signal is much longer than d, we can assume that the input signal into the substituting quadrupole has certain undefined states (with duration time of the order of d) at the start and the end of a pulse, and a defined state within the pulse. In the defined state there is also a displacement of the phase of the carrier vibration, and the signal amplitude at the output changes in proportion to the value of the second term of (D.1.7) [D.1.4]. The simplifying assumption in question consists in omitting the undefined states. This is possible because for radar practical antennas the time duration of an undefined state is very small compared to the pulse length[2].

[1]Usually achievement of a uniform transfer band of the antenna which is much wider than the width of scanning signal is the goal, because of the possibility of re-tuning.

[2]For an antenna span of several meters the time duration of an undefined state (for angles within $\pm 5°$ from electrical axis of the antenna) would be of the order of 10^{-3} μS, while the lengths of the scanning pulses in applications of interest to us are usually larger than 1μS.

The introduction of this assumption allows a very important simplification of the expression for the pulse response of an antenna. Namely, it can be rewritten, in accordance with the above, as follows:

$$h_{A_{\infty}} = g_n(\psi)\,\delta\left(t - \frac{r}{c}\right). \qquad \text{(D.1.12)}$$

where $g_n(\psi)$ is the so-called voltage characteristis of the transmitting antenna as a function of angle ψ (D.1.3).

In the case of space scanning, $g_n(\psi)$ is a function of time. For the most common case, when scanning takes place by displacement of a characteristic with constant shape in angular coordinates (in revolving antennas), $g_n(t)$ - $g_n(t) = g_n[\gamma_0 + \gamma(t)]$. If the displacement takes place with a constant angular velocity γ, then $g_n(t) = g(\gamma_0 + \gamma t)$.

Thus we can write the pulse response of the substituting quadrupole with variable parameters as follows:

$$h_{A_{\infty}}(t, t') = g_n(t')\,\delta\left(t - t' - \frac{r}{c}\right). \qquad \text{(D.1.13)}$$

This is a pulse response of a quadruple of the so-called class of separable quadrupoles, which can be represented in the form of a serially connected filter with constant parameters and an ideal amplitude modulator. In the case of the transmitting antenna it will be the so-called separable type II quadrupole according to the Kailath classification (D.1.9), i.e. the filter is connected after the modulator. The separability of the quadrupole makes it much easier to operate the pulse response.

As shown by Mayo, Howells et al., with simplifying assumptions analogous to those for the transmitting antenna, we can assume for the receiving antenna a similar form of the pulse

response (D.1.4). However, because of the opposite direction of signal propagation in space during reception, the substituting quadrupole of the receiving antenna should rather be represented in a form corresponding to type I according to the classification in ref. [D.1.9].

It is easy to see from these considerations that such a signal reflected from a point object can be represented as follows:

$$u_p(t) = k \cdot g_n\left(t - \frac{2r}{c}\right) \sigma_n(t)\, w\left(t - \frac{2r}{c}\right). \qquad \text{(D.1.14)}$$

where k - signal reduction defined by the radar range equation.

References.

D.1.1. Zadeh, L.A. A General Theory of Signal Transmission Systems. J. Franklin Inst., April 1952.

D.1.2. Szulkin, P. The Response Function of Linear Systems Varying in Time. Arch. Autom. i Telemechaniki, vol. V, No. 1, 1960.

D.1.3. Silver, S. Microwave Antenna Theory and Design. New York, 1949.

D.1.4. Mayo, B.R., Howells, P.W., Adams, W.B. Generalized Linear Radar Analysis. Microwave Journal, Aug. 1961.

D.1.5. Campbell, G.A., Foster, R.M. Fourier Integrals for Practical Applications New York, 1948.

D.1.6. Osiowski, J. Significance and Applications of Distribution in Circuit Theory. Electrotechnical Discourses, No. 4, 1960.

D.1.7. Kerr, D. Propagation of Short Radio Waves. New York, 1951.

D.1.8. Polk, C. Transient Behavior of Aperture Antennas. PIRE, July, 1960.

D.1.9. Kailath, T. Time-Variant Dispersive Channels. Ch. 6 of the book edited by E. Baghdada: Lectures of Communication Systems Theory. New York, 1961.

APPENDIX 2

SOME PROPERTIES OF NARROW-BAND STOCHASTIC PROCESSES.

The narrow-band stationary stochastic process $\xi(t)$ can be represented in the form (D.2.1.):

$$\xi(t) = A(t)\cos\Phi(t), \tag{D.2.1}$$

where the processes $A(t)$ and $\phi(t)$ are defined by the relations:

$$A(t) = \sqrt{\xi^2(t) + \eta^2(t)}, \tag{D.2.2}$$

$$\Phi(t) = \operatorname{arc\,tg}\frac{\eta(t)}{\xi(t)}, \tag{D.2.3}$$

and the process $\eta(t)$ is related to the process $\xi(t)$ by the Hilbert transformation:

$$\eta(t) = -\frac{1}{\pi}\lim_{T\to\infty}\int_{-T}^{T}\frac{\xi(\tau)}{\tau - t}\,d\tau; \tag{D.2.4}$$

The integral in (D.2.4) should be understood as the principal value of Cauchy (D.2.2). The Process $A(t)$ is called the envelope, and $\phi(t)$ - the phase of the stochastic process $\xi(t)$. Both A and ϕ are processes that change relatively little with time, and:

$$\Phi(t) = \omega_0 t - \varphi(t). \tag{D.2.5}$$

Substituting (D.2.5) into (D.2.1) we will obtain:

$$\xi(t) = A(t)\cos\varphi(t)\cdot\cos\omega_0 t + A(t)\sin\varphi(t)\cdot\sin\omega_0 t. \tag{D.2.6}$$

Denoting:

$$P(t) = A(t)\cos\varphi(t), \quad Q(t) = A(t)\sin\varphi(t), \tag{D.2.7}$$

we can write the narrow-band process in the equivalent form:

$$\xi(t) = P(t)\cos\omega_s t - Q(t)\sin\omega_s t. \qquad (D.2.8)$$

When processes P and Q are Gaussian, the probability distribution of process A(t) is determined by the Rayleigh law, and the distribution of process ϕ is uniform in the range 0-2π (D.2.1).

It can be shown that (D.2.3) the autocorrelation functions of processes P(t) and Q(t) are equal

$$R_P(\tau) = R_Q(\tau) = R_0(t). \qquad (D.2.9)$$

The reciprocal correlation function $R_{PQ}(\tau)$ equals zero, if the /208
power spectrum $W(\omega)$ of process $\xi(t)$ is symmetrical with respect to the carrier frequency ω_s (D.2.3). In this case:

$$R_0(\tau) = \frac{1}{\pi}\int_0^\infty W(\omega)\cos\omega\tau\, d\omega. \qquad (D.2.10)$$

It follows from (D.2.10) and (D.2.8) that the autocorrelation functions of the narrow-band process $\xi(t)$ is equal to:

$$R(\tau) = R_0(\tau)\cos\omega_s\tau. \qquad (D.2.11)$$

References:

D.2.1. Middleton, D. An Introduction to Statistical Communications Theory. New York, 1960.

D.2.2. Tichmarsh, E. Introduction to the Theory of Fourier Integrals. Oxford, 1950.

D.3.2. Lewin, B.R. The Theory of Random Processes and Its Application to Radar. Moscow, 1957.

SOLUTION OF THE FREDHOLM EQUATIONS OF THE FIRST KIND BY THE METHOD OF ORTHOGONAL EXPANSIONS

In considering problems related to optimization of reception with clutter it is important to obtain effective solutions of integral equations of the type

$$s(t) = \int_{t_1}^{t_2} \Gamma(t, t') q(t') dt'. \qquad (D.3.1)$$

This is the so-called Fredholm equation of the first kind (D.3.1). Let us assume that

$$q(t) = \sum_n a_n \mu_n(t), \qquad (D.3.2)$$

where functions μ_n form a complete system within the interval (t_1, t_2).

Then

$$s(t) = \sum_n a_n \int_{t_1}^{t_2} \Gamma(t, t') \cdot \mu_n(t') dt', \qquad (D.3.3)$$

or

$$s(t) = \sum_n a_n \nu_n t, \qquad (D.3.4)$$

where

$$\nu_n(t) = \int_{t_1}^{t_2} \Gamma(t, t') \cdot \mu_n(t') dt'. \qquad (D.3.5)$$

The solution of (4.2.1) is thus reduced to finding the coefficients a_n, using the known properties of functions q(t) and $\gamma(t)$.

This problem is considerably simplified in two cases:
a. if the series appearing in (D.3.3) and (D.3.4) is a power series; the unknown coefficients can be determined by comparing appropriate terms of the sum appearing on the right-hand side with the power expansion of function q(t);
b. if functions $\gamma(t)$ form an orthogonal system, i.e. if:

$$\int_{t_1}^{t_2} \gamma_n(t)\, \gamma_m(t)\, \rho(t)\, dt = N_n \delta_{mn}. \tag{D.3.6}$$

Then the coefficients a_n can be determined in the form:

$$a_n = \frac{1}{N_n} \int_{t_1}^{t_2} \bar{\gamma}_n(t)\, q(t)\, \rho(t)\, dt. \tag{D.3.7}$$

In more general cases one can use orthogonalization of the function system by creating appropriate linear combinations of functions γ_n, e.g. by the method of Schmidt, or by using biorthogonal expansions (D.3.1). We will not consider these methods further here, because they are not necessary in later considerations. /210

A case that is directly usable for expansion of type a is the equation with a kernal of the type $e^{-(t-t)2}$. As presented in part 2, this is an approximation of the correlation function of some types of passive interference that is frequently used. For expansion we use here one of the properties of the Gauss function, namely

$$\exp[-(t-t')^2] = \sum_{n=0}^{\infty} \frac{e^{-t'^2} \cdot H_n(t')}{n!}\, t^n, \tag{D.3.8}$$

where H_n are the appropriate multinomials of Hermite;

$$H_n(t) = -1^n e^{-t^2} \frac{d^n}{dt^n} (e^{-t^2}).$$

Evidently, in this case $r_n \sim t^n$. Thus we can e.g. simply obtain the solution of the integral equation

$$s(t) = \int_{-\infty}^{\infty} \exp[-(t-t')^2]\, q_1(t')\, dt'. \tag{D.3.9}$$

Namely, let us take $q_1(t') = \sum_{n=0} a_n H_n(t')$; ; (cf. eq. D.3.4).

Since (D.3.1):

$$\int_{-\infty}^{\infty} H_n^2 e^{-t^2} dt = 2^n n! \sqrt{\pi}, \tag{D.3.10}$$

equation (4.2.9) is reduced to the form:

$$s(t) = \sqrt{\pi} \sum_{n=0}^{\infty} a_n 2^n t^n. \tag{D.3.11}$$

From this we will obtain after transformation:

$$q_1(t) = \frac{1}{\sqrt{\pi}} \sum_{n=0} \frac{s^{(n)}(0)}{2^n n!} H_n(t). \tag{D.3.12}$$

However, we should consider in more detail the case b, since it plays an important role in problems related to signal detection. Using the fact that the nucleus $\Gamma(t, t')$ is the autocorrelation function of a stationary process, we can introduce the following limiting assumptions with respect to $\Gamma(t, t')$.

$\Gamma(t, t)$ will now be a symmetric positive definite function. Secondly, we have $\Gamma(t, t') = \Gamma(t - t') = R(\tau)$ (D.3.2). Thirdly, we can assume that R(τ) is, in accordance with the Wiener-Chinchin theorem, a Fourier transform of the spectral density function, and the latter is a measurable function of ω^2, e.g.

$$W(\omega) = C_0 \prod_{n=0}^{M} (c_n^2 + \omega^2) \Big/ \prod_{n=1}^{N} (b_n^2 + \omega^2), \tag{D.3.13}$$

and $M+1 \leqslant N$, $c_0 > 0$; ; for $n = 0$, $c_n^2 + \omega^2$ is replaced by unity (D.3.2). We can also introduce the assumption that $R(\tau)$ is expressed by /211 the sum of exponential functions (D.3.2).

$$R(\tau) = \sum_{n=1}^{N} a_n e^{-b_n|\tau|}; \quad b_n > 0; \tag{D.3.14}$$

as follows from part. 3, this is actually true in the problems considered here, because one of the cases in question is simply $R(\tau) \sim e^{-0.\tau|}$.

Using the above assumptions we solve (D.3.1) using one of the best known orthogonal expansions, namely the Fourier transform. In order to simplify later transformatins we will rewrite (D.3.1) in a somewhat different form, which is equivalent to the assumptions made above:

$$\int_{-\infty}^{\infty} R(|t - t'|) Z_T(t') dt' = G(t - t_0 - a), \tag{D.3.15}$$

where

$$0 < t < T, \quad T = |t_1 - t_2|$$

$$Z_T(t) = \begin{cases} \eta_T(t') \text{ also } 0 < t' < T \\ 0 \text{ for other values of } t'. \end{cases}$$

Since the kernal is continuous everywhere, we can introduce an "expanded" function G:

$$G_r(t, t_0 + a) = \begin{cases} G^+ e^{-c(+)}(t - T), & t > T \\ G(t - t_0 - a), & 0 \leqslant t \leqslant T \\ G^- e^{c(-)} t, & t < 0 \end{cases} \tag{D.3.16}$$

where $G^+ = G(T - t_0 - a)$; $G = G(-t_0 + a)$. Constants $c^{(\pm)}$ should be selected such that the exponential functions in (D.3.16) assure appropriate behavior of the function G_r at infinity, making it possible to represent it in the form of the Fourier integral (D.3.2).

The integral equation (D.3.15) can thus be rewritten in the form to which the technique of Fourier tranform is easily applied, namely:

$$\int_{-\infty}^{\infty} R(t-t')\, Z_T(t')\, dt' = G_r(t, t_0 + a) - \chi^+(t) + \chi^-(t), \qquad \text{(D.3.17)}$$

where

$$\chi^+ = \begin{cases} G^+ e^{-\alpha(+)}(t-T), & t > T \\ 0, & t \leqslant T \end{cases} \qquad \text{(D.3.18a)}$$

$$\chi^- = \begin{cases} 0, & t \geqslant 0 \\ G^- e^{\alpha(-)} t, & t < 0 \end{cases} \qquad \text{(D.3.18b)}$$

Let us denote:

$$S(p) = \mathcal{F}\{Z_T\};\ X^+(p) = \mathcal{F}\{\chi^+\};\ X^-(p) = \mathcal{F}\{\chi^-\}. \qquad \text{(D.3.19)}$$

where p-jω. Using the Fourier transform on both sides of (D.3.16) we will also obtain:

$$S_r(p) = \mathcal{F}\{G_r\} = \int_0^T G(t - t_0 - a)\, e^{-pt}\, dt + \frac{G^{(+)} e^{-pt}}{p + \alpha^{(+)}} - \frac{G^{(-)}}{p - \alpha^{(-)}} \qquad \text{(D.3.20)}$$

Using further the Fourier transform on both sides of (D.3.17) /212 and taking advantage of relations (D.3.19-20), we obtain:

$$S(p) = \frac{2S_r(p)}{W(p/2\pi j)} + 2\,\frac{X^{(+)}(p) + X^{(-)}(p)}{W(p/2\pi j)}, \qquad \text{(D.3.21)}$$

where W is the spectral power density, corresponding to the correlation function R(τ).

The desired solution $Z_T(t)$ will thus be obtained in the form:

$$Z_T(t) = \int_{-j\infty}^{j\infty} S(p)\, e^{pt} \frac{dp}{2\pi j}. \qquad \text{(D.3.22)}$$

In order to obtain effective solution, however, it is necessary to define the unknown functions $X^{(+)}$ and $X^{(-)}$.

This is usually a rather tedious procedure, unless the specific properties of the functions appearing in the equation simplify the definition of $X^{(\pm)}$.

It can be demonstrated that (D.3.2):

$$X^{(-)}(p) = \sum_{n=2}^{N} \gamma_n^{(+)} e^{pT} \frac{b_1 - b_n}{(b_n + p))\,(b_1 + p)} \qquad \text{(D.3.23a)}$$

and

$$X^{(-)}(p) = \sum_{n=2}^{N} \gamma_n^{(-)} \cdot \frac{b_1 - b_n}{(b_n - p)\,(b_1 - p)}. \qquad \text{(D.3.23b)}$$

where $b_1 \ldots b_n$ have identical meaning as in (D.3.14), and the unknown coefficients γ_n are defined as

$$\gamma_n^{(+)} = a_n e^{-b_n T} \int_{-\infty}^{\infty} e^{b_n \tau} Z_T(\tau)\, d\tau, \qquad \text{(D.3.24a)}$$

$$\gamma_n^{(-)} = a_n \int_{-\infty}^{\infty} e^{-b_n \tau} Z_T(\tau)\, d\tau. \qquad \text{(D.3.24b)}$$

Substituting quantities $X^{(\pm)}$ obtained on the basis of (D.3.23) into formula (D.3.21), we obtain the desired solution of equation (D.3.1) but with 2N-2 unknown coefficients $\gamma_n^{(\pm)}$. They are determined by substituting relations (D.3.23) and (D.3.21) into (D.3.15), and treating them as an identity. As an example we can state that the solution of integral (D.3.1) in the case of a kernal in the form $Be^{-b\tau}$ (correlation functions of this type appear e.g. with waves reflected from interfering objects - cf. part 3) is (D.3.2):

$$Z_T(t) = \frac{1}{2bA}\left\{[b^2G(t-u) - G''(t-u)] + (G' + bG)_{T-u}\,\delta(t-T) + \right.$$
$$\left. + (bG - G)_{-u}\,\delta(t-0)\right\}; \qquad 0 < t < T. \qquad \text{(D.3.25)}$$

where $u-t_0+a$, $T=|t_1=t_2|$.

In the work of Middleton [D.3.2] one can find the solutions of more complicated integral equations of a similar type, e.g. for a nucleus of the form $B_1 \cdot e^{-b_1\tau} + B_2 \cdot e^{-b_2\tau}$, etc.

References.

D.3.1. Morse, P.M., Feshbach, H. Methods of Theoretical Physics. New York, 1953.

D.3.2. Middleton, D. An Introduction to Statistical Communications Theory. New York, 1960.

THE DISPLACEMENT THEOREM FOR INTEGRAL EQUATIONS

The scanning signals in radio- and sonar ranging are usually pulses of high frequency vibrations with a carryer frequency f_0. However, the examples of the solutions of the integral equation described in Appendix 3 refer to the paths which do not have a carrier frequency. Although there are no reasons to prevent us from solving this equation using the methods described in Appendix 3 even in the case of narrow-band path with a carrier frequency. It is also possible to prove a more general relation which simplifies the solution in the case of narrow-band paths with carrier frequency, if the solution of the appropriate integral equation for the envelope is known. We will call this relation the displacement theorem for an integral equation, formulated as follows:

If Z_T is the solution of the integral equation

$$\int_{-\infty}^{\infty} R(|t-t'|)\, Z_T(t')\, dt' = G(t-t_0), \tag{D.4.1}$$

then the solution of the integral equation

$$\frac{1}{2}\int_{-\infty}^{\infty} R(|t-t'|)\cos\omega_0(t-t')\, Z_{0T}(t')\, dt' = G(t-t_0)\,[A\cos\omega_0 t + B\sin\omega_0 t] \tag{D.4.2}$$

is

$$Z_{0T} = Z_T(t)\,[A\cos\omega_0 t + B\sin\omega_0 t] + \Delta(t), \tag{D.4.3}$$

where

$$\Delta(t) = \mathcal{F}^{-1}\left\{2(A-jB)\left[\frac{X^{(+)}(p+p_0)+X^{(-)}(p-p_0)}{W(f-f_0)} + \frac{X^{(+)}(p+p_0)+X^{(-)}(p-p_0)}{W(f+f_0)}\right]\right\}. \tag{D.4.4}$$

The formulation (D.4.2) follows from the fact that when the stationary process $\xi(t)$ has a correlation function $P(\tau)$, then the path $\xi(t)\cos(\omega_0 t + \phi)$ will have a correlation function equal to $\frac{1}{2} R(\tau) \cos \omega_0 \tau$, for any phase angle ϕ (cf. App. 2).

Based on the known relationships with imaginary argument functions and an exponential function with imaginary argument and on the displacement theorem known from the Fourier transform theory (D.4.1), it is possible to represent the solution of (D.4.1) in the form (see App. 3, eq. D.3.21):

$$
\begin{aligned}
S_0(p) &= \frac{2S_{0r}(p)}{W_0(p/2\pi j)} + \frac{X_0^{(+)}(p) - X_0^{(-)}(p)}{W_0(p/2\pi j)} = \\
&= \frac{2A}{W(f+f_0) + W(f-f_0)} [S_r(p+p_0) + S_r(p-p_0) + \\
&+ X^{(+)}(p+p_0) + X^{(+)}(p-p_0) + X^{(-)}(p+p_0) + X^{(+)}(p-p_0)] - \\
&- \frac{2jB}{W(f+f_0) + W(f-f_0)} [S_r(p+p_0) + S_r(p-p_0) + \\
&+ X^{(+)}(p+p_0) + X^{(+)}(p-p_0) + X^{(-)}(p+p_0) + X^{(-)}(p-p_0)].
\end{aligned}
\qquad (D.4.5)
$$

/214

Since both $S_r(\omega)$ and $W(\omega)$ are narrow-band spectra, we can write (D.4.5) approximately in the form:

$$
\begin{aligned}
S_0(p) = 2(A - jB) \Bigg[&\frac{S_r(p+p_0)}{W(f+f_0)} + \frac{S_r(p-p_0)}{W(f-f_0)} + \\
&+ \frac{X^{(+)}(p+p_0)}{W(f+f_0)} + \frac{X^{(+)}(p-p_0)}{W(f-f_0)} + \frac{X^{(-)}(p+p_0)}{W(f+f_0)} + \\
&+ \frac{X^{(-)}(p-p_0)}{W(f-f_0)} + \frac{X^{(+)}(p+p_0)}{W(f-f_0)} + \frac{X^{(+)}(p-p_0)}{W(f+f_0)} + \\
&+ \frac{X^{(+)}(p+p_0)}{W(f-f_0)} + \frac{X^{(-)}(p-p_0)}{W(f+f_0)} \Bigg].
\end{aligned}
\qquad (D.4.6)
$$

The solution of (D.4.2) is found by taking the inverse Fourier transformation of function $S_0(p)$ (see App. 3); using again the displacement theorem for the Fourier transform we can

thus write on the basis of (D.4.6):

$$Z_{oT} = Z_T(t)[A \cos \omega_\varphi t + B \sin \omega_\varphi t] + \Delta(t), \qquad (D.4.7)$$

where $\Delta(t)$ is defined by (D.4.4). The displacement theorem is proven in this way.

The displacement theorem (in its application to detection problems) can also be proven using the statistical independence of the quadratic components of the narrow-band stochastic process, expressing the process realization probability in terms of the probability of the components mentioned above.

References.

D.4.1. G.A. Campbell, R.M. Foster. Fourier Integrals for Practical Applications. New York, 1948.

ON THE MODULATION OF STATIONARY STOCHASTIC PROCESSES

In many applications one may encounter paths generated by periodic vibrations or almost periodic vibrations by amplitude modulation of these vibrations by a stationary stochastic process. If the carryer vibration is denoted by x(t), and the given stationary process by Z(t), we will obtain in this case the stochastic process

$$M(t) = x(t) \cdot Z(t). \tag{D.5.1}$$

Processes of this type are sometimes called in the literature the non-stationary periodic processes [D.5.1, D.5.2] . Because of the symmetry of (D.5.1) it can also be interpreted as the modulation of a stationary stochastic process by a periodic path (or almost periodic path).

We describe below some simple relations relating the properties of a modulated stochastic process with appropriate characteristics of the stationary process Z(t) and vibration parameters x(t). The author has demonstrated in a previous paper [D.5.3] that the modulation of a periodic (or almost periodic) vibration by a defined path is, for certain kinds of modulation, equivalent to the modulation of any harmonic vibration by this path. We will show here that a similar theorem in the case of amplitude modulation is also true with respect to stationary stochastic processes.

As we know [D.5.4 and D.5.5], every stationary process (in a more general sense) which obeys the condition

$$\lim_{t-s\to 0} E\{|Z(t) - Z(s)|^2\} = 0, \tag{D.5.2}$$

can be represented in the form of a Fourier-Stieltjes integral:

$$Z(t) = \int_{-\infty}^{\infty} e^{j\omega t}\, dS(\omega). \qquad (D.5.3)$$

The function of spectral distribution $S(\omega)$ is a process with orthogonal increases. We have

$$E[S(\omega)] = 0 \qquad (D.5.4)$$

and

$$E[(S(\omega_1 + \Delta\omega_1) - S(\omega_1))\overline{(S(\omega_2 + \Delta\omega_2) - S(\omega_2))}] = 0 \qquad (D.5.5)$$

for disjoint intervals $(\omega_1, \omega_1 + \Delta\omega_1) \text{ i } (\omega_2, \omega_2 + \Delta\omega_2)$[1].

The inverse relation between $S(\omega)$ and $Z(t)$ can be written in the form:

$$S(\omega + \Delta\omega) - S(\omega) = \frac{1}{2\pi} \lim_{T\to\infty} \int_{-T}^{T} \frac{e^{-j\omega t} - e^{-j(\omega+\Delta\omega)t}}{-jt} Z(t)\, dt. \qquad (D.5.6)$$

We will use these relations in proving the theorem about amplitude modulation.

As we know [D.5.6], if the path $y(t)$ has a spectrum $S_y(\omega)$ determined by the Fourier transform /216

$$S_y(\omega) = \mathcal{F}\{y(t)\} = \int_{-\infty}^{\infty} y(t)\, e^{-j\omega t}\, dt, \qquad (D.5.7)$$

then the path $z(t) = y(t)\, e^{j\omega_n t}$ has a spectrum $S_z(\omega)$

$$S_z(\omega) = \mathcal{F}\{y(t)\, e^{j\omega_n t}\} = S_y(\omega - \omega_n). \qquad (D.5.8)$$

---

[1] Because of the form of equations in App. 5, the coupled value will be denoted here by a bar above appropriate terms, and not by a star, as in the other formulas in the present work.

An analogous theorem holds for the spectral distribution of stationary processes. For the function $Z(t) = Z(t)\, e^{j\omega_n t}$ we can write formally on the basis of (D.5.6):

$$S_1(\omega + \Delta\omega) - S_1(\omega) = \frac{1}{2\pi} \lim_{T\to\infty} \int_{-T}^{T} \frac{e^{-j\omega t} - e^{-j(\omega+\Delta\omega)t}}{-jt} Z_n(t)\, dt =$$

$$= \frac{1}{2\pi} \lim_{T\to\infty} \int_{-T}^{T} \frac{e^{-j(\omega-\omega_n)t} - e^{-j(\omega-\omega_n+\Delta\omega)t}}{-jt} Z(t)\, dt =$$

$$= S(\omega - \omega_n + \Delta\omega) - S(\omega - \omega_n), \tag{D.5.9}$$

or

$$S_1(\omega) = S(\omega - \omega_n). \tag{D.5.10}$$

A periodic or almost periodic path x(t) can be written in the form of a Fourier series

$$x(t) = \sum_{n=-\infty}^{\infty} A_n\, e^{j\omega_n t}. \tag{D.5.11}$$

Substititing (D.5.11) into (D.5.1) we will obtain

$$M(t) = \sum_{n=-\infty}^{\infty} A_n\, e^{j\omega_n t} \cdot \int_{-\infty}^{\infty} e^{j\omega t}\, dS(\omega). \tag{D.5.12}$$

Because of (D.5.10)

$$M(t) = \int_{-\infty}^{\infty} e^{j\omega t}\, d\left[\sum_{n=-\infty}^{\infty} A_n S(\omega - \omega_n)\right]. \tag{D.5.13}$$

Since the infinite series is a Fourier series, and - because of (D.5.3) - there exists an integral in (D.5.12), the existence of the integral (D.5.13) follows from the Lebesgue theorem about limited convergence (which can be formulated as a theorem about series integration) (D.5.7).

The relation (D.5.13) can be written in the form:

$$M(t) = \int_{-\infty}^{\infty} e^{j\omega t}\, d\, S_2(\omega). \qquad \text{(D.5.14)}$$

where

$$S_2(\omega) = \sum_{n=-\infty}^{\infty} A_n\, S(\omega - \omega_n). \qquad \text{(D.5.15)}$$

In practical applications one needs primarily the power spectrum or the autocorrelation function of a path.

Before determining the spectrum, we should consider briefly the kind of spectrum we will deal with. It follows from /21/ the general theory which considers the possibility of determining the energy property of a path with its spectral distribution, that in contrast to the power spectrum in the case of stationary processes, for processes considered here there exists an "averaged" spectrum, i.e. a spectrum with respect to the

average power defined as $\lim_{T\to\infty} \frac{1}{2T} \int_{-T}^{T} E|Z(t)|^2\, dt$ (D.5.8).

It corresponds to an appropriately understood autocorrelation function (D.5.2, D.5.9). This should be remembered in the interpretation of results in practical applications.

In order to determine the power spectrum understood in this way we have to determine the mean of the product (D.5.8):

$$W(\omega + \Delta\omega) - W(\omega) = E\{[S_2(\omega + \Delta\omega) - S_2(\omega)]\overline{[S_2(\omega + \Delta\omega) - S_2(\omega)]}\}. \qquad \text{(D.5.16)}$$

Because of (D.5.15) we obtain:

$$W(\omega + \Delta\omega) - W(\omega) = E\left\{\sum_{r=-\infty}^{\infty} A_r\,[S(\omega - \omega_r + \Delta\omega) - S(\omega - \omega_r)]\right\}\overline{\left\{\sum_{q=-\infty}^{\infty} A_q\,[S(\omega - \omega_q + \Delta\omega) - S(\omega - \omega_q)]\right\}}. \qquad \text{(D.5.17)}$$

It is easy to see that relation (D.5.17) can be written in the form:

AD-A098 433 FOREIGN TECHNOLOGY DIV WRIGHT-PATTERSON AFB OH F/G 17/9
REDUCTION OF STATIONARY CLUTTER IN RADAR.(U)
OCT 80 J KROSZCZYNSKI
UNCLASSIFIED FTD-ID(RS)T-0132-80 NL

4 OF 4

END
DATE
FILMED
8-81
DTIC

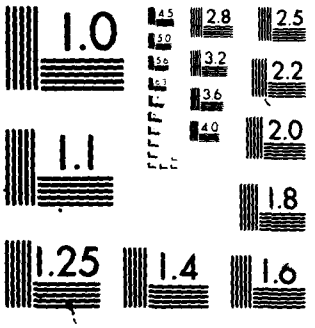

MICROCOPY RESOLUTION TEST CHART
NATIONAL BUREAU OF STANDARDS-1963-A

$$W(\omega+\Delta\omega)-W(\omega)=\mathrm{E}\left\{\sum_{n=-\infty}^{\infty}A_n^2\left|S(\omega-\omega_n+\Delta\omega)-\right.\right.$$
$$\left.-S(\omega-\omega_n)\right|^2+\sum_{r=-\infty}^{\infty}\sum_{\substack{q=-\infty\\ r\neq q}}^{\infty}A_rA_q\left[S(\omega-\omega_r+\Delta\omega)-\right.$$
$$\left.\left.-S(\omega-\omega_r)\right]\overline{\left[S(\omega-\omega_q+\Delta\omega)-S(\omega-\omega_q)\right]}\right\}. \tag{D.5.18}$$

For $\Delta\omega<\inf\ (\omega_r-\omega_q)$ the intervals $(\omega-\omega_r,\omega-\omega_r+\Delta\omega)$ and $(\omega-\omega_q,\omega-\omega_q+\Delta\omega)$ are disjoint, and therefore, on the basis of (D.5.5), the second term of (D.5.18) equals zero.

$$W(\omega+\Delta\omega)-W(\omega)=\sum_{n=-\infty}^{\infty}A_n^2[W_z(\omega-\omega_n+\Delta\omega)-W_z(\omega-\omega_n)], \tag{D.5.19}$$

and

$$W_z(\omega+\Delta\omega)-W(\omega)=\mathrm{E}\left\{[S(\omega+\Delta\omega)-S(\omega)]\overline{[S(\omega+\Delta\omega)-S(\omega)]}\right\}. \tag{D.5.20}$$

On the basis of *Wiener-Chinchin* formula we can define the autocorrelation function of the modulated path M(t):

$$R_M(\tau)=\int_{-\infty}^{\infty}e^{j\omega\tau}dW(\omega)=\int_{-\infty}^{\infty}e^{j\omega\tau}d\left[\sum_{n=-\infty}^{\infty}A_n^2W_z(\omega-\omega_n)\right]. \tag{D.5.21}$$

Equation (D.5.21) is equivalent to the relation introduced in (D.5.10) for the case of amplitude modulation. Since the autocorrelation function of path x(t) is $\sum_{n=-\infty}^{\infty}A_n^2e^{j\omega_n\tau}$ we can write (D.5.21) in a form where we will have the product of the autocorrelation function of path x(t) and the power spectrum of process Z(t), as in ref. [D.5.10] for the operation of the inverse Fourier transformation.

On the basis of (D.5.19) and (D.5.21), the theorem of /218 amplitude modulation for stationary stochastic processes can be considered proven. In fact, as follows from these equations, the power spectrum or the autocorrelation function for a modu-

lated path is obtained in such a form as if every harmonic of path x(t) was subject to the modulation process by a stochastic process individually.

The theorem proven here is of practical importance for all cases where a modulation of the periodic path by a stationary stochastic process is present; because of the symmetry of (D.5.1) the same applies to the modulation of a stationary process by the periodic path. Therefore, these are applications useful when considering radar signals, sampling problems, etc.

References.

D.5.1. Zadeh, L.A. Correlation Functions and Spectra of Phase and Delay-Modulated Signals. PIRE, April 1951.

D.5.2. Gudzenko, L.I. On Periodically Non-stationary Processes. Radiotechnika i Elektronika, No. 6, 1959.

D.5.3. Kroszczynski, J. On Some Modulation Properties. Pzheglad Telekomunikacyjny, No. 11, 1954.

D.5.4. Doob, J.L. Stochastic Processes. New York, 1953.

D.5.5. Jaglom, A.M. Introduction to the Theory of Stationary Random Functions. Usp. Mat. Nauk, No. 5(51), 1952.

D.5.6. Campbell, G.A., Foster, R.M. Fourier Integrals for Practical Applications. New York, 1948.

D.5.7. Cramer, H. Mathematical Methods in Statistics, PWN, 1958.

D.5.8. Blanc-Lapierre, A., Fortet, R. Theorie des fonctions aleatoires, Ch. IX, Paris, 1953.

D.5.9. Charkiewicz, A.A. On the Calculation of Spectra of Random Signals, Radiotechnika, No. 5, 1957.

D.5.10. Zadeh, L.A. Correlatic. Functions and Power Spectra in Variable Networks. PIRE, Cct. 1950.

SOME INTERRELATIONS FOR THE SIGNAL AND INTERFERENCE SPECTRA

6.1. The width of fluctuation spectrum of passive interference W_p.

The sepctrum $W_p(f)$ can be approximated by the expression (cf. eq. 5.3.4):

$$W_p(f) = \text{const} \cdot \exp\left[-a\left(\frac{f}{f_s}\right)^2\right]. \qquad \text{(D.6.1)}$$

where

a - coefficient dependent on the character of correlated noise;

f_s - carrying frequency of the signal.

(D.6.1) can be written also in the form:

$$W_p(f) = \text{const} \cdot \exp\left[-\left(1{,}666\,\frac{f}{\Delta_f^p}\right)^2\right]. \qquad \text{(D.6.2)}$$

where Δ_f^p - the width of fluctuation spectrum of correlated interference at the level of half-power (Fig. D.6.1), therefore Δ_f^p is related to f_s by the dependence:

$$\Delta_f^p = \frac{1{,}666\, f_s}{\sqrt{a}}. \qquad \text{(D.6.3)}$$

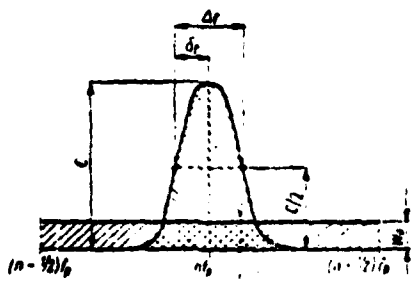

Fig. 6.1. Spectra of correlated and non-correlated noise.

6.2. The width of modulation spectrum generated by antenna revolution W_A.

Let us assume a Gaussian shape of the directional antenna characteristic

$$G(\psi) = \exp\left[-2{,}776\left(\frac{\psi}{\psi_0}\right)^2\right]. \qquad \text{(D.6.4)}$$

where ψ_o - the width of antenna beam at the half-power level. The time of transition of the beam by an angle equal to ψ_o is: /220

$$t_0 = (N-1)\,T_p = \frac{N-1}{f_p}, \qquad \text{(D.6.5)}$$

where N - number of pulses falling within the beam width.

Using (5.3.5) and the known properties of the Gaussian pulse spectrum we can write the power spectrum $W^A(f)$ in the form:

$$W_A(f) = \text{const}\cdot\exp\left\{-\left[2{,}066\,(N-1)\frac{f}{f_p}\right]^2\right\}. \qquad \text{(D.6.6)}$$

Thus the width of spectrum Δ_f^A is:

$$\Delta f = 0{,}6238\,\frac{f_p}{N-1}. \qquad \text{(D.6.7)}$$

In Fig. 7.2.2 we have introduced as a parameter the quantity $\delta_f/f_p = \frac{1}{2}\,\Delta_f/f_p$.

Thus, if the fluctuations were caused by the motion of the antenna only, we would have:

$$\frac{\delta f}{f_p} = \frac{0{,}3119}{N-1}. \qquad \text{(D.6.8)}$$

6.3. The total width of the interference fluctuation spectrum W_p

Based on (7.1.12), for Gaussian shapes of spectra $W_p(f)$ and $W_A(f)$ we can write:

$$W_f(f) = \text{const} \cdot \exp\left\{-\left[\frac{(1.666 \cdot f)^2}{(\Delta_p^f)^2 + (\Delta_f^A)^2}\right]\right\}. \tag{D.6.9}$$

and therefore:

$$\Delta_f = \sqrt{(\Delta_f^p)^2 + (\Delta_f^A)^2}. \tag{D.6.10}$$

6.4. The ratio of power of correlated and non-correlated noise.

The power of non-correlated noise, falling within a bandwidth equal to the period of a periodic filter characteristic in frequency domain is:

$$P_n = W_0 f_p, \tag{D.6.11}$$

where

W_0 - spectral density of noncorrelated noise;

f_p - the period of the periodic filter characteristic (Fig. D. 6.1).

The power of correlated noise, falling within the same bandwidth, is (for a Gaussian spectrum shape): /221

$$\begin{aligned} P_{ak} &= \int_{\left(n-\frac{1}{2}\right)f_p}^{\left(n+\frac{1}{2}\right)f_p} C \cdot \exp\left[-\left(\frac{1.666 f}{\Delta f}\right)^2\right] df \cong \\ &\cong \int_{-\infty}^{\infty} C \cdot \exp\left[-\left(\frac{1.666 f}{\Delta f}\right)^2\right] df \cong \\ &\cong 0{,}532\, C \Delta_f. \end{aligned} \tag{D.6.12}$$

Therefore, the ratio of the power of correlated and non-correlated noise is:

$$\frac{P_{ak}}{P_n} \cong 0{,}532 \cdot \frac{C}{W_0} \cdot \frac{\Delta_f}{f_p}. \tag{D.6.13}$$

SOME ASPECTS OF THE RADAR RECEPTION WITH NONCOHERENT INTEGRATION

The system of optimal reception of strongly fluctuating signals, discussed in Ch. 4.2, contains a linear filter with constant parameters, followed by a switch, quadratic detector, and integrator. We should note the following aspects of the operation of this system. The integration time must be appropriately adjusted to the time duration of the detected signal. If the integration time is too short, we do not use part of the signal; if it is too long, we integrate the noise unnecessarily[1]. In the case of signal modulation in the process of space scanning, weighted integration should be used, with the weight function appropriately adjusted to the directional antenna characteristic. Since the time of arrival of the packet is not known, the realization of the above requirements is not easy. An ideal integration system of this type would have to contain a special switch (mentioned in Ch. 4), which makes successive readings of the voltage at the output of the linear filter and transmits them to appropriate integration systems. This problem is considered in more detail in ref. [D.7.1].

In practical systems a similar operation can be approximated by various methods. During integration on the screen of the image tube of a panoramic display, the integration characteristics of the luminofore and the revolving motion of the radial time base give a mode of operation somewhat resembling the one described above. In applying visual integrators of the analog type (e.g. with a delay line and feedback - see Ch. 8, their characteristics are also chosen appropriately for the parameters of the pulse packet. In devices mentioned above the "switch"

[1]Let us note that at the input of a noncoherent integrator (unlike in the coherent integrator), the noise has only positive values becauseof quadratic detection.

does not appear explicitly in the practical system[1]. The need for a "switch" is more apparent, in the case of systems of automatic numerical detection and determination of object coordinates. Since these problems go far beyond the scope of the present volume, we will only say that by appropriate programming of computers used for this purpose it is possible to realize the noncoherent numerical signal integration which approaches the optimal, and at the same time to estimate the coordinates of the detected objects. This problem is discussed in detail in ref. [D.7.2] .

References.

D.7.1. Middleton, D. On New Classes of Matched Filters and Generalizations of the Matched Filter Concept. IRE Trans., IT-6, June 1960.

D.7.2. Klujev, N.F. Detection of Pulse Signals Using Collectors with Discrete Operation. Moscow, 1963.

[1]therefore it was omitted in Fig. 6.2.5

END

DATE

FILME

6

DTIC